Author:
Fewtrell, Timothy J

Title:
Development of simple numerical methods for improving two-dimensional hydraulic models of urban flooding

Timothy J. Fewtrell

Development of simple numerical methods for improving two-dimensional hydraulic models of urban flooding

A dissertation submitted to the University of Bristol
in accordance with the requirements of the degree
of Doctor of Philosophy in the Faculty of Science.

School of Geographical Sciences, December 2008

Word Count: 51272

Abstract

Severe flood events throughout Europe in recent years have increased political, public and scientific awareness of the risks posed by large flood events. In response, engineers and researchers have transferred their attention from rural studies to consideration of urban areas where risk is concentrated. Computational fluid dynamics methods have been extensively employed in the evaluation of in-channel and out-of-bank flow processes in natural rivers in the last 20 years. In the case of urban flood events, computationally efficient methods are required to estimate flood risk at fine scale details over wide areas. The overall aim of this thesis was therefore to understand the controlling features of urban areas for floodwave propagation and subsequently, develop computationally efficient methods to evaluate flood risk.

The first component of this research was focused on determining the features of urban areas that modulate floodwave dynamics. Subsequently, the effect of grid resolution on the representation of urban features and flood propagation was investigated to determine the compromise between computational cost and model performance. It was found that floodwave propagation through urban areas in the UK is controlled by the distribution of building sizes and separation distances.

The second part of this thesis details the development and evaluation of sub-grid scale porosity techniques aimed at harnessing high resolution topographic data sets within coarse resolution numerical models. For the first time, this research presents a consistent and rigorous evaluation of a variety of porosity techniques for flood modelling. The results suggest that representing the broad scale effect of buildings and obstacles on flood flows provides the best compromise between data demands, pre-processing requirements and computational cost. Indeed, the use of a porosity techniques yielded model performance at least as good as standard model configurations at double the resolution for an order of magnitude less computation time. The techniques developed here provide a structured approach towards flood risk assessment for engineers in data rich areas as well as proposing methodologies for data sparse regions.

Blank Page

Acknowledgements

First and foremost, this thesis would not have been possible without the constant support and guidance of my supervisors Paul Bates and Matt Horritt. Thanks also to Jon Wicks for hosting me at Halcrow on the odd occasions I made the trip along the M4. Special thanks to Paul for allowing me to develop my own ideas and yet still putting up with my outbursts when they didn't go as planned. I owe a considerable amount to you for my professional (and personal) development over the past 4 years (and counting).

As every PhD student who has finally finished is very quick to recall, the three (four) years are punctuated by ups and downs, the size of which no one can ever describe. Along the way, colleagues have turned to friends and everyone from my two offices, Browns and the Hydro Postdoc office, have made my working hours infinitely more enjoyable. From Browns, my fellow fourth years, Graham Felce, Laura Edwards and Sam Kelly, deserve a special mention for keeping me going. However, Browns would not have been the place it was without the constant encouragement and input from Anne Le Brocq, Andrew Sole, Liz Bagshaw, Gina Moseley and Jonny Day.

My last year of frantic coding and writing would not have been possible without the support of the Hydro Postdoc office (it will always be 'our' office...). The sparks of creativity from Jeff Neal, Liz Holcombe, Guy Schumann, Giuliano Di Baldassarre (despite our football and motorsport rivalries) and our honorary hydrologist, Anne-Laure Daniau (and the occasional visits from Malcolm Anderson) definitely added to the scientific (and otherwise) content of the thesis. The scientific input would not have been complete without past and present members of the Hydrology Research Group - Katerina Michealides, Debbie Lister, Charlotte Lloyd, Wouter Buytaert, JP Renaud, Jim Freer and especially Neil Hunter.

As with all things in life, there are some bits of research best left to other people. Unfortunately, with a PhD that just isn't possible. However, without the input of Duncan Baldwin and Gethin Williams on all things computing, babysitting my simulations would have been significantly more difficult. Further thanks to Jenny Griggs for offering to read the drafts and final proofs of this thesis, and then actually doing it. I also owe a huge thank you to Mark Trigg for all the knowledge imparted on hydrology, hydraulics and computer code - your experience has had an immeasurable impact on me and my research career.

These four years in Bristol were made considerably more enjoyable by the never-ending banter and 'occasional' work chats with my (now ex-)housemates - Asa Morris and Charlie Flood. Without the distractions from work you two provided, there would be no thesis. Thank you for keeping me 'chilled'.

Without the unwavering love and support of my parents, grandparents and Emma, Bart, Thijs and Jitske, this mammoth task would not have been possible. Special thanks to Mummy for reading the drafts, despite admitting to wondering what on earth it was all about and to Daddy for helping me talk through problems and understanding it all (or at least pretending to).

Author's Declaration

I declare that the work in this dissertation was carried out in accordance with the requirements of the University's Regulations and Code of Practice for Research Degree Programmes and that it has not been submitted for any other academic award. Except where indicated by specific reference in the text, the work is the candidate's own work. Work done in collaboration with, or with the assistance of, others, is indicated as such. Any views expressed in the dissertation are those of the author.

SIGNED:.....T.Fenstall..... DATE:....01/07/09..

Blank Page

Contents

List of Figures

List of Tables

CHAPTER 1

Introduction

Recent severe flood events in the UK, in particular Carlisle in January 2005 and Gloucestershire in the summer of 2007, have raised public, political and scientific awareness of flood risk and the need for effective flood protection and alleviation measures. Furthermore, events across Europe in the summer of 2002 highlighted the need of effective but justifiable flood managements schemes as annual damage estimates far outstretch current management expenditure. Current flood management expenditure in the UK for fluvial and pluvial urban flooding is estimated at £800 million whereas average annual damage estimates in 2004 were as much as £1,400 million (Evans *et al.*, 2004). In the UK alone, nearly two million properties are located on floodplains along rivers, estuaries and coasts and The Department of the Environment, Food and Rural Affairs (DEFRA) further estimate that 200,000 properties are classified as at risk of flooding as they do not have the Government prescribed standard of protection against a 1-in-75 year flood event. Furthermore, the Association of British Insurers (ABI) note that member companies have reported a total of 165,000 claims totaling £3 billion as a result of the summer 2007 floods in the UK (ABI, 2007).

Climate change scenarios and development projections suggest that flood risk in Europe is likely to increase. Firstly, sea level rise, increased storm frequency, changing seasonal patterns and an increase in the probability of extreme events mean that low-lying areas will be at greater risk from flooding in future years (IPCC, 2007). Secondly, increased public and private development in floodplains will have a dramatic effect on both the annual damage estimates and the distribution of areas at risk. Evans *et al.* (2004) project as much as £30 billion of annual damage from fluvial and pluvial flooding by 2080 based on high emission scenarios and current management expenditure. Despite these projections, a recent proposal from the Office of the Deputy Prime Minister details the development of a further 250,000 properties and ~£500 million of investment located on floodplains in south east England (Prescott, 2005). However, the practicality of this investment is undermined by the fragmented approach to responsibilty for flood risk between UK Government and the private insurance industry as levels of *sufficient* protection and *risk awareness* are, as yet, undefined (Huber, 2004). There is a clear disparity between attitudes towards planning and management and the perception of present and potential flood risk.

Increasing flood risk requires the development and application of an appropriate set of tools to inform local and regional government on management policy, engineers for planning and design purposes and (re-)insurers to calculate exposure. However, Gouldby and Samuels (2005) note a discrepancy in the definition of *risk* across the wide range of disciplines and activities concerned with risk assessment. Furthermore, these definitions have multiple dimensions depending on the needs of the particular decision-maker and application. Therefore, in terms of quantifying flood risk, it is necessary to reduce the ambiguity of the term and provide a coherent approach for its application to flooding, particularly in urban environments. In this case, there is a vital distinction between the 'hazard' and the 'consequences' of the hazard; the product of which can be considered the risk of a given flood event. Gouldby and Samuels (2005) detail the source-pathway-receptor-consequence model to include associated probability, fragility and depth-damage curves from Sayers *et al.* (2002). This model provides the basis for a consistent method for dealing with the assessment of flood risk from identification and understanding of the hazard through to quantification of vulnerability and exposure.

The recognition of flood risk and the need for effective assessment and management strategies is paramount prior to any planning, design or policy discussions. In response, the commissioning and subsequent publication of the Foresight Future Flooding report (Evans *et al.*, 2004) and the funding of large flood risk assessment projects (e.g. Flood Risk Management Research Consortium (FRMRC) and FLOODsite) by UK and EU funding streams are prime examples of the realisation of, and reaction to, this need.

1.1 The role of flood inundation modelling

Wheater (2002) noted that decision-support modelling tools are required to inform strategic planning, flood design and management and climate change scenarios. The aim of simulation models is to 1) 'explore the implications of making certain assumptions about the nature of the real world system' and 2) 'to predict the behaviour of the real world system under a set of naturally-occurring circumstances' (Beven, 1989). To date, flood inundation modelling applications have mainly been concerned with the former in the form of event *validation* or *history-matching* (Konikow and Bredehoeft, 1992). However, in terms of flood risk assessment in current and future environmental and political climates, flood inundation models and their application are required to fulfill both these aims. There is no guarantee that a

model designed under one specific set of naturally-occurring circumstances will respond in a realistic manner when subject to extreme events, which is precisely when the answers matter most (Kirchner, 2006).

Floods and floodplain inundation are inherently spatio-temporal phenomena that, in the absence of field observations, require a distributed physically based modelling approach. The practical application of flood models, therefore, requires the ability to extrapolate across space and/or time and to predict situations where no measurements are available (Hunter, 2005). The final report of the EU Concerted Action on Dam Break Modelling (CADAM) project (Morris, 2000) suggested the information required for satisfactory assessment of the consequences of flooding at any point of interest within the flood zone may include:

- time of first arrival of flood water
- peak water level and extent of inundation
- time of peak water level
- instantaneous depth and velocity of flood water
- duration of flooding

Consequently, flood inundation modelling is required to simulate the movement of a flood wave along a river valley through compound channels, over complex topography and through areas of varied topology and land-use and provide a time-accurate solution. The problem then arises of how to conceptualise the problem of flooding and translate that into a reasonable numerical approximation.

1.1.1 From concepts to numerics

The utility of flood modelling relies on the appropriate definition of the problem, both conceptually and numerically, and subsequent evaluation of the performance of the modelling tool prior to use in a decision support framework (Wheater, 2002). A conceptual model is a hypothesis pertaining to current understanding, or perceptual model, of the physical phenomenon (in this case, fluvial flow processes) in which the relative importance of known processes are represented in detail, represented simply or ignored. Any conceptual model will be wrong and will be known to be wrong (Morton, 1993), but will still have the possibility of being approximately realistic (Beven, 2002). Until recently, the dominant practice in environmental modelling was to ensure that any conceptual model, and the numerical representation thereof, was 'as real as possible' by employing a reductionist approach (see

Freeze and Harlan, 1969). However, models based on this approach often incur considerable setup and computational costs and are often characterised by a large number of unknown parameters with varying degrees of measurement tractability (Beven, 1989). On the other hand, over-simplification and lumping of processes can lead to redundancy of (high resolution) input data and indistinguishable model configurations (see Beven (2006)). Ultimately, the most appropriate method will be the simplest one that provides the information and functionality required by the user whilst fitting the available observational data as defined by some appropriate measure of acceptability limits (Bates and De Roo, 2000). This approach implicitly employs some notion of the principle of parsimony (Box and Jenkins, 1970) which recommends selecting the simplest method that describes the available data based on an analysis of the trade-off between bias and variance of the parameter estimates (Di Baldassarre *et al.*, in press).

The hydraulic processes of in-bank, channel flow are well understood and numerically, the de St. Venant equations of gradually varied unsteady flow in open channels are generally accepted as an appropriate basis for flood modelling (Wheater, 2002). Various simplifications of these equations exist (e.g. Muskingum-Cunge routing, kinematic or diffusion wave approximations etc.) and site-dependent characteristics will determine the complexity required for modelling channel flows. On the other hand, out-of-bank flows in compound meandering channels are known to be highly three dimensional and involve the development of i) a strong shear layer between the main channel and the floodplain (Knight and Shiono, 1996) and ii) significant conveyance between meander loops, both acting to transfer momentum across the channel-floodplain boundary.

The question that arises is then how to structure these assumptions numerically and a number of approaches of varying complexity have been developed since the 1960s (Xanthopoulos and Koutitas, 1976; Zanobetti *et al.*, 1968, 1970). A fully three dimensional numerical treatment of these hydraulic processes is not currently viable at reach-scale as computational costs, turbulence closure schemes and the transient nature of the shoreline limit practical application of these models (Hunter *et al.*, 2007). Furthermore, the data available for model building and evaluation may not support this level of detail. In the other extreme, until recently, most flood risk assessments were undertaken using 1D models which, although being computationally efficient, are limited by the inability to simulate lateral floodplain flows, the subjectivity of cross-section location and orientation and the representation of the floodplain as either extended cross-sections or storage cells based on the underlying

topography. A number of authors have shown that a 2D representation of floodplain flow is sufficient detail to represent gradually varying flow over complex topography (see review in Hunter *et al.*, 2007). Regardless of the process complexity, models need to be parameterised and evaluated prior to any application within a decision support framework.

1.1.2 Parameterising flood models

Constructing a hydraulic flood model of any given reach requires a substantial amount of boundary data to parameterise and constrain the computation in the form of i) topographic data to define the model grid, ii) flow conditions, internal and external to the model domain, and iii) definition of the flow resistance parameter values. Until the mid-1990s, elevation data for the UK was derived from a combination of surveyed contour information, with some interval and accurate to ± 1.25 m, and spot heights, with a relative accuracy of $\pm$ 5 mm but poorer absolute accuracies (Marks and Bates, 2000). These data are combined to produce digital elevation models of roughly 10 m horizontal resolution with an error of at least ± 50 cm, an error of significant magnitude to have complex effects on flow patterns (Bates and Anderson, 1996). The advent and proliferation of **Li**ght **D**etection **a**nd **R**anging (LiDAR), has reduced the errors of digital elevation data to 0.15 m vertically and 0.10 m horizontally at sub-metre spatial resolution (Mason *et al.*, 2007). In rural areas, a number of studies (Cobby *et al.*, 2003; Mason *et al.*, 2003) have shown the utility of these topographic data to drive unstructured mesh generation and friction parameterisation for hydraulic models. In urban areas, LiDAR data has been used to drive flood models, at grid (Hunter *et al.*, 2008) and sub-grid scales (Yu and Lane, 2006b), and to derive building characteristics (Forlani *et al.*, 2006). The errors associated with LiDAR data and their effect on flood modelling have been investigated (Néelz and Pender, 2006) and explored in detail (Raber *et al.*, 2007), and such data has significantly improved the representation of topographic variations in hydraulic models.

Flow boundary conditions for hydraulic modelling of floods, whether 1D or 2D, are generally specified as flow hydrographs derived from gauging stations, both internal and external to the modelled reach. These hydrometric data are routinely archived from nationally maintained gauging stations (e.g. UK National River Flow Archive) and are usually in the form of a time series of water stages and/or discharge estimates. Despite the spatial coverage and ease of data acquisition, it should be noted that there is a clear discrepancy between the design specifications of flow gauging stations and the data requirements for hydraulic

flood modelling. Most gauging stations in the UK were originally designed for low flow monitoring for water resource management such that during floods, these stations operate outside the designed measurement range. Moreover, most discharge records are derived from stage-discharge rating curves relating measured water levels to a flow (Herschy, 1999) but errors in rated discharge data can be up to ±20% for large out of bank flows (Pappenberger *et al.*, 2006). Uncertainties in measured rating curves, when subject to extrapolation to larger events or into the future, may generate significant deviations in model results to reduce confidence in the model's predictive ability. Furthermore, the assumption that present observations are indicative of future conditions is not guaranteed as natural systems are dynamic (Oreskes *et al.*, 1994). Uncertainties in gauged flows resulting from these assumptions and problems initiate an uncertainty cascade (Pappenberger *et al.*, 2006) that propogates to model predictions of water depths and consequently to estimates of flood damage.

Perhaps the most controversial and least determinable aspect of model parameterisation in hydrology is the definition of an appropriate flow resistance parameter formulation and value. A number of formulations of flow resistance or 'roughness parameters' have been derived empirically (e.g. Manning's n, Chezy, Darcy-Weisbach) and their relative applicability depends greatly on the field of interest. However, most engineering applications of flooding adopt the Manning's n approximation to represent bed shear. Theoretically, roughness can be defined for each computational cell based on empirically derived estimates from field measurements (e.g. Chow, 1959). However, studies have reported difficulty in resolving 'optimum' model performance from a single model realisation using field derived friction values (Beven, 1989) implying the need for calibration strategies (Hunter, 2005). Furthermore, Horritt *et al.* (2007) have demonstrated the difficulty of reconciling model and application specific 'optimum' friction values with published tables (Chow, 1959) or 1D modelling approaches (Fisher and Dawson, 2003) after calibration and subsequent validation of the hydraulic model. Calibrated roughness parameters in hydraulic models of varying complexity actually account for differences in process representation (Horritt and Bates, 2001b, 2002) and may belie limitations in other model parameterisation data (Pappenberger *et al.*, 2006). Most hydraulic models limit the variation in roughness parameters to a few distinct classes, generally split between a channel flow resistance and a floodplain flow resistance to reduce the dimensionality of the problem. However, roughness values will vary in space and time depending on conditions prior to the flood event and evolving conditions during the flood event. Roughness parameterisation, therefore, will be model specific, site specific and

event specific (Lane, 2005). As such, calibrated parameters should be recognised as being 'effective' values that may not have a physical interpretation outside of the model within which they were calibrated (Beven, 2000b).

1.1.3 Evaluating models in a risk framework

The utility of flood modelling in any decision support system relies on the modeller's and decision maker's confidence in the validity of the model results. The former requires objective evaluation of model output compared to observed features of the flood or benchmark results. The latter requires clear and appropriate communication of model findings conveying the relevant and necessary aspects of the modelled scenario. The following section concerns the former, where methods for evaluating models and model results are discussed within a framework of analysing risk from natural hazards. Model evaluation is conventionally done within a calibration and validation process. In all but the simplest of cases, numerical models contain variables or parameters relating to a physical property of the domain that require adjusting for use in the modelled reach. In the case of flood models, channel and floodplain friction coefficients are calibrated so that the model is best able to reproduce available observational data. The data available to constrain the calibration and validation process of any hydraulic model is generally some combination of bulk flow measurements, wide-area synoptic maps (e.g. satellite imagery) and point measurements of maximum water level.

Very often, modellers will use values from literature look-up tables of the chosen roughness coefficient (i.e. values of Manning's n from Chow (1959)), as a substitute for detailed model calibration. This approach is only applicable if the basis of the model is the same as the assumptions of the original derivation of the roughness coefficient (Yu and Lane, 2006a). Until recently, modellers tended to maximise a convenient 'goodness-of-fit' (dependent on available observational data) to obtain an optimised parameter set and proceed into a predictive phase with this model configuration. This relies on the premise that one model parameterisation will prove optimum in representing the modelled phenomenon, regardless of how this phenomenon changes over time or space. This assumes that values of friction parameters are independent, firstly, of objective function and calibration data and secondly, of numerical code used and combination of modelled site and event. However, a number of authors in many fields of hydrological science (Beven and Binley, 1992; Freer *et al.*, 2004; Pappenberger *et al.*, 2005; Wagener *et al.*, 2003; Werner *et al.*, 2005b) have shown that

rather, a range of behavioural (Spear and Hornberger, 1980) or acceptable model parameterisations, with 'effective' parameter values, exist, leading to a range of possible outcomes during a predictive phase.

The previous section detailed the data necessary to construct models and in particular, hydraulic flood models, noting specifically that there is significant uncertainty associated with input data. Pappenberger *et al.* (2006) note that models sit at the bottom of an uncertainty cascade where errors in input data propagate through the model system and are inherent in the results. Therefore, even if all parameters are known accurately and parameterised accordingly, uncertainties in input data will still lead to a range of possible model parameterisations, and thus predictions, after calibration (Beven, 2000b).

The data available to constrain the calibration and validation process can be broadly divided into spatially lumped and spatially distributed measurements. Bulk flow measurements of catchment or reach discharge or water levels indicates spatially lumped catchment response whereas wide-area synoptic maps (e.g. satellite imagery) or maximum inferred water levels are indicative of spatially distributed data. Refsgaard (2000) noted that bulk flow characteristics do not allow the potential of a model to make spatially distributed predictions to be tested, a vital component for the analysis of risk. However, gauged bulk flows, internal and external to the model domain, should still be a significant part of any calibration/validation strategy (e.g. Bates *et al.*, 1998a; Fawcett *et al.*, 1995).

Spatially distributed datasets of flood extents and water heights may be gathered from remotely sensed imagery, either directly (flood extents) or after processing (intersecting a DEM to retrieve water heights (Schumann *et al.*, 2007a)). Airborne and satellite remote sensing can deliver wide-area synoptic views of flooding that are generally processed into a discrete, binary classification of wet/dry areas. The classification of these images can result in error. The delineation of a flood boundary is subject to noise from both local ground conditions (i.e. emergent vegetation) and sensor properties (i.e. incidence angle, spectral band). Furthermore, there is large variation in the ground resolution of remotely sensed imagery depending on the type and age of the sensor. Point measurements of local water depth maxima can be inferred from wrack marks or discolouration of fixed structures (e.g. buildings and bridges) (see McMillan and Brasington (2007) and Neal *et al.* (2009a)). However, Freer and Beven (2005) highlighted the mismatch between the nature of variables used to run and evaluate a model and the nature of the observed variable. At the local point scale (e.g. a surveyed water level measurement compared to the free surface elevation predicted

at the effective model grid scale), this difference arises as a result of scale, heterogeneity and non-linearity effects so that the predicted variable is not the same quantity as that measured (Beven, 2006), which may not even be indicative of the natural phenomenon (Oreskes *et al.*, 1994). Oreskes *et al.* (1994) further note that observations and measurements of both independent and dependent variables are laden with inferences and assumptions attributed to the environmental modeller. In practical terms, what is perceived as a maximum water level mark may purely be the level at which water remained ponded during floodwave recession. The important feature here, is that regardless of the data used in model validation, a range of acceptable model parameterisations will always exist (Beven, 2006).

Based on current data collection and modelling approaches, a range of acceptable model parameterisations and therefore, model predictions will always occur. However, as Beven (2000a) noted, this range of possible model realisations should be considered as the risk of a given event. As such, models should always be evaluated within a risk framework, given current limitations in data and models. Modellers and decision makers should not view this as a problem, but rather as a means of communicating the translation of a hazard to a risk.

1.2 A changing emphasis

Until recently, most hydraulic modelling applications, whether 1D or 2D, have been limited to rural flood events. Rural areas have long been the focus of much hydrology-related research mainly stemming from a geomorphological heritage and a reductionist approach originating as a result of quantification in physical geography (Richards, 1996). As a result of this reductionist approach, process interactions in compound meandering channels of rural reaches are well understood (Knight and Shiono, 1996). Although rural reaches can be both topographically and topologically complex, the spatial scales of this complexity mean that their hydraulic behaviour is somewhat easier to define.

Surveying over large areas of the UK has delivered contour data to ± 1.25 m accuracy and spot heights with a relative error of ± 5 mm provided topographic data sets for early modelling studies (Bates and Anderson, 1993). Advances in laser altimetry in the 1990s led to a dedicated data collection programme over the UK's coastal regions and large river floodplains (Marks and Bates, 2000). This, in turn, proliferated studies of flooding on rural river reaches (e.g. Cobby *et al.*, 2003; Horritt and Bates, 2001a; Werner *et al.*, 2005a). As a result, processing algorithms for LiDAR data were originally designed for rural floodplains

(Mason *et al.*, 2003) and have been extended to other remotely sensed topographic data for larger river basins (Wilson *et al.*, 2007). As noted above, the calibration of friction parameters represents the greatest area of uncertainty in flood modelling and so relationships between land use and empirically derived friction factors has been extensively explored (Mason *et al.*, 2003; Werner *et al.*, 2005b). Such relationships are only meaningful if the model and friction bases are similar but as most friction formulations are based on rural river reaches, such methods may at least provide satisfactory initial parameterisations. In addition, Bates (2004) noted that data used to validate hydraulic models consists largely of bulk flow measurements from gauging stations and remotely sensed imagery giving direct measurements of relevant processes. However, these data were, until recently, only available on rural reaches.

The changing emphasis which has sparked the sudden interest in urban flood modelling studies (as a simple count of papers on the topic since 2004 will show) is largely a result of the consideration of risk rather than hazard modelling. The increased communication between the engineering and insurance industries and academia, in response to the large flood events of recent years, has further highlighted the need for research in this area. More specifically, the important features of a flood (outlined in §1.1) become increasingly important in urban areas where asset value is high and depth-damage curves are highly sensitive. Therefore, there is clear need to develop appropriate techniques for urban environments that are characterised by significantly different hydraulic processes. Urban flood events contribute most to overall flood risk and thus there is a clear need for appropriate flood risk management strategies able to cope with current and future flooding scenarios.

1.3 The challenge of urban applications

Mignot *et al.* (2006) note that urban areas are characterised by obstacles of varying shapes and length scales and Yu and Lane (2006a) recognise the importance of these structural features in terms of flow direction and storage volume on the floodplain. Many urban areas are also characterised by linear features such as hedges and fences which may significantly affect flood flow fields. Moreover, Mason *et al.* (2007) note that these structures are of high spatial frequency and Mark *et al.* (2004) quantify this by arguing that any model of urban flooding must be of high enough resolution (1-5 m) to resolve these features. Harnessing the high resolution topographic data made available through LiDAR is required to describe this topographic variation. The storage volume and flow paths in urban environments are

also a product of complex topological artefacts that must be quantified. The MasterMap® data product combines high resolution topological and land use data in a set of GIS vector layers and its combination with LiDAR topography (Mason *et al.*, 2007) has provided the first attempt at fully representing urban environments in a digital form.

Braschi *et al.* (1991) argue that, from a hydraulic viewpoint, flooding in an urban environment is a series of storage areas (road junctions) connected by channels (roads) carrying flow. In fact, the channelised flow is driven by surface slopes and urban structures and may be sub- or super-critical depending on local conditions. Depending on the source of flooding, flow in these channels may also be of high velocity and shallow depths (Mark *et al.*, 2004) and subject to hydraulic jumps and shocks. Thus, it will be necessary to determine how important these super-critical, high velocity flows are for determining flood risk and ultimately, flood damage. This in turn has an impact on the complexity of numerical scheme required for urban flood models (see Hunter *et al.*, 2008).

The storage of water on the floodplain is, however, not limited to road junctions and the extent to which storage in buildings affects flood propagation is a challenge not previously encountered in rural areas. Although this will have a significant impact on estimates of damage, Hingray *et al.* (2000) argue that the velocity of the passing floodwave is so much greater than the seepage velocity that this component can be ignored. Furthermore, any estimates of seepage will be reliant on detailed knowledge of building infrastructure and layout, further adding to the growing data costs of urban flood modelling.

Friction parameters are still the most important optimisation parameter in flood models. As noted above, the relationship between rural areas and friction factors is well known and has been explored in much detail although the values remain effective. However, little is known about how these empirical relationships, or indeed the effective values, transfer across to the urban setting. Indeed, the move to urban environments precludes the use of these empirical relationships as rural river reaches were used as the basis for their derivation. The need to investigate the impact of friction parameterisation, and how this changes with scale, is, therefore, of paramount importance in urban flood models.

Nonetheless, event mapping in urban areas may actually be more successful than rural areas as a wealth of calibration and validation data may exist:

- anecdotal evidence
- water marks on buildings
- trash lines and wrack marks

- aerial photography (news, police, etc.)
- satellite imagery

Until recently, however, these data have not been routinely collected and the lack of these data still represents the largest barrier to the wholescale deployment of rigorous urban flood modelling studies.

1.4 Research scope

1.4.1 Research niche

The preceding review has highlighted the need for detailed and rigorous flood risk assessment in urban areas in response to large urban flood events (e.g. November 2000 in UK, August 2002 in Europe) and increased planning for developments on floodplains (e.g. South East Growth Areas (Prescott, 2005)). The CADAM report (Morris, 2000) highlighted the need for detailed information on depths and durations of flooding, which will be even more important in urban areas where depth-damage curves are highly sensitive to water depth predictions. This requires a rigorous evaluation of current tools and techniques, balancing computational burdens, numerical complexity of the modelling framework and investment in bespoke data collection and model building. If these prove unsatisfactory at providing reliable and practical tools for the end-user, new methods are required to provide the required hydraulic information in an appropriate format and to an appropriate level of detail.

1.4.2 Thesis focus

The broad aspiration of the thesis is, therefore, **'to improve the quality of hydraulic information gathered from spatially distributed flood inundation models of urban floods'**. Specifically, it will seek to:

(i) elucidate the controlling features of urban environments on models of flood propagation and as such, assess the utility of simple model codes for modelling dynamic urban floods.

(ii) identify limitations of current approaches to urban flood modelling and to attempt to overcome these by developing new methods, specifically designed for urban applications.

(iii) develop computationally efficient methods to yield fine scale, wide area predictions of urban floods

(iv) identify simple to implement, practical approaches for engineers to apply flood models to urban areas.

In order to identify specific objectives to address these research aims, it is necessary to understand in detail how numerical flood models are constructed, the advantages and disadvantages of the different methods and how these techniques may be applied to urban flood scenarios. This will be the focus of the following chapter, in which 'state-of-the-art' flood models will be discussed in relation to current practice in order to identify specific research objectives and a methodology to meet these.

CHAPTER 2

Numerical modelling of fluvial flow processes

2.1 Introduction

In Chapter 1, flood inundation modelling was shown to be an important practical problem where spatially-distributed model predictions are required and used to inform major decisions relating to flood hazard and risk mitigation. Increased demand for accurate predictions of quantities relevant to the management of floodplains, such as discharge, water surface elevation, inundation extent and flow velocity, has arisen out of a shift in emphasis from rural to urban floodplain systems. The specific interest in urban floodplains is a result of the need to consider the risk rather than the hazard and has been influenced by large flood events (e.g. autumn 2000, Carlisle 2005, summer 2007) causing substantial damage. Clearly, from an insurance and planning perspective, confidence in the modelling output is paramount as the ramifications of mis-prediction in urban areas are significant.

Chapter 1 has thus outlined the broad problem of flooding in today's society and noted the generic requirements created by the shift to consideration of urban flood events. In addition, the specific challenges arising from this shift have been noted and the need for the adaptation of existing tools or the development of new modelling techniques is apparent. Chapter 2 aims to move from this general context to a detailed examination of current approaches to ultimately define a research direction to address specific objectives. Firstly, the numerical modelling tools created to resolve flow processes on urban floodplains will be explored by considering the dimensionality of the problem. Secondly, the challenges presented to flood modellers by a shift to urban environments are explored and thirdly, the approaches within current urban flood modelling frameworks are examined. Finally, specific research objectives will be identified and an outline of the thesis will be presented.

2.2 Hydraulic modelling of floodplain inundation

2.2.1 Flow processes in compound channels

Flow processes in open compound channels have been extensively studied experimentally (e.g. Carling *et al.*, 2002; Ervine *et al.*, 1993; Shiono and Knight, 1991) and numerically (e.g. Lane *et al.*, 1999, 2002). Complex flow interactions exist between the channel and adjacent floodplain across a variety of spatial and temporal scales. During the passage of floodwave down a river reach, water may gradually or rapidly extend and retreat over the neighbouring floodplain (Hunter, 2005). As a result, floodplains may either act as temporary storage or provide an additional mode of conveyance down the valley. At the reach scale, the combination of channel-floodplain interactions and friction effects acts to decrease wave speed, or *celerity*, and attenuates the flood peak as it is translated downstream. In natural rivers, the relationship between celerity and discharge is such that wave speed reaches a maximum at about two thirds of bankfull discharge (Q_{bf}) and reduces to a minimum at roughly 1.5 times bankfull discharge. The latter point is associated with the maximum channel-floodplain interaction effect at which time the shallow floodplain depth is most effective at attenuating flood peaks (see NERC (1975) for a more detailed discussion).

In the near-channel zone, a complex set of processes interact to create substantial momentum exchange between the in-channel and out-of-bank portions of the floodwave. The dominant processes governing this momentum transfer are largely dependent on the shape of the channel. If the channel is straight, flows in the faster flowing main channel and slower moving floodplain are essentially aligned causing a shearing layer at their interface (Shiono and Knight, 1991). The vertical vortices and secondary circulation that this shear layer creates is the principal mode of momentum transfer as high-momentum fluid from the main channel is convected onto the floodplain (Knight and Shiono, 1996). In the case of meandering compound channels, the shear layers created at the interface are generally much more intense which has a profound effect on channel conveyance (Hunter, 2005). Sellin *et al.* (1993) observed the general flow patterns in compound meandering channels on the UK Flood Channel Facility at HR Wallingford where water spills from the apex of the downstream meander and flows over the floodplain before interacting with the channel at the following meander. In this case, water is expelled vigorously from the main channel onto the floodplain and provides a route for rapid floodplain flow conveyance. It is worth noting, however, that floodplain flows beyond the meander belt will not be subject to such modifica-

tions (Hunter, 2005), or indeed influenced substantially by these energy losses and complex flow channel-floodplain processes.

In the far field, a floodwave can be approximated as a gradually varied, shallow water wave where vertical velocities can be assumed negligible compared to the horizontal velocities. This is based on the premise that horizontal extent of typical floods is large (up to several kilometres) compared to the depth (usually <10 m and typically ~1 m) (Hunter, 2005). In terms of hydraulic modelling, these dynamic flow fields can therefore be assumed to be two-dimensional and thus only varying in the x and y Cartesian directions. Bates and Horritt (2005) note that whilst it is clear complex 3D processes dominate the near-channel zone, their impact can often be assumed negligible in terms of the evolution of the out-of-bank floodwave. Furthermore, the types of data routinely collected during or after flood events do not resolve these three-dimensional flows, and thus there is little data with which to evaluate models of this behaviour. In addition, these 3D processes do not sufficiently affect the system to be necessary for adequate predictions of the information required from hydraulic models (e.g. Morris, 2000).

Flow interactions with micro-topography (e.g. Bradford and Sanders, 2002), vegetation (e.g. Cobby *et al.*, 2003) and structures (e.g. Haider *et al.*, 2003; Mignot *et al.*, 2006) on the floodplain may also be important, thereby complicating the modelling problem (Hunter, 2005). In particular, where these features actively influence the flood routing behaviour, in addition to their effect on storage, explicitly representing these effects is necessary adding further complexity to the modelling process. Furthermore, consideration of water exchange with the surrounding environment may be important for particular model applications (e.g. long river reaches, urban drainage systems). Integration of these additional features into the modelling framework may add a significant computational burden and may also be difficult to parameterise (Beven, 2002).

It is clear that one-, two- and three-dimensional processes exist during the extension and retreat of a floodwave along a river channel and over the floodplain. However, these spatially varied processes have considerably different magnitude effects on the overall description of floodplain inundation. Although 3D processes clearly exist in the near-channel zone, their effect on far-field inundation is negligible and, indeed a 3D model of reach scale flood dynamics would be computationally prohibitive. As a result, most work to date on natural and urban rivers has been concerned with 1D and 2D descriptions of inundation processes which are therefore discussed in the following section.

2.2.2 One-dimensional approaches

One-dimensional models of fluvial flows have been extensively applied in academic (e.g. Horritt and Bates, 2002) and industrial (e.g. HR Wallingford, 2004) applications for investigating flood behaviour at reach scales of tens to hundreds of kilometres. This class of hydraulic model has been shown to provide consistent approximations of bulk flood routing properties such as propagation and attenuation of the flood wave and backwater effects. As a result, these methods can rapidly evaluate variations in water level and discharge in the downstream direction (Hunter, 2005). The premise of 1D codes is the simplification of the full Navier-Stokes equations for fluid flow to assume only longitudinal variation in hydraulic conditions. Therefore, the continuity equation can be expressed as (Bates and Anderson, 2001):

$$\frac{\partial Q}{\partial x} + \frac{\partial A}{\partial t} = 0 \tag{2.1}$$

where Q is the discharge (m^3s^{-1}), A is the cross-sectional area (m^2), x is the distance between cross-sections (m) and t is the time. Similarly, the conservation of momentum can be considered between two cross-sections Δx apart and yields a first order partial differential which can be expressed in the conservative form as:

$$\frac{\partial Q}{\partial t} + \frac{\partial (Q^2/A)}{\partial x} + gA(\frac{\partial h}{\partial x} + S_f) = 0 \tag{2.2}$$

where h is the height of water (m), g is the gravitational acceleration (m^2s^{-1}) and S_f is the non-dimensional friction slope. Although Equations 2.1 and 2.2 have few exact analytical solutions, with appropriate boundary and initial condition specification these can be solved numerically to yield estimates of Q and h in both space and time.

The one-dimensional simplification of the Navier Stokes equations yields predictions of system state variables that are commensurate with point field measurements of river discharge. As such, these models provide good predictions of wave routing for in-bank flows where lateral and vertical velocity variations can be assumed negligible (Knight and Shiono, 1996). Consequently, these models form the basis of a number of standard hydraulic river modelling codes such as HEC-RAS and ISIS. The UK Environment Agency routinely collect channel bathymetric data at discrete cross-sections that are then directly incorporated into the 1D modelling platforms. Delineation of flood extents from 1D models requires an additional processing step as there is no information content between the prescribed cross-sections. Therefore, results are often coupled with high resolution topographic data to yield distributed flood depth information throughout the floodplain (Lane *et al.*, 2003; Schumann

et al., 2007b). However, there is considerable skill required in analysis of appropriate cross-section data (Samuels, 1990) and where floodplain flows are complex and unknown *a priori*, a two-dimensional approach is necessary to fully understand flood dynamics. In an attempt to tackle this problem, storage cells or reservoirs can be incorporated to represent the dynamics of flow on the floodplain. However, these rely heavily on good topographic data and detailed knowledge of the embankment spill sections. Furthermore, as cross-sections are generally spaced hundreds of meters apart, these storage cells calculate instantaneous floodwave propagation speeds between adjoining units. Therefore, in order to more accurately resolve floodplain dynamics, two-dimensional treatment of the flows on the floodplain is required.

2.2.3 Two-dimensional codes

During extreme flood events, flows overtop river banks and the entire floodplain becomes inundated such that the dominant flow is in the downstream direction, and thus flows can still be considered as one-dimensional (Cunge *et al.*, 1980). However, in less extreme flood events, complex flow patterns emerge on the floodplain that necessitate a two-dimensional numerical treatment. In this case, the depth-averaged Navier Stokes equations, otherwise known as de St Venant equations, may be used to represent these flows. Neglecting wind stress and applying Mannings's roughness formulation to represent the net effects of turbulent diffusion, dispersion and surface roughness these may be expressed as:

$$\frac{\partial h}{\partial t} + \frac{\partial (uh)}{\partial x} + \frac{\partial (vh)}{\partial y} = 0 \tag{2.3}$$

$$\frac{\partial u}{\partial t} + u\frac{\partial u}{\partial x} + v\frac{\partial u}{\partial y} + g\frac{\partial h}{\partial x} + \frac{n^2 u\sqrt{u^2+v^2}}{h^{4/3}} = 0 \tag{2.4}$$

$$\frac{\partial v}{\partial t} + v\frac{\partial v}{\partial x} + u\frac{\partial v}{\partial y} + g\frac{\partial h}{\partial y} + \frac{n^2 v\sqrt{u^2+v^2}}{h^{4/3}} = 0 \tag{2.5}$$

These can then be solved using some appropriate numerical procedure (e.g. finite difference (FD, Falconer and Owens, 1987), finite element (FE, Hervouet *et al.*, 2000) or finite volume (FV, Horritt, 2004)) to obtain predictions of the water depth, h, and the two components of the depth-averaged velocity, u and v, in the x and y Cartesian directions (Hunter, 2005). As these equations assume no variation in vertical velocities, they are well suited to describe flow processes where the horizontal extent far exceeds the vertical depth. Two-dimensional models have the added advantage of being able to capture some aspects of the near channel flow structures, in addition to representing moving boundary effects in the far field.

Numerous formulations and simplification of these equations exist within the modelling community, some of which will be discussed in detail with reference to urban applications below (§2.4). However, broadly speaking, these can be divided into models that solve the full 2D de St Venant equations (Bradford and Sanders, 2002; Hervouet and Van Haren, 1996; Horritt, 2004) and diffusion wave based approximations of these equations (Bates and De Roo, 2000; Bradbrook *et al.*, 2004; Zanobetti *et al.*, 1970). The advent of LiDAR data has proliferated a large number of studies using 2D models as the topographic component of these models has become parameterised more completely. However, the broad scale adoption of these methods for practical applications has been largely limited by the lack of contiguous channel bathymetric data and the significant processing power required to run these models.

2.2.4 Coupled 1D-2D methods

In response to physical shortcomings of 1D models and the significant computing requirements of 2D models, a suite of models have been developed that couple a 1D representation of channel flows with a 2D floodplain description (Bates and De Roo, 2000; Bradbrook *et al.*, 2004). Coupled 1D-2D models were developed to reduce the high resolution required in 2D models to resolve channel flows and as such a 1D-2D model can be a combination of full 1D and full 2D or any simplification thereof. The 1D component of these models vary in complexity and thus simplified forms of Equations 2.1 and 2.2 can be employed:

$$S_f = S_0 - \frac{\partial h}{\partial x} - \frac{u}{g}\frac{\partial u}{\partial x} - \frac{1}{g}\frac{\partial u}{\partial t} \tag{2.6}$$

$kinematic \longrightarrow$

$diffusion \longrightarrow$

$dynamic \longrightarrow$

For example, TRENT (Villanueva and Wright, 2006) and TUFLOW (Syme, 1991) solve the full dynamic equation whereas LISFLOOD-FP (Bates and De Roo, 2000) employs the kinematic approximation. The kinematic approach ignores the latter terms such that the momentum equation is reduced to the friction slope, S_f, and is generally solved using empirical formulas for steady flow (i.e. Manning's, Chezy's) which yields the following (assuming Manning's equation):

$$S_0 - \frac{n^2 P^{4/3} Q^2}{A^{10/3}} = 0 \tag{2.7}$$

where P is the wetted perimeter (m) and n is Manning's friction coefficient. This formulation is implemented in the original LISFLOOD-FP code (Bates and De Roo, 2000) by assuming that channels are wide and shallow such that the wetted perimeter can be approximated by

the channel width (Hunter, 2005). However, the kinematic assumption may not be applicable where backwater effects dominate the flood signal (e.g. the Amazon floodplain) and therefore, it is necessary to use higher-order schemes, such as the diffusion approach (e.g. Bradbrook *et al.*, 2004). This method also has the added advantage of being able to incorporate complex changes in slope direction in the longitudinal channel direction. Regardless of approximation chosen, these equations are typically discretised using implicit finite differences to avoid numerical instabilities and permit the use of time steps comparable with the physical phenomena under consideration (Cunge *et al.*, 1980).

The representation of floodplain flows in two dimensions in this class of model is often approximated using a diffusion wave based model (Bradbrook *et al.*, 2004) or a storage cell approach using an analytical equation (e.g. Manning's equation) to represent the inter-cell fluxes (Hunter *et al.*, 2005b). These equations are generally implemented in a finite difference formulation on structured grids such that the depth of water in a given cell is a function of the change in volume in the cell defined as the fluxes into and out of cell during a given time step. Use of the higher-order diffusive wave approximation was found not to provide significant improvements to model results to justify the additional computational expense for a rural application (Horritt and Bates, 2001a). Therefore, fluxes in the x and y Cartesian directions can be considered independently and can be resolved using Manning's equation (Equation 2.8).

$$Q_x = \frac{h_{flow}^{5/3}}{n} \left(\frac{\Delta h}{\Delta x} \right)^{1/2} \Delta y \tag{2.8}$$

where h_{flow} is the depth of water available for flow between two neighbouring cells, specifically the elevation difference between the highest water level and ground level of neighbouring cells. Once more, regardless of numerical scheme chosen, these equations are generally solved using explicit schemes whereby floodplain flows are calculated first followed by the updating of water heights throughout the domain. However, such codes have well documented stability constraints (e.g. Cunge *et al.*, 1980; Hunter, 2005) that require flow limiter formulations to prevent numerical oscillations (Bates and De Roo, 2000). However, this has the added impact of calculating unrealistic wave propagation characteristics and displaying insensitivity to floodplain friction parameterisation (Hunter *et al.*, 2005b).

The interaction between the 1D and 2D solvers in these hybrid codes is effected by allowing fluxes from both domains to be included as either: (i) the source term; or (ii) as part of the volume updating procedure, respectively. In this manner, there is no exchange of

momentum between the channel and floodplain although a number of authors (Bradbrook *et al.*, 2004; Horritt and Bates, 2002; Yu and Lane, 2006a) have found this effect to be negligible in terms of far field inundation extents and depths.

Table 2.1 presents a summary of the available techniques and models classified in terms of model complexity and dimensionality, and their potential applications adapted from Pender (2006).

Method	Distinguishing features	Available software	Potential application
$0D$	No physical laws included in simulations	ArcGIS, DeltaMapper, etc.	Broad scale assessment of flood extents and flood depths
$1D$	Solution of the one-dimensional de St Venant equations	Infoworks RS, ISIS, MIKE11, HEC-RAS	Design scale modeling which can be of the order of 10s to 100s km depending on catchment size
$1D^+$	1D plus a flood storage cell approach to the simulation of floodpain flow	Infoworks RS, ISIS, MIKE11, HEC-RAS	Design scale modeling which can be of the order of 10s to 100s km depending on catchment size with the potential for broad scale application if used with sparse cross-section data
$2D^-$	2D model without the conservation of momentum for floodplain flow	LISFLOOD-FP, JFLOW	Broad scale modelling or urban inundation depending on cell dimensions
$2D$	Solution of the full two-dimensional shallow water wave equations	TUFLOW, MIKE 21, TELEMAC-2D	Design scale modelling of the order of 10s km and may have the potential for use in broad scale modelling if applied with very coarse grids
$2D^+$	2D model with a solution for vertical velocities using the continuity equation only	TELEMAC-3D	Predominantly coastal modelling applications where 3D velocity profiles are important and has been applied to reach scale river modelling problems in research projects
$3D$	Solution of the the three-dimensional Reynolds averaged Navier Stokes equations	CFX, FLUENT, PHOENIX	Local predictions of three-dimensional velocity fields in main channels and floodplains

Table 2.1: Summary of available methods for floodplain inundation modelling grouped by model complexity and dimensionality adapted from Pender (2006)

2.3 Challenges of urban complexity in hydraulic modelling

Flow processes in compound channels are, clearly, well understood and the equations, and their simplifications, governing these processes have been successfully incorporated into nu-

merical models. However, urban environments have significant effects on the nature of these flow processes in open channels and on floodplains. In particular, urbanisation distinctly changes the dynamics of flood flow processes. Furthermore, urban areas are characterised by distinct topographic and topological features that affect flooding processes and patterns. The effects of urbanisation on catchment hydrology and small-scale flood hydraulics are thus discussed in more detail to determine the appropriate numerical scheme to resolve floods in urban environments.

2.3.1 Effects of urbanisation on flood processes

Urban development typically involves the removal of trees, the replacement of soils and vegetation with impervious surfaces and the replacement of the natural drainage system with a network of storm sewers (Nelson *et al.*, 2009). The increase in impervious surfaces acts to reduce: (i) interception of rainfall by the canopy; and (ii) infiltration into the subsurface both of which increase the fraction of rainfall that becomes runoff. Overland flow velocities are substantially faster on smooth surfaces (e.g. concrete, asphalt) and runoff enters the channel system more quickly, whereupon the high velocities are maintained in a dense and efficient network of sewers (Richards, 1982) or urban rivers. Leopold (1973) and Smith *et al.* (2002) recognise the decreased lag time and increased hydrograph peak and total runoff volume for a given rainfall depth created by these effects. Carter (1961) considers the changes in runoff volume and lag time as independent and subsequently calculates a growth factor analogous to 2.5 times greater runoff volume for a completely urban area (i.e. 100% impermeable). Work by Epsey *et al.* (1969) and Brater and Sherril (1975) suggests an inverse 1:1 relationship between increasing runoff volume and lag time for regional analysis of unit hydrographs in the United States. In terms of flood frequency, a number of authors have shown a diminishing effect of urbanisation on flood peaks with increasing flood return periods (Hollis, 1975; Martens, 1968). Nonetheless, the complex relationship between percentage urbanised, percentage sewered, and drainage basin area and slope ultimately determine the changes to runoff properties during urbanisation.

A number of authors have observed channel enlargement and incision in response to urbanisation and the associated changes in the flow and sediment regimes of the catchment. Specifically, Leopold (1973) found the number of floods exceeding channel capacity increased significantly with increased urbanisation as a result of decreased channel cross-sectional area. An increase in sediment yield during urban development is also enhanced during the smaller,

more frequent flood events. As the flood regime becomes more *flashy*, channel enlargement may, therefore, tend towards bed incision rather than lateral bank erosion. However, channel enlargement varies significantly with channel, basin and flood frequency characteristics where enlargement is increased in regimes that adapt to more frequent, low return period events. Nelson *et al.* (2009) found that although there were significant increases in flood peaks due to urbanisation for the Dead Run catchment in Baltimore, the channel planform remained remarkably stable. It is clear that understanding changes to channel and floodplain dynamics in response to urbanisation is vital to appreciating flood causing mechanisms throughout an urbanising catchment. This impacts on any assessment of future flood risk as any modelling framework must be robust enough to incorporate the effect of such changes on both flood hazard and flood risk.

2.3.2 Urban topology and topography

Mason *et al.* (2007) note that high spatial frequencies of elevation change are characteristic of urban topography. From a hydraulic viewpoint, these have a significant effect on floodwave propagation and storage (Mignot *et al.*, 2006; Yu and Lane, 2006a) and from a modelling standpoint, the varying shapes and length scales should determine the grid resolution of any model (Mark *et al.*, 2004). In fact, the surface drainage network may be approximated as a series of channels (i.e. roads) connected at storage areas (i.e. road junctions, squares) and thus modelled as such (Braschi *et al.*, 1989). However, this assumes that the flow paths are known *a priori* and that open areas act purely as storage rather than as a mode of conveyance. Furthermore, urban floods are often *flashy* and as such are high velocity, shallow flows that can be subject to hydraulic jumps, shocks and reflections (Hunter *et al.*, 2008) which will dramatically influence the complexity of the numerical scheme required. Mark *et al.* (2004) note that the combination of high frequency topographic features and the complex topology in urban areas necessitates at least a 2D treatment of flows at high resolution. This high resolution requirement exposes a dichotomy in urban flood risk assessment whereby computationally efficient city-wide predictions are required with local scale detail for damage and risk evaluation. Therefore, any numerical modelling scheme must be able to reproduce fine scale detail over large areas efficiently for the end-user and decision maker.

In the rural case, flow paths are determined purely by the topographic features of the floodplain. However, in the urban case, flood flows are determined by the alignment of storm sewers, culverts and the road network. The incorporation of an artificial drainage

system in the form of sewers means that urban flooding may occur as a result of sewer surcharge and/or river overbank flows. A number of authors (Mark *et al.*, 2004; Schmitt *et al.*, 2004) have noted the importance of the complex relationship between surface and subsurface drainage systems for conveying water through the urban network. Parameterising subsurface flows requires detailed knowledge of the sewer network, flow conditions prior to the event and individual connections between the surface and the subsurface. In addition, the grid resolution of any numerical models must be such that manholes and drains can be incorporated directly into the description of local topography (<1 m). An increase in parameter dimensionality coupled with the high resolution requirements of any such scheme make the problem computationally unattractive and the magnitude of local information required limits this approach to small-scale studies (e.g. Schmitt *et al.* (2004); Xiao *et al.* (2009)). However, in certain applications the contributing influence of the sewer system to flooding may not be ignored as this source can lead to significant overland flow and damage. Specifically, a large proportion of the insured losses from the summer 2007 floods in the UK were a direct result of sewer surcharge. Nonetheless, the proportion of flows from these systems may be negligible compared to overall flood volume (e.g. in the Carlisle 2005 event) and will be modelled implicitly in any 2D model of surface flow once water has surcharged to the surface (although the magnitude of this surcharge is difficult to quantify). Therefore, when addressing the issue of urban flooding, it is necessary to determine the origin of the dominant floodwaters in order to determine suitable hydraulic modelling frameworks with which to assess current and future flood risk.

2.4 Approaches to urban flood modelling

The review of flood modelling methods has highlighted the significant development of techniques designed for the simulation of flooding over reach-scale rural areas (~10-60 km). However, the shift to encompass risk and hazard modelling has brought urban environments to the fore and the intricacies thereof necessitate different approaches to flood inundation modelling. A number of authors have adapted current modelling tools while others have developed entirely new techniques to address this problem. The section that follows details the mounting body of work concerning calibration and validation of urban flood models, benchmarking models of varying complexity, compensating for urban topographic effects through friction parameterisation and the development of sub-grid scale methods for representing the

complex topography of urban environments.

2.4.1 Applied calibration and validation

Spatially distributed calibration and validation data, in the form of inundation extent imagery or water level records, has been found to offer considerable potential for constraining uncertainties in calibration parameters for flood inundation models (Aronica *et al.*, 2002; Hunter *et al.*, 2005a). To date, most work in this area has been limited to rural areas, although recent work has attempted to apply this form of model evaluation to urban areas (McMillan and Brasington, 2007; Neal *et al.*, 2009a; Yu and Lane, 2006a). Synchronising inundation extent imagery, often derived from satellite imagery, with the flood peak is essential in urban areas as these tend only to inundate during very high flows or due to some unexpected failure in the drainage network (Neal *et al.*, 2009a). Yu and Lane (2006a) calibrate the diffusion-based 1D-2D model JFLOW using aerial photography on the falling limb of the hydrograph for a flood event in November 2005 on the River Ouse in Yorkshire, UK. The authors explore the grid resolution sensitivity of inundation extent predictions and results from this work suggest that uniform values of Manning's n cannot be used to resolve the correct temporal variations in floodwave propagation for coarse resolution models. These results question both the reliability of n as a calibration parameter particularly without some form of spatial distribution and the validity of a field-estimated friction value for use in 2D diffusion wave type models for urban applications. However, Horritt (2000a) notes that due to computational cost, friction parameterisation is generally limited to calibration of a uniform friction factor or at best a crude representation of the spatially heterogeneous friction surface. Satellite inundation extent imagery may be further complicated in urban areas as these have generally been derived from Synthetic Aperture Radar (SAR) images which are difficult to process in these areas due to a large amount of backscatter and indeed, the resolution may be less than the gaps between buildings (Neal *et al.*, 2009a).

Field measurement of water levels, whether in the channel or on the floodplain, have been shown to provide considerable information regarding the spatial variation in flood response in rural applications (e.g. Tayefi *et al.*, 2007; Werner *et al.*, 2005a) and more recently for urban applications (e.g. McMillan and Brasington, 2007; Mignot *et al.*, 2006; Neal *et al.*, 2009a). The quality of such data is rather variable and thus different model evaluation strategies are required. Butler *et al.* (2009) acquired a binary measure relating to flooded/not flooded properties from a survey following a flood in Hull, UK in June 2007. Results from this

analysis suggest a diffusion-wave based model (FLOWROUTE^{TM}) can adequately describe pluvial flood propagation and does not portray a bias towards under- or over-prediction. McMillan and Brasington (2007) describe a more complete data set whereby a survey of riparian residents yielded maximum water depth information at discrete building locations in the floodplain for a flood on the River Granta in Cambridgeshire, UK. In this study, a different diffusion-based flood model employing a flow limiter was shown to largely under-predict flood depths. Calibration of channel friction parameters yielded different optimum parameter sets depending on the observational data used, a finding similar to previous studies in rural areas for a diffusion-wave based model with a flow limiter (Horritt and Bates, 2001a).

A further level of detail is obtained by carrying out a detailed post-event survey of water marks and wrack lines (Mignot *et al.*, 2006; Neal *et al.*, 2009a). The latter report a data set of 263 point measurements of maximum water surface and extent elevations collected following a 1-in-150 year flood event in Carlisle, UK in January 2005. In this study, a 25 m grid resolution LISFLOOD-FP storage cell model is calibrated to a root mean squared error (RMSE) of 0.32 m between measured and simulated maximum water levels. Mignot *et al.* (2006) calibrate Manning's n for a flood in Nîmes, France in 1988 by minimising the difference between modelled and observed maximum water level over the whole domain. This calibration procedure resulted in a peak water elevation $\sim$0.13 m lower than measured flood marks with a standard deviation of $\sim$0.53 m. This was an acceptable technique as in this case, the friction coefficient alters the mean maximum water level without affecting the main features of the flow or local water surfaces. It is clear from both these applications that model calibration of friction parameters was a useful method for parameterising the frictional resistance of buildings. Furthermore, Mignot *et al.* (2006) provide the first known independent validation of an urban flood model by assessing the performance of the calibrated model on a less extreme event from September 2002. In this case, the model appeared to show a lower standard deviation ($\sim$0.20 m) but significant over-prediction of the mean peak water depth ($\sim$ +0.3 m). As urban floods become more prevalent (Lane, 2008), the need for detailed data sets for model evaluation of urban flooding scenarios will become increasingly necessary.

2.4.2 Model benchmarking procedures

As urban flood risk assessment is in its infancy, only a few studies have benchmarked models of varying complexity for modelling inundation processes in urban areas (HR Walling-

ford, 2004; Hunter *et al.*, 2008). In the former, the ISIS, LISFLOOD-FP, TUFLOW and TELEMAC-2D models were evaluated comparatively for flood inundation in the Greenwich embayment of the River Thames, UK by defence overtopping/failure scenarios. The models were evaluated by comparing (i) the depth time series at seven discrete locations within the embayment to allow comparison of wave propagation speed and flow depth, (ii) discharge time series at point(s) of defence failure to determine both the volume of water entering the domain and the ability to model breach flows, and (iii) flood extent maps. Predictions from ISIS (a 1D model), TUFLOW (a full-2D depth averaged finite difference code) and TELEMAC-2D (a full-2D depth averaged finite element model) were considered satisfactory for in each case. However, LISFLOOD-FP (a quasi-2D model solving Manning's equation for floodplain flows), was shown to markedly underpredict the both spatially distributed (i.e. inundation extent, flood depths) and bulk (i.e. wave volume, travel time) flood characteristics. Specifically, these shortcomings may be summarised as: (i) systemic underprediction of flood extents and water depths; (ii) wave propagation speeds highly dependent on grid resolution (Δx) and time step (Δt); and (iii) the appearance of numerical instabilities and oscillations in cells of deep water. It should be noted, however, that the version of LISFLOOD-FP employed in this study employed a flow limiter to dampen oscillations in areas of sharp free surface slopes (i.e. around the breach) which caused the unrealistic propagations observed in this study. Despite previous findings (e.g. Horritt and Bates (2001a)), calibration of Manning's n was not undertaken to resolve differences between the different models. However, unreported investigations by the authors conceded that the model was capable of accurately reproducing either the bulk wave dynamics or inundation extent if specifically calibrated to do so (Hunter, 2005).

As a result of this and other studies, Hunter *et al.* (2005b) developed an unconditionally stable version of LISFLOOD-FP that adapts the time step based on a CFL condition for advective flows. This model was shown to overcome the observed numerical oscillations in areas of deep water and produce realistic sensitivity to floodplain friction variations. Following these developments, Hunter *et al.* (2008) benchmarked a number of models of varying complexity for a pluvial-induced flood event in July 2002 in Greenfield, Glasgow. This work found that floods in urban areas are characterised by numerous transitions to supercritical flows and numerical shocks and reflections, the effect of which are localised and do not appear to affect overall wave propagation (Hunter *et al.*, 2008). Furthermore, the diffusion based models (LISFLOOD-FP and JFLOW) were shown to under-predict maximum

flood extents and as such, at this site, the inclusion of inertial effects appear to be important to understand inundation extent. However, this is likely to be a result of the steep slopes and alignment of roads in the dominant flow direction. What is clear, however, is that correct prediction of local water elevations within urban areas is broadly achievable with a wide range of numerical schemes and that uncertainties in both friction parameterisation and flow condition specifications are likely to dominate results in practical applications.

2.4.3 Physical roughness value parameterisation

The most common approaches to representing frictional resistance on rigid structures are: (1) to calibrate the friction parameter in the computational model to observed flow or water level data (see §2.4.1); or (2) to assign friction values based on scale models of the given region. The latter is a labour intensive and costly exercise but has been attempted by a few authors (e.g. Haider *et al.*, 2003; Soares-Frazão and Zech, 2008; Zanichelli *et al.*, 2004). Haider *et al.* (2003) compare a 2D explicit finite volume model (Rubar 20) with a 1:100 scale model of the Toce River Valley. There were slight differences between the setup of the scale and computational model as individual buildings from the scale model were grouped into units of 10 for the numerical simulation. The Manning's n value was set as 0.0162 as recommended by the Italian Agency for Electricity and Dams (ENEL) although no physical basis was provided for this value. Generally, the inclusion of structures in the model lead to higher water levels at the observation points which was largely due to the reduction of flow area and subsequent constriction of flow. Moreover, no physical basis was provided for the Manning's n value used although an increased Manning's n value was tested to investigate its success at replicating the effect of buildings but this was found to be inappropriate. Similarly, Soares-Frazão and Zech (2008) compares a full 2D, depth averages model to a scale model of a dam break scenario through an idealised urban area and set the Manning's n value to 0.01 based on steady-flow experiments. However, the blocks used to represent the buildings were wooden and thus will have different fiction characteristics to concrete or brick houses.

Zanichelli *et al.* (2004) construct a 1:100 scale model of the Po River Delta in Italy to examine the sensitivity of numerical models to friction parameterisation. The authors note that empirical values of roughness (e.g. Chow, 1959) were generally developed for 1D models to account for surface roughness, water depth, vegetation effects and channel sinuosity. However, in full 2D, depth averaged models, these factors are represented differently and thus will lead to changes in the empirical model required to represent friction effects. This

change is probably more relevant to the main channel than in the floodplain where velocities are moderate and roughness values depends largely on vegetation height, distribution and type. In urban areas, friction is largely a result of building height and distribution, and road surfaces so this premise may still hold. As a result, the authors develop a relationship between Manning's n and the physical scale model whereby n scales like $\lambda^{1/6}$ where λ is the scale of the physical model.

In addition to scale models, methods for determining a friction value based on vegetation features have been investigated for rural environments (e.g. Fathi-Maghadam and Kouwen, 1997; Mason *et al.*, 2003) although few studies have considered urban applications. Hervouet *et al.* (2000) devise an extension of the de St. Venant Equations in order to simulate the dynamic effects of obstacles through incorporation of an appropriate friction factor based on the drag force exerted by cylindrical obstacles. This is incorporated into the momentum equation as a stress term such that the effect of cylindrical structures is:

$$F_x = -\left(\frac{n}{A}\right)\left(\frac{D}{2}\right)C_D U^2 \tag{2.9}$$

where n is the number of structures in area, A, with diameter D and drag coefficient, C_D. Translation of this formula into a standard expression for friction such as the Chèzy Law or the Manning-Strickler Law would give a value dependent on water height which would be computationally demanding to update friction values at every time step. Consequently, Hervouet *et al.* (2000) add the force equation (2.9) directly into the momentum equation. Therefore, this requires *a priori* knowledge of the detailed structure density, diameter and drag coefficient, which is generally unavailable and of questionable quality, and thus limits the generality of the model. This also assumes that the structures are cylindrical which may be appropriate in a rural setting (i.e. trees) but may not be applicable in an urban setting where most structures are rectangular and anisotropy may play a significant role. The local resistance due to obstacles in this formulation can be changed into a friction resistance in terms of the drag coefficient, and structure density and diameter. Nonetheless, Hervouet *et al.* (2000) test TELEMAC-2D using the friction formulation and note the lack of ability to reproduce the constriction effect exerted by these features. Empirical relationships do exist for cuboid and rectangular shapes in immersed flows that relate planform area to a drag coefficient, C_D (Munson *et al.*, 2005). However, there have not been any studies to date that have assessed these relationships for emergent bodies and as such, these have not been incorporated into numerical models for water flow around these features.

Tarrant *et al.* (2005) use MasterMap® land coverage to determine spatially distributed Manning's n values for the Greenwich Embayment on the River Thames. The sensitivity of TUFLOW, a full 2D hydraulic model, to friction values is investigated by increasing the originally high value of building roughess from a Manning's n of 0.5 to 1.0. However, the final flood extent appears relatively insensitive to changes in friction. The same authors further note that due to the lack of sensitivity of flood models to friction values in urban areas, it is likely that flood evolution and extent is more dependent on the volume of water entering the floodplain and the small-scale topographic variability than on surface roughness. However, the insensitivity may well be a function of the high roughness values used in the original simulation and thus is not representative of the sensitivity of flood models to friction parameterisation in urban areas.

Lane (2005) notes that the roughness and frictional resistance of the surface over which a fluid flows is one of the fundamental parameters of geomorphological and hydrological research and yet is generally implemented as a calibration parameter in most numerical modelling exercises. Furthermore, Yu and Lane (2006a) note that friction should be set in relation to the complexity of the model used for any given application. Indeed, empirical friction values should only be applied in numerical models if the basis for derivation of the empirical value is the same as the basis for the equations in the numerical model. For example, empirical values of Manning's n should strictly only be used in situations comparable to those for which they were originally devised (i.e. steady flow in natural rivers). Beven (2002) further suggests that friction values will be highly scale dependent suggesting values devised from physical scale models will bear little relation to values yielding optimal model performance. In addition, there are likely to be multiple parameter sets that will yield similar model performance given uncertainties throughout the modelling framework (Beven, 2006). As such, friction values should be considered a scale dependent calibration parameter that is a component of topography to be parameterised, rather than a component that has any physical meaning itself (Lane, 2005).

2.4.4 Porosity and sub-grid scale techniques

Recent advances in processing speed and data collection have clearly facilitated a number of studies into the representation of urban areas within hydraulic models although the increase in computer power, and the adaptation of numerical models, has not been such that these models can explicitly represent urban structure over large areas. Consequently, a suite of

sub-grid scale algorithms have been developed to incorporate the effect of fine scale urban media on coarse scale flood routing models with varying success and complexity. Molinaro *et al.* (1994) note that it is possible to approach the flooding of urban areas in two distinct manners. The first approach is to implement a channel network type model and the second approach is to retain a two-dimensional representation and realise that water only flows through part of the urban domain as a result of urban structures. The first type of model is employed by Braschi *et al.* (1989) as an initial attempt at modelling flood wave propagation and inundation extent for urban areas by implementing the concept of storage capacity of an urban media. The model domain is discretised into a set of discrete nodal points, acting as reservoirs, at squares or road crossings connected by a series of channels in which the flow direction and nature (sub- and/or super-critical) may change rapidly and vary throughout the channel. The model calculates the water stored at a given node as the sum of the inflow to the node, outflow from the node and any external inputs (e.g. rainfall). The storage of water is concentrated at discrete nodes in the domain determined by squares, gardens or road intersections. The porosity of a given node in the computational domain is determined by the ratio of the unobstructed area to the total plan area and is defined as time invariant. Therefoe, the reduction in node storage volume as a result of urban media is represented. However, Braschi *et al.* (1991) make the observation that the storage area will increase with increasing water level and so one could implement a time varying porosity value. The time-invariant approach was tested on the 1966 flooding in Florence and validated against flood extent derived from photographs and flood depth maxima observed on urban structures. However, this study still included the calibration of both the friction and porosity parameters to determine a best-fit to the observed data. The actual value of urban porosity for this study was found to be insignificant for determining an optimum model calibration and not physically based (Braschi *et al.*, 1991).

Molinaro *et al.* (1994) implement a similar porosity concept in a finite volume two dimensional flood inundation model (FLOOD2D) such that for a particular grid cell, the total area that can be flooded is reduced by the area obstructed by buildings (Figure 2.1). The model solves a simplified form of de St. Venant Equations where the convective inertial terms are neglected which is suitable for flood modelling of gradually varied flow as spatial variations in kinetic energy are generally negligible. An important characteristic of FLOOD2D is that the computational grid adapts to the propagation of the flood (i.e. during flood expansion, a set of grid cells is automatically added to the domain after each time step) (Molinaro *et al.*,

1994). In order to implement the concept of urban porosity within FLOOD2D, the authors define an effective area, A_e, that can store water for a given grid cell.

$$A_e = n_l \Delta x \Delta y + n_l \Delta y \left(1 - n_l\right) \Delta x \tag{2.10}$$

where n_l is the ratio between the 'free length' and the total length of each cell side and Δx and Δy are the cell side lengths. Subsequently, it is possible to define a ratio, n_A, between the effective area and the total area as a function of n_l:

$$n_A = \frac{A_e}{\Delta x \Delta y} = n_l + n_l \left(1 - n_l\right) = n_l \left(2 - n_l\right) \tag{2.11}$$

Molinaro *et al.* (1994) define the two new parameters, n_l and n_A, as the *linear porosity* and the *aerial porosity*, respectively, of a given built up area. Consequently, the continuity equation is modified to include the effective area of a cell and 'free length' of each cell side and can be expressed as follows:

$$n_l \left(2 - n_l\right) \frac{\Delta h}{\Delta t} + \frac{\tilde{n}_{l,i+1} q_{x,i+1} - \tilde{n}_{l,i} q_{x,i}}{\Delta x_i} + \frac{\tilde{n}_{l,j+1} q_{y,j+1} - \tilde{n}_{l,j} q_{y,j}}{\Delta y_i} = 0 \tag{2.12}$$

where

$$\tilde{n}_{l,i} = min\left(n_{l,i}; n_{l,i+1}\right) \quad \tilde{n}_{l,j} = min\left(n_{l,j}; n_{l,j+1}\right) \tag{2.13}$$

The same authors note that this makes the assumption that the water storage in buildings is relatively insignificant. This is justified as the temporal variations in this storage will be small with respect to the temporal variations in water exchange between cells. Notably this formulation of porosity takes into account the scaling of the cell volume accessible to floodwaters as well as recognising that the porosity at cell boundaries is the controlling factor

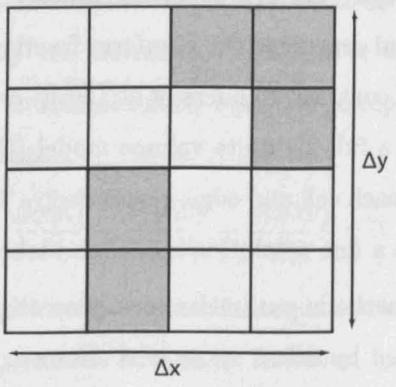

Figure 2.1: Schematic of a computational grid cell with sub-grid scale blockages where buildings are drawn in black. From Molinaro *et al.* (1994).

for the fluxes between cells. However, this method does not incorporate any topographic information of the sub-grid scale units used to determine the areal and linear porosity of a given cell.

Moramarco *et al.* (2005) attempt to use FLOOD2D to simulate flooding of the Upper Tiber basin in Italy with and without the incorporation of a porosity value. A 10 m resolution grid was derived from a detailed cartographic map and individual topographic surveys and two Manning's roughness coefficients were determined for the channel and the floodplain separately. However, using the inflow conditions computed by the hydrologic model, results from FLOOD2D showed that the water level did not exceed the capacity of the river channel and thus, would never have caused the observed flood extent. Consequently, having inspected the local topography and urban layout, it is clear that the flooding was likely caused by a progressive blocking of a significantly placed bridge. Therefore, Moramarco *et al.* (2005) assume a progressive obstruction of P. Nuovo Bridge up to 50% and apply the urban porosity approximation. No detail is given as to the spatial distribution or time evolution of the porosity values but the model does appear to be in good agreement with the observed water depths around the bridge and in the main town square.

Guinot and Soares-Frazão (2006) developed a *storage porosity* formulation based on the unobstructed to total area ratio for the flux and source terms of a full-2D depth averaged model using a modified Riemann solver for unstructured grids. The model was shown to perform well in analytical test cases with uniform porosity distributions. Soares-Frazão *et al.* (2008) extend this model to incorporate a *conveyance porosity* as the fraction of cross-sectional area available for flow (similar to the *linear porosity* of Molinaro *et al.* (1994)). The authors apply this model to a large scale experiment aimed at simulating a dam break on the Toce River Valley in Italy. In this case, the porosity values are assumed uniform throughout the urban area and represent the planform fraction of the urban area available for water storage and flow. In contrast, Sanders *et al.* (2008) develop similar storage (ϕ) and conveyance (ψ) porosities for a full-2D finite volume model (BreZo (Bradford and Sanders, 2002)) but calculate both for each cell and edge, respectively. This new formulation provides good results in comparison to a fine resolution model and laboratory experiments.

The porosity treatment methods outlined above generally incorporate a scaling factor based on the area encompassed by urban structures. However, this only accounts for large scale features that obstruct flow throughout all feasible flow depths. The ground height variation in an urban area can be substantial however and it is necessary to consider that

the small scale vertical variations in topography may largely affect the overall flow direction and water storage. Therefore, the need to incorporate sub-grid scale topography is apparent. Defina *et al.* (1994) note that the ground surface is often represented as a piecewise constant or a piecewise linearly varying surface which neglects surface unevenness within a computational cell in the domain. However, when dealing with small water depths, the surface irregularities and height variations play a large role in defining the extent of a flood event. Consequently, an adaptation of the shallow water equations are developed to incorporate this surface unevenness. A new parameter, η, is introduced to represent the wetted percentage of a cell as a function of the water depth, h. Therefore, the new continuity equation is written as:

$$\eta \frac{\partial h}{\partial t} + \frac{\partial hu}{\partial x} + \frac{\partial hv}{\partial y} = w \tag{2.14}$$

where η is the wetted percentage of a cell, h is the water depth, u and v are directional velocity components and w is a sink/source term. The parameter η is defined by examining the relationship between the mean water depth and the top bed elevation above the mean for a number of real topographical profiles and can be summarised as follows:

$$\eta = \begin{cases} e^{-\alpha\left(1-\frac{Y_a}{Y_{lim}}\right)^2} & \text{if } Y_a < Y_{lim} \\ 1 & \text{if } Y_a > Y_{lim} \end{cases} \tag{2.15}$$

where Y_a is the difference between water depth and mean bottom elevation, Y_{lim} is the difference between highest ground elevation and mean bottom elevation and α is 0.7. Bates and Hervouet (1999) adapted these curves by parameterising the relationship between η and Y_a for each computational element using LiDAR data of a tidal mud flat in the UK. However, it is unlikely that the topographical profile in an urban area will fit this standard form and a new relationship may have to be determined for each urban area under investigation. Hervouet *et al.* (2000) modify the technique of Defina *et al.* (1994) to enable temporal variations in local porosity, η, in the continuity equation to represent constriction effects and the volume occupied by obstacles.

$$\frac{\partial(\eta h)}{\partial t} + \frac{\partial(\eta hu)}{\partial x} + \frac{\partial(\eta hv)}{\partial y} = 0 \tag{2.16}$$

Incorporating this same concept into the momentum equation is a necessary step as the porosity is a limiting factor in the available flow area. However, using the non conservative momentum equation and simplifying the diffusion term, the momentum equation is unchanged by the inclusion of a porosity concept. Using this concept in tandem with TELEMAC-2D for

dam break flood wave cases near urban areas, Hervouet *et al.* (2000) found that the adaptation simulated the constriction effect of obstacles successfully but failed to incorporate the head-losses caused by obstacles or the friction losses on vertical structures.

Yu and Lane (2006b) derive a theoretical sub-grid scale topographic treatment in order to enable a simple raster based inundation model to adequately represent small scale features and yet still provide the speed of simulation associated with this class of model. To adequately present this approach numerically, it is necessary to discuss the cell storage volume and cell flux effects separately. In terms of the sub-grid scale representation of the storage effects, it is necessary to consider a grid cell divided into sub-grid cells as in Figure 2.2. Standard approximations of topography in coarse grid models assume bed elevation of the cell to be the average of the sub-grid scale cell elevations and storage volume is calculated with reference to this datum. Consequently, this is likely to under-estimate the true volume of storage for $min(E_{i,j}) < H < max(E_{i,j})$ and this will lead to over-estimation of water levels and may contribute to the relatively fast diffusion of water over the floodplain in this class of model (Yu and Lane, 2006b). Therefore, Yu and Lane (2006b) develop a DEM pre-processing step to accurately represent the actual storage of water in any given cell based on the sub-grid scale topography:

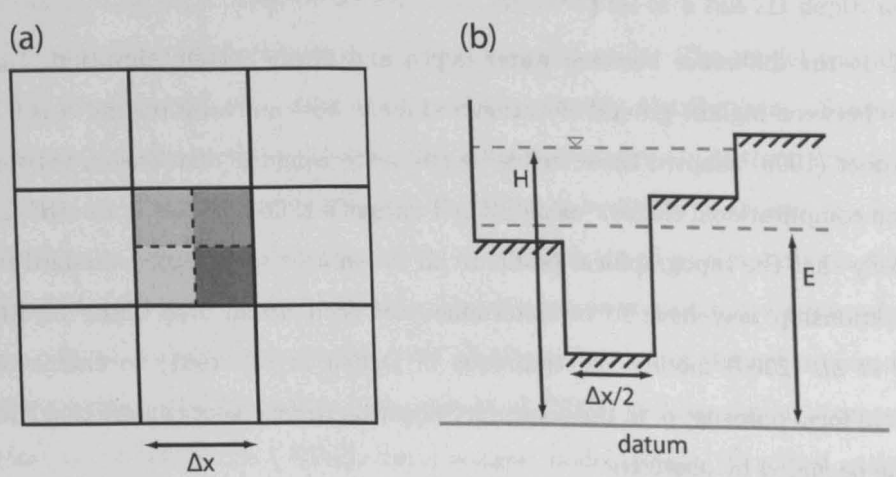

Figure 2.2: Schematic view of hypothetical sub-grid topography. *a*) shows the model with its sub-grid cells; $e1$, $e2$, $e3$ and $e4$ are sub-grid cell bed elevations; w is the resolution of the model grid. *b*) shows the four elevations unwrapped onto a 1D plain; H is the sub-grid water surface elevation; E is the bed elevation of the model cell which is equal to the average of its sub-grid cell elevations. From Yu and Lane (2006b).

$$V_{ij} = \frac{w^2}{N_{ij}} \left(N_{ij}^2 H_{ij} - \sum_{k=1}^{N_{ij}^k} e_k \right) \tag{2.17}$$

where V_{ij} is the water volume, H_{ij} is the water surface elevation, e_k is the bed of elevation of the sub-grid cell k, w is the width of the grid cell containing N_{ij} sub-grid cells and N_{ij}^k is the number of wet sub-grid cells. This formulation reduces the water volume and water surface elevation errors associated with the rate of wetting and drying process both within individual cells and across the floodplain as a whole (i.e. rapid diffusion across the floodplain at coarse grid scales) (Yu and Lane, 2006b). The concept is implemented by solving the governing equations at a given model resolution but calculating the water volume and extent based on the sub-grid model resolution. However, it should be noted that the model developed in Yu and Lane (2006a) does not incorporate a rigorous time stepping stability criterion shown to be a significant requirement for physically realistic results from such codes. Indeed, the authors use grid cell effective velocities in a standard CFL criterion for shallow water waves (see Eqn. 3.6), which is not strict enough, or numerically based, for this model formulation. In addition, as this constraint yields very small time steps, the authors implement a numerical fix based on the maximum CFL. Hunter *et al.* (2005b) showed considerable numerical oscillations and unrealistic wave propagation in diffusion wave based models without strict time stepping control. McMillan and Brasington (2007) adopt a similar approach to Yu and Lane (2006b) as a pre-processing step by calculating a porosity value as the ratio of unblocked area to total plan area at a set of discrete height increments (i.e. at a slice or plane through a porous medium (Sanders *et al.*, 2008)) for each cell. A relationship between water height and storage volume is then derived at those same increments with linear interpolation between them. This method assumes that porosity variation is a linear function but as topography is described in a discrete step-wise manner, the porosity function will also be a step-wise function. Furthermore, the authors calculate porosity values in vertical slices up to 12 m above the base DTM with few increments between 0 and 1 m depth, the range in which most urban flood depths appear to occur.

Molinaro *et al.* (1994) noted the importance of scaling fluxes between cells based on the 'free length' of adjoining cell boundaries which should also take into account the effect of small scale topographic changes. Yu and Lane (2006b) implement this concept as a set of rules that define whether adjacent sub-grid scale cells are hydraulically connected based on the sub-grid scale topography and water surface elevations. Given l sub-grid scale cells along a given cell face, there will be $l+1$ possible values of porosity for the cell depending on the number of sub-grid cells contributing to the flux (Yu and Lane, 2006b). Therefore, the porosity value is expressed as a percentage of the number of sub-grid cells along a common

face. For example, if there are 4 sub-grid cells, the possible values of porosity for any given cell are 0, 0.25, 050, 0.75, 1.0. The porosity values, defined as a DEM pre-processing to retain computational efficiency, are used to scale the flux explicitly. However, as Manning's equation determines the flux as a non-linear function of the water depth, it is necessary to ensure that the correct water depth is used in the evaluation of the flux (Yu and Lane, 2006b). Consequently, the effective depth for the flux from any give cell is:

$$d_e = \sqrt[3/5]{\frac{\sum_{i=1}^{n} d_i^{5/3}}{n}} \tag{2.18}$$

where n is the number of sub-grid cells that are wet along the outflow side of the cell and d_i is the effective water depth in the individual sub-grid cell contributing to the outflow. McMillan and Brasington (2007) also note the importance of sub-grid scale topography for controlling flow direction. Consequently, the porosity values are incorporated directly into their two methods for computing fluxes between neighbouring cells. Firstly, a relationship between depth and cross-sectional area at each cell boundary is derived and secondly, the inter- and intra-cellular porosities are explicitly included in the flow limiter equation (see McMillan and Brasington, 2007 for details).

Yu and Lane (2006b) incorporate this sub-grid scale topography algorithm into a simple cellular storage model detailed in Yu and Lane (2006a) and apply this model to the River Ouse in Yorkshire. Yu and Lane (2006a) note that this reach is suitable for such model testing because of the "availability of a one-dimensional hydraulic model of the main river flow, high quality LiDAR data for the floodplain surface, the presence of structural features on the floodplain characteristic of urban areas and remotely sensed data on inundation extent and water levels of a large flood event in November 2000." In order to adequately assess the new model formulation, it esd necessary to undertake a model validation and verification exercise whereby the model esd validated using the at-a-point in time data from ~300 hours in the November 2000 flood. The model was then verified using high resolution benchmark simulations at 4 m resolution. The model is set up using 4 m, 8 m, 16 m and 32 m resolution DEMs and uses the sub-grid treatment in a ratio of 2:1 so that the 8 m DEM uses the 4 m DEM to define the sub-grid scaling. The results confirm that the rate of diffusion across the floodplain is greatly reduced thus greatly impacting upon the timing of inundation. Further results suggest that the sub-grid scale treatment also reduces the maximum inundation area for all mesh resolutions at all time periods (Yu and Lane, 2006b). Regardless of the measure used to assess model accuracy, it is evident that the sub-grid

treatment improves the predictions compared to the original model configuration (without sub-grid treatment).

2.5 Research design

2.5.1 Identified research objectives

The preceding sections have documented the growing body of research concerning the representation of urban areas within different hydraulic modelling platforms. A clear dichotomy has presented itself where flood risk assessment is required over *wide areas* of the urban landscape (i.e. whole cities) but *fine scale* local detail is necessary to assess the hazard and risk to individual properties for planning and insurance needs. This requirement comes at a high computational cost, unlikely to be resolved with computing power alone, and therefore methods must be developed to optimise the performance of coarse resolution models. The aim of this thesis is therefore to **'develop computationally efficient methods for fine scale, wide area models of urban flooding and to undertake the rigorous testing thereof within a consistent modelling framework'**.

Specifically, this literature review has highlighted a number of areas within this broad focus that require significant investigation and clarification. Firstly, although there has been a proliferation of studies on urban floods, there have been few studies that consider the features of urban areas modulating floodwave propagation. Indeed, most studies have arbitrarily chosen resolution based on trade-offs between computation time and available data, and a degree of modeller skill. To date, although studies have analysed the effect of grid and topographic resolution on the ability of hydraulic models to adequately simulate floodwave propagation in rural areas, issues of scale in urban areas have thus far been left largely unaddressed. Furthermore, studies of urban floods have not dealt explicitly with the quality of representation of buildings, in terms of fidelity to the known building footprint, and the few studies that have considered scale have dealt with the broad scale effect of model resolution. Therefore, it is clearly necessary to evaluate the effect of coarse resolution topographic descriptions of urban environments on predictions from hydraulic models.

Secondly, although a number of numerical porosity techniques have been developed for urban flood models, the detailed formulations and their complexity, in terms of topographic representation, vary significantly. In addition, the apparent performance of these porosity methods may be masked considerably by the differences in model complexity, and indeed, in

the specific implementation of that complexity (i.e. FV vs. FE, implicit vs. explicit solvers, diffusion wave vs. full 2D de St Venant). Importantly, the use of porosity techniques in diffusion wave type models has largely been conducted in models that employ variations of flow limiters which have been shown to dramatically alter floodwave propagation characteristics (Hunter *et al.*, 2005b). Judgement of the appropriate porosity method to use for a given applications is therefore hampered not only by the variation in porosity techniques, but also by the variability of models. Clearly, research is required to develop and evaluate porosity methods within a consistent modelling platform to objectively assess the relative performance of these methods. Consequently, it will be possible to provide guidance on the necessary level of complexity required for porosity techniques for particular test cases.

Thirdly, the discussion of both scale and porosity techniques has been largely limited to a single flood event at one particular site or to scale laboratory experiments. It is well known that there is considerable inter- and intra-urban environmental variability. Furthermore, events of varying magnitude develop and propagate in significantly different manners. Therefore, it is necessary to evaluate the performance of new methods within a number of different urban areas to provide further guidance for the appropriate technique for any given urban flood risk assessment.

These defined research objectives are summarised within the thesis outline that follows (§2.5.2).

2.5.2 Thesis outline

Chapter	Title	Description
1	Introduction	- Identification of the need for urban flood risk assessment
2	Numerical modelling of fluvial flow processes	- Identification of the effects of urbanisation on flooding - Review of current approaches to urban flood modelling - Identification of detailed research objectives
3	Requirements for hydraulic modelling of urban floods	- Selection and description of the LISFLOOD-FP model - Analysis of the data requirements for urban flood models - Identification of possible test cases
4	Evaluation of the scale dependence of urban environments	- Evaluation of coarse resolution representations of topography - Analysis of gridding techniques for DEMs - Effects of friction parameterisation in coarse resolution urban models - Chapter conclusions and recommendations regarding length scales and processing power for urban flood models
5	Sub-grid porosity approaches for finite difference models	- Development of simple sub-grid porosity approaches - Analysis of the position of these methods within current research programmes - Testing of new methods on verifiable test cases - Chapter conclusions regarding appropriate techniques for idealised case studies
6	Application of sub-grid scale porosity techniques	- Application of porosity approaches to Glasgow, Greenwich and Carlisle test sites - Evaluation of the suitability of the various methods - Conclusions and recommendations concerning urban characteristics and sub-grid scale techniques
7	Conclusions and discussion	- Conclusions regarding scale in urban areas - Limitations of research design and methodology - Considerations on future work

Table 2.2: Thesis outline

CHAPTER 3

Requirements for hydraulic modelling of urban floods

The previous chapters have highlighted the need for effective flood risk assessment tools and the opportunities for research within the context of improving current approaches to urban flood modelling have been identified. Specifically, the need for rigorous evaluation of current approaches within a strict modelling framework has been recognised. Furthermore, the development of techniques to characterise urban areas for urban flood modelling practitioners are required. Finally, porosity methods need to be developed and assessed within a consistent modelling approach to identify the necessary complexity for their practical application. A number of authors have highlighted the significant data requirements for successful flood modelling studies in rural areas (Bates, 2004; Hunter *et al.*, 2005a). However, it is important to consider how these data requirements change with a shift of emphasis to urban environments.

The data requirements can be considered as two distinct but inherently linked units; the data needed to build, and the data needed to evaluate, hydraulic flood models. The successful application of hydraulic models to flooding scenarios requires a substantial amount of data (e.g. floodplain topography, channel bathymetry and flow conditions) and observational data to constrain model predictions. Therefore, the chapter that follows will develop the detailed research design in order to meet the objectives outline in §2.5. Firstly, this chapter will seek to evaluate the available modelling platforms and select an appropriate model with which to conduct the research. Secondly, a discussion of the data available for investigating urban flood events will be presented and as such the specific data required for successful urban flood modelling projects will be highlighted. Finally, this chapter will act as a justification and explanation of the chosen model data sets for evaluating current techniques and developing new approaches to inundation modelling in urban areas.

3.1 Selection of modelling framework

3.1.1 Model code selection

Table 2.1 details the spectrum of model structures and complexity available for the numerical modelling of floodwave propagation. Specifically, Chapter 2 demonstrated that any model of urban flooding episodes must incorporate a two-dimensional representation of the flow structures in order to adequately resolve the detailed spatial variation without sacrificing computational cost. The chosen model should therefore be a 2D hydraulic model with a track record of successful application to urban flood events. In addition, there are a number of other requirements in order to undertake the identified research objectives. Firstly, the source code must be available in order to allow the development of the new numerical techniques and secondly, the model must have simple numerics in order to successfully implement these methods and provide practical advice for engineers. Referring back to Table 2.1, these requirements prohibit the use of a number of models and as such, limit the available modelling tools.

Building on early studies using a 2D diffusion wave approximation of floodplain flow (e.g. Han *et al.*, 1998; Hromadka and Yen, 1986; Xanthopoulos and Koutitas, 1976), a number of raster-based models have been developed to exploit high resolution topography data available through LiDAR. These models generally employ a 1D representation of channel flow linked to a 2D representation of floodplain flow, commonly involving a diffusion-wave treatment (Bradbrook *et al.*, 2004). These models minimise the degree of process representation and thus are extremely computationally efficient, especially on the coarse resolution grids for which they were originally designed. A number of authors (e.g. Bates and De Roo, 2000; Horritt and Bates, 2001a; Hunter *et al.*, 2005a; Werner, 2004; Wilson *et al.*, 2007) have shown the utility of this class of model for reproducing single patterns of observed flooding over large rural reaches. More recently, these models have been applied to urban applications with some success (e.g. Butler *et al.*, 2009; McMillan and Brasington, 2007; Yu and Lane, 2006a). Most notably, the diffusion wave approximation has been shown to perform well in relation to more complex numerical codes (Hunter *et al.*, 2008; Prestininzi, 2008) where local discontinuities and small scale oscillations have a small influence on the overall dynamics of the flood. As a result, models of this class have been developed for the insurance (Butler *et al.*, 2009; Lohmann *et al.*, 2009) and engineering (Bradbrook *et al.*, 2004) industries where practical methods for wide-area modelling are most necessary. Morris (2000) noted that in order to

adequately assess flood risk, water depths and velocities must be known throughout the model domain. However, as the diffusion wave approximation ignores the local acceleration and advective terms in the de St. Venant equations, instantaneous velocities from such models are not representative of the real-world quantity. As a result, such diffusion wave models can only be used in situations where the depth term dominates the velocity term in damage calculations. This is the case in most fluvial floods in the UK where flows are slowly propagating and gradually varying such that velocities are negligible compared to water depths.

Here, the LISFLOOD-FP code of Bates and De Roo (2000) and Hunter *et al.* (2005b) is selected as representative of this class of hydraulic model which fits the above requirements with which to explore its suitability for urban flood modelling. This model was initially jointly developed at University of Bristol, UK and EU Joint Research Centre, Italy (Bates and De Roo, 2000) and has since been developed by a number of researchers at University of Bristol (Hunter *et al.*, 2005b). As a result, the program source code is available for manipulation. Furthermore, the simplicity of process representation allows for more straight forward incorporation of additional numerical techniques. LISFLOOD-FP uses a 1D kinematic wave equation for channel flow linked to a 2D representation of floodplain flows calculated using an analytical flow equation (Manning's equation). Channel flow is computed as in Eqns 3.1 and 3.2 using an implicit finite difference scheme.

$$\frac{\partial Q}{\partial x} + \frac{\partial A}{\partial t} = q \tag{3.1}$$

$$S_0 - \frac{n^2 P^{4/3} Q^2}{A^{10/3}} = 0 \tag{3.2}$$

where Q is the volumetric flow rate (m^3s^{-1}), A is the cross sectional area of the flow (m^2), q is a source term from other sources (i.e. floodplain, tributaries), S_0 is the bed slope, n is Manning's friction coefficient, P is the channel wetted perimeter and h is the flow depth. The flow between floodplain elements is calculated using the continuity equation (Eqn. 3.3) and Manning's equation (Eqn. 3.4).

$$\frac{\partial h}{\partial t} = \frac{\partial Q}{\partial x^2} \tag{3.3}$$

where

$$Q_x = \frac{h_{flow}^{5/3}}{n} \left(\frac{\Delta h}{\Delta x} \right)^{1/2} \Delta y \tag{3.4}$$

where Q is the flow between floodplain cells (m^3s^{-1}), h is the height of water in any given cell (m), Δx and Δy are the grid spacings (m) and n is Manning's friction parameter.

The numerical scheme is setup using an explicit finite difference discretisation of the time derivative and a 5-point stencil finite difference discretisation of the space derivative:

$$\frac{^{t+\Delta t}h^{i,j} - {}^{t}h^{i,j}}{\Delta t} = \frac{{}^{t}Q_x^{i-1,j} - {}^{t}Q_x^{i,j} + {}^{t}Q_y^{i,j-1} - {}^{t}Q_y^{i,j}}{\Delta x \Delta y} \tag{3.5}$$

where Δt is the time step, the left exponent represents the time step and the right exponent represents the spatial index. However, explicit models are conditionally stable such that the time step must be small enough to satisfy the Courant-Freidrichs-Lewy condition and prevent numerical instabilities. The CFL condition for the de St Venant equations is expressed as follows:

$$\text{CFL} = \frac{\Delta t}{\Delta x}\max\left(\sqrt{u_{i,j}^2 + v_{i,j}^2} + \sqrt{gh_{i,j}}\right) \leq 1 \tag{3.6}$$

where u and v are velocities (m^2s^{-1}) and g is gravitational acceleration (m^2s^{-1}). In this case, the u and v terms are not applicable as the diffusion wave approximation removes the local velocity and inertial acceleration terms from the 2D shallow water equations and thus it is not possible to define a wave speed. Some model formulations (e.g. Bradbrook *et al.*, 2004; Yu and Lane, 2006a) approximate the velocity terms as Q/A although this provides a grid square effective instantaneous velocity rather than the physical property and thus wrongly estimates the stable time step. This often leads to a computational time step which is very small compared with the physical phenomena under consideration (Bradbrook *et al.*, 2004; Cunge *et al.*, 1980). In the original formulation of LISFLOOD-FP, small time steps relative to the grid resolution were selected which offered a partial solution although instabilities still remained when addressing flow over complex topography.

As a first solution to this problem and in order to prevent numerical instabilities with a prescribed time step, a floodplain flow limiter was invoked to prevent 'over' or 'undershoot' of the solution and is a function of flow depth (h_{flow}), grid cell size (Δx) and time step (Δt):

$$Q_x^{i,j} = \min\left(Q_x^{i,j}, \frac{\Delta x \Delta y (h^{i,j} - h^{i-1,j})}{4\Delta t}\right) \tag{3.7}$$

The limited flow value is determined by considering the change in depth of a cell, and ensuring it is not large enough to reverse the flow in or out of the cell at the next time step (Hunter, 2005). However, this flux limiter is largely responsible for the lack of sensitivity to floodplain friction often reported about this class of model as there is no friction term (Manning's n) in Eqn. 3.7. Nevertheless, anecdotal evidence from developers of other storage cell codes indicates that the majority include a similar condition (e.g. Bradbrook *et al.*, 2004; McMillan and Brasington, 2007.

In response to the lack of friction sensitivity, observed instabilities in areas of deep water and oscillations between neighbouring cells (explored in more detail in Cunge *et al.* (1980)), Hunter *et al.* (2005b) developed an optimally stable version of LISFLOOD-FP. An adaptive time-step algorithm based on considerations of model stability, analagous to a Courant-Freidrichs-Lewy condition for advective flows, was developed which effectively solved these problems. Here a von Neumann stability analysis for the explicit discrete diffusion equation yields a time step that is controlled by the grid spacing (Δx) and the depth available for flow (h_{flow}). Further stability analysis suggests that an optimal time step for this hydraulic model is given by:

$$\Delta t = \frac{\Delta x^2}{4} \min \left(\frac{2n}{h_{flow}^{5/3}} \left| \frac{\Delta h}{\Delta x} \right|^{1/2}, \frac{2n}{h_{flow}^{5/3}} \left| \frac{\Delta h}{\Delta y} \right|^{1/2} \right) \tag{3.8}$$

A more detailed discussion of the derivation of this adaptive time stepping algorithm is given in Hunter *et al.* (2005b). However, as the timestep (Δt) is a quadratic function of the grid size (Δx), this method comes at a high computational cost when applied on the high resolution grids necessary for urban simulations (1-10 m) (Hunter *et al.*, 2008) but still retains efficiency on coarse resolution grids (10-100 m) for which the code was originally developed.

As an explicit method is employed, negative depths may occur on the floodplain during the drying phase where more water may leave a cell than the cell actually contains (Bates and De Roo, 2000). As a result, a non-dimensional scaling coefficient is introduced such that mass is conserved and water depths return smoothly to zero as the cell dries.

$$w = \frac{V^{i,j}}{\Delta t(Q_x^{i-1,j} + Q_x^{i,j} + Q_y^{i,j-1} + Q_y^{i,j})} \tag{3.9}$$

The LISFLOOD-FP model is a representative example of diffusion-based storage cell type models that has been extensively evaluated for rural applications (e.g. Bradbrook *et al.*, 2004; Horritt and Bates, 2001a; Werner *et al.*, 2005b) and more recently, urban test cases (e.g. Hunter *et al.*, 2008; Neal *et al.*, 2009a). To meet the objectives outlined in §2.5, significant development of the current model code was required and is outlined below.

3.1.2 Program structure

LISFLOOD-FP was originally written in the PC-Raster programming language (Bates and De Roo, 2000) but was subsequently recoded into the `C` programming language. In order to develop the techniques for the research objectives, it was necessary to restructure the

model code to facilitate the addition of new modules specifically developed for urban applications. Furthermore, as this model is being applied to a number of different applications of significantly different scope (i.e. Amazonian rural floodplains (Wilson *et al.*, 2007) vs. small-scale urban areas (Hunter *et al.*, 2008)), having a model structure into which modules can be added easily was advantageous. The restructured program call graph is displayed in Figure 3.1. The function in green shading correspond to sections of the code that are responsible for loading in external data and setting up model variables, such as arrays holding the digital elevation data, channel parameters and the boundary conditions. `IterateQ` initiates the main time iteration loop from which core model functions are called. Initially, the program calculates fluxes in the channel, followed by conveyance on the floodplain using through Manning's equation (`CalcFPQx` and `CalcFPQy`). Floodplain flow may also be calculated using standard weir equations (`CalcWeirQx` and `CalcWeirQy`) at specific locations. The functions that follow are concerned with applying boundary conditions (`BCs` and `BoundaryFlux`) and updating water depths (`UpdateH` and `DryCheck`). Each time loop then finishes with file output and mass balance calculations before returning to `IterateQ`. When the simulation is completed, there are several file output calls before the model documents the total simulation time and returns to the command prompt.

The `C` code was updated to object oriented `C++` using data `structures` within a modular framework (see Figure 3.2). The first row is split up into files concerning reading and writing functions, the second row is the core processing functions for time and space iteration and the third row documents optional and utility functions. Modularising the code in this way and splitting `functions` according to their purpose eases the addition of new procedures within a defined framework. In the process of re-coding, a number of bugs were also highlighted that would have significantly hindered the progress of the project.

3.2 Building urban flood models

The data required to build robust but site specific model applications can be broadly classified into two groups, namely topographic data, whether that be floodplain elevations, channel bathymetry or land use classifications, and boundary conditions, describing the flow characteristics and domain delineation. Beven (2002) notes that the perceived complexities of environmental models precludes knowledge of all the boundary conditions, auxiliary conditions and system characteristics given the current state of measurement technology.

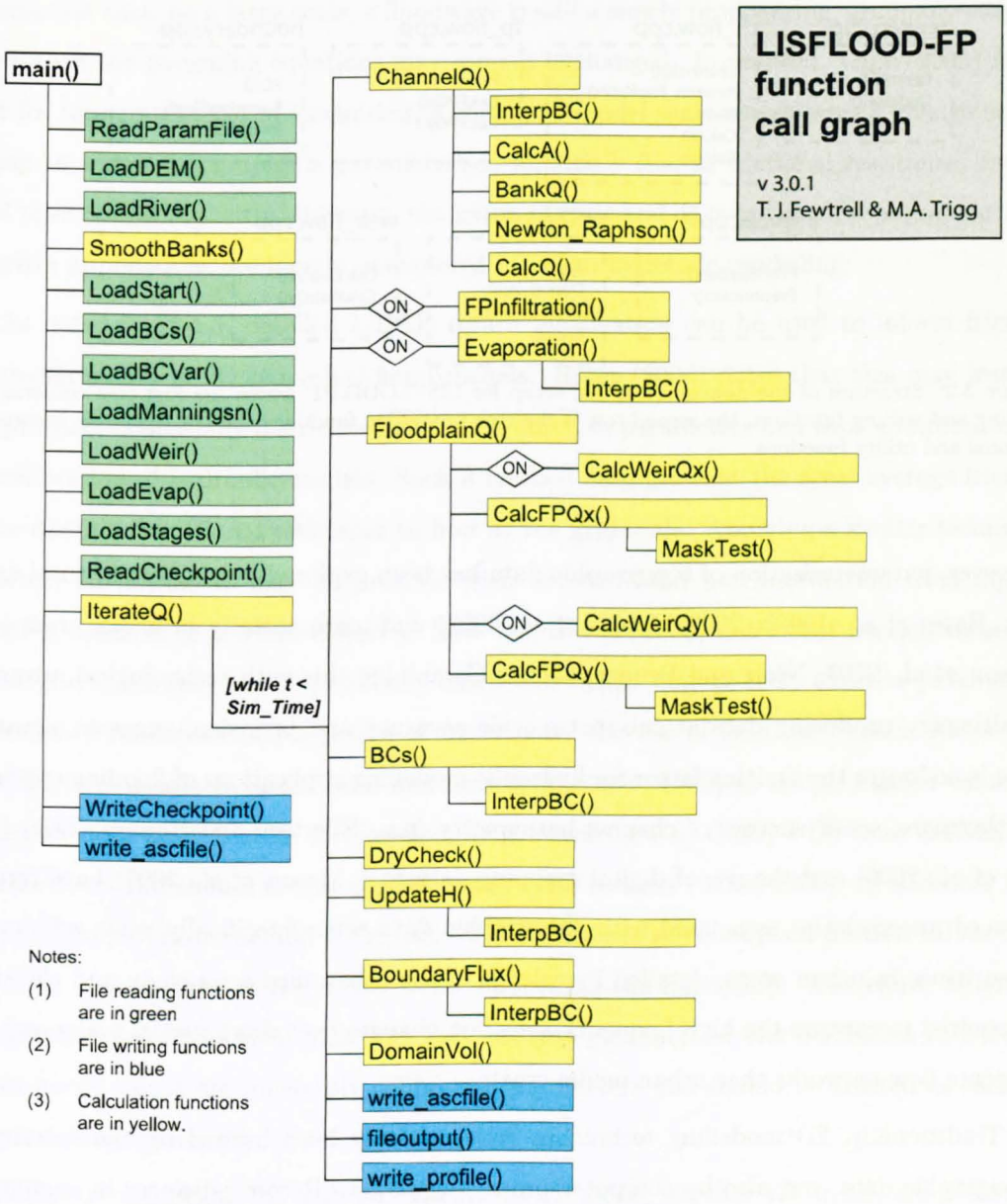

Figure 3.1: Program call graph for modularised LISFLOOD-FP in C++

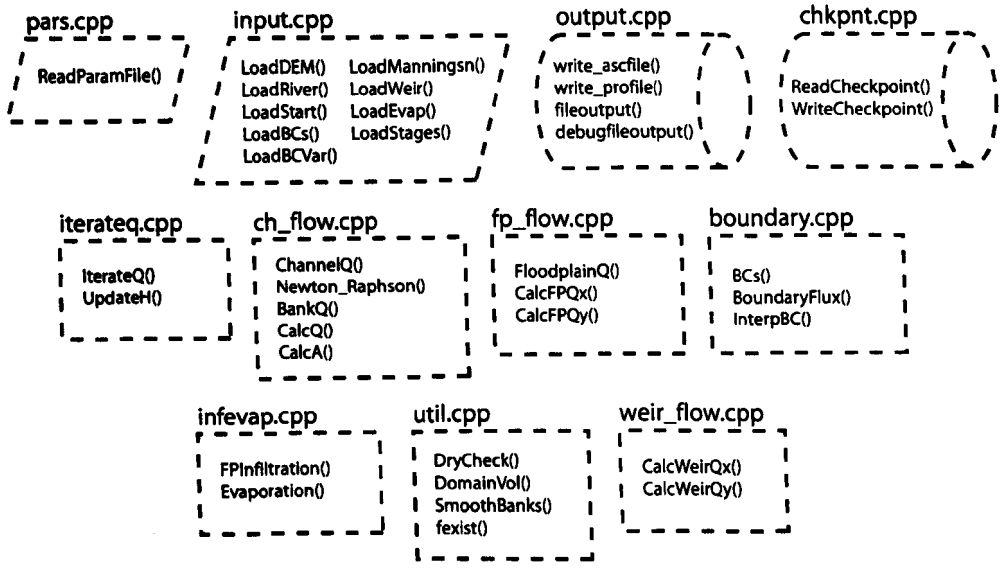

Figure 3.2: Structure of the new modular file setup for LISFLOOD-FP where the first row concerns file reading and writing functions, the second row is the core processing functions and the third row documents optional and utility functions.

However, parameterisation of topographic data has been explored extensively in rural areas (e.g. Bates *et al.*, 1998b, 2003; Cobby *et al.*, 2003) and more recently in urban areas (e.g. Mason *et al.*, 2007; Néelz and Pender, 2006). Combining this with technological advances in altimetry producing data at sub-metre scale accuracy and precision, suggests elevation data is no longer the limiting factor for hydraulic modelling applications of flooding episodes. Furthermore, sonar surveys of channel bathymetry (e.g. Eilertsen and Hansen, 2008; Horritt *et al.*, 2006) and the use of digital mapping data (e.g. Mason *et al.*, 2007) have further reduced uncertainties associated with topographic data sets. Specifically when addressing these issues in urban areas, detailed knowledge of the urban media topology and elevation is required to capture the high frequency elevation changes over short spatial scales and the intricate flow networks that urban media create.

Traditionally, 2D modelling techniques have not only been limited by the sparsity of topographic data, but also by computer processing power. Recent advances in computing technology (e.g. Accelerator boards (ClearSpeed^{TM}, GPUs, etc) and High Performance Computing) have relaxed these constraints such that the new, high resolution data sources can be exploited to their full potential. The responsibility now lies with environmental modellers to adapt current models to take full advantage of the available resources. In the interim, intuitive and physically-based methods for aggregating such data to scales at which the cur-

rent suite of numerical models are computationally feasible and efficient for engineering and planning applications, are required. However, aggregation to coarse model grid scales generally assumes that the governing equations still hold and that effective parameters can be found appropriate to the model scale (Beven, 1995). With reference to flood modelling, if the assumption that, on a large scale, a floodwave is still a slowly propogating, gradually varying wave, then the governing equations may remain unchanged. In practice, Lane (2005) notes that for topographic parameterisation, a change of model scale necessitates a change in the degree to which topography is parameterised implicitly (i.e. as frictional resistance) rather than represented explicitly. However, the issues of scale and aggregation of topographic data in urban applications are largely unexplored in urban hydraulic modelling.

As noted in §2.4.3, detailed LiDAR return information can be used to inform friction parameterisation in 2D numerical flood models. Bates (2004) notes that this may lead to the prospect of spatially distributed grid scale effective parameters and thus a reduced need for calibration of hydraulic models. Such a method assumes that the areal average friction is the dominant frictional resistance to flow at the grid scale. Applying a similar technique in urban environments may be possible with detailed land use information from digital mapping datasets (e.g. MasterMap®). However, Beven (2006) notes that friction values at coarse grid scales may not be physically based, but rather may be truly effective parameters that cannot be determined *a priori*. Furthermore, the use of land use classifications and empirically determined values from literature (e.g. Chow, 1959) to assign friction values is meaningless as most friction formulations (e.g. Manning's n, Chezy's C) were derived for natural rivers and should not be applied outside this context (Lane, 2005). In addition, this is only an appropriate method if the basis of derivation of the floodplain friction values uses the same assumptions as the model being applied to the floodplain. Therefore, although topographic and topological data sets may provide guidance for the derivation of friction values, these values are inherently calibration parameters and should be treated as such in any modelling framework.

Boundary conditions for hydraulic modelling of floods, whether 1D or 2D, are generally specified as flow or water stage hydrographs derived from gauging stations at the top (and sometimes, bottom) of the modelled reach. However, there is a clear discrepancy between the design specifications of nationally maintained flow gauging networks and the data requirements for hydraulic flood modelling. These gauging stations were originally designed with either water resource management or flood warning, rather than hydraulic modelling

in mind. As such, during flood events these gauges often operate outside the designed measurement range introducing significant uncertainties to these data. Furthermore, as typical gauge spacing in the UK is 10 - 60 km or more apart, few such data are available (Bates, 2004). Uncertainties in input data, when subject to extrapolation to larger events or into the future, may generate significant deviations in model results that can negate any predictive ability (Oreskes *et al.*, 1994). Furthermore, the assumption that present observations are indicative of future conditions is not guaranteed as natural systems are dynamic (Oreskes *et al.*, 1994). The alteration of gauging station reaches and flow dynamics by vegetation, floodplain development and sediment transport represent practical limitations to current gauging station data sets.

3.3 Assessing urban flood models

The combination of uncertainties in parameter values and initial and boundary conditions initiate an uncertainty cascade (Pappenberger *et al.*, 2006) that propogates to model predictions of water depths and consequently to estimates of flood damage. Until recently, validation data for hydraulic models has largely been bulk measurements (stage of discharge at points on the river network) representing the spatially aggregated catchment response. However, flood inundation modelling is a spatially and temporally distributed problem that requires distributed, rather than lumped, observational data to constrain and validate model predictions (Bates, 2004). The integration of remotely sensed imagery with flood models (e.g. Horritt *et al.*, 2007; Schumann *et al.*, 2007b) and the use of spatially distributed point measurements (e.g. Hunter *et al.*, 2005a; McMillan and Brasington, 2007) provide large data sets with which to evaluate competing model structures and parameterisations.

Bulk flow measurements represent an uncertain aggregate catchment response to that point and thus evaluating hydraulic models with these data can lead to a wide range of conjectures. For any given model, many different combinations of flow conditions and grid-scale effective parameter values may lead to the same aggregate catchment response but give different spatial predictions and, thus, process inferences. In fact, replication of aggregate catchment response often only requires single values of model parameters spatially lumped at the catchment scale (Bates, 2004). As such, stage and discharge data are unlikely to provide a sufficiently rigorous test for competing model structures (Hunter, 2005) and indeed, render model parameterisations indistinguishable from each other (Beven, 2002). Nonetheless, flow

records have proven their utility in testing the wave routing behaviour of flood models and have been shown to be replicable by even the simplest of numerical schemes (Horritt and Bates, 2002).

A consideration of measurements for driving models highlights the mismatch between the nature of variables used to run and evaluate a model and the nature of the observed variable (Freer and Beven, 2005). At the local point scale (e.g. a surveyed water level measurement compared to the free surface elevation predicted at the effective model grid scale), this difference arises as a result of scale, heterogeneity, non-linearity and incommensurability effects so that the predicted variable is not the same quantity as that measured (Beven, 2006), and which may not even be indicative of the natural phenomenon (Oreskes *et al.*, 1994). Oreskes *et al.* (1994) further note that observations and measurements of both independent and dependent variables are laden with inferences and assumptions attributed to the environmental modeller. In practical terms, what is perceived as a maximum water level mark may purely be the level at which water remained ponded during floodwave recession. Similarly, ponded water may deposit wrack marks that may be incorrectly interpreted as maximum flood extents. Given the noise in observations (spatially and/or temporally) used to evaluate model predictions (Beven, 2006), model states will inevitably be both equifinal and indistinguishable. Furthermore, Hunter *et al.* (2005a) note that there is a trend in environmental modelling to ignore the errors and uncertainties associated with field measurements due to the difficulties in collecting these data. However, errors and uncertainties in these data may have a significant impact on the predictive ability of flood models or values of effective parameters estimated within distributed models depending on the modelling application.

Synoptic scale maps of floods processed from remotely-sensed data provide wide-area, spatially distributed and spatially and temporally discrete information on flood extents. Such data have been extensively used and evaluated for constraining hydraulic models on rural reaches (see Horritt and Bates, 2002; Hunter *et al.*, 2005a; Schumann *et al.*, 2007b) where topographic variation has a fractal nature at large spatial scales. However, significant elevation changes on short spatial scales in urban areas and the channelised nature of many urban floods requires that remotely-sensed imagery of flooding capture the detailed variation in flood extent between urban structures. In fact, the resolution requirements of remotely sensed imagery for evaluating urban flood patterns (~1-2 m) far exceed current satellite capabilities (~20 m ground resolution) and the availability of airborne data is lim-

ited. Furthermore, even with future advances in satellite technology (e.g. TerraSAR-X at ~3 m ground resolution), problems of detecting building/ground/water transitions will still remain as complex radar returns from these surfaces will make flood delineation problematic.

As a consequence of errors in observational data and the mismatch of scales in remotely sensed imagery, Beven (2006) suggests that modellers can (or should) only look for application specific consistency between modelled and observed data.

3.4 Specific data requirements

The discussion above has highlighted the wide range of high resolution data required to build and assess hydraulic models of urban floods. However, the sparse availability of all these data for any given site significantly restricts the sites at which urban flood risk can be analysed in detail. The research design in §2.5 outlined a need to understand the controlling features of urban floods and the need to develop a suite of approaches specifically designed for urban flood risk analysis. As a consequence, the study sites will specifically need to have high resolution topographic and topological data, estimates of flood hydrographs and data with which to evaluate the models. It has been noted that topogaphic and topological datasets of urban areas are readily available but flow estimates and model evaluation data are scarce.

A further issue to consider is the number of test sites required to adequately investigate urban floods. A compromise must exist between the number of study sites, the time available for the research and the level of detail considered at each site. In addition, the choice of urban flood scenario is also significantly limited by the quality and quantity of available data. The selected test sites should cover a spectrum of urban characteristics, type and severity of floods, and areas of national and international interest. A review of the current literature and available data sets has highlighted three possible flooding scenarios, the aspects of which are discussed in detail below.

3.5 Greenfield, Glasgow, UK

3.5.1 Site and event description

In July 2002, much of the UK was affected by large storms characterised by extreme rainfall depths and localised high intensity downpours (see Table 3.1). On 30th July, a large storm was situated over much of west and central Scotland delivering approximately 75 mm of

Region	Rainfall (mm)	Rainfall Anomaly (%)	Raindays (days)	Raindays Anomaly (%)
UK	98.3	134	14	3
England	84.7	144	12	3
Wales	74.2	89	12	1
Scotland	126.3	132	18	4
N Ireland	104.7	147	16	3
Scotland W*	118.6	110	18	5

Table 3.1: Monthly average rainfall amounts for Met Office regions of the UK for July 2002. The anomalies show the difference from or percentage of the 1961-1990 long term average. * denotes the district of Scotland containing Glasgow.

rainfall in ten hours from early morning to late evening with a maximum intensity of 94.5 mm/hr (Jolley, 2002). The storm can be roughly divided into 3 sub-storms, each displaying markedly different characteristics. The first storm started at 10:30 and finished at 11:45, measured 5 mm depth with a maximum intensity of 25 mm/hr. The second storm started at 12:55 and lasted for ~20 minutes delivering 8 mm of rain with a maximum observed intensity of 69.3 mm/hr. These two sub-storms are typical of high intensity summer storms observed in the UK and have a return period of ~1 - 2 years. The third storm started at 14:15 and lasted for 6 hours, measuring 61 mm depth and had a maximum intensity of 94.5 mm/hr. However, 38 mm depth and the maximum rainfall intensity were observed in the first hour of the storm which equates to a 1-in-100 year rainfall event. The remaining 5 hours of the storm delivered 23 mm depth with a maximum intensity of 44 mm/hr which is a 1-in-3 year return period storm (Jolley, 2002). The maximum inter-event time in the ten hour period is 70 minutes suggesting that event can be considered as a single storm. The implications of this are that the event does not portray the typical characteristics of a high intensity, short duration summer storm but rather it can be regarded as a winter storm with high intensity summer storms interspersed within it. The short inter-event time and the small proportion of dry periods throughout the storm combined with the high return period sub-events limited the capacity of the catchments around Glasgow to recover between events (Jolley, 2002).

The long rainfall event duration combined with high intensity sub-events overwhelmed the local drainage capacity in the east end of Glasgow and resulted in internal property flooding in >250 properties (see Figure 3.3). In particular, the Greenfield suburb of Glasgow experienced localised flooding in >90 properties when a local stream exceeded culvert capacity and spilled onto the street network. The catchment area upstream of the culvert is < 5 km^2 and the stream responds rapidly to heavy rainfall. Observations of the flooding in Greenfield

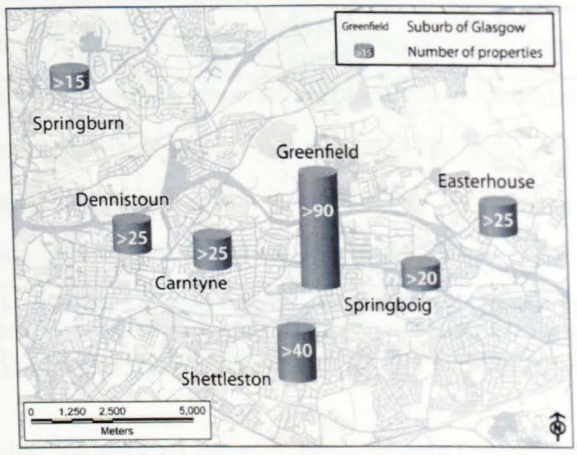

Figure 3.3: Internal property flooding in east end of Glasgow from July 2002 flood event adapted from Jolley (2002) overlain on MasterMap®. © Crown copyright Ordnance Survey. All rights reserved.

suggested water flowed along two main streets oriented east-west before interacting with the complex building configuration in the centre of the domain and then ponding at the western edge. The study site consists of a combination of apartment blocks, semi-detached houses and a school set within a topologically complex network of streets and open park land. Furthermore, the flood waters are constrained by the railway embankment running east-west along the southern boundary of the domain.

3.5.2 Data availability

The digital elevation data used to characterise the topography and topology of the area is a 2 m resolution LiDAR survey undertaken by Infoterra Ltd. fused with Ordnance Survey (OS) MasterMap® digital map data to define building locations, the road network and other significant land use types (see Figure 3.4). The raw LiDAR data was processed by Infoterra Ltd using their standard processing algorithms to produce a 'bare-earth' DTM with horizontal and vertical accuracies of less than 50 cm and 15 cm root mean square error (RMSE) respectively. Building and kerb height information was not retained from the original LiDAR data but rather buildings were defined as either 12 m (for apartment blocks and the school) or 6 m (for small houses) above ground level. Kerbs were assigned a uniform height of 10 cm above road level and the road camber was re-introduced to the DSM based on location in the MasterMap® digital map data set. Although the resultant DSM does not represent actual 'ground-truth' topography, it does represent urban topography as smooth, heterogeneous surfaces with significant breaks of slope (Figure 3.5).

Figure 3.4: The Greenfield study site in Glasgow, UK where a) is an aerial photograph and b) is the Ordnance Survey MasterMap® of the area. © Crown copyright Ordnance Survey. All rights reserved.

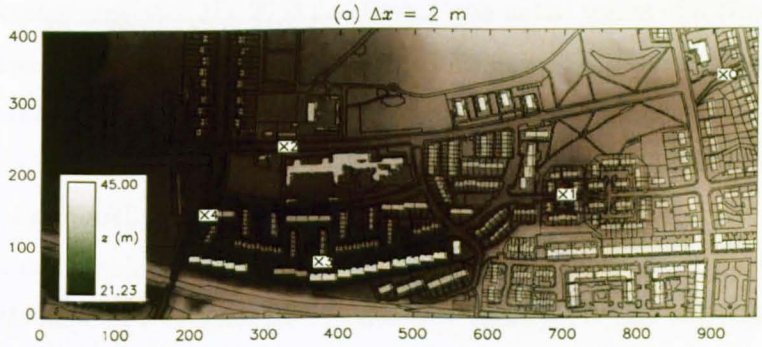

Figure 3.5: Digital elevation model (DEM) of Greenfield site with buildings and kerbs reinserted based on their location in the MasterMap® data represented by the black lines.

The data requirements discussed above highlight the need for accurate knowledge of flow conditions for a given flood event in order to adequately assess model results in comparison to observational data. Unfortunately, no flow measurements were available from the localised flooding event in July 2002. Therefore, the inflow conditions for this model application (Figure 3.6) were approximated from eye-witness accounts, historical photography and culvert geometry (Hunter *et al.*, 2008). Furthermore, there is little quantitative data available for model evaluation. Historical photography, anecdotal evidence and detailed knowledge of the drainage system provides qualitative information. Nevertheless, Hunter *et al.* (2008) demonstrated similar flooding patterns from a set of standard 2D flood models of varying complexity, providing results consistent with the qualitative observations, suggesting that flooding at this site is well represented in two-dimensional flood models.

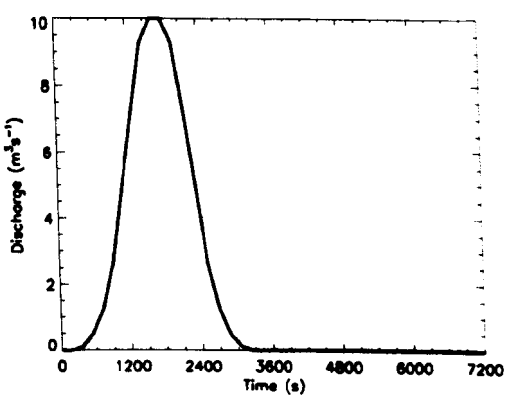

Figure 3.6: Event hydrograph used in this scenario derived from observations of flooding in July 2002.

3.6 Carlisle, UK

3.6.1 Site and event description

In January, 2005, the city of Carlisle in Cumbria, UK experienced substantial flooding as a result of water levels approximately one metre above the 1822 level, the previous highest recorded flood level in Carlisle. The city is situated at the confluence of one major river (River Eden) and two significant tributaries (Rivers Petteril and Caldew) with a combined catchment area of ~2,400 km^2 (see Figure 3.7). The Petteril and Caldew rivers are both subject to rapid flood response as a result of the steep upper regions of the catchments (Clarke, 2005). Furthermore, the majority of the catchment is rural with the major urbani-

sation concentrated around Carlisle. As a result, the region around Carlisle is at risk from substantial flooding. However, high flows are generally contained by the defence structures although these defences are estimated at only providing protection up to the 1-in-70 year event.

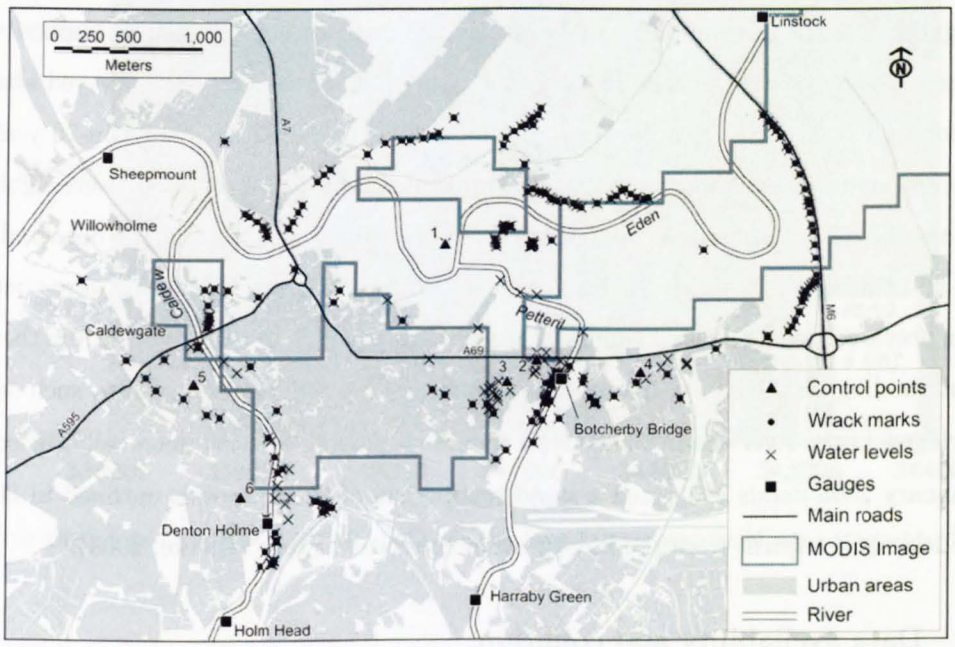

Figure 3.7: MasterMap® topological data of Carlisle delineating land use types. © Crown copyright Ordnance Survey. All rights reserved.

Initial estimates suggested the 2005 flood event was in the region of a 1-in-250 year flood event on all three rivers but subsequent investigations have found the event to be a 1-in-150 year event on the River Eden and a 1-in-100 year event on the Caldew and Petteril rivers (Clarke, 2005). The flooding was largely caused by high river levels as a result of almost continuous heavy rainfall from January 6^{th} to 8^{th} but overwhelming of the local drainage system contributed significantly to localised flooding. The storm event began on January 6^{th} and was accompanied by gale force winds on January 7^{th} and 8^{th}. The River Eden catchment received up to 175mm of rain in the 36 hour period (Day, 2005). Furthermore, the wet antecedent catchment soil conditions and the associated full lakes offered little storage capacity causing rapid runoff into the rivers. The resulting river flows were up to 1,600 m^3s^{-1} on the River Eden in Carlisle city centre. These high river flows overwhelmed a number of defences in the Carlisle region causing widespread flooding throughout the city. The flooding affected approximately 6,000 residents and 3,500 homes (of which approximately

1,900 properties were directly flooded) and 60,000 homes were cut off from electrical supplies (Day, 2005). Furthermore, the fire station, police station, bus depot and football ground were severly affected by the flooding with the bus depot forced to scrap the entire fleet. Clarke (2005) estimates the monetary damage from the flood to be ~£500 million.

In October 2004, the Environment Agency published a revised Flood Risk Management Strategy for Carlisle and the Lower Eden for public consultation in order to cope with the significant flood risk in the area. The current state of flood defences was surveyed after the 2005 flood and defence standards varied significantly from 1-in-20 year to 1-in-70 year protection and some affected areas were not protected at all. Furthermore, there were significant differences between the forecast predictions from operational models and the observed flood extent and timings (Clarke, 2005). Firstly, forecasting models and thresholds were operating oustide previously observed and validated ranges and secondly, observations during the event suggest flooding on the rivers Caldew and Petteril was caused by obstructions, such as trees and bridges, in the river channel and flood waters by-passing existing defences. The scale of the January 2005 floods prompted a rapid reappraisal of the proposals outlined in 2004 to ensure lessons are learnt from the largest event in recent history (Clarke, 2005).

3.6.2 Data availability and collation

The January 2005 Carlisle flood event provides a unique opportunity to evaluate common data sources available for setting up distributed flood models and assessing model accuracy for urban applications. Data for model setup is in the form of LiDAR elevation data, river cross-sections and river discharge time-series. Field measurements of high water marks and flood extents combined with remotely-sensed satellite data form the basis of model evaluation schemes. This is representative of data that would be routinely gathered before, during and after a flood event.

Airborne scanning laser altimetry data (LiDAR) at metre spatial resolutions are becoming increasingly available (Marks and Bates, 2000) for the generation of digital surface and terrain models for urban areas. Mason *et al.* (2007) detail the development of a LiDAR post-processing framework specifically designed for urban applications which incorporates digital map data and pattern recognition techniques. As a result, it is possible to construct a DTM of the ground surface and a DSM incorporating buildings and vegetation of a 6 x 4 km area surrounding Carlisle. Figure 3.8 shows the digital surface model constructed using LiDAR data flown by the Environment Agency in 2003 and MasterMap® digital map data.

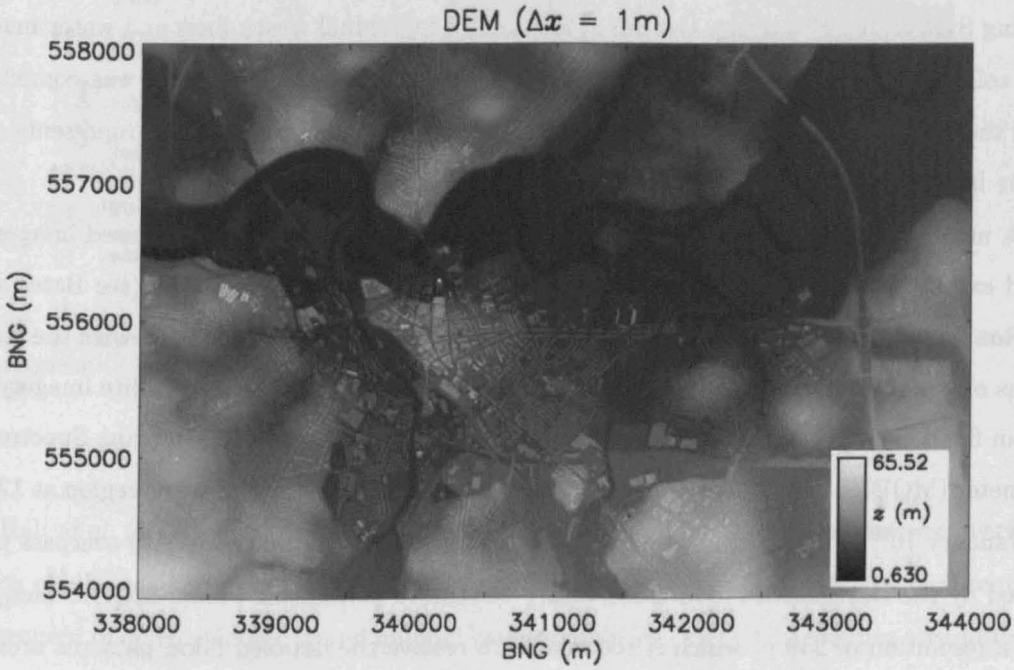

Figure 3.8: Digital elevation model (DEM) of Carlisle site from LiDAR segmented using MasterMap® data.

As discussed above, flood inundation models are driven by discharge or water level measurements as upstream, downstream and/or internal boundary conditions. During the Carlisle flood, significant out of bank flows at both rated and unrated gauging stations resulted in substantial uncertainty surrounding flow estimates for the event. For hydraulic modelling purposes, the presence of a number of level-only gauges around Carlisle complicates the delineation of a model domain, although the gauges internal to the domain can act as important tools for model calibration and validation. On the River Eden, the lack of a rated gauge upstream of the area of interest and the known problems with the rating curve above 7.0 m water depth at the Sheepmount gauge require significant attention prior to any hydraulic modelling. Furthermore, uncertainty surrounding the Sheepmount rating curve limits the use of this data to internal calibration and validation of water stages. On the River Caldew at Cummersdale and on the River Petteril at Harraby Green, substantial out of bank flows necessitate an evaluation and subsequent possible revision of current rating curves prior to any hydraulic modelling exercise.

In order to exploit this opportunity to increase our understanding of flooding in the urban environment, a post-event mapping survey of water levels in Carlisle was undertaken.

Although undertaking a survey directly after the event is somewhat inappropriate, water levels, trash lines and wrack marks are temporary features. Using a differential Global Positioning System (dGPS) setup, the [x,y,z] location of individual wrack lines and water marks was collected throughout Carlisle city centre. This data set of ~75 points was combined with the EA post-event mapping data set of ~500 points (see Figure 3.7) and represents one of the largest data sets of urban flood extents and water heights.

A number of studies have demonstrated the utility of satellite remotely sensed images of flood extent to inform and constrain model predictions of rural flood events (see Bates and De Roo (2000); Horritt and Bates (2001b, 2002); Schumann *et al.* (2007b)). As with the other forms of observational data presented here, there are few applications of satellite imagery to urban flood events. During the Carlisle event, the Moderate Resolution Imaging Spectroradiometer (MODIS) instrument aboard NASA's Aqua satellite passed over the region at 12:40 on January 10th. Figure 3.7 shows the flood extents derived from the MODIS overpass processed by the Dartmouth Flood Observatory to remove permanent water. MODIS imagery has a resolution of 250 m which is too coarse to resolve the detailed flood patterns around the complex structures on urban floodplains, typically of higher spatial frequency (~5–10 m (Mark *et al.*, 2004)). It is clear from Figure 3.7 that the MODIS imagery does not capture the spatial pattern of flooding and the coarse resolution does not provide the detail required for urban flooding applications.

3.7 River Thames at Greenwich, London, UK

3.7.1 Site description

London is home to 7.5 million people, of which 1 million people and 300,000 properties are in the tidal flood risk area (Dawson *et al.*, 2005). The indicative tidal flood risk area for the Thames Region of the Environment Agency (EA) lies between Teddington Weir and Dartford Creek (approx. 116 km^2) (Figure 3.9) and would be liable to frequent flooding from surge tides without the existing tidal walls and embankments. London is defended by a complex system of over 200 km of embankments and walls, the Thames Barrier and a suite of warning systems. However, recent development in London's previously derelict docklands and the emergence of the the new financial district around Canary Wharf combined with plans for significant future development over the next 15-30 years (Prescott, 2005) poses significant questions over future flood risk.

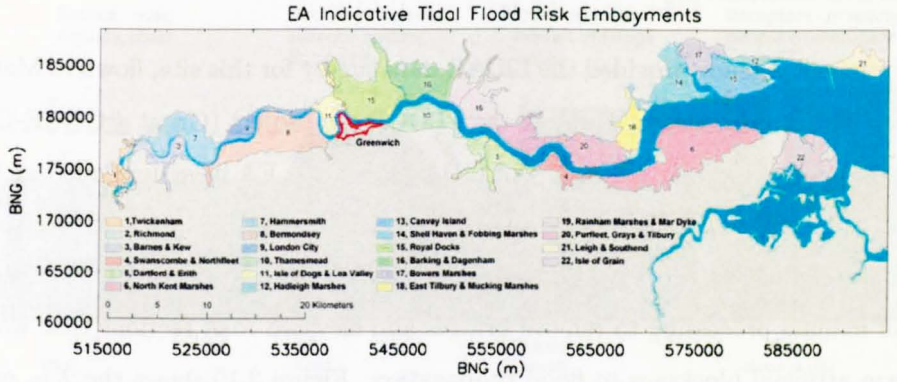

Figure 3.9: Map of the delineated Greenwich tidal embayments. Data supplied courtesy of the UK Environment Agency.

Hall *et al.* (2003) note that flood risk in estuaries is dominated either by defence overflow, which can be calculated using standard weir equations, or defence breaching, which requires assessment of defence integrity and inundation probabilities. The latter requires an additional computational burden (Hall *et al.*, 2003) and Dawson *et al.* (2005) note that if extreme sea level rise scenarios are considered for flood risk assessment, the contribution to total inundation volume from breaching is negligible compared to the inundation volume from overflow events. Furthermore, Gouldby *et al.* (2007) note that the flood defences along the River Thames are in good condition and thus breach events are less likely than overtopping scenarios. Dawson *et al.* (2005) found significant increases in flood risk to London and the surrounding Thames region from comparatively small increases in sea level which supports the need for modelling of individual areas to assess detailed flood risk.

For flood management purposes, the EA delimit the tidal flood risk area into embayments which are considered to be in hydraulic isolation from each other, with high ground, tributaries or artificial constraining features extending from inland to the river Thames to form boundaries between embayments. In order to investigate detailed urban flood risk, the Greenwich embayment is chosen as a suitable study site indicative of defence integrity and urban topography and topology for the wider Thames tidal flood risk region (see Figure 3.9). The 11.5 km^2 embayment is characterised by areas of densely clustered terraced housing and large industrial units and machinery surrounded by substantial open spaces. Furthermore, the embayment incorporates significant assets (e.g. Blackwall Tunnel) and flooding of these features would cause substantial business and service interruption for the UK's capital.

3.7.2 Data availability

The Environment Agency provided the LiDAR data survey for this site, flown in March 1999 and collected at 2 m resolution, through the FLOOD*site* project (Grant #GOCE-CT-2004-505420). In order to increase the utility of LiDAR data, the EA have developed an in-house segmentation algorithm that delivers a DSM, a DTM and a mask of buildings and vegetation based on pattern recognition in the raw LiDAR signal. The EA also perform a significant amount of manual processing to remove bridges and elevated road sections that would otherwise form artificial blockages to flood propagation. Figure 3.10 shows the 2 m resolution digital elevation model for the Greenwich embayment processed by the Environment Agency.

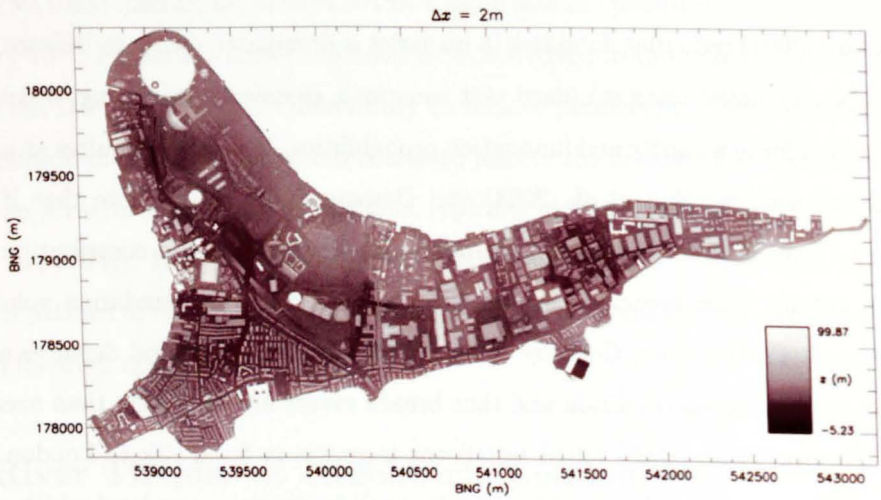

Figure 3.10: Digital elevation model (DEM) of Greenwich site from LiDAR segmented using the Environment Agency in-house processing algorithm.

The simulation of overtopping and breach scenarios for hydraulic modelling of individual flood embayments was conducted by HR Wallingford Ltd using a model based on the RASP procedure (see Hall *et al.* (2003)). This method involves the development of fragility curves which integrates a full range of loading conditions (water levels) with the performance and integrity of flood defences (Gouldby *et al.*, 2008). Each defence section is considered independent and has a different resistance to flood loading which is characterised by structure type, crest level or condition. The fragility curve for each defence section, defined as a continuous random variable of defence failure conditional on the load, was derived from failure models for either, or a combination of, overflow and piping (see Figure 3.11). The

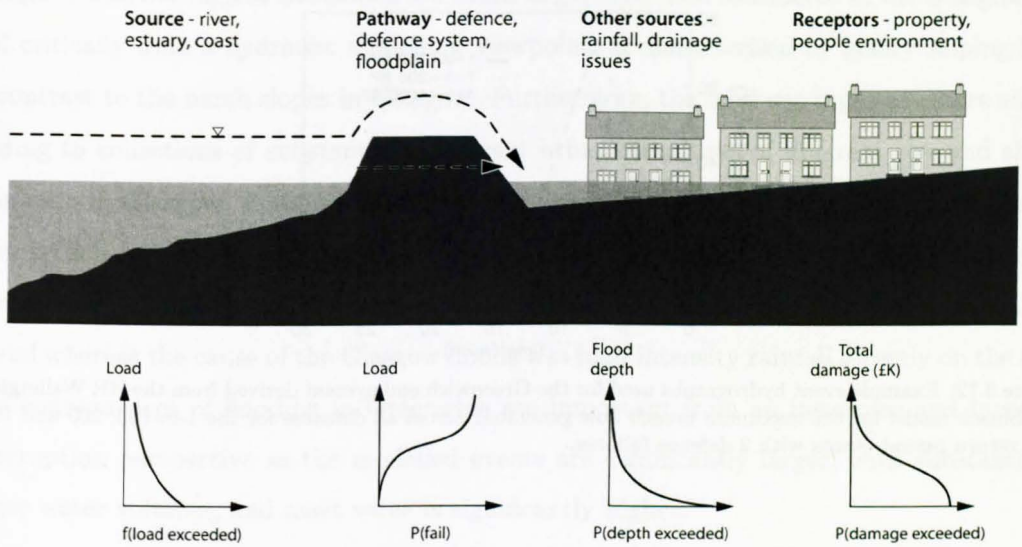

Figure 3.11: RASP source-pathway-receptor-consequence model of the risks of flooding based on Gouldby *et al.* (2008).

occurrence of extreme water levels is defined as a continuous random variable associated with each defence section. The defence system state (failed/not failed) is addressed using a Monte Carlo framework where the defence state is sampled with reference to the defence specific fragility curve for a given loading. Peak flow rates into the floodplain for each defence are calculated using the broad-crested weir equation and converted to a water volume assuming a triangular hydrograph for a given duration (Gouldby *et al.*, 2008).

Overtopping and breach volumes are calculated for each defence section and applied as point source inflows at the centroid of the defence section in the LISFLOOD-FP model. Inflows are derived as 1-100, 200 and 1000 year events with 2, 5 or 10 breach locations and overtopping fluxes at other locations. This provides a catalogue of events of varying magnitude to evaluate uncertainties in estimation of event size and characteristics on flood propagation in a complex urban area. Figure 3.12 shows the an example hydrograph derived from the water volume and breach duration estimates for three different event sizes.

3.8 Selected data sets

The above sections have highlighted the requirements for successful and rigorous flood modelling studies and the particular intricacies of urban environments that require detailed treatment. The data available to investigate the performance and test the development of spe-

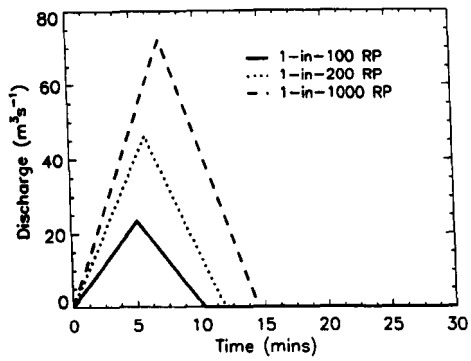

Figure 3.12: Example event hydrographs used for the Greenwich embayment derived from the HR Wallingford Ltd breach model for the maximum breach flow generated across all defences for the 1-in-100, 200 and 1000 year return period events with 2 defence failures.

cific urban flood models have also been presented. Based on the data requirements and the characteristics of the available data sets, only a subset of these data satisfy the criteria for improving the quality of hydraulic information gathered from spatially distributed flood inundation models of urban floods.

Flooding at the Glasgow site provides an ideal opportunity to examine model consistency for an urban flood event as practically, its features are characteristic of urban flood episodes and a number of models of varying complexity have been shown to provide commensurate patterns of flooding (Hunter *et al.*, 2008). For hydraulic modelling purposes, this site represents a rigorous test of model ability to represent flow around buildings, along defined road networks and over open ground as well as high velocity, shallow flows along steep streets and ponding in low lying areas. The flow conditions at this site consist of a rapid rise and fall of the hydrograph which is typical of urban flooding scenarios. Furthermore, the flood illustrates the ability of small catchments to generate relatively high peak flow rates as a result of the impervious, low friction surfaces of urban environments. Observations at the field site also suggest the ponded water at the western edge takes considerable time to drain through the storm water drainage system. Practically, the computational requirements for this test case are such that numerous experiments can be formulated and methods tested prior to their application to more computationally expensive test cases both in terms of domain extent and flood magnitude.

The Greenwich test case provides a unique opportunity to investigate the consequences of flooding during the planning phase of a large flood defence scheme (Thames Estuary 2100 Project (TE2100)) in addition to presenting significantly different urban characteristics than

Glasgow. The borough of Greenwich is a much larger area than considered at the Glasgow site and critically from a hydraulic modelling viewpoint, is characterised by gently sloping land in contrast to the harsh slopes in Glasgow. Furthermore, the land use types are more varied leading to collections of substantially different urban structures of different size and shape than seen in Glasgow. Possible flooding at this site is characterised by multiple flow inputs, from breach and overtopping locations, and thus provides a rigorous test of flow interactions in any new techniques and approaches. In addition, the flood scenarios at Greenwich are fluvial whereas the cause of the Glasgow floods was high intensity rainfall directly on the site. The consequences of flooding in Greenwich are important from an insurance and business interruption perspective as the modelled events are significantly larger, with substantially larger water volumes, and asset value is significantly higher.

The lack of validation data at Glasgow and Greenwich enables model evaluation across scales and development of new methods for flood propagation in models of the urban environment without consideration of errors in observations. Therefore, evaluation of these methods can be defined as a benchmarking procedure (see Oreskes *et al.* (1994)) within a model verification framework (Lane and Richards, 2001). The product is, therefore, a consistent methodology for evaluating the consistency of modelling methods and results and as such, assess new approaches to urban flood modelling.

As noted above, the flooding at Carlisle, although well-documented, has a number of uncertain features that may limit the utility of this data set during testing. Firstly, the aim of this research is to investigate complex flow fields that occur in urban environments and how to resolve these in hydraulic models. However, the Carlisle flood event is characterised by complex river-floodplain interactions between the three river systems but with 90% of the flow contained in the rural River Eden catchment. Therefore, uncertainties in the description of the rivers and their flows may mask, or indeed counteract, increased model performance from any new methods and approaches. Furthermore, there are significant uncertainties in the boundary flow conditions used to drive flood models which requires substantial re-evaluation of boundary conditions. The Carlisle data set has also highlighted practical limitations of gathering and processing point measurements of water depths and flood extents for model assessment for large urban catchments and flooding episodes (Neal *et al.*, 2009a) and the significant time required to assimilate these data. As a consequence, the delivery of the Carlisle test site as coherent case study was not timely for each research objective.

Nevertheless, these three study sites represent a wide spectrum of urban characteristics,

flood types and magnitudes and topographic features (Figure 3.13) and as such will allow detailed and rigorous testing of modelling techniques for urban flood events.

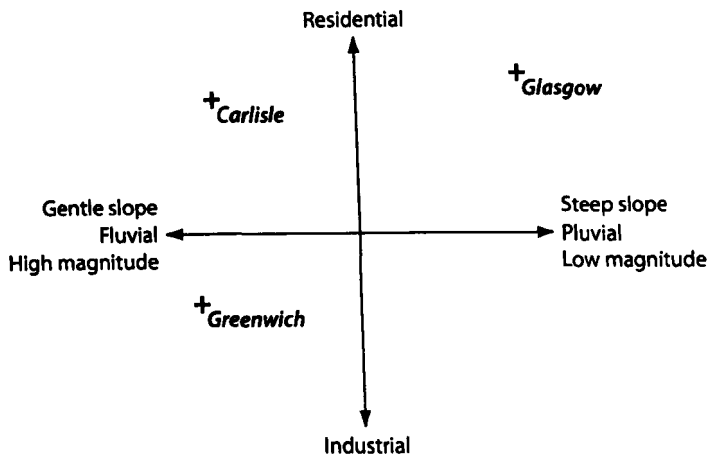

Figure 3.13: Spectrum of urban study sites positioned within a range controlling features for floodwave dynamics.

3.9 Conclusions

The preceding chapter has highlighted the significant data requirements for building a detailed urban flood model, with the emphasis being on high resolution topographic data, detailed topological information about the particular urban area and knowledge of the event boundary conditions. The emergence of LiDAR and other remotely sensed elevation data and MasterMap® topological data has helped to constrain the topography but uncertainties still remain in flow data (Pappenberger *et al.*, 2006). In terms of the former, although a few studies (e.g. McMillan and Brasington, 2007; Yu and Lane, 2006a) have observational used data of flooding episodes in urban areas, the availability of spatially and temporally distributed information on particular flooding episodes is limited. In addition, the test site in Yu and Lane (2006a) does not represent a solely urban test case and the observational data available in McMillan and Brasington (2007) has considerable uncertainty as a result of the collection methodology. Therefore, a different approach to model evaluation is required, namely model verification, which in itself provides a different framework for developing and assessing urban flood models. The flooding scenarios at Glagow and Greenwich allow the behaviour of urban flood models to be investigated without consideration of errors in observational data. Furthermore, a model verification approach in these regions allows the controlling features

of urban environments and the utility of new techniques to be determined. The following chapters will therefore document the evaluation of the scale dependence of urban features and utility of sub-grid scale porosity techniques for the improvement of flood risk assessment over wide urban areas.

CHAPTER 4

Evaluation of the scale dependence of urban environments

4.1 Introduction

The need for effective and efficient flood risk assessment tools is driven by a dichotomy of scales within flood risk analysis where *fine scale* detail is required over *wide areas*. The fine scale detail is required to assess risk and possible damage to individual assets and properties (i.e. for insurance purposes) but is also required over wide areas as flood events are rarely localised. Furthermore, wide area application is a necessity to assess the consequences of a return to a flood rich period (Lane, 2008), in addition to the long-standing planning and management needs. A number of authors (Hunter *et al.*, 2005b; Sanders, 2008) have noted the significant computational requirement of numerical models on high resolution grids invoked by stringent time step constraints to maintain model stability. Consequently, in order to address the large scale problem, the ability of coarse resolution models to provide fine scale, detailed flood risk predictions needs to be assessed.

The effect of model resolution on estimates of flooding in rural areas has been extensively explored (see Hardy *et al.*, 1999; Horritt and Bates, 2001a; Horritt *et al.*, 2006, 2007; Tayefi *et al.*, 2007) and models at coarse resolution are generally shown to perform well compared to observed data, especially when reprojected onto higher resolution elevation models (Horritt and Bates, 2001a). Analysis of natural topography displays a fractal property (Marks and Bates, 2000) that can be retained at resolutions up to ~250 m (Horritt and Bates, 2001a). Chapter 2 has highlighted the hydrologically complex nature of urban environments and a number of authors (Mark *et al.*, 2004; Yu and Lane, 2006a) have noted that the structures on urban floodplains significantly alter the storage capacity and conveyance characteristics. Mark *et al.* (2004) note that urban areas are characterised by length scales of 1-5 m but few authors have explored the effect of not representing these length scales explicitly in numerical models of urban flooding. Yu and Lane (2006a) considered the effect of coarse resolution models for a mixed urban and rural test case although the majority of the flow was contained

in the rural floodplain. The authors found a significant reduction in model performance at coarse resolutions and non-stationarity of response of numerous model performance measures with respect to the friction parameter in a sensitivity analysis.

In this chapter, the analysis of Yu and Lane (2006a) is extended to consider model resolution, friction and resampling effects on hydraulic model predictions for a wholly urban case without the influence of channel-floodplain interactions. This allows the evolution of flow around structures to be examined in greater detail and the quality of representation of the urban environment to be assessed. Specifically, the effect of scale on predictions of surface water heights and flood extents will be evaluated (§4.3). Secondly, the influence of different grid resampling strategies will be evaluated within the same framework to quantify the effects of uncertainty in feature representation and discretisation noise. Thirdly, the effects of the inclusion of different data layers for deriving coarse resolution representations of topography is undertaken (§4.4). Finally, the sensitivity of the model to friction calibration at different scales will be addressed to determine how effective parameter values may add to uncertainties in flood prediction (§4.5). The lack of detailed observational data requires a different approach to model calibration and validation. Assuming the high resolution simulations represent a set of benchmark predictions, it is possible to verify that coarse resolution models are consistent abstractions of the benchmark simulation. Consequently, model verification is undertaken by assessing coarse model predictions of flood depths and extent with respect to the benchmark solution (Lane and Richards, 2001).

4.2 Model evaluation methods

In order to establish the variability in model predictions associated with changing resolution, resampling strategy and friction sensitivity, the effect of these model configurations was evaluated separately prior to a combined analysis to determine detailed model sensitivities. This study is a model verification exercise as there is no appropriate quantitative data for any observed event. Consequently, model predictions of water heights are evaluated against the benchmark high resolution simulation using root mean squared error (RMSE) (Eqn. 4.1).

$$RMSE = \sqrt{\frac{1}{NC}\sum(h_{i,j}^{D} - h_{i,j}^{M})^2} \tag{4.1}$$

where $h_{i,j}$ is the water height at cell $[i,j]$ in the benchmark (D) or modelled (M) simulation and NC represents the number of cells classified as wet in the benchmark model result or

the coarse resolution model result. The ability of the coarse resolution models to adequately predict propagation extent is analysed by calculating a global fit statistic (Eqn. 4.2) (Werner *et al.*, 2005b) as follows:

$$F^{\langle 1 \rangle} = \frac{M_1 D_1}{M_1 D_1 + M_1 D_0 + M_0 D_1} \tag{4.2}$$

where $M_{1/0}$ represents the modelled cell state (wet (1) or dry (0)), $D_{1/0}$ represents the benchmark cell state and NC represents the number of cells in the benchmark model domain (96,000 cells). $F^{\langle 1 \rangle}$ therefore varies between 0 for model with no overlap between predicted and benchmark inundated areas and 1 for a model where these coincide perfectly. In order to deal with the changing resolution, coarse model results were resampled to the benchmark domain size using a simple nearest neighbour approach which ensures all values within the output stencil are equal to the predicted model result and no averaging or interpolation of values occurs. Hunter (2005) notes that $F^{\langle 1 \rangle}$ ignores the areas of correct predictions of non-flooding ($M_0 D_0$) and thus this measure is not dependent on the size of the model domain. In other words, $F^{\langle 1 \rangle}$ is only concerned with areas that are wet and as such can be regarded as a surrogate for the active floodplain area within the domain (Hunter, 2005). This measure has been used in a number of studies (e.g. Aronica *et al.*, 2002; Horritt and Bates, 2001a) to calibrate a variety of flood models against observed inundation area but yields a single broad optimum region in a two-parameter space (channel and floodplain n). As a result, a number of other measures, ($F^{\langle 2 \rangle}$, $F^{\langle 3 \rangle}$, $F^{\langle 4 \rangle}$) with minor modifications to the numerator, have been proposed in order to further constrain the regional of optimal model performance (Hunter, 2005). As this study employs a benchmarking approach, $F^{\langle 1 \rangle}$ seems the most appropriate measure as it provides a relatively unbiased result, equitably discriminating between under- and over-prediction. The $F^{\langle 1 \rangle}$ measure discriminates between modelled and observed data at the margins of the flooded area. Examining this statistic throughout a flood event will inevitably lead to an increase in the fit statistic as the flooded area increases relative to the number of cells at the flood margins. This reduces the discriminatory power of the statistic when assessing competing model structures. Nonetheless, once the flood wave dynamics have subsided, the $F^{\langle 1 \rangle}$ measure will provide an indication of the error introduced by variations in model structure.

4.3 Influence of model resolution on flood propagation

In order to test the importance of scale, the original high resolution DEMs of Greenfield and Greenwich are progressively coarsened to examine the effect of introducing quantisation noise into the description of building locations, dimensions and shape. As urban areas are characterised by obstacles and structures that dramatically affect the flow area and storage capacity of floodplains, coarse representations of these obstacles will tend to alter the dynamics of the urban flood. However, this effect has remained largely unquantified and the controlling features of flood propagation have not been fully elucidated in studies to date.

4.3.1 Greenfield, Glasgow, UK

In order to test the significance of scale, the original $\Delta x = 2$ m (96,000 cells) DSM is aggregated to three progressively coarser resolution DEMs ($\Delta x = 4$ (24,000 cells), 8 (6,000 cells), 16 m (1,500 cells)) using the default method nearest neighbour approach. This resampling method defines the elevation of the output coarse grid cell as the elevation of the fine resolution cell in the centre of the output resolution stencil. Figure 4.1 shows the maximum predicted flood depths using the high resolution, benchmark 2m DEM used to evaluate the coarse resolution model predictions. These results appear to be consistent with observations of the flood event in July, 2002 as the model simulates shallow flow depths down the northern street, running east to west, interactions with the building fabric and ponding in the low lying streets north of the railway embankment.

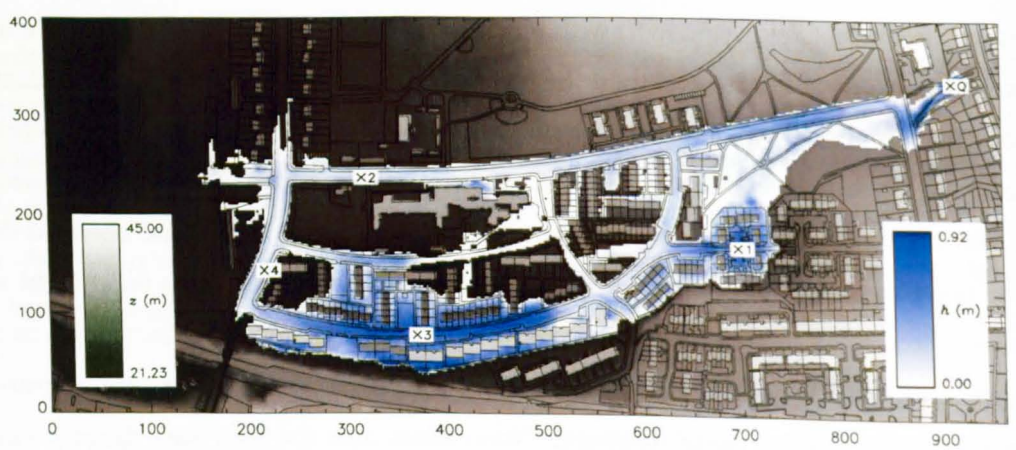

Figure 4.1: Maximum simulated flood extent from the high resolution, benchmark 2m LISFLOOD-FP solution of Greenfield with the surface height (z) from the DEM shown as a grey scale overlain by water depths (h).

Figure 4.2 shows the maximum predicted flood depths using the coarse resolution DSMs. The most notable features are the ability of the 4 and 8 m resolution models to simulate the shallow flow down the northern street, the ponding in low-lying region north of the railway embankment, and the complex interactions with the building network. At 16 m, the model simulates the former two features adequately but fails to replicate water depths around the buildings in the centre of the domain. Nonetheless, the 16 m model appears to replicate areas of deep water which will contribute most to damage estimates from this flood event. However, there is a substantial difference in the spatial distribution of the water depths such that the 16 m model overpredicts depths in the region of point X1 and underpredicts depths in the region of X3 (see Figure 4.1 for locations). These analyses provide indications of model performance, although only qualitative, but do not provide an insight into the ability of coarse resolution models to predict the dynamic propagation of the floodwave.

Figure 4.3 shows the evolution of quantitative model performance over the course of the simulation for $\Delta x = 4$, 8, 16 m compared to the benchmark solution using the default nearest neighbour resampling technique. Analysis of these global measures of performance provide contrasting conclusions about the ability of the model to predict flooding at coarse resolutions. Assessing the RMSE of predicted water levels requires a choice between evaluating water elevations and water depths. In ponded regions, the use of water elevations is likely to provide a better result than water depths as a flat water surface will be predicted regardless of bed elevation. However, in areas of dynamic flow, such as down the steep slopes present in the Greenfield domain, the model is likely to more accurately predict the water depth. It should be noted, however, that the diffusion wave approximation will become less appropriate as slope (and hence, velocity) increases. Nonetheless, Hunter *et al.* (2008) found similar results for a range of 2D flood models at this site and Prestininzi (2008) has shown the utility of diffusion wave models for transient flows. In relation to flood risk at the Greenfield site, the use of water depths therefore provides a conservative estimate of risk which has practical application for the planning and insurance industries. The RMSE of predicted flood depths over the entire domain is less than the typical vertical error of LiDAR data of ± 15 cm RMSE. In this case, the RMSE is describing changes in relative submergence as the water slopes are negligible compared to the topography such that only the dynamic portion of the event will affect the error distribution. This is observed in the evolution of the RMSE as the error rises until the time of peak inflow and remains fairly constant thereafter.

In constrast, the binary measure of flood extent is temporally more variable and decreases

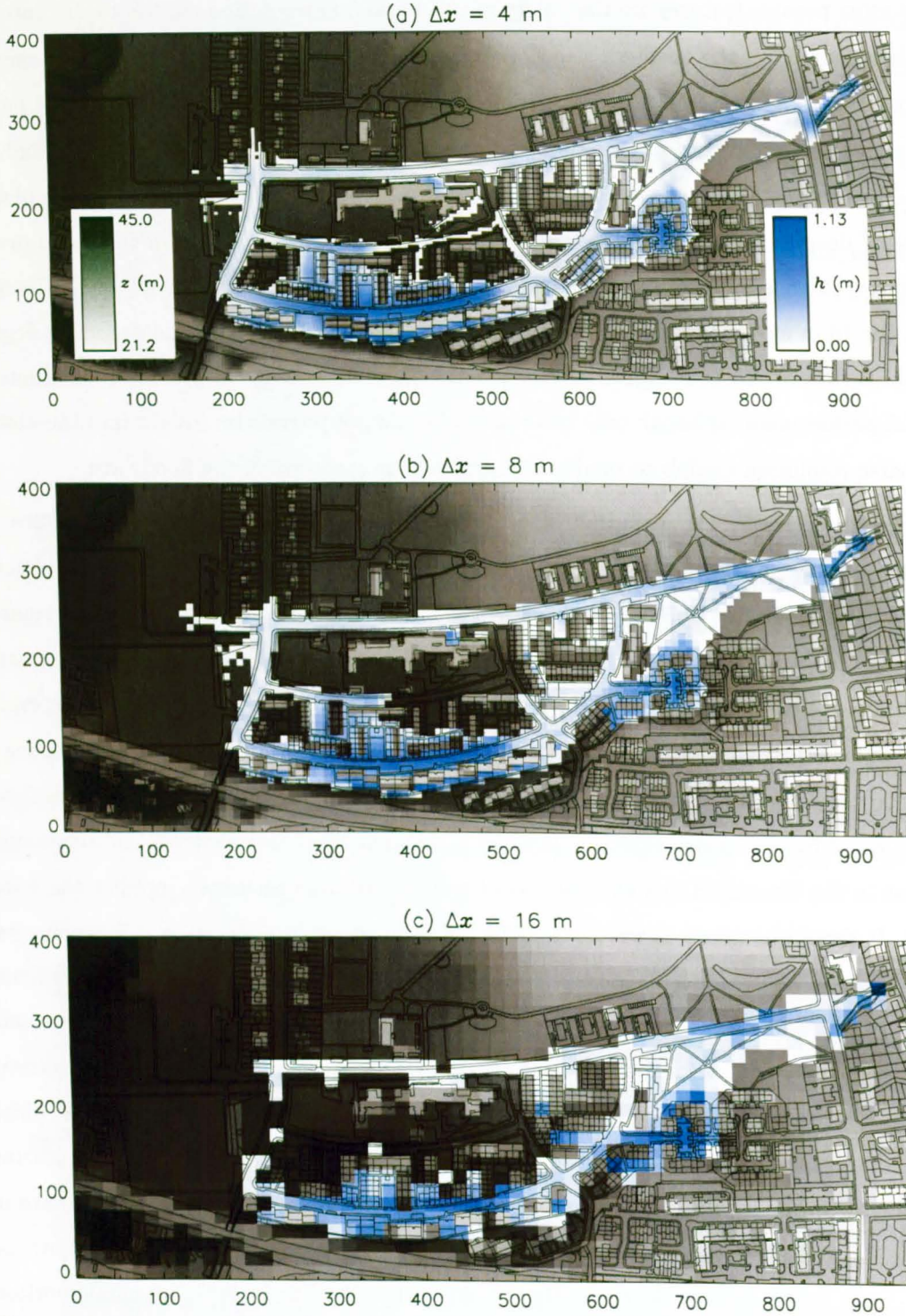

Figure 4.2: Maximum simulated flood depths from the 4, 8 and 16 m LISFLOOD-FP solutions with the surface height (z) from the DEM shown as a grey scale overlain by water depths (h).

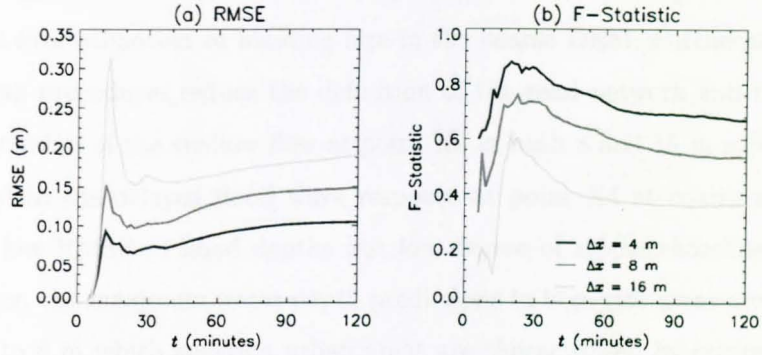

Figure 4.3: Evolution of global measures of model performance throughout the simulation at $\Delta x = 4$, 8 and 16 m compared to the benchmark solution where *a*) is the RMSE of predicted flood depths and *b*) is the F^2 binary measure of fit of flood extents.

substantially with decreasing model resolution and suggests poor process or topographic representation within the coarse models. Horritt and Bates (2001a) note that predictions at coarse resolutions will be subject to two types of error when comparing model shorelines to a benchmark dataset. Firstly, the coarse resolution models will provide only a crude approximation of the model shoreline as a result of the quantisation noise introduced in the resampling process (discussed in more detail in §4.4). Secondly, there will be a bulk effect on coarse model predictions resulting from changes to flow paths and local slopes that is independent of quantisation noise. The evolution of the model fit measurement (Figure 4.3b) suggests that although the prediction of water heights is within expected error bounds, significant error is introduced into the flood wave propagation at coarse resolutions. These conflicting conjectures indicate that it is necessary to consider internal model predictions when analysing flood predictions at coarse resolutions (after Bates *et al.*, 1998a; Fawcett *et al.*, 1995).

Accordingly, time series of water depth predictions at four characteristic locations within the Greenfields site (see Figure 4.1 for locations) are compared. Point X1 represents an area of rapid ponding at the start of the simulation followed by the slow release of water as the simulation proceeds. Point X2 is indicative of shallow, high velocity flow down a well-defined road and point X3 represents an area of permanent ponding with little drainage. Point X4 represents an area of convergent flow receiving water from both the northern and southern road networks. In this case, the low resolution models show significant over- and under-prediction of water depths at the chosen locations (Figure 4.4). The overprediction at point X1, the associated under-prediction at point X3 and analysis of the DEM in the

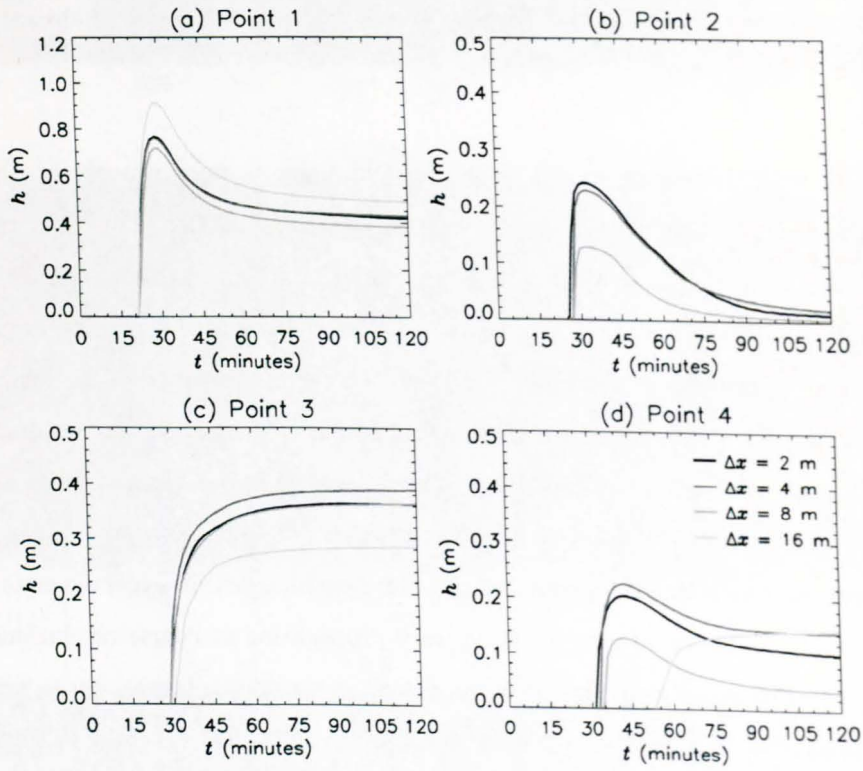

Figure 4.4: Evolution of water depths throughout the simulation at four control points, X1-4, at each resolution. Note the black line in each diagram represents the benchmark 2 m solution.

16 m model suggest that water release from point X1 is inhibited by the blockage of flow paths and the overestimation of building size in the coarse DEM. Furthermore, it is likely that resampling procedures reduce the definition of the road network and thus may cause the under-prediction of the shallow flow at point X2 in both 8 and 16 m model resolutions. This may explain the delayed flood wave response at point X4 at coarse resolutions and the apparent low RMSE of flood depths but low degree of model shoreline fit mentioned above. However, the maximum water depth predictions in high risk areas are well predicted in models up to 8 m which suggests urban areas are characterised by critical length scales and model performance deteriorates significantly at resolutions above these thresholds.

4.3.2 Greenwich, London, UK

The Greenwich tidal embayment has distinctly different characteristics from the Greenfield site and also portrays significant spatial variation in land use and, as a result, building size and distribution. From a hydraulic modelling viewpoint, the area is characterised by gentle slopes throughout and a combination of dense networks of interconnecting streets and large expanses of open land. Terraced residential housing dominates the south west region and industrial docklands dominate the western edges with large areas of open land in between. Figure 4.5 shows the location of the inflow points along each defence section and characteristic inflow hydrographs for the 1-in-100 year return period event for a number of the defences on the 5 m DSM.

Figure 4.6 shows the maximum predicted flood depths from a 1-in-100 year return period event with breaches lasting ~20 minutes over an event of ~2 hours. The results suggests that the model is able to simulate channelised flow between the complex terraced houses in the south west corner of the domain and flow over complex open land in the northern most regions. Furthermore, regardless of building size, the dominant flow paths appear to be ultimately governed by the street network. This effect is particularly noticeable in the east of the domain where the building axis length is ~20 m and the street width is ~5 m. There is also substantial evidence for complex local topography controlling storage patterns in the north of the domain and flows in this region are also substantially influenced by the Millenium Dome (visible as cicular feature east of X2) and Blackwall Tunnel (south of X2). Therefore, models at coarse resolution need to be able to resolve these complex channelised flow patterns and topographically controlled storage areas.

The spatial distribution of maximum predicted flood depths throughout the simulation at

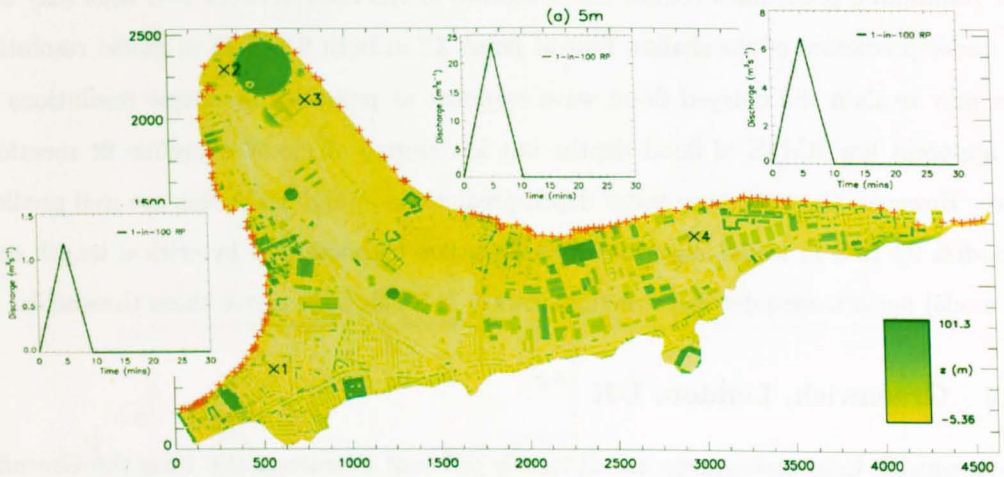

Figure 4.5: The 5 m DSM of the Greenwich study area showing the location of the four control points, X1-4, the middle of the defense sections (+) and characteristic flow hydrographs for a sample of the defenses for the 1-in-100 year flood event.

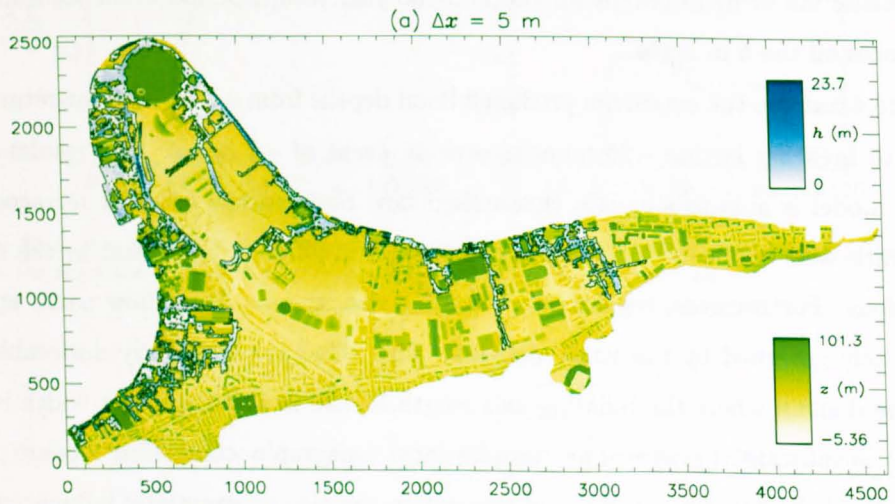

Figure 4.6: Maximum simulated flood extent from the high resolution, benchmark 5 m LISFLOOD-FP solution of Greenwich with the surface height (z) from the DEM shown as a grey scale overlain by water depths (h).

grid resolutions of 10, 25 and 50 m are shown in Figure 4.7. Detailed analysis of the Greenfield study site suggested that critical length scales exist within urban environments that control the propagation of flood waters. A visual comparison of maximum predicted flood extents for Greenwich imply a similar controlling mechanism. The 10 m resolution model appears to replicate the complex flow paths between buildings observed in the benchmark simulation in the south east and south west regions of the domain. In addition, this model appears to capture the topographic variations in areas of open land that determine the dominant modes of storage around the Millenium Dome. However, artificial deceleration of the floodwave through the dense street network is apparent in the reduction of the maximum flood extent in these regions.

On the other hand, the 25 and 50 m grid resolution models appear to significantly alter the dominant flow paths for floodwave propagation. Firstly, these coarse models portray substantial over-prediction of flood extents in areas of open land which is a result of excessive smoothing of topographic features in the resampling process. Secondly, prediction of water depths and flood extents in the regions where the street network controls floodwave progression, is poorly resolved. In particular, artificial blockages created by overestimating building size characterises the 25 m model result where water ponds behind these blockages (i.e. eastern area of Figure 4.7b) or the floodwave propagation is impeded (i.e. south west region). Notably, these artefacts are also visible in areas of the 50 m resolution model (i.e. eastern regions) but at this resolution, the buildings are underestimated in places which may lead to overestimates of floodwave propagation (i.e. south west corner). Furthermore, both the 25 and 50 m models exhibit emergent flow paths not apparent in the high resolution models (5 and 10 m) due to diversion of flows in new directions and excessive smoothing of topographic features.

Global model performance can be determined by analysing the temporal evolution of measures throughout the simulation compared to the benchmark 5 m simulation (Figure 4.8), as conducted for the Greenfield study. In contrast to the previous study, the RMSE and F^2 measures provide similar conclusions about the utility of coarse models in this area. The evaluation of flood depths shows a rapid deterioration in model performance initially to an RMSE of $\sim$1 m which then remains constant throughout the simulation. A similar response is seen in the model fit statistic (F^2) where model performance is consistently poor ($<$0.5) throughout the event at each resolution. These global performance measures suggest that the 10 m resolution model does not provide adequate predictions of flood depths or

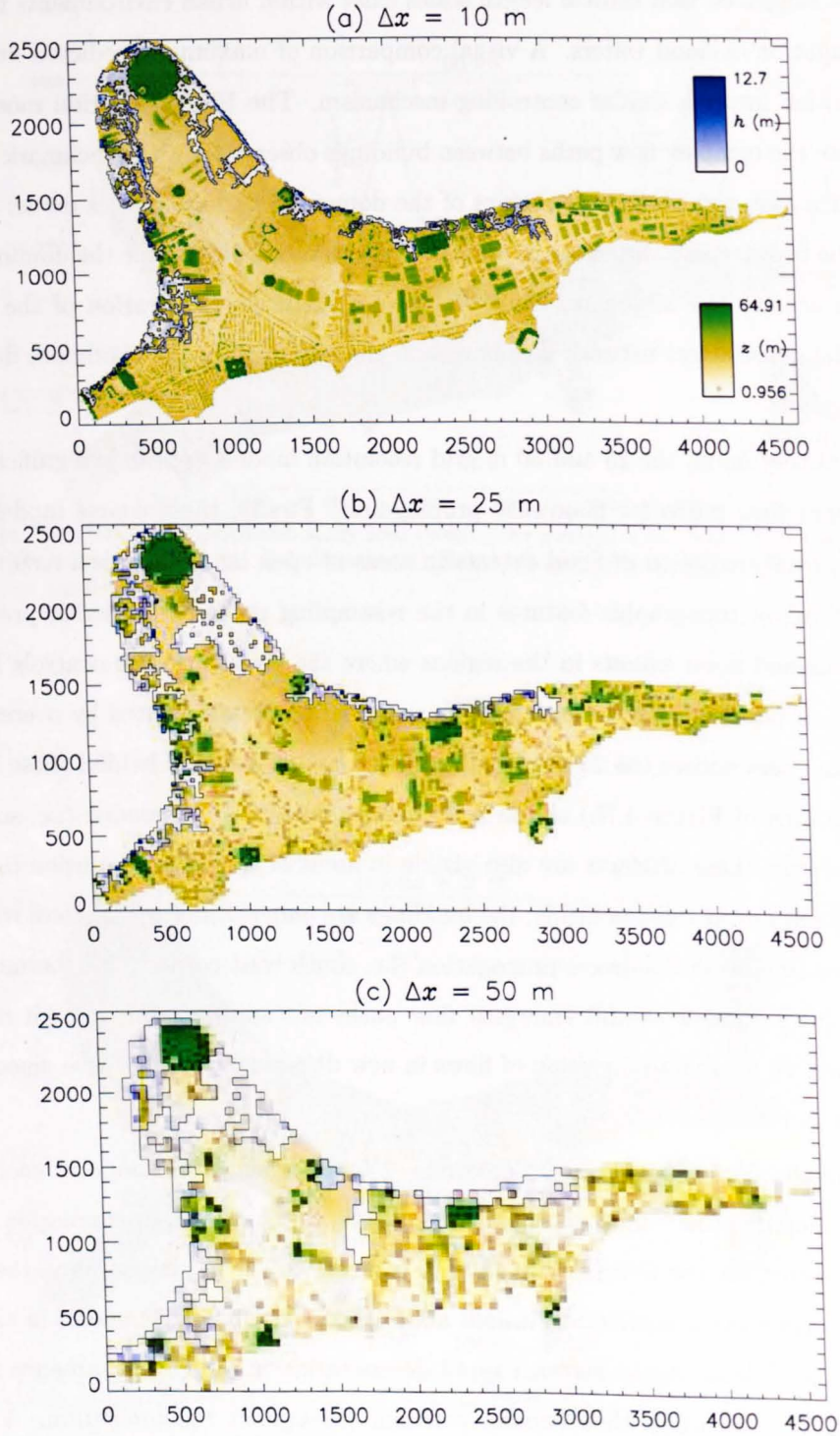

Figure 4.7: Maximum simulated flood extent from the 10, 25 and 50 m LISFLOOD-FP solutions with the surface height (z) from the DEM shown as a grey scale overlain by water depths (h).

extents. Although all the detailed flow paths in the densely urbanised areas are not resolved in the 10 m grid, it provides consistent patterns of flooding at most sites in the domain. Furthermore, the large RMSE across all resolutions may be, in part, caused by the flooding of Blackwall tunnel in the 5 m benchmark that is not observed in the 10 m model, or indeed in the 25 and 50 m models. As expected from the analysis at Greenfield, there is a systematic decrease in model performance with decreasing model resolution. Notably, the small reduction in performance from 25 to 50 m resolution which suggests there may be a degree of emergent behaviour at these resolutions. Global performance measures do not provide information about the prediction of local water level variability. This is necessary for assessing the utility of coarse resolution models for damage and loss estimation.

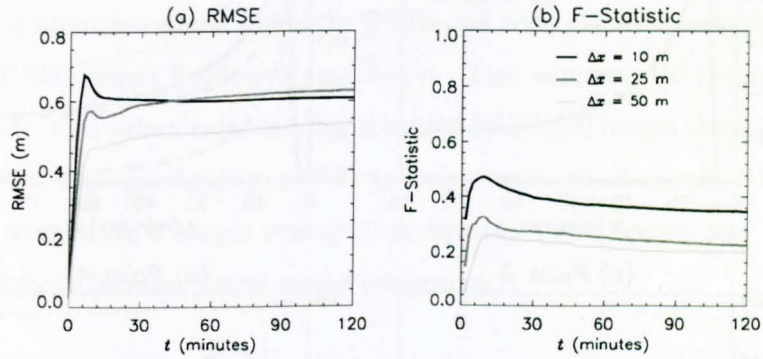

Figure 4.8: Evolution of global measures of model performance throughout the simulation at $\Delta x = 10$, 25 and 50m compared to the benchmark solution where *a*) is the RMSE of predicted flood depths and *b*) is the F^2 binary measure of fit of flood extents.

Subsequently, time series of water depth predictions at a number of locations with different characteristics within the model domain (see Figure 4.5 for locations) are compared. The area surrounding point X1 is characterised by terraced, residential housing, with walled, hydraulic disconnected gardens, connected by an irregular, narrow street network. Point X2 is an area of industrial docklands with buildings of XX m and large expanses of open land in between whereas point X3 is an area of paved, open land. Finally, point X4 is an industrial area with large buildings separated by narrow alleyways and streets. Echoing findings from the Greenfield site, the coarse resolution models show substantial over- and under-prediction of water depths at the control points. Furthermore, there is little discernable pattern across the four sites although the 25 and 50 m models consistently under-predict the water depths regardless of land use type.

Figure 4.9 shows the evolution of water depth at the four control points for the coarse

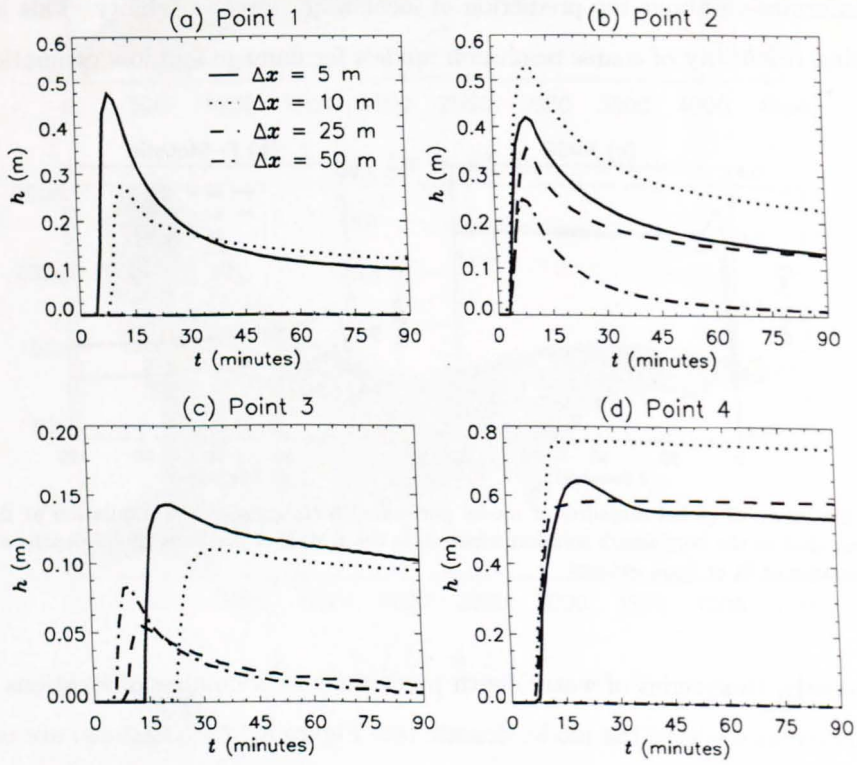

Figure 4.9: Evolution of water depths throughout the simulation at four control points, X1-4, at each resolution. Note the black line in each diagram represents the benchmark 5m solution.

resolution and benchmark model simulations. At point X1, the lack of water depth results at 25 and 50 m grid resolution is a direct result of not resolving the street network that conveys water to this location at these resolutions and the artificial blockages created by overestimating building size in this region. The 10 m resolution model predicts a later arrival time and a lower water depth, a consequence of increased tortuosity caused by the orthogonal nature of the solver in LISFLOOD-FP. Point X2 and point X4 shows similar responses at coarse resolutions with the 10 m model over-predicting water depths and the 25 and 50 m models under-predicting depths although all models appear to adequately predict floodwave arrival times. The shallow water depths and floodwave timings predicted at X3 are poorly resolved in the coarse resolution models but these shallow depths will have little impact on flood damage and loss estimates. This analysis combined with the global performance measures and qualitative comparison of the DEMs and flood maps suggests that the resolved street network determines floodwave progression. This supports the conjecture from the Greenfield study, that urban areas are characterised by critical length thresholds and model resolutions below this threshold do not adequately resolve flood dynamics through urban environments suggesting a simple reprojection strategy (see (Horritt and Bates, 2001a)) would be unlikely to increase coarse model performance.

4.3.3 Conclusions and recommendations

Results of model simulations at both Greenfield and Greenwich imply that urban areas are characterised by critical length scales that determine the dominant mode of water conveyance. At these specific sites, channelised flow along street networks seems to be the dominant mode and thus the length scale that needs to be resolved is defined by the width of the streets. Figure 4.10 shows the distribution of shortest building dimensions and shortest building separation distances for the Greenfield site. The shortest building dimension is calculated by approximating all buildings to rectangles and using the area and perimeter data available in MasterMap® to determine the rectangle dimensions. This suggests that, for this particular site, the critical length scale is of the order of 8m and is determined by both the shortest building dimension and the distance between buildings.

Figure 4.11 shows the results of the same analysis of the building distribution at the Greenwich test site. This suggests a critical shortest building dimension of $\sim$12 m and a building separation threshold of $\sim$5 m. In the context of the coarse resolution modelling results, this would explain the restricted flow observed in the resolved streets in the 10 m

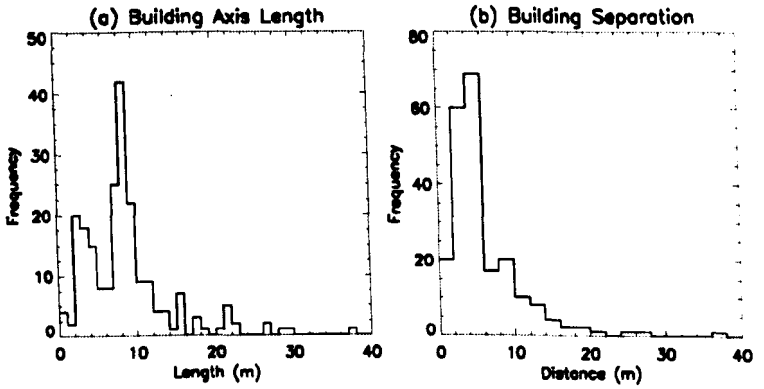

Figure 4.10: Distribution of length scales in the Greenfields area where *a*) is the distribution of shortest building dimension derived from MasterMap® and *b*) shows the distribution of shortest distance between buildings.

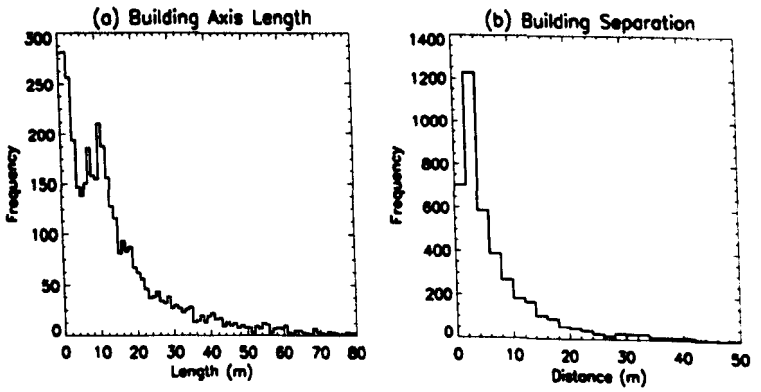

Figure 4.11: Distribution of length scales in the Greenwich area where *a*) is the distribution of shortest building dimension derived from MasterMap® and *b*) shows the distribution of shortest distance between buildings.

simulations and the complete lack thereof in the coarser resolution models. However, this does suggest that in order to adequately understand flooding at this site, a grid resolution of <10 m is required. This is commensurate with studies of other UK sites (see Yu and Lane (2006a)) and around the world (see Mark *et al.* (2004)). However, it is likely that this critical value will be site specific and needs to be determined prior to any urban hydraulic modelling study.

As set out in §1.4, the aim of this thesis is to develop computationally efficient yet accurate numerical models of urban environments. Therefore, it is necessary to consider relative model runtimes to determine an acceptable trade-off between model performance and efficiency. Table 4.1 shows the model runtimes, efficiency and associated performance for coarse resolution models at the two test sites. Model efficiency is defined as event length / computational time such that an efficiency of greater than 1 means the computational time is less than the length of the flood event. Clearly, the high time-step dependence on water depth and the larger domain size in Greenwich reduces the practical utility of models of <10 m resolution despite the poor performance of coarse resolution models. However, the good performance and high efficiency of the 8 m resolution model at Greenfield, coupled with the length scale analysis in this region provides a practical trade-off between computation time and model performance for models of this size with similar characteristics. Notably, these results suggest a detailed analysis of critical length scales and a consideration of model computation time is necessary *a priori* to determine the practical utility of a given model configuration.

	Resolution (m)	Event time (mins)	Runtime (mins)	Model efficiency	Minimum timestep (s)	Model performance ($F^{\langle 1 \rangle}$)
Glasgow						
	2	120	1087.08	0.11	0.003	-
	4	120	119.43	1.00	0.008	0.784
	8	120	4.77	25.16	0.028	0.629
	16	120	0.43	279.07	0.079	0.474
Greenwich						
	5	120	35080.01	0.003	<0.001	-
	10	120	1027.33	0.12	0.002	0.347
	25	120	17.78	6.75	0.013	0.223
	50	120	0.17	720.00	0.566	0.199

Table 4.1: Relative model efficiency, minimum time step and model performance at the end of the simulation for models of varying resolution at the Greenfield and Greenwich study sites run using a 2.0 GHz Pentium IV processor.

4.4 Sensitivity to urban media configurations

Floods in urban environments are clearly controlled by the building configuration and associated road network and resolving these features in coarse resolution models determines the success of any given model application. The preceding analysis has taken a naive approach to grid resampling without consideration of the quality of representation of the urban environment. Therefore, this section will examine the utility of different resampling strategies and combinations of elevation data to resolve flood information at coarse scales.

4.4.1 Greenfield, Glasgow, UK

Effects of gridding technique

In the analysis thus far, the default, nearest neighbour resampling strategy from the ArcGIS software package (Geographical Informations Systems) was employed with no consideration of the details of the technique. However, as noted above, predictions at coarse resolutions are subject to both quantisation and scale reduction errors and both need to be minimised. Thus, the method used to obtain coarse resolution DEMs thus may be influential in minimising that error. Urban environments are characterised by high spatial height variability and the method of grid interpolation will greatly affect the representation of buildings at coarse scales. Furthermore, there are a large number of possible techniques incorporated into standard geographical information systems (GIS) software packages. The effect of these techniques will be assessed by deriving coarse resolution grids using either (i) nearest neighbour interpolation, (ii) bilinear interpolation, (iii) mean or (iv) cubic spline convolution methods. Each method uses a different configuration of the high resolution cells for processing. The nearest neighbour method uses the value of the input cell defined as the closest to the centre of the output cell whereas the bilinear interpolation uses the four cells closest to the centre. The mean technique is defined as the mean of all cells in the output stencil and the cubic convolution applies a cubic spline function over the 16 cells nearest the centre of the output cell.

Yu and Lane (2006a) analysed model results using bilinear, nearest neighbour and cubic spline resampling techniques and found inconsistent results across model scales and throughout model simulations. Figure 4.12 shows the RMSE and fit statistic at 8 m resolution for each resampling strategy and suggests a consistent model response throughout the course of the simulation with different resampling techniques, although there is large variability

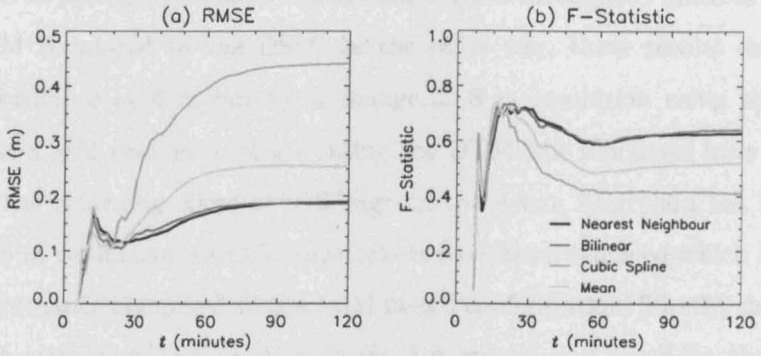

Figure 4.12: Evolution of the global measures of model performance at $\Delta x = 8$ m for each resampling strategy compared to the benchmark solution where *a*) is the RMSE of predicted flood depths and *b*) is the F^2 binary measure of fit of flood extents.

between the different methods which is also observed across all resolutions. The variability between methods is likely a result of the default stencil used in the averaging in each method in the ArcInfo GIS software package. The largest error is associated with the cubic spline interpolation which uses a 16-cell stencil whereas the smallest error is associated with 4-cell bilinear and 1-cell nearest neighbour stencil methods. Therefore, the original resolution and quality of the input data will have a significant effect on coarse resolution representations of topography. Internal verification of water depth predictions show a similar pattern, namely that the nearest neighbour method provides results most consistent with the benchmark data set for predicting high water stands (Figure 4.13). On the other hand, the bilinear approach appears to compromise the prediction of deep areas for improved predictions in shallow areas. However, it is clear that standard, 'off-the-shelf' resampling techniques provide no clear substantive improvement to model results over a naive resampling strategy.

Effects of data layer combinations

A DEM of an urban area can be considered as having two distinct layers with a mask of building locations and elevations overlaying the 'bare earth' terrain (e.g. a DTM). If the overall slope of the terrain is captured in coarse resolution 'bare earth' DTMs, then it may be possible to drive urban flood models with a 'bare earth' description of topography. This approach relies on the premise that the underlying topography, rather than the buildings, controls local flow paths. Figure 4.14 compares the global model performance of the nearest neighbour DSM model configuration with the nearest neighbour DTM driven models at 4, 8 and 16 m resolution throughout the simulation. These results show an increased ability of

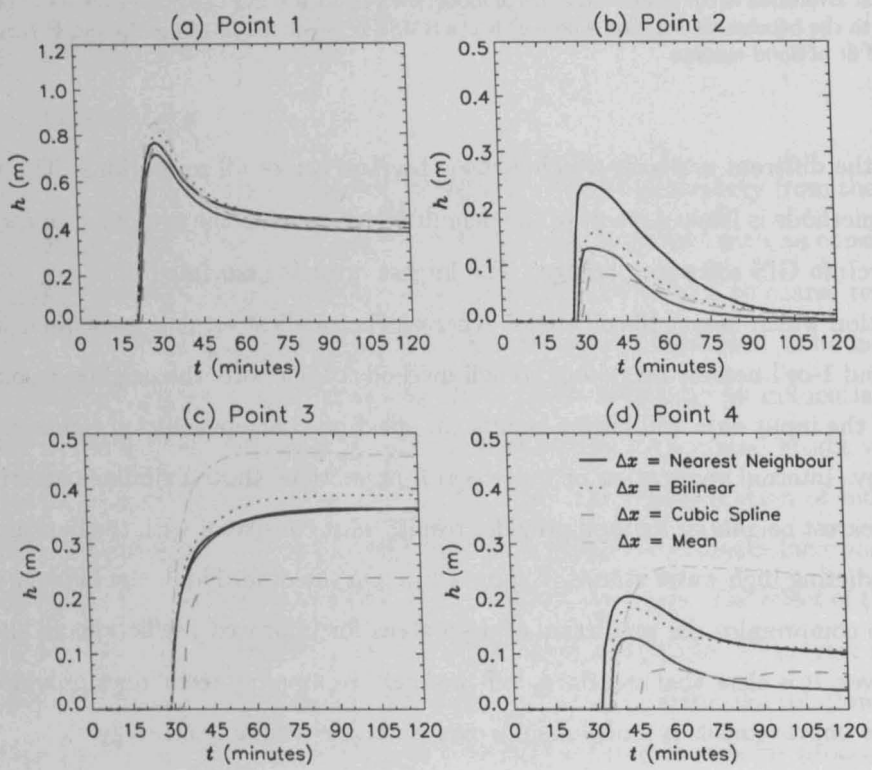

Figure 4.13: Evolution of water depths throughout the simulation at four control points, X1-4, at $\Delta x = 8$m resolution for each resampling strategy. Note the black line in each diagram represents the benchmark 2 m solution.

the 16 m model to predict both flood depths and extents throughout much of the simulation using the DTM compared to the DSM. In the same way, these results show a decrease in model performance at 4 m but little change at 8 m resolution using the 'bare earth' topography. At a grid resolution of 4 m using the DTM, the blockages have been removed meaning that the retarding effect of buildings on the urban floodplain has been removed. Similarly, at 16 m resolution, two blockage effects have been removed which act to increase the global performance compared to the DSM model configuration. Firstly, there is an effect associated with removal of buildings, as in the 4 m model, and secondly, there is an effect associated with removal the blockage artefacts introduced by resampling to coarse resolution. Notably, worse model performance is apparent at resolutions higher the critical length scale and increased model performance below this threshold using the terrain models. This would imply that the overall flood pattern is largely driven by the underlying topography whereas the local building locations only influence predictions around the buildings.

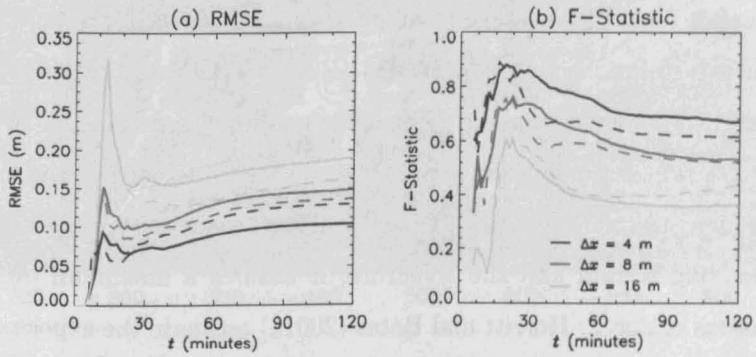

Figure 4.14: Evolution of global measures of model performance throughout the simulation at $\Delta x = 4$, 8 and 16m compared to the benchmark solution where *a*) is the RMSE of predicted flood depths and *b*) is the F^2 binary measure of fit of flood extents where the solid lines represent the DSM result and the dashed lines represent the DTM result.

Figure 4.15 shows the maximum water depth predictions on the 4, 8 and 16 m resolution DTMs overlain with the MasterMap® to provide the locations of the buildings that have effectively been removed. There is one main feature noticeable across all resolutions that highlights: (i) the lack of local information in global performance measures, and (ii) the problems of using DTMs to drive flood models. As the buildings have been removed, there is increased area available for storage and a substantial amount of water 'in' the buildings, most noticeably around X3. This increased storage area has the effect of decreasing water levels at X3 and X4 throughout the simulation. Furthermore, the removal of major buildings

like the school south of X2 has acted to create a new flow path, diverting water away from the road, leading to decreased water depths at X2 across all resolutions. These results would imply that the artificial blockages created when including buildings at resolutions below the critical length scale have a substantial effect on slowing flood propagation. In addition, it would suggest that a method capable of representing the buildings implicitly, such as porosity techniques (see Braschi *et al.* (1989) and McMillan and Brasington (2007)), would provide realistic results as long as the underlying topography used to drive the model was consistent across model scales.

The utility of a DTM-based model configuration is founded in the idea that the underlying topography is well represented in coarse models and ultimately controls the broad-scale pattern of inundation. However, local scale detail of flooding around buildings is not captured and indeed, the removal of buildings provides spurious areas for water storage. If an urban DEM can be considered as two distinct layers and the DTM captures the underlying, large-scale topographic features, it may be possible to consider the resampling of each layer separately (hereafter termed 'two-stage resampling') which allows the quantisation noise introduced at coarse resolutions to be quantified (Horritt and Bates, 2001a). Based on the findings thus far, a bilinear resampling approach is employed hereafter for resampling both the 'bare earth' DTM and the building mask. The two-stage method reduces the uncertainty of building size estimates at coarse resolutions as rather than smoothing the transition between the underlying terrain and the structure, it ensures a maximum overprediction of building dimensions of $\Delta x/2$. Horritt and Bates (2001a) estimate the expected quantisation noise at any given resolution by degrading the benchmark data set to the model resolution and comparing this back to the original benchmark data set using Eqn. 4.2. The results from this analysis at different times during the simulation are shown in Figure 4.16. These suggest that during the dynamic portion of the event model results at low resolutions are greatly affected by the blockage of flow paths and overestimation of building dimensions in both the direct and two-stage resampling methods. Furthermore, the lack of significant increase in model performance over the standard resampling approaches suggests that resampling the 'bare earth' DTM to resolutions greater than the critical length scale of ~8 m still averages out the road network blocking a significant flow path at this site. However, after the dynamic portion of the event, the coarse resolution models appear to be functioning as well as could be expected given the magnitude of the quantisation noise. At a site less dominated by steep slopes where the 'bare earth' topography varies more gradually, the two-stage resampling

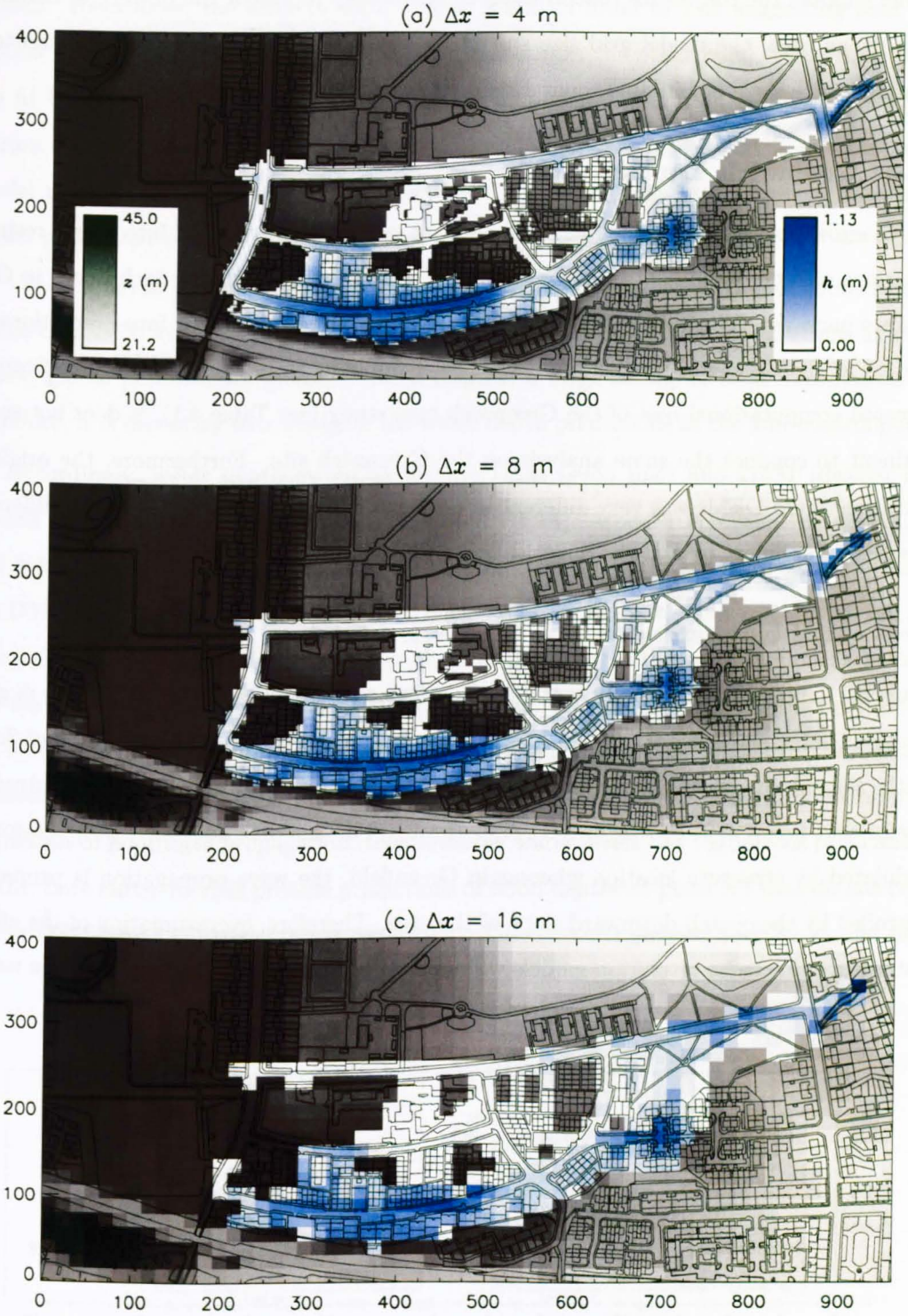

Figure 4.15: Maximum simulated flood depths from the 4, 8 and 16 m LISFLOOD-FP solutions using the DTMs with the surface height (z) from the DEM shown as a grey scale overlain by water depths (h).

method may however provide a significant increase in model performance. These results further support the conjecture that in order to adequately represent the pattern of flooding in an urban area, the model grid size should be of the order of the minimum of shortest building length scale or building separation distance at the individual site.

4.4.2 Greenwich, London, UK

The Glasgow case study highlighted the significant variability introduced into coarse respresentations of topographic data sets by the range of standard resampling techniques in GIS software packages. Theoretically, the same variability will be introduced into predictions of flooding at the Greenwich test site. As a result of preliminary testing and this significantly increased computational cost of the Greenwich case study (see Table 4.1), it does not seem pertinent to conduct the same analysis on the Greenwich site. Furthermore, the original derivation of the DEMs was very different in both cases. Therefore, only the use of different data layer combinations and the quantisation effect will be examined here.

Effects of data layer combinations

Figure 4.17 compares the evolution of global performance measures at 10, 25 and 50 m grid resolution using the 'surface' and 'bare earth' model configurations. The evaluation of flood depths suggests increasing model performance with increasing resolution which is contradictory to that found at the Glasgow test site. However, in this case floodwave propagation is modulated by structure location whereas in Greenfield, the wave propagation is primarily controlled by the overall downward slope of the area. Therefore, overestimation of the effect of structures in coarse resolution models will artificially retard flow, and thus increase water

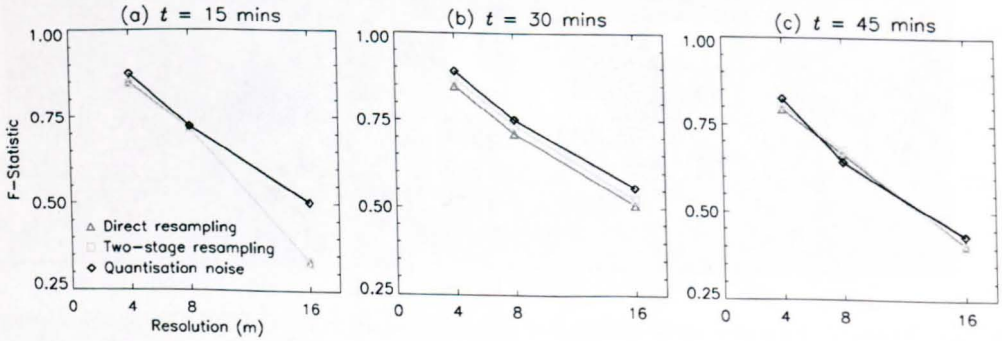

Figure 4.16: Fit between predicted and benchmark inundated area at *a*) $t = 15$, *b*) $t = 30$ and *c*) $t = 45$ mins for two different resampling strategies and the maximum expected taking quantisation noise into account.

depths which is compensated for by the removal of buildings in the 'bare earth' DTM-based models. Regardless, the error in water depth is still of order of 1 m suggesting poor prediction of the variable controlling damage estimates. On the other hand, when considering the fit between flood extents in the benchmark and coarse resolution models, the use of a terrain model appears to portray similar to the Glasgow test case, that is an decrease in model performance at resolutions higher than the critical length scale and an increase in model performance at grid resolutions lower than the critical threshold.

Visual analysis of flood depth maps suggests a systemic over-prediction of flooded extent in the coarse DTM-based models compared to their DSM counterparts. However, as noted above, global performance measures often disguise a large degree of local information and therefore, it is necessary to investigate the water depth predictions at the four control points.

Accordingly, water depth evolution for the DSM (solid line) and DTM (dashed line) models at multiple resolutions is analysed (Figure 4.18). Model response at points X2, X3 and X4 appears to display a systemic under-prediction of peak and final water depths in the DTM-based models compared to both their DSM counterparts and the benchmark 5 m simulation at all resolutions. The timing of water depth arrival appears stationary between the 'surface' and 'bare earth' model configurations which may be a result of the proximity of the control points to the defence overtopping and breach locations. Therefore, the removal of blockages, both actual and artificial, in coarse resolution DTMs at this site reduces the restriction of floodwave propagation, thus lowering water levels. At resolutions of 25 and 50 m, the 'bare earth' models provide predictions of flood depths at point X1 that do not occur in the DSM-based models at these resolution. These results suggest that at 25 and 50 m

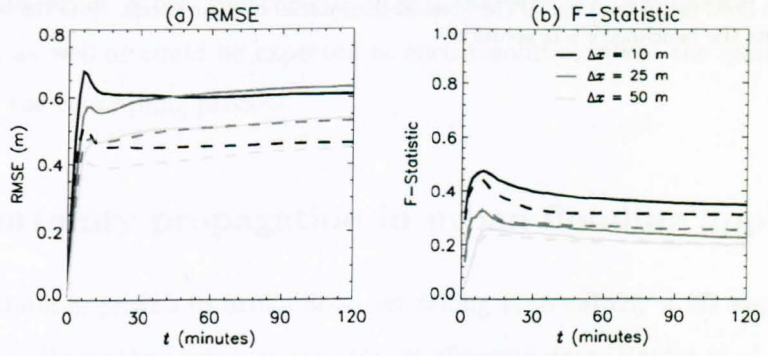

Figure 4.17: Evolution of global measures of model performance throughout the simulation at $\Delta x = 10$, 25 and 50m compared to the benchmark solution where *a*) is the RMSE of predicted flood depths and *b*) is the F^2 binary measure of fit of flood extents for the DSM (solid line)and DTM (dashed line) results.

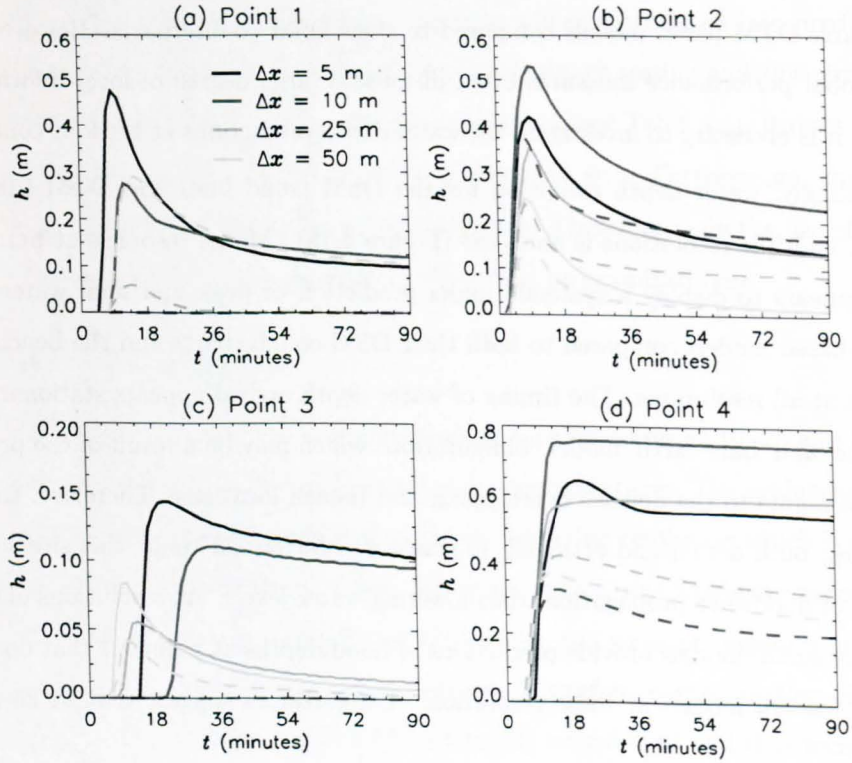

Figure 4.18: Evolution of water depths throughout the simulation at four control points, X1-4, at each resolution for the DSM (solid line) and DTM (dashed line) model configurations. Note the black line in each diagram represents the benchmark 5 m solution.

resolution, the DTM is adequately representing the actual underlying topography in these regions and thus, if buildings can be adequately represented in coarse resolution models (e.g. porosity techniques), there is scope for using such descriptions of topography.

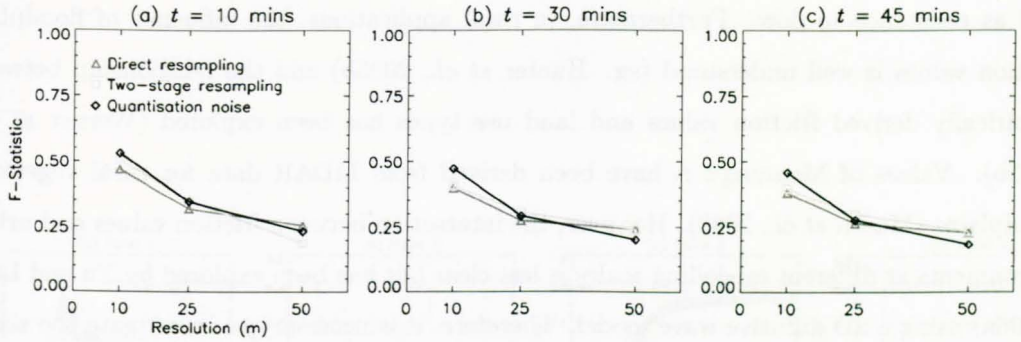

Figure 4.19: Fit between predicted and benchmark inundated area at *a*) $t = 10$, *b*) $t = 30$ and *c*) $t = 45$ mins for two different resampling strategies and the maximum expected taking quantisation noise into account.

Figure 4.19 shows the results of a 'two-stage' resampling approach using the DTM and MasterMap® building map for the Greenwich test site. Echoing findings from the Glasgow test site, the 'two-stage' resampling approach does not appear to provide substantial or systemic improvement over the standard bilinear resampling approach. Models at 10 m slightly under perform the quantisation noise at all times and a detailed look at the DEMs suggests this is a function of the orthogonal, 5-point stencil used in LISFLOOD-FP causing artificial blockage of flow in the densely urbanised areas around points X1 and X4. In this case, there appears to be little difference in the magnitude of the quantisation noise throughout the simulation. As water continues to propagate through the urban area for the duration of the simulation (unlike the Glasgow site where water ponds for much of the simulation), this result is not unexpected. In general, however, the models also appear to be performing as well as could be expected at each resolution given the quantisation noise introduced by the resampling process.

4.5 Uncertainty propagation in urban flooding applications

The most common approach to urban flood modelling is to employ a 2D approach at high resolution and calibrate the friction parameters to observed data (Haider *et al.*, 2003; Mignot *et al.*, 2006; Tarrant *et al.*, 2005). However, actual values of the friction parameters will be model and possibly scale dependent, as within models of varying complexity friction values

account for a variety of artefacts and unrepresented processes. In complex models, these friction values compensate for a combination of drag forces aligned in the flow direction and shear stresses acting on the sides of the flow, whereas in more simplified models the roughness value accounts for lack of physical process representation in the controlling equations as well as resistance to flow. Furthermore, in rural applications, the influence of floodplain friction values is well understood (eg. Hunter *et al.*, 2005b) and the relationship between empirically derived friction values and land use types has been explored (Werner *et al.*, 2005b). Values of Manning's n have been derived from LiDAR data for rural vegetated floodplains (Mason *et al.*, 2003). However, the interaction between friction values and urban evironments at different modelling scales is less clear but has been explored by Yu and Lane (2006a) using a 2D diffusive wave model. Therefore, it is necessary to investigate the shape of the response surface to changes in the Manning's n friction coefficient used in LISFLOOD-FP. Digital map data can be used to assign friction values to standard land use classifications based on empirically determined values from the literature (e.g. Chow, 1959) although these "standard" values of n are generally considered as a guide and calibrated values will be model and scale specific. In addition, this is only an appropriate method if the basis of derivation of the floodplain friction values uses the same assumptions as the model being applied to the floodplain. Furthermore, using a spatially distributed friction value based on land use classification at coarse resolutions incorporates further uncertainty as a result of the coarse representation of the land use regions. The sensitivity of model predictions to variations in friction parameterisation was therefore explored by conducting 30 simulations for each resolution and resampling method where the spatially uniform Manning's n varied from 0.01 to 0.1. A large range of friction values was employed to test if friction parameterisation can compensate for grid resolution effects. However, the range of friction values used is likely to introduce a bias into the resulting flood depth distributions as the benchmark value (0.035) is skewed towards the lower end of the parameter range. Nevertheless, the premise in this research is to investigate the utility of empirically derived values from the literature to provide guidance for practitioners attempting to determine appropriate parameter ranges *a priori* for operational purposes.

4.5.1 Greenfield, Glasgow, UK

At the Glasgow site, the results from this analysis are shown as variations in the predicted water levels at the four control points (Figure 4.20). The upper and lower lines represent the

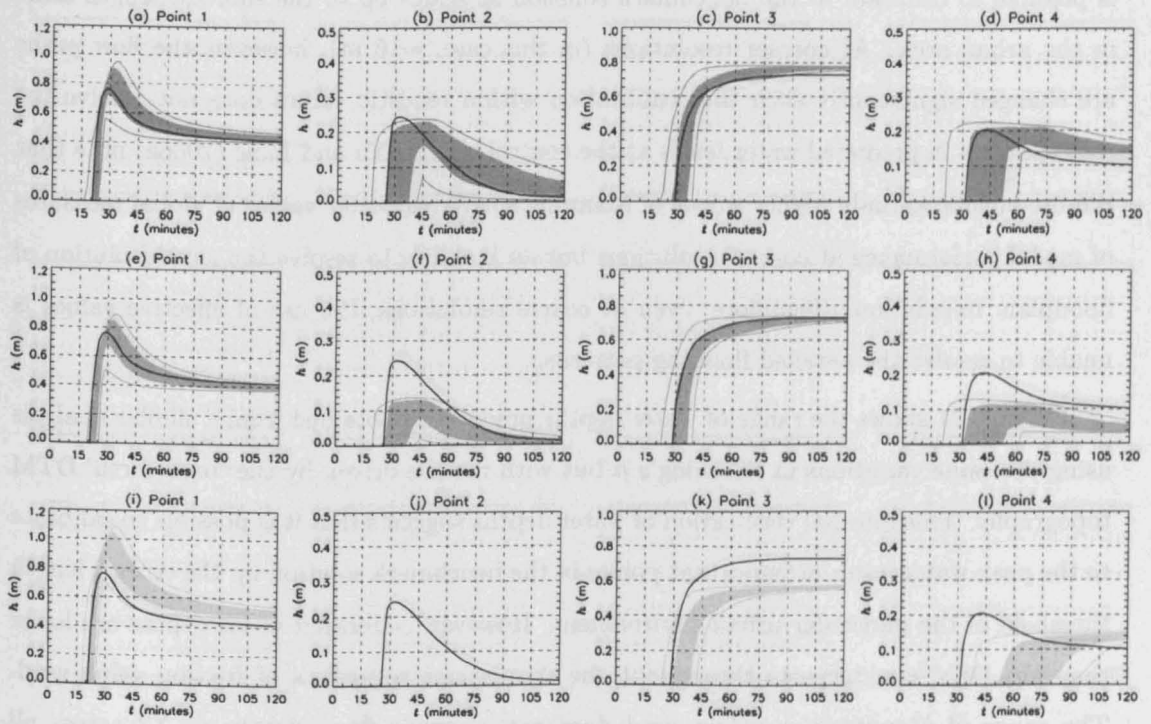

Figure 4.20: Percentile range of water depth at control points, X1-4, for the ensemble of varying friction coefficient simulations at $\Delta x = 4$ (panels a-d), 8 (panels e-h) and 16m (panels i-l). The solid lines represent the minimum and maximum water depths predicted over the ensemble, while the shaded area represents the 25-75 % percentile range. The solid black line represents the benchmark 2m solution.

maximum and minimum predicted water levels respectively and the shaded region represents the interquartile range of predictions. The benchmark solution data set is shown as the solid black line on each graph. At 4 m grid resolution, it is possible to calibrate to within 10% of peak water levels at all points and to final water levels at all but point X4. Similarly, in areas of deep water where damage will be greatest, the 8 m resolution model appears to calibrate to maximum and final water depths. However, although the water depth evolution is well predicted at X1, the 16 m models underpredict water levels at points X2 and X3, and cannot resolve floodwave dynamics at point X4. In general, it would appear that it is possible to calibrate to the benchmark solution at scales up to the shortest length scale in the urban area. At coarser resolutions (in this case, ~16 m), however, the flow paths are changed significantly such that calibration within realistic values does not resolve the discrepancies in predicted water levels at the control points. Yu and Lane (2006a) note that the use of substantially higher values of Manning's n yields better values of global measures of model performance at coarse resolutions but an inability to resolve the time evolution of floodplain inundation. Therefore, even at coarse resolutions, the use of effective values is unable to resolve the detailed flooding patterns.

Figure 4.21 shows the range of water depths predictions obtained from a similar analysis using the same variations in Manning's n but with models driven by the 'bare earth' DTM topography. This internal verification of water depths suggests that it is possible to calibrate to the peak water levels at important points in the benchmark solution up the critical length threshold of the particular urban environment. However, calibrated water depths are lower than the DSM counterparts throughout the simulations regardless of friction value used. The range of Manning's n values used does not reconcile flood depths at X2 across all resolution or X3 and X4 at 16 m resolution. This implies that an increase in friction value cannot account for the effect removal of blockages has on the flow patterns or pathways at resolutions below the critical length scale and that parameters become effective at resolutions above this threshold. Furthermore, without the benefit of observed data to constrain effective parameters, uncertainty in these parameters is high leading to effective parameter values that cannot be determined *a priori*.

The magnitude of the range in maximum water depths predicted in each model grid cell at any time during the simulation on the 'two-stage' resampling and DTM grids at 16 m grid resolution are shown in Figure 4.22. This is the uncertainty in predicted maximum water depth generated by forcing the models with a range of friction coefficients. As noted

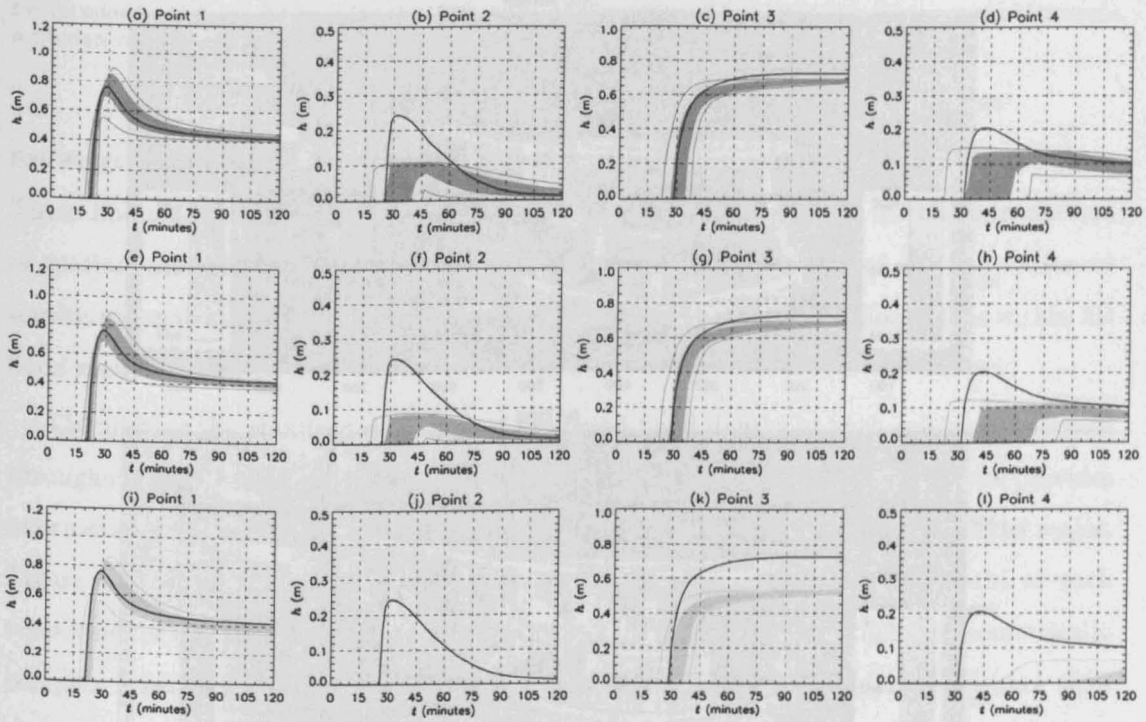

Figure 4.21: Percentile range of water depth at control points, X1-4, for the ensemble of varying friction coefficient simulations at $\Delta x = 4$ (panels a-d), 8 (panels e-h) and 16m (panels i-l) using the DTMs. The solid lines represent the minimum and maximum water depths predicted over the ensemble, while the shaded area represents the 25-75 % percentile range. The solid black line represents the benchmark 2m solution.

in Hunter *et al.* (2008), this confirms that changes to uniform parameter values invoke a spatially complex response in non-linear distributed models. Furthermore, the uncertainties associated with the topographic description introduce a further non-linear spatial response such that even though a model may replicate observed data at particular points, there is no guarantee of similar levels of performance throughout the whole model domain. Specifically, this provides further evidence that calibration of friction values cannot account for changes to flow paths brought on by the removal of buildings.

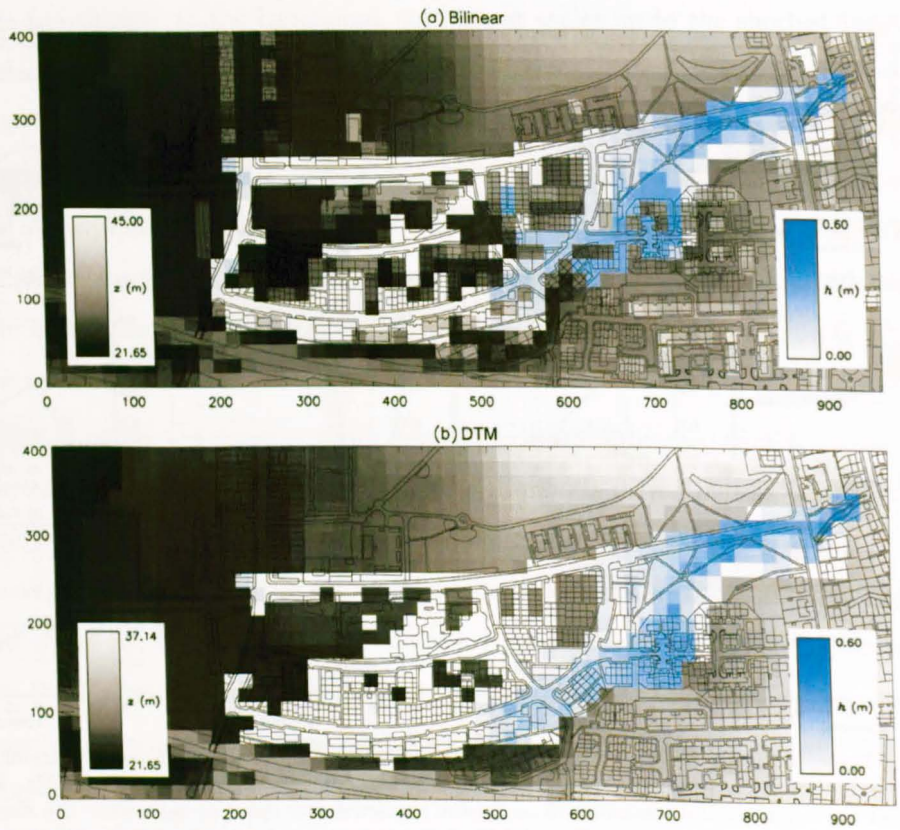

Figure 4.22: Magnitude of range in water depth (h) predicted by LISFLOOD-FP at 16 m resolution using a) the bilinear two stage resampling method or b) the DTM for the ensemble of varying friction coefficients.

The response surface to changes in the Manning's n friction coefficient across different scales is stationary with respect to the optimum value for changes in model resolution up to values roughly the size of the shortest building dimension (~8 m) (Figure 4.23). In addition, there is significant variability in model performance at 4 and 8 m grid resolution at friction values away from the optimum. Furthermore, Figure 4.23 suggests that at coarser resolutions the optimum friction value is significantly reduced and the shape of the response surface does

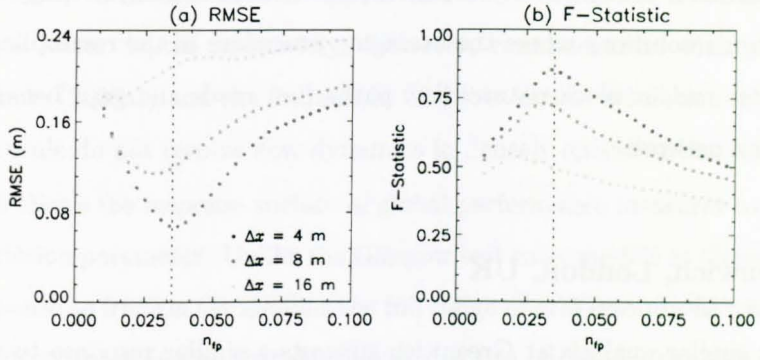

Figure 4.23: Model response of RMSE and F^2 for the ensemble of varying friction coefficient simulations at $t = 30$ mins for each resolution using the DSM model configuration. The dotted line represents the Manning's n friction value used in the benchmark 2 m solution.

not suggest any further improvement in model performance at high values of Manning's n. These findings are similar to Yu and Lane (2006a), suggesting scope for the introduction of spatially distributed friction values, increasing the dimensionality of any calibration or sensitivity analysis problem but recognising the effective nature of friction values within 2D flood models.

Calculating the standard deviation of predicted flood depths at each cell in the domain throughout the simulation for the range of resampling strategies and friction values provides information on the relative importance of each model configuration across all model scales. Figure 4.24 shows the mean of the standard deviation of predicted flood depths at each resolution for the different model configurations. This suggests that within the geometrically complex urban area, accurately representing the topography is of greater significance than the value of the roughness parameter within realistic bounds as found by Yu and Lane

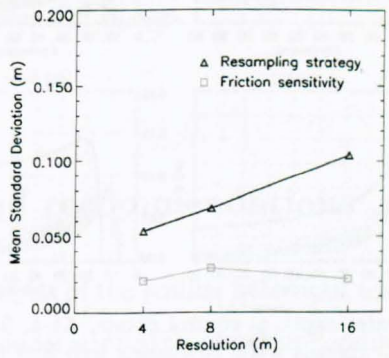

Figure 4.24: The mean standard deviation of predicted flood depths throughout the domain for the range of resampling strategies and ensemble of friction coefficients at each resolution ($\Delta x = 4$, 8 and 16m).

(2006b). Furthermore, the sensitivity of model results to resampling strategy is significantly greater at coarser resolutions where the averaging procedure in the resampling method can significantly alter and/or block natural flow paths (i.e. roads and gaps between buildings) within the urban network.

4.5.2 Greenwich, London, UK

Undertaking a similar analysis at Greenwich suggests a similar response to varying values of Manning's n for decreasing model resolutions (see Figure 4.25). The 10 m grid resolution model is near the threshold length scale of the Greenwich embayment such that in areas of open land (points X2 and X3) it is possible to calibrate to maximum benchmark water depths. However, in the dense urban network at points X1 and X4, this sensitivity analysis in Manning's n does not resolve peak water depths or the floodwave dynamics. Therefore, it would seem that friction calibration cannot account for misrepresentation of the building network, even if grid resolution is similar to, but larger than, the critical length scale. In

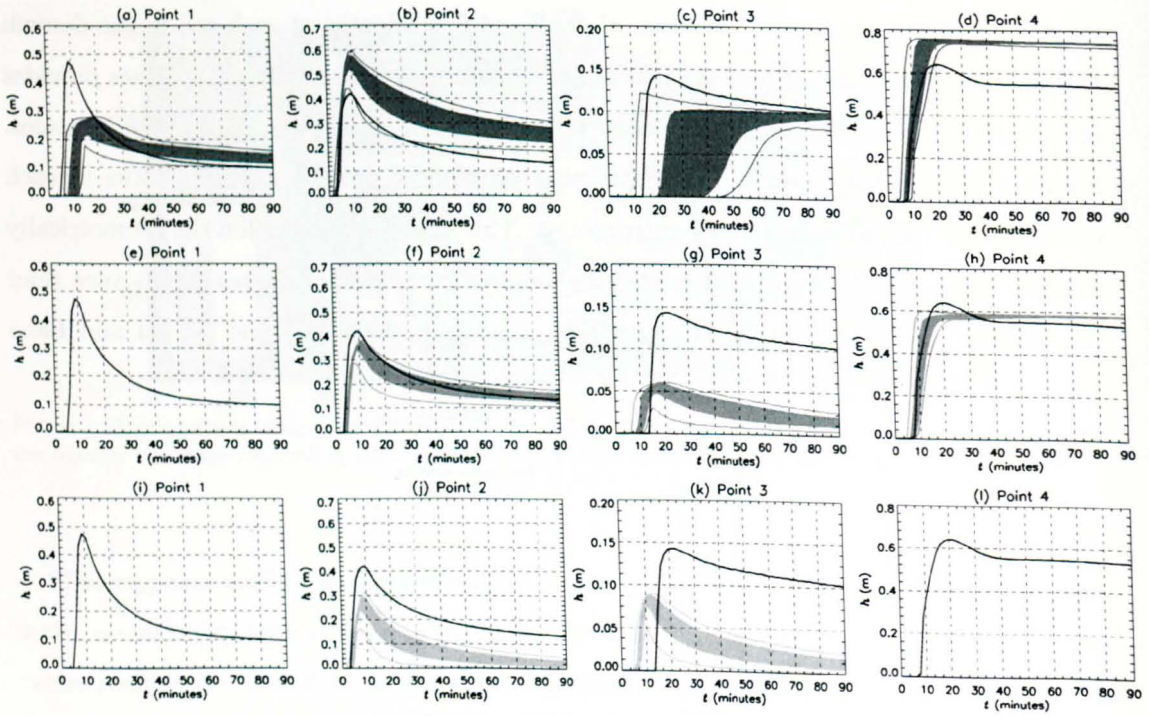

Figure 4.25: Percentile range of water depth at control points, X1-4, for the ensemble of varying friction coefficient simulations at Δx = 10 (panels a-d), 25 (panels e-h) and 50 m (panels i-l). The solid lines represent the minimum and maximum water depths predicted over the ensemble, while the shaded area represents the 25-75 % percentile range. The solid black line represents the benchmark 5m solution.

areas of open land, the coarse models appear to resolve floodwave dynamics even if they do not simulate water depths adequately. However, commensurate with previous studies (e.g. Yu and Lane (2006a)) and the findings in Glasgow, coarse resolution models above the critical length scale do not resolve flow dynamics in densely spaced urban areas.

Figure 4.26 shows the response surface of global performance measures to changes in the Manning's n friction parameter. Unlike the Glasgow test case, models at Greenwich exhibit a stationary response to friction throughout the full range of grid resolutions which is probably caused by the deep water depths that develop at this site. However, analysis of the building fabric suggested that a resolution of 10 m in this area of Greenwich may only just be high enough resolution to fully capture floodwave dynamics. Similarly, this suggests that models of flooding at Greenwich are highly dependent on the representation of the structures on the floodplain and that calibration cannot account for any deficiencies therein. Furthermore, similar to the analysis of Yu and Lane (2006b), the value of friction in any model of urban flooding will only be informative if the topography is resolved adequately within the model.

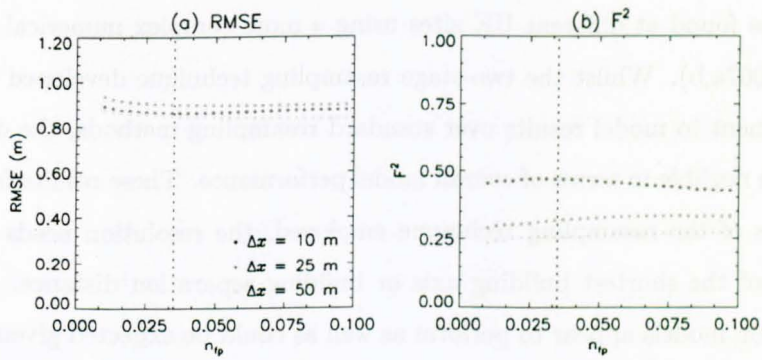

Figure 4.26: Model response of RMSE and F^2 for the ensemble of varying friction coefficient simulations at $t = 10$ mins for each resolution using the DSM model configuration. The dotted line represents the Manning's n friction value used in the benchmark 5 m solution.

4.6 Conclusions and recommendations

In this chapter, a rigorous analysis of the scaling behaviour and sensitivity to floodplain friction of a 2D storage cell type model applied to an urban flooding scenario has been presented. The topographically and topologically complex nature of the urban environment introduces ambiguity in model results when considering global measures of model performance. Consid-

eration of internal predictions of water depth is therefore necessary to understand detailed flood dynamics and evolution. In practical terms, estimates of flood damage for insurance and defence design applications are reliant on accurate predictions of water depths. The combination of global performance measures and internal predictions of water depth highlights an initial estimate of the minimum grid cell size for urban applications being roughly equal to the shortest length scale of the urban structures.

The method used in deriving a coarse resolution DEM from a high resolution, processed LiDAR output induces significant variability in the predicted flood extents and large differences in water level predictions thoughout the domain creating substantial variation across resolutions when compared to the benchmark solution. Indeed, standard GIS resampling techniques introduce a large degree of variability but here the results are consistent across model scales and throughout the simulation in contrast to previous findings (see Yu and Lane (2006a)). The utility of 'bare earth' digital terrain models to resolve these variations at coarse resolutions was explored and found to be particularly significant where the underlying topography ultimately controls floodwave propagation (e.g. Greenfield test site) in preference to building location and alignments (e.g. Greenwich test site). These conclusions are similar to those found at different UK sites using a more complex numerical model (Neelz and Pender, 2007a,b). Whilst the two-stage resampling technique developed here provides some improvement to model results over standard resampling methods, the differences observed here are neglible in terms of overall model performance. These results further suggest that regardless of the resampling technique employed, the resolution needs to be similar to the length of the shortest building axis or building separation distance. Nevertheless, coarse resolution models appear to perform as well as could be expected given the degree of quantisation noise.

As noted by Hunter *et al.* (2008), the lack of observational data for urban floods induces the need for modellers to consider a range of predictions from a physical range of friction values and how sensitivity of friction values varies across scales. Calibration of the friction parameter is the standard way of reducing uncertainty over model parameters and fitting model predictions to observed inundation conditions. Using a spatially uniform friction value to reduce uncertainty at coarse resolutions suggests a stationary model response up to the threshold grid cell size and a lack of identifiable values which provide a match to the benchmark solution at coarser resolutions. Furthermore, unrealistically high friction values do not appear to provide a feasible approach in this case as model performance decreases

substantially across the friction range used in this application, a result also demonstrated by Yu and Lane (2006a).

Finally, the topographical complexity of urban areas and computational restraints of high resolution grids requires that a compromise between detail and model runtime is achieved. This work suggests that model resolutions up to the characteristic length scale of building size and street width provide consistent and sufficiently accurate predictions of flooding. Furthermore, the accurate representation of the topography and topology is of greater importance than the individual value of the roughness parameter regardless of model resolution. Therefore, work should concentrate on the incorporation of high resolution topographic data into coarse resolution models through sub-grid scale approaches (see McMillan and Brasington, 2007; Molinaro *et al.*, 1994; Yu and Lane, 2006b). The development and testing of sub-grid scale techniques will be explored in Chapter 5 and the application of these techniques to real test cases will form the basis of Chapter 6.

CHAPTER 5

Sub-grid scale porosity approaches for finite difference models

The previous chapter highlighted the significant sensitivity of model results to coarse resolution representations of topography on urbanised floodplains, whether that be surface or terrain models. Specifically, coarse resolution models artificially increase the flood wave propagation speed but also dramatically alter flow direction and storage capacity due to blockage effects and coarse structure representation (see Yu and Lane (2006a) for further examples). The use of coarse resolution models stems from the practical need for efficient and fast numerical models for near real-time flood forecasting and wide-area application. The high computational cost incurred by fine resolution model grids limits the practical usage of such configurations. Therefore, model and application specific techniques are required to improve the utility of coarse resolution models and overcome the computational demands of higher resolution numerical models. As a result, a number of authors (Braschi *et al.*, 1991; McMillan and Brasington, 2007; Molinaro *et al.*, 1994; Yu and Lane, 2006b) have developed porosity techniques for hydraulic models of urban flooding and shown the utility of retaining sub-grid scale topographic information to more correctly represent urban flood propagation and storage. However, the variability in terms of algorithm complexity, topographic representation, and model dimensionality and structure means no guidelines exist to help decide on the appropriate technique for a given application. Furthermore, the limited data available for model evaluation and the lack of a clear evaluation methodology suggests that identifying an optimum configuration from competing model structures and sub-grid scale techniques is difficult.

The chapter that follows will develop a number of sub-grid scale porosity algorithms of varying complexity with increasing data and pre-processing requirements. The first technique (§5.1.1) is an extension of that developed by Braschi *et al.* (1991) to two dimensions and additionally includes the incorporation of the porosity into the flux calculation. Introduction of a water height dependency extends this technique further (§5.1.2), although the utility of this approach was noted by the same authors (but not formally developed by them). Section

5.2.1 details the development of a porosity that realises the effect of blockages and linear elements along boundaries of coarse resolution cells. The technique is inspired by that of Molinaro *et al.* (1994) although different in application. The final porosity technique (§5.2.2) is very similar to those developed by Yu and Lane (2006b) and McMillan and Brasington (2007). Model verification against the optimally stable LISFLOOD-FP code (Hunter *et al.*, 2005b) is used to objectively assess the sub-grid techniques. Moreover, the ability of the algorithms to represent common flow phenomena in urban environments (e.g. constriction, expansion etc.) is evaluated and the sensitivity of model results to issues of scale (e.g. sub-grid topography, structure orientation etc.) is also addressed. Such a framework allows a coherent evaluation methodology to be developed and subsequently applied to real-world flooding scenarios. It is hoped that through the research presented, a clear understanding of the utility of sub-grid scale porosity techniques may be produced. Given the limited data available for evaluation of these methods, the simplest explanation that matches the available observations should provide the basis for any guidance for practical application of these techniques.

5.1 Areal-based porosity approaches for flood models

5.1.1 Development of a simple porosity scaling

Braschi *et al.* (1989) developed a simple scaling parameter to represent the storage capacity of the urban area associated with a node in a 1D network model. This simple porosity algorithm scales the area available for storage based on the ratio of the unblocked area to the total area around a given computational node. Braschi *et al.* (1989) estimate the urban porosity from maps of the built environment. However, the availability of LiDAR datasets for urban areas provides 3D spatially distributed topographic data in discrete form, allowing a more accurate determination of the area available for storage. Given an elementary area A larger than the resolution of the underlying topography, a value of porosity can be defined for A. In discrete form, each cell in the computational domain can be assigned a porosity value based on the areas permanently blocked to flow in the higher resolution sub-grid scale topography. Computationally, the value of porosity (η) can be expressed as:

$$\eta(\mathbf{x}) = \begin{cases} 1 & \langle z \rangle > z_b \\ 0 & \langle z \rangle \leq z_b \end{cases} \tag{5.1}$$

$$\eta_A = \langle \eta(\mathbf{x}) \rangle \tag{5.2}$$

where η_A is the porosity of A, η is the blocked (0) and unblocked (1) state of each sub-grid cell in A, $\langle \eta(\mathbf{x}) \rangle$ is the mean of $\eta(\mathbf{x})$ over the coarse grid, $\mathbf{x}$ denotes the vector of spatial coordinates (x, y) of the fine scale grid, $\langle z \rangle$ is the elevation of the coarse resolution grid and z_b is the elevation of an individual sub-grid cell in A. Assuming that water will not breach above a certain height above the ground surface allows the determination of a time-invariant porosity for most floodplain applications given a few simple assumptions. Specifically within an urban area, it is possible to assume that water will not overtop the buildings and consequently, it is possible to define a fixed porosity based on high resolution maps of building layout (e.g. MasterMap®) fused with elevation data. It should be noted that water may enter buildings during a flood, further increasing the area available for storage. However, parameterising seepage into buildings requires detailed building information and introduces further uncertainty into the modelling process. Furthermore, Hingray *et al.* (2000) note that, in most cases, the velocity of the passing floodwave is significantly greater than the velocity of seepage into buildings and therefore, the latter can be disregarded.

The method developed by Braschi *et al.* (1989) and extended in Braschi *et al.* (1991), specified the flow in an urban environment as a network of 1D channels, such that applying a porosity scaling to the momentum equations was not necessary. As such, the porosity scaling was only applied to the storage term in the continuity equation. When considering a 2D model, where flow is explicitly modelled throughout the urban domain, such a simple scaling algorithm must also account for a reduction in the area available for flow. Therefore, the porosity approach derived in Eqns. 5.1 and 5.2 is extended to include this and is incorporated directly into both the momentum and continuity equations for floodplain flow in LISFLOOD-FP. The momentum transfer across the floodplain cells is determined by Manning's equation:

$$Q = \frac{AR^{2/3}S^{1/2}}{n} \tag{5.3}$$

where Q is the flow rate ($m^3 s^{-1}$), A is the cross-sectional area (m^2), R is the hydraulic radius (m), S is the bed slope and n is Manning's friction coefficient. In a regular, finite difference hydraulic model:

$$A = wd \tag{5.4}$$

$$R = \frac{A}{P} = \frac{wd}{w} = d \tag{5.5}$$

where w is the cell width (m) and d is the depth of water available for flow (m) and the wetter perimeter, P, is approximated by the cell width. Therefore, Manning's equation,

rewritten for LISFLOOD-FP, is:

$$Q = \frac{wd^{5/3}S^{1/2}}{n} \tag{5.6}$$

In the momentum equations, the porosity value is intended to represent the reduction in area available for flow between neighbouring cells and flow through individual cells. This requires an alteration of the areal based terms in the momentum equation:

$$A = wd\eta_A \tag{5.7}$$

$$R = \frac{A}{P} = \frac{wd\eta_A}{w\eta_A} = d \tag{5.8}$$

Therefore,

$$Q = \frac{wd^{5/3}S^{1/2}\eta_A}{n} \tag{5.9}$$

Thus far, the porosity scaling accounts for reduction in flow area at coarse resolutions but the area available for storage in any given cell will also be reduced by the presence of buildings. Therefore, the porosity value is also incorporated directly into the continuity equation such that:

$$\eta_A \frac{\partial h}{\partial t} = \tilde{\eta}_{A,x}\frac{\partial Q_x}{\partial x} + \tilde{\eta}_{A,y}\frac{\partial Q_y}{\partial y} \tag{5.10}$$

where

$$\tilde{\eta}_A = min\left(\eta_{A,i}; \eta_{A,i-1}\right) \tag{5.11}$$

where i represents the x or y subscript of the computational cell. Adopting a similar nomenclature to Molinaro *et al.* (1994), such a technique can be termed an *areal* porosity as it accounts for the reduction in area available for water storage and flow across a given computational cell. In applying this technique, the slope calculation in Eqn. 5.9 is determined by the slope of the coarse resolution topography but the magnitude of the fluxes is ultimately scaled by the porosity value. This assumes that the coarse resolution topographic variability in the DTM represents a good first order approximation to the high resolution terrain model.

5.1.2 Water height dependent areal porosity

The method outlined above assumes that areas are either blocked or unblocked throughout the full range of flow depths which removes the sub-grid scale complexity and assumes that a coarse DTM is an adequate representation of the small-scale topographic variability. It is clear that within an urban area, most urban structures exceed the maximum flow depth, making this a valid assumption. Nevertheless, there is a large degree of small horizontal and vertical topographic variability in urban and rural areas that may exert a large impact on

flow paths at low water depths. Braschi *et al.* (1989) noted the variability of small scale topography in urban areas so that the urban porosity may change with increasing water level to include water entering cellars, gradually flooding courtyards, etc. although this formulation was not explicitly tested in their work.

It is possible to define the porosity as above in Eqn. 5.1 but extend this to make η dependent on the depth of water. Such a variable porosity is analagous to the η defined by Defina (2000) representing the wet fraction of a partially wet cell incorporated directly into the St Venant equations for shallow water flow. However, the method proposed by Defina (2000) was implemented in an unstructured grid hydraulic model where elevations are defined at element vertices yielding sloping elements. Consider the elementary area A with an elevation based on the associated sub-grid topography (Figure 5.1), where the computational units are defined as horizontal. For a given height of water, h, above the minimum elevation of A, the porosity will vary based on the sub-grid topography and as a consequence, more topographic information will be stored in the porosity values.

$$\eta^h(\mathbf{x}) = \begin{cases} 1 & \langle z \rangle + h > z_b \\ 0 & \langle z \rangle + h \leq z_b \end{cases} \tag{5.12}$$

$$\eta_A^h = \left\langle \eta^h(\mathbf{x}) \right\rangle \tag{5.13}$$

where η_A^h is the porosity of A at water height h, η is the blocked (0) or unblocked (1) state of a sub-grid cell at water height h, $\mathbf{x}$ denotes the vector of spatial coordinates (x, y) at the sub-grid scale, $\langle z \rangle$ is the minimum elevation of A and z_b is the elevation of the sub-grid cells in A. This is implemented in LISFLOOD-FP as in Eqns. 5.9 and 5.10. Practically speaking, the free surface slope is determined based on the coarse resolution digital terrain and the inter-cellular fluxes are consequently scaled by the porosity value. The porosity values are determined *a priori* by applying a planar water surface to each coarse grid cell on a cell-by-cell basis at any number of discrete water height increments between which the function is assumed linear. LISFLOOD-FP uses this data in the form of a look-up table for each water height to determine the porosity at any given time step. As in McMillan and Brasington (2007), a corresponding lookup table for the water height based on the cell volume is also required as storage cell models update the cell water height based on changes in volume over a time step. Considering the same generalised topography as in McMillan and Brasington (2007) (Figure 5.1a-b), and the associated variation in porosity and volume (Figure 5.1e), the method implemented here is physically different. In McMillan and Brasington (2007),

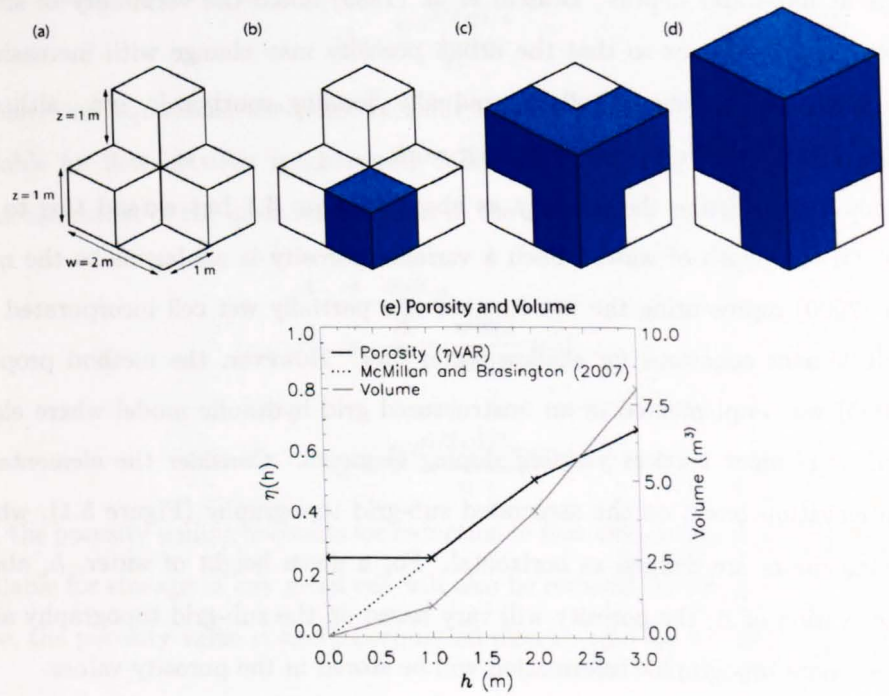

Figure 5.1: Variation in porosity and volume for an idealised 2 m cell based on 1 m sub-grid scale topography where (a)-(d) show the sub-grid scale resolution topography and flood depth variation and (e) shows the variation in porosity and volume with water depth compared to McMillan and Brasington (2007).

the porosity of a cell with an infinitesimally small, but greater than zero, water depth is zero and assumed linear up to the first increment calculation. This leads to an underestimation of porosity up to the first water height increment, which will have the added impact of artificially reducing inter-cellular fluxes. However, in the method developed here, once water has entered the cell, it has the same porosity throughout the range up to the first increment (see Figure 5.1e) which should provide better estimates of inter-cellular fluxes.

Incorporating a dependency on local water height into the value of urban porosity recognises the importance of small scale vertical and horizontal elevation variability. This approach should, therefore, more accurately represent small scale storage and flow on a coarse resolution model grid. Furthermore, the ability of the model to resolve shallow flows and flows over sloping terrain will be increasingly improved as model resolution decreases and topographic averaging increases.

5.2 Boundary-based porosity approaches for flood models

The areal porosity techniques, outlined above, rely on the premise that the flow between adjacent computational cells is controlled by the total cellular area available for flow. However, as fluxes are calculated at cell boundaries, the topography at the boundary is in fact the controlling feature for flow between cells (see also McMillan and Brasington, 2007; Molinaro *et al.*, 1994; Yu and Lane, 2006b). A porosity value can then be determined for each cell edge to control both the direction/orientation of flow and its magnitude. An additional feature of introducing a porosity based on the boundary topography is that, theoretically, this should reduce the impact of instantaneous wetting of caorse grid cells observed in coarse resolution configurations of storage cell models (see Bates and De Roo, 2000; Hunter *et al.*, 2005b). The section that follows develops two methods of incorporating the boundary porosity, the latter of which represents a method similar to that presented in McMillan and Brasington (2007).

5.2.1 Development of a linear porosity concept

Molinaro *et al.* (1994) noted the blockage and reduced storage effects of urban environments and thus defined two parameters, η_l and η_A, as the *linear porosity* and the *areal porosity*, respectively, of a given built up area. It is clear that the height of water in any given cell is scaled by the *areal porosity* and the fluxes between cells are scaled by the *linear porosity*. Using the concept of *linear porosity* to determine the cellular net flux, a linear porosity η_l can be defined as the ratio of unblocked area to blocked area of the sub-grid topography at the boundary of a coarse resolution model grid cell.

$$\eta\left(\mathbf{x},\mathbf{d}\right) = \begin{cases} 1 & \langle z_l \rangle > z_{l,b} \\ 0 & \langle z_l \rangle \leq z_{l,b} \end{cases} \tag{5.14}$$

$$\eta_l\left(\mathbf{d}\right) = \langle \eta\left(\mathbf{x},\mathbf{d}\right) \rangle \tag{5.15}$$

where η_l is the linear porosity of A, η is the blocked (0) or unblocked (1) state of a sub-grid cell at the edge of A, $\mathbf{x}$ denotes the vector of spatial coordinates (x, y) at the sub-grid scale, $\mathbf{d}$ denotes the direction out of the grid cell (N,E,S,W), $\langle z_l \rangle$ is the elevation of A and $z_{l,b}$ is the elevation of the boundary sub-grid cells in A at a given boundary. This formulation of η_l replaces the value η_A in Eqn. 5.9 for each direction out of any given computational cell. Such a formulation will necessarily represent the flows between cells more accurately than

a porosity based on the total unblocked area of the computational cell (Eqns. 5.1 and 5.2). However, it does assume that the stencil of floodwave propagation is limited to one sub-grid cell width, an assumption that will become increasingly limited at very coarse model resolutions. The volume of water in a given cell is scaled as a function of the area available for storage based on the sub-grid topography (i.e. η_A) calculated as in Eqns. 5.1 and 5.2 and applied to the continuity equation as in Eqn. 5.10.

5.2.2 Water height dependent boundary porosity

As discussed above, topographic irregularities in A may exert a large impact on the overall flow dynamics through an area highlighting the need for a porosity dependent on water height (similar to the ϑ and η functions in Defina (2000)). Consequently, as boundary porosities (η_l) determine inter-cellular fluxes, a water height dependency is clearly necessary in any such formulation (see Eqns. 5.16 and 5.17). As resampling ratios between the resolution of the coarse cell A and the sub-grid resolution increase, it is likely that the influence of boundary topographic variations in the averaging process will decrease. Therefore, less information about the sub-grid boundary elevations is retained in the coarse resolution grid cells and boundary fluxes will represent broad scale flow features rather than fine scale flows. Therefore, incorporating boundary topographic effects by supposing a water height dependency in this region will necessarily provide a more realistic representation of flow between neighbouring regions.

$$\eta^h(\mathbf{x},\mathbf{d}) = \begin{cases} 1 & \langle z_l \rangle + h > z_{l,b} \\ 0 & \langle z_l \rangle + h \leq z_{l,b} \end{cases} \tag{5.16}$$

$$\eta_l^h(\mathbf{d}) = \langle \eta(\mathbf{x},\mathbf{d}) \rangle \tag{5.17}$$

where η_l^h is the linear porosity of A at water height h, η the blocked (0) or unblocked (1) state of a sub-grid cell at the edge of A at a given water height h, $\mathbf{x}$ denotes the vector of spatial coordinates (x, y) of the sub-grid scale, $\mathbf{d}$ denotes the direction out of the grid cell (N,E,S,W), $\langle z_l \rangle$ is the minimum elevation of the sub-grid cells in A, $z_{l,b}$ is the elevation of the boundary sub-grid cells in A at a given boundary. Similarly, the storage volume in the elementary area is also defined as a function of water height as in Eqns. 5.12 and 5.13.

This formulation will necessarily represent the flows between cells more accurately than a porosity based on the total unblocked area of the computational cell. The volume of water in a given cell is scaled as a function of the area available for storage based on the sub-grid

topography (η) calculated as in Eqn. 5.1. Eqn. 5.18 provides the detailed application of such an approach to the LISFLOOD-FP governing equations for floodplain flow.

$$\eta_A \frac{\partial h}{\partial t} = \tilde{\eta}_{l,x} \frac{\partial Q_x}{\partial x} + \tilde{\eta}_{l,y} \frac{\partial Q_y}{\partial y} \tag{5.18}$$

where

$$\tilde{\eta}_l = min\left(\eta_{l,i}; \eta_{l,i-1}\right) \tag{5.19}$$

where $\tilde{\eta}_l$ is determined as in Eqn. 5.11 using the linear porosities and η is from Eqn. 5.1. It is computationally simple and physically feasible to implement this boundary porosity approach within a framework dependent on water depth as detailed above for a simple areal porosity as an extension to the original formulation.

A number of authors have noted the artificially increased flood propagation speeds at coarse resolutions in storage cell diffusion based models (Bradbrook *et al.*, 2004; Hunter *et al.*, 2005b; Yu and Lane, 2006a). This effect was countered in JFLOW (Bradbrook *et al.*, 2004; Yu and Lane, 2006a) by including a percentage wet parameter based on grid-scale effective velocities and in LISFLOOD-FP by introducing an unconditionally stable time stepping procedure (Hunter *et al.*, 2005b). In the former, the percentage wet parameter is derived using velocities based on a non-numerical stability criterion that is not applicable to the equations the model solves (see §2.2.3 for a more detailed discussion). In the latter formulation, coarse models still over-predict the flood extent at any time by one grid cell width. Therefore, although the linear porosity approaches will resolve fluxes between cells more physically, the model may still over-predict flood propagation at coarse resolutions as there is nothing controlling the rate of flow across a given cell to the other boundary.

5.3 Summary of techniques

A number of authors have developed similar porosity techniques for a variety of models of different complexity dependent on application and Table 5.1 summarises how the porosity techniques developed here relate to the techniques already in the literature. The fixed areal porosity (ηFIX) developed here is an extension to two dimensions of the method originally proposed by Braschi *et al.* (1989) for a 1D road network model. The original technique was used to represent the area available for water storage associated with each node in the network whereas in this case, the porosity value is used to represent blockages smaller than the model grid cell which reduce the area available for storage. Furthermore, it is also

explicitly incorporated into the momentum equation for flow between floodplain cells unlike the 1D road model developed by Braschi *et al.* (1989) where such a method was not required. The possible importance of incorporating a water height dependency into the areal porosity (ηVAR) was recognised by Braschi *et al.* (1989) to represent water ponding in cellars and buildings themselves. In this case, the water height dependency is to represent small scale horizontal and vertical topography variability that affect both the storage of water on the floodplain and the propagation of the floodwave through the urban fabric.

Molinaro *et al.* (1994) initially developed the concept of linear and areal porosities for a fully hydrodynamic finite difference 2D model; the concept of which was used here to develop the ηBOUND and ηBVAR sub-grid porosity approaches. The fixed linear porosity scales the fluxes out of any given cell in each direction based on individual boundary porosities and the water storage in the cell is scaled by the areal porosity (ηBOUND). The original formulations were derived in a different manner than presented here but form the basis of the concept. The water height dependent boundary porosity (ηBVAR) approach is similar to the technique developed in McMillan and Brasington (2007) but does not require incorporation into the flow limiter equation as the adaptive time stepping routing in LISFLOOD-FP negates the necessity for such a formulation.

These techniques represent a progression of increasing complexity from the simple areal based fixed porosity approach to the incorporation of boundary effects and the influence of small scale vertical topographic variability into the porosity value. In addition, this research represents the first time the methods are developed in a single model structure and consistently implemented to allow comparative testing.

5.4 Verifiable solutions for model testing

To assess model performance effectively, we require a structured sequence of numerical experiments that are simple enough to isolate the effect of the algorithm being studied but complex enough to provide a rigorous and realistic test of the model. A number of studies (Bradford and Sanders, 2002; Horritt, 2000b, 2002; Hunter, 2005) have shown the utility of analytical solutions to the governing flow equations as a rigorous test of model and algorithm performance. These analytical tests allow the effects of numerical techniques to be assessed in isolation from additional sources of uncertainty, such as friction parameterisation, boundary conditions, bed topography and inaccurate process representation, which all affect

Method	Description	Equations	Derivation and application
ηFIX	A fixed areal porosity value for each coarse computational grid cell based on any sub-grid resolution and on the location of blockages to flow throughout all flow depths that is applied to both the momentum and continuity equations	5.1, 5.2, 5.9, 5.10, 5.11	Adapted for 2D from 1D model proposed by Braschi *et al.* (1989, 1991)
ηVAR	A height variable areal porosity value for each coarse resolution computational grid cell based on the sub-grid scale topography and derived from a coarse resolution DTM using the minimum of the sub-grid resolution input DTM that is applied to both the momentum and continuity equations	5.12, 5.13, 5.9, 5.10, 5.11	Idea mentioned in Braschi *et al.* (1989) but not derived or tested by them
ηBOUND	A linear porosity value determined for each direction out of a coarse resolution cell based on the location of permanent blockages to flow throughout all flow depths that is applied to the momentum equation. Uses the areal porosity (ηFIX) to scale the area available for storage in the continuity equation	5.14, 5.15, 5.9, 5.18, 5.19	Derived from a method proposed by Molinaro *et al.* (1994) for a full 2D flood model
ηBVAR	A linear porosity value determined for each direction out of a coarse resolution cell based on the sub-grid scale topography and derived from a coarse resolution DTM using the minimum of the sub-grid resolution that is applied to the momentum equation. Uses the areal porosity (ηVAR) to scale the area available for storage in the continuity equation	5.16, 5.17, 5.9, 5.18, 5.19	Similar to McMillan and Brasington (2007) and Yu and Lane (2006b) developed for 2D diffusion wave models but with minor adjustments

Table 5.1: Summary of the porosity techniques developed here compared to published techniques

the model. Unfortunately, for the problem under consideration here, the need to include micro-topography and large-scale floodplain structures in any testing regime will introduce non-linearities into the model configuration, removing the possibility of using analytical solutions for algorithm testing. As a result, a sequence of numerically verifiable tests to highlight the utility of the various porosity algorithms are devised and implemented.

In a one-dimensional sense, flows in urban areas are characterised by constrictions and expansions along roads and at road junctions (Braschi *et al.*, 1989) and in a two-dimensional sense, by flows around prominent urban structures. Therefore, the ability of the porosity algorithm to simulate constriction, expansion and complex flow structures around obstacles needs to be assessed objectively. Hunter *et al.* (2008) have shown the consistency of LISFLOOD-FP with relation to more complex numerical schemes for propagation of flood flows around urban structures at fine scales. Furthermore, Prestininzi (2008) has shown the utility of a diffusion wave model for simulating an impulsive dam break wave over complex topography where the model adequately predicts floodwave arrival times and peak water levels. In both cases, the diffusion wave models fail to represent high-frequency oscillations, bores and wave reflections but these can be regarded as 2^{nd} order effects that have a small influence on the overall dynamics of the event at larger scales and have little impact on assessments of possible flood damage. In addition, Hunter *et al.* (2008) showed that shock-capturing numerical schemes do not produce results substantially different from non shock-capturing schemes in full 2D hydrodynamic models. Consequently, the performance of the porosity algorithms can be evaluated using verifiable tests of the prominent modes of flow in urban areas. The verification of model results takes the form of Ch. 4 and as in Yu and Lane (2006b), where the performance of coarse resolution models is assessed with respect to a high resolution benchmark solution.

5.4.1 Flow around structures

The simulation of flow fields around a complex configuration of buildings requires that the water levels around these structures are represented accurately. Consequently, the performance of the porosity algorithms to represent flow around a prominent structure is assessed objectively. Flooding of a domain of 120 m x 120 m with one building centred at [55, 65] with dimensions 10 m x 10 m, at a resolution of $\Delta x = 2$ m is driven by a wave of constant velocity of 0.5 ms^{-1} with a Manning's n of 0.035 on a horizontal plane ($S_0 = 0$). Coarse resolution models often portray blockage of flow paths, redirection of flow and misrepresen-

tation of storage area. To assess the performance of the simple areal sub-grid algorithm at coarse resolutions, the computational grid is resampled to DEMs at Δx = 5, 10, 20 and 40 m resolution, using the two-stage resampling technique outlined in Ch. 4. Figure 5.2 shows the computational grid at a number of resolutions, to highlight the resampling effect on individual buildings, and the associated porosity values in the coarse resolution models.

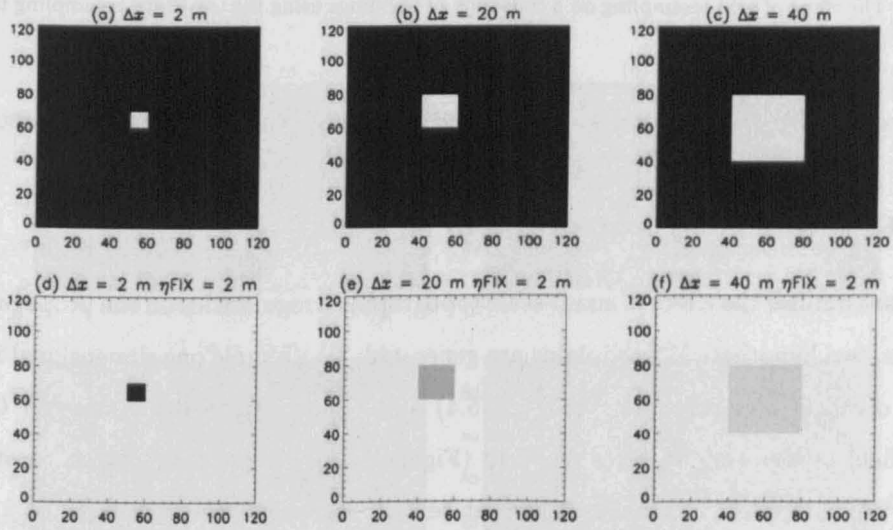

Figure 5.2: The effect of grid resampling on a single building using the two-stage resampling technique and the associated porosity values where (a) and (d) show the 100 m^2 building on the 2 m grid, explicitly and using porosity, (b) and (c) show the effect of resampling to 20 m and 40 m resolutions respectively and (e) and (f) show the associated porosity values. Note the grey scale on plots (d) to (f) represent a decrease in porosity values.

5.4.2 Multiple blockages, constrictions and expansions

The propagation of a flood wave through a series of blockages, constrictions and expansions should identify the ability of the porosity algorithms to accurately represent the wetting front and the water height variation upstream and downstream of these features. It should be noted, however, that LISFLOOD-FP does not incorporate local acceleration or inertia and thus will not represent hydraulic transients such as shocks (Hunter *et al.*, 2008) which may occur when a floodwave impacts a building. A wave of constant velocity of 0.5 ms^{-1} is propagated over a horizontal plane (S_0 = 0) from the western edge through a domain of 120 m by 120 m with a Manning's n of 0.035. Based on the length scale analysis in Ch. 4, the spacing between buildings and the building dimensions on UK floodplains can be approximated as ~5 m. Therefore, the benchmark solution is configured at Δx = 5 m. Figure 5.3a show the aligned building configurations within the 5 m computational grid. The

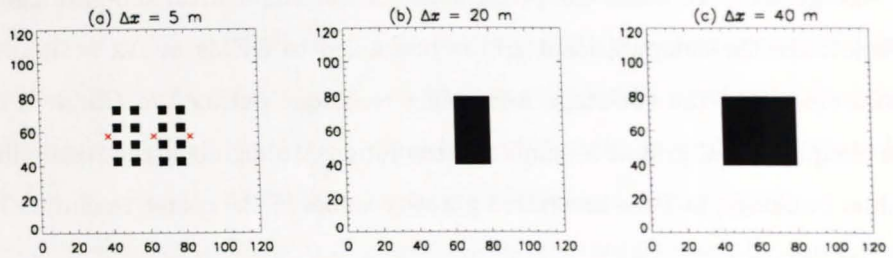

Figure 5.3: The effect of grid resampling on a collection of buildings using the two-stage resampling technique.

effect of resampling (a) to resolutions of 20 and 40 m is shown in (b) & (c), respectively.

5.4.3 Flow over complex topography

In order to establish the effect of small-scale topographic irregularities on the propagation of a floodwave, two hypothetical floodplains are generated: (i) a simple one-dimensional flowpath with an obstacle half way along (Figure 5.4) and (ii) stochastically generated Gaussian random field topography on a regular grid (Figure 5.5a). In the first case, a constant flux of 0.5 $m^2 s^{-1}$ is applied in the western most cell propagating down a channel of 2 x 10 m. The north and south boundaries are assumed closed and at the eastern boundary, a normal depth condition is imposed. In the second case, a synthetic modelled variogram is used to derive the topography with a sill of 0.1 m and a range of 1 m. The generated field has dimensions 320 m by 96 m and a resolution of $\Delta x = 2$ m to enable regular resampling to 4 coarse resolution DEMs ($\Delta x = 4$, 8, 16 and 32 m). A initial buffer region of 64 m, using

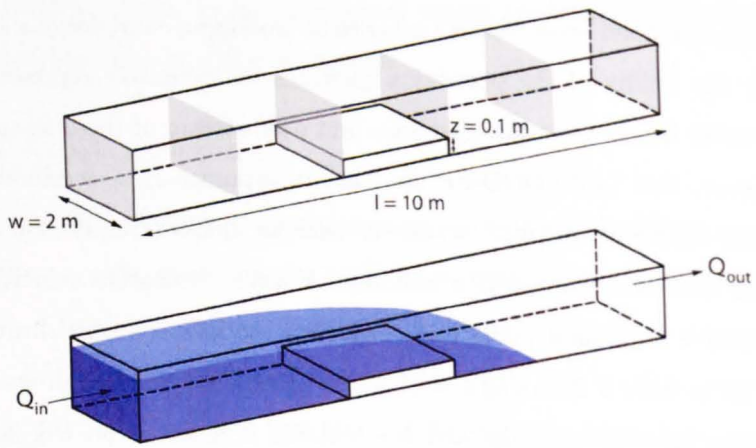

Figure 5.4: Setup of the simple 1D channel test case with a small obstruction for the water height dependent porosity technique (ηVAR) showing the obstacle and flow direction.

the average elevation of the high resolution grid, is added to the western edge of the domain to allow flow to develop in each model configuration before interaction with the small-scale topography. Figure 5.5 shows the variation of this surface with model resolution. A wave of constant velocity of 0.5 ms^{-1} is applied at the western boundary, the northern and southern boundaries are specified as zero-flux, and at the eastern boundary, a normal depth condition is imposed. A Manning's n of 0.035 is applied across the entire domain in both cases.

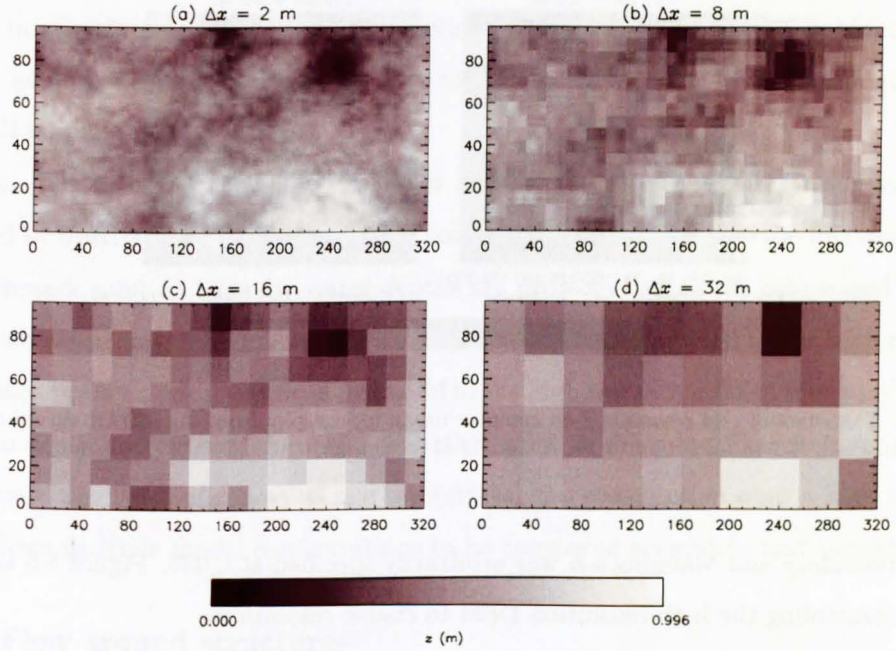

Figure 5.5: The effect of grid resampling on Gaussian random field topography from a benchmark of 2 m resolution to 8, 16 and 32 m resolution.

5.4.4 Flow through complex urban environments

The final test of the porosity algorithms is a more representative application to spatially-complex urban topography, attempting to capture the effect of grid and sub-grid scales, and wetting and drying effects. Accordingly, a 200 by 200 m indicative subset of urban topography is extracted from the Carlisle LiDAR dataset at a resolution of 2 m. The data were then simply aggregated to provide 4 coarse resolution DEMs ($\Delta x = 5$, 10, 20 and 40 m) with each cell being assigned an elevation using the nearest neighbour resampling technique. A wave of constant velocity of 0.75 ms^{-1} provided the flow boundary condition imposed along the west boundary of the domain to simulate the wetting process. Zero-flux conditions were specified at the north and south boundaries with a normal depth condition imposed at

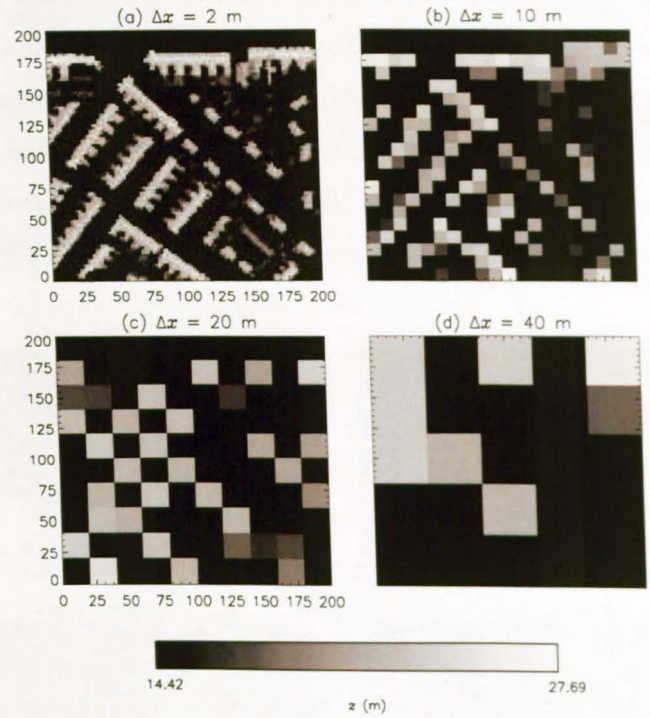

Figure 5.6: The effect of grid resampling on complex urban topography from the LiDAR survey of Carlisle from a benchmark of 2 m resolution to 10, 20 and 40 m resolution.

the east boundary and Manning's n was arbitrarily specified at 0.035. Figure 5.6 shows the effect of resampling the high resolution DSM to coarse resolutions.

5.5 Model results and discussion

The appropriate representation and display of results from porosity type approaches has a significant effect on the apparent model performance. Yu and Lane (2006b) evaluate their sub-grid approach by coarsening the benchmark data set (observed or modelled) to the model resolution (i.e. projecting a 2 m benchmark to a 4 m model grid resolution) and thus deriving a wetting front (Figure 5.7a&b) (Yu, 2005). This strategy is likely to under- and over-estimate model extent performance as there is a loss of precision in the evaluation data. However, Yu (2005) recognised that synoptic observations of flood extent (e.g. areal photography) will be subject to averaging and subsequent possible mis-classification at the flood edge so the use of a wetting front cell approach reduces these uncertainties. However, as the work reported here is a pure model verification study, the results are a measure of relative model performance (rather than absolute when comparing to observational data)

and therefore, uncertainties in benchmark results do not need to be considered.

The assessment of predicted water depths will be influenced by the choice of comparison of water depths above the DEM or comparison of water elevation predictions. The use of a sub-grid porosity approach implies a need to represent small-scale topographic variation in order to adequately resolve flood information (water depth and extent). Therefore, comparing water depths/elevation on a coarse grid induces an averaging process that the use of a porosity-type approach aims to avoid. In addition, Chapter 4 has shown the significant changes in structure location in coarse resolution grids and therefore, if water depths are assessed at a coarse resolution, the ability to assess damage and loss for any given flood event will be limited.

As an alternative, Figure 5.7c&d shows a model evaluation strategy, similar to that suggested in Horritt and Bates (2001a), for comparing model results at the fine resolution of the benchmark solution whereby water depths are projected on to the coarse grid to derive free surface elevations. The free surface elevations are then resampled to the high resolution using a linear interpolation and reprojected on to the high resolution DEM thus resolving high resolution depth and extent information. Furthermore, as the sub-grid techniques used here can compare any ratio of coarse to fine resolutions, the reprojection onto a high resolution DEM, allows multiple model configurations to be compared accurately and consistently.

5.5.1 Flow around structures

The correct implementation and subsequent utility of the simple areal porosity technique can be assessed with respect to changing model resolution and the consistent prediction of water surface elevations around a prominent building on the floodplain compared to the high resolution benchmark. Figure 5.8a-c and d-f show the RMSE of predicted flood depths on the 5, 10, 20 and 40 m resolution grids using the coarse DSM and the ηFIX porosity algorithm at discrete times during the simulation. The timings of panels (a) to (c) coincide with: i) the initial interaction with the building; ii) the floodwave reaching the boundary; and iii) approaching steady state in the fine resolution 2 m benchmark solution. The top panel shows the assessment of flood depths prior to reprojection whereas the bottom panel shows the results after reprojection onto the fine resolution grid. In terms of the porosity approach, this reprojection step is vital to resolve the water depths around individual buildings that are represented implicitly where porosity values are greater than zero.

The identical prediction of flood depths in the coarse resolution and ηFIX models at

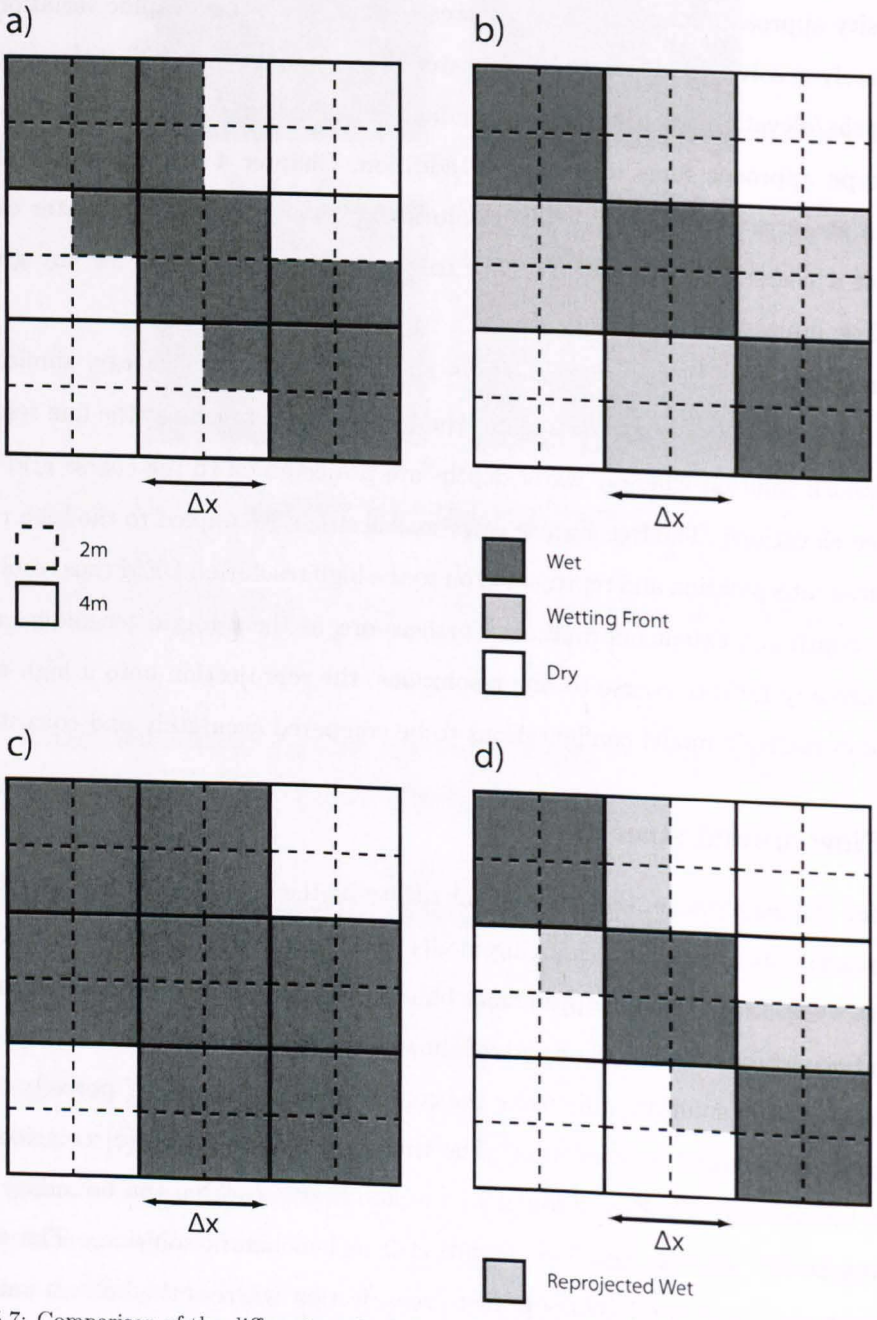

Figure 5.7: Comparison of the different methods for evaluating coarse and fine resolution model results.

5 and 10 m resolution verifies that the algorithm has been implemented correctly within LISFLOOD-FP. In addition, the very similar nature of the results at 20 m and 40 m at the time of interaction with the building further implies that where the porosity value is equal to one, the original model formulation and the porosity approaches are identical. However, the results at resolutions of 20 and 40 m later in the simulation suggest poor prediction of water levels throughout the domain with significantly higher RMS errors when incorporating the buildings into the grid directly. The ηFIX algorithm significantly increases the accuracy of predicting water depths around buildings on a coarse mesh reducing errors by over 50% at steady state on the 40 m grid.

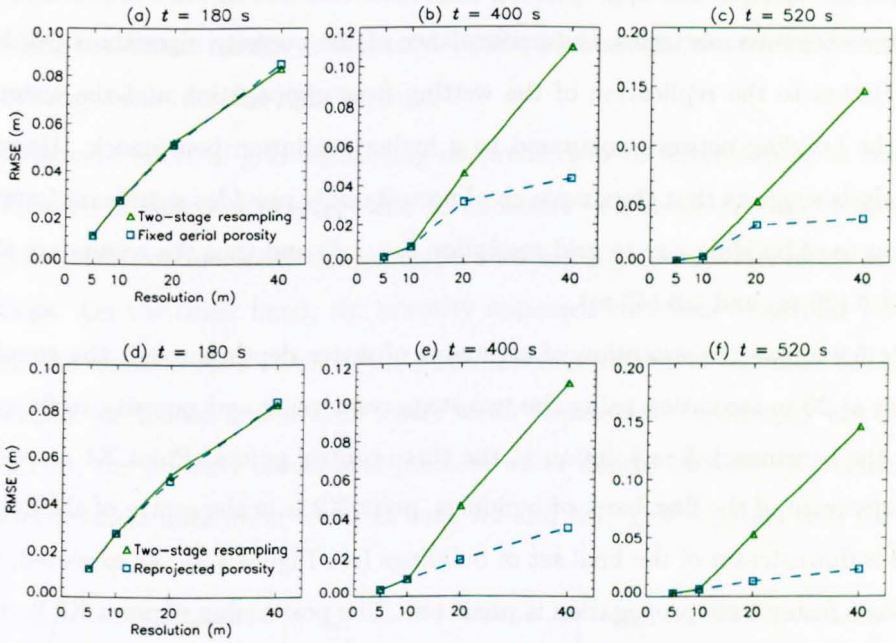

Figure 5.8: RMSE of predicted flood depths compared to 2 m benchmark solution at each resolution where the top row (a) - (c) is the flood depths before reprojection and the bottom row (d) - (f) is the flood depths after reprojection onto the high resolution DSM.

These errors are due to the overprediction of flood extents by one cell when comparing models at coarse resolution to those at a finer resolution or a result of the discrete nature of the predictions such that a horizontal water surface is determined for each cell. The initial errors at all resolutions provide an insight into the magnitude of the noise introduced at coarse resolutions despite identical representations of topography.

Scaling the water depth and fluxes by an areally defined porosity value appears to provide increased model performance in terms of water depths and domain flux when considering a single floodplain irregularity (i.e. a building). However, urbanised floodplains are char-

acterised by sequences of buildings with different orientations and floodwave dynamics are determined by the interaction of flow with these features. Therefore, it is necessary to consider how the floodwave interacts with a complex network of buildings to convey water on an urbanised floodplain.

5.5.2 Multiple blockages, constrictions and expansions

To demonstrate the importance of flows interacting with a number of buildings and configurations of buildings, a floodwave is propagated through a variable set of buildings, constrictions and expansions using the DEMs shown in Figure 5.3. As LISFLOOD-FP does not incorporate the physics to represent the high frequency oscillations and head loss effects that occur when waves encounter obstacles, the performance of the porosity algorithms can be evaluated in relation to the replication of the wetting front propagation and the water heights through the building network compared to a higher resolution benchmark. However, the above analysis suggests that the simple areal porosity only provides significant improvement at large ratios of building size to grid resolution (i.e. 1:4) and thus the results are shown for ratios of 1:4 (20 m) and 1:8 (40 m).

Figure 5.9 shows the evolution of estimates of water depth through the course of the simulation at 20 m resolution using the two-stage resampling and porosity techniques compared to the benchmark 5 m solution at the three control points. Point X1 corresponds to directly upstream of the first bank of buildings, point X2 is in the centre of the domain and point X3 is downstream of the final set of buildings (see Figure 5.3). As expected, at coarse resolutions a faster wave propagation is predicted. The positioning of point X2 is critical for comparison of water levels in this case as a shift in the x-direction would cause a prediction of zero water depths as a result of the overestimation of building size. On the other hand, regardless of location, the ηFIX formulation predicts a water surface profile similar to that in the benchmark simulation (considering the over-prediction associated with coarse resolution models). The most interesting result occurs at point X3, where the coarse DSM model predicts a more accurate water depth evolution than the porosity formulation. However, Fawcett *et al.* (1995) and Bates *et al.* (1998a) note the importance of internal validation of model predictions wherever possible and the exact location of point X2 will greatly impact on any conclusions from this internal validation. Kirchner (2006) stresses the need for getting the right answers for the right reasons and notes the tendency of environmental modellers to trust model results without consideration of the causes of the results. These guidelines are

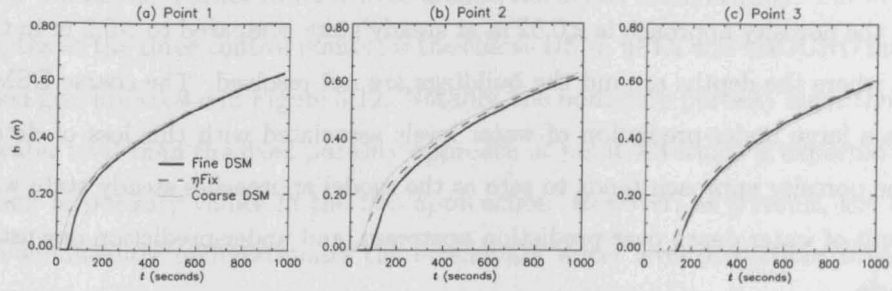

Figure 5.9: Evolution of water depth at control points X1-X3 in the model domain at 20 m resolution for the resampled DSM and ηFIX approaches compared to the benchmark 5 m solution on the aligned model grid.

of paramount importance in this case where the porosity approach is behaving as expected and providing consistent results at this model scale whereas the coarse DSM configuration is not providing results for the right reasons.

The significant effect of grid resampling on predictions of water depths at coarse resolutions is shown in Figure 5.10 where the 40 m model fails to predict water levels in the centre of the urban configuration and simulates substantially lower water levels in the lee of the buildings. On the other hand, the porosity approach simulates consistent water levels throughout the domain. As a result of the instantaneous wetting of an entire cell in storage cell approaches (or indeed any scheme where water depths and topography are discretised at cell centres), the porosity model over-predicts water depths initially. Nevertheless, this model under-predicts final water levels at both X2 and X3. This suggests that the porosity

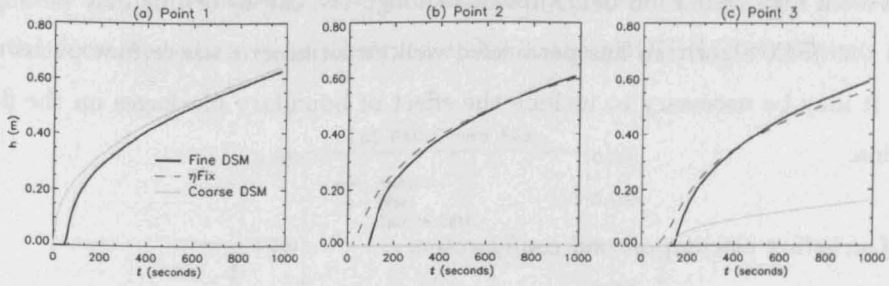

Figure 5.10: Evolution of water depth at control points X1-X3 in the model domain at 40 m resolution for the resampled DSM and ηFIX approaches compared to the benchmark 5 m solution on the aligned model grid.

algorithm is artificially decreasing water levels too much and as such, is compensating for the tendency of coarse resolution models to overestimate wave propagation velocities.

Figure 5.11a shows the RMSE of, and bias in, water level predictions in the coarse DSM

and ηFIX models compared to the high resolution benchmark. Notably, the RMSE of flood depths in the porosity approach is <0.02 m at steady state compared to >0.2 m in the DSM approach where the depths around the buildings are not resolved. The coarse DSM results also show a large under-prediction of water levels associated with this loss of detail. The bias in the porosity approach tends to zero as the model approaches steady state which is a direct result of water depth over-prediction upstream, and under-prediction downstream, of the obstacle.

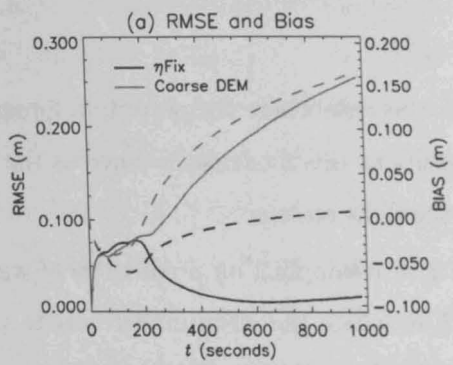

Figure 5.11: Evolution of RMSE and bias in water level predictions for the 40 m DSM and ηFIX methods where the solid line represents the RMSE on the left y-axis and the dashed line corresponds to the bias on the right y-axis.

In this case, the areal porosity value accounts for the reduction in flow and storage area adequately, within the accuracy expected at coarse resolutions. Furthermore, conditions have been highlighted where coarse resolution models without porosity may provide results consistent with high resolution benchmarks although the causes of this may be unphysical. Although the ηFIX algorithm has performed well, in situations where flow paths are more tortuous, it may be necessary to include the effect of boundary blockages on the floodwave propagation.

Effects of structure orientation and configuration

To investigate the impact of structure orientation on the utility of porosity formulations, the boundary porosity formulation is applied to the aligned building case. In this case, at 40 m resolution in the centre cell, the boundary porosity is 0.5 in the x-direction at the east and west boundaries and is 0.5 in the y-direction at the south boundary and 1.0 at the north boundary compared to a direction independent porosity of 0.75 in the ηFIX method. This will act to retard floodwave propagation in the x-direction, and specifically into the porous

cell, which will further reduce water depths around the urban configuration. The evolution of water depths at the three control points for the coarse DSM, ηFIX and ηBOUND methods on the aligned grid are shown in Figure 5.12. Notably, the boundary porosity algorithm predicts a lower water level than the fixed porosity approach at point X3 which is expected given the distribution of porosity values in the two approaches. However, as a result, the boundary approach significantly underestimates the benchmark water level predictions suggesting an over-emphasis of the effect of the buildings on overall flood propagation in the boundary approach.

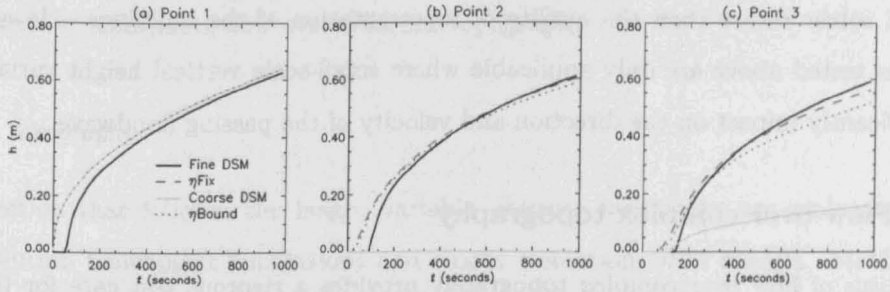

Figure 5.12: Evolution of water depth at control points X1-X3 in the model domain at 40 m resolution for the resampled DSM, ηFIX and ηBOUND approaches compared to the benchmark 5 m solution on the aligned model grid.

The evolution of RMSE and bias of flood depths for the ηFIX and ηBOUND methods show a decrease in overall performance for the boundary porosity formulation (see Figure 5.13). An increase in the RMSE and bias suggests an over-estimation of the impact of the boundary cells on the overall floodwave propagation. Furthermore, the increase in bias is a result of the decreased water levels observed at X3 in the ηBOUND formulation.

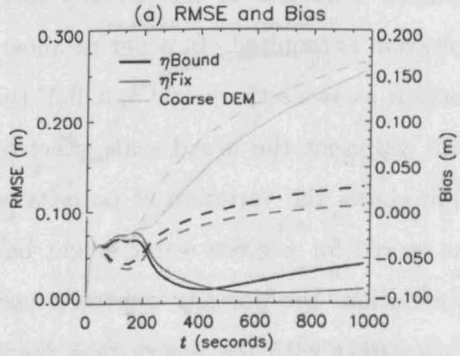

Figure 5.13: Evolution of RMSE and bias in water level predictions for the 40 m DSM, ηFIX and ηBOUND methods where a) the solid line represents the RMSE on the left y-axis and the dashed line corresponds to the bias on the right y-axis.

The simple areal porosity approach appears to resolve broad scale flow dynamics and internal water depths in coarse resolution models when compared to high resolution benchmark solutions. However, the ratio between the building size and the grid resolution needs to be sufficiently high (i.e. 1:8) to significantly improve model results. Furthermore, the boundary porosity approach does not appear to improve model performance further and indeed, in these simple test cases, actually decreases model performance by over-estimating the impact of boundary cells. These tests have also highlighted the need to ensure models are getting the right answers for the right reasons (Kirchner, 2006), in that coarse resolution DSM models may, at times, appear to perform adequately but for reasons related to the numerical solver rather than the quality of representation of the buildings. However, the techniques tested above are only applicable where small-scale vertical height variations do not significantly impact on the direction and velocity of the passing floodwave.

5.5.3 Flow over complex topography

The analysis of flow over complex topography provides a rigorous test case for the water height dependent porosity approaches. The most important first step is to ensure that the formulation and implementation in the C++ code is functioning as expected. Once this has been established, it is possible to explore how the methods perform over more complex topography.

Channelised flow

The first test consists of propagating a wave down a simple channel with an obstacle of 2 x 2 m and 0.1 m height between 4 and 6 m along the channel as shown above in Figure 5.4. In order to simulate similar behaviour in the porosity method, a slight modification from the benchmark configuration is required. In order to allow propagation in the ηVAR method, the obstacle is specified as twice the height but half the width when determining the ηVAR values as this will represent the broad scale effect of the obstacle on the flow (Figure 5.14a). Figure 5.14b shows the variation of porosity with water height and the associated volumes of water stored for a given water height based on the high resolution topography. During the simulation, the porosity approach uses a DEM with a flat bed as underlying topography, consistent with the theory that the porosity value accounts for small-scale topographic variation.

The variation in water elevation along the channel at various times during the simulation

is shown in Figure 5.14c. During the initial passage of the floodwave, the variable porosity approach under-predicts water levels upstream and over-predicts water levels downstream of the obstacle. However, this is due to the initially open nature of the porosity description of topography compared to the completely blocked nature of the DSM up to 0.1 m water depth. Nevertheless, it is clear that once the obstacle becomes substantially submerged, and the models approach steady state, the DSM and ηVAR models converge on consistent solutions. These results suggest that the height variable porosity is formulated correctly and thus, capable of representing the broad scale effect of small-scale topographic irregularities. Consequently, it is necessary to evaluate the utility of the ηVAR and ηBVAR porosity formulations at simulating flow over complex topography.

Complex topography

In the section that follows, the height variable porosity techniques are evaluated against high resolution benchmark simulations and coarse resolution DSM models. McMillan and Brasington (2007) noted the significant small-scale variation in topography in an urban area as justification for the development of the height dependent porosity (similar to ηBVAR developed here). The authors specify the porosity and volume as initiating from the minimum elevation of the high resolution DSM in the coarse grid stencil but conduct the model simulation on the coarse resolution DTM (normally derived as the average of the high resolution DSM). As long as the coarse resolution DTM is representative of the underlying topography, this approach will retain the slope characteristics of the topography. In this case, the use of both the coarse DTM and the mimumum elevation models (MEM) will be assessed.

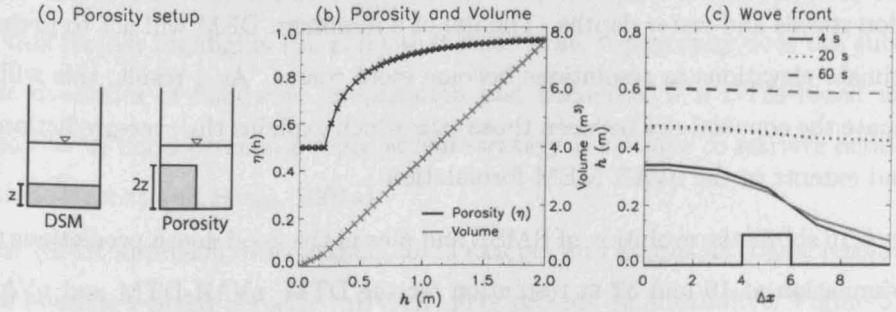

Figure 5.14: Water height dependent areal porosity for the channelised 1D flow over a single obstacle where (a) shows the porosity and DSM setups, (b) shows the variation in porosity values and volume for the centre cell and (c) shows the progression of the wetting front down the channel where the black represents the benchmark and the grey line represents the porosity method.

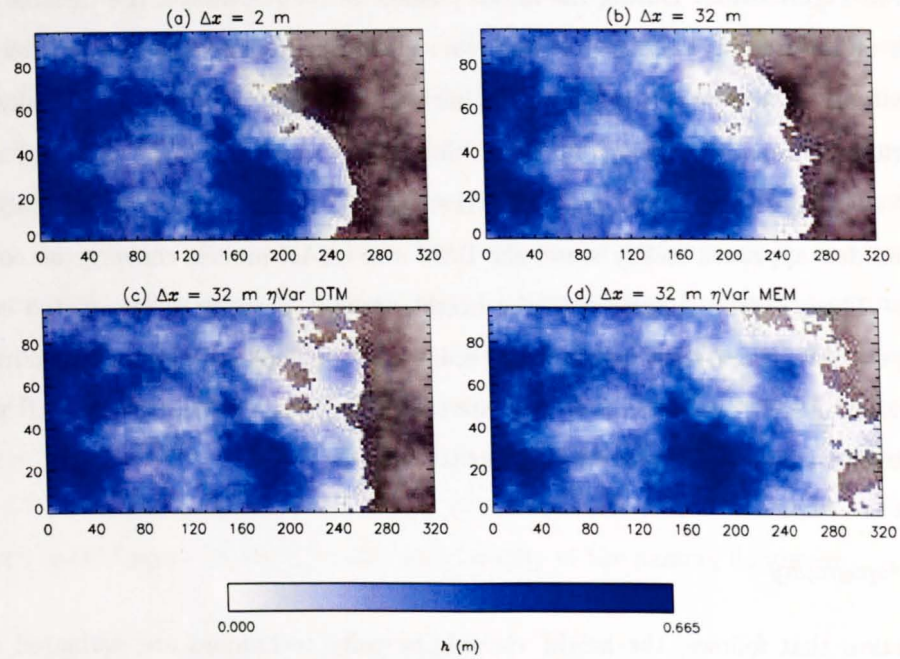

Figure 5.15: Distribution of simulated water depths (h) after 600 s using the ηVAR porosity technique reprojected onto the high resolution DEM (z) where (a) is the benchmark 2 m simulation, (b) is the coarse resolution DSM, (c) is the ηVAR using the DTM and (d) is the ηVAR using the MEM at 32 m resolution.

Figure 5.15 shows the simulated distribution of water depths after 600 s for the high resolution benchmark, and the coarse resolution DTM and ηVAR porosity methods using the DTM and MEM at 32 m grid resolution. All the coarse resolution results have been reprojected onto the high resolution DSM using the method outlined in Horritt and Bates (2001a). The most notable feature is the good agreement in terms of water depths between the high resolution benchmark, coarse resolution DTM and the ηVAR method using the DTM. On the other hand, the ηVAR MEM method appears to substantially over-estimate propagation speeds and water depths. The use of a minimum DEM will act to progressively under-estimate elevations as resolutions become more coarse. As a result, this will tend to over-estimate the connectivity between those cells which explains the over-prediction of flood depths and extents in the ηVAR MEM formulation.

Figure 5.16 shows the evolution of RMSE and bias in the flood depth predictions throughout the simulation at 16 and 32 m resolution for the DTM, ηVAR-DTM and ηVAR-MEM methods compared to the 2 m benchmark solution. The evolution of the RMSE and bias further suggests that the ηVAR-MEM method overestimates flood depths throughout the simulation. Furthermore, once reprojected, these results suggest that the coarse DTM ap-

proach provides a more consistent prediction of water depths than the use of a porosity approach. This result supports earlier findings that if a coarse resolution model is a good predictor for flood extent, reprojection onto a high resolution DEM will provide good predictions of water depth (Horritt and Bates, 2001a). Despite these findings, it is clear that although the height variable porosity should be calculated from the minimum grid, the models should be driven by the averaged DTM topography.

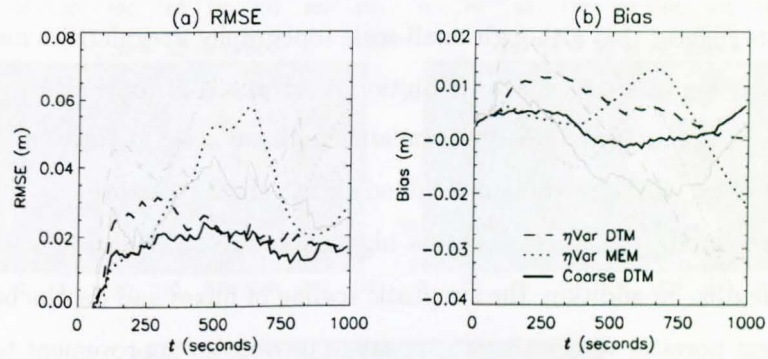

Figure 5.16: Evolution of RMSE and bias of water depth predictions at 16 and 32 m resolution using the DTM, ηVAR-DTM and ηVAR-MEM methods where the dark line corresponds to the 16 m resolution and the grey line corresponds to the 32 m resolution.

Analysis of the variation in the porosity and volume for a representative 32 m grid cell and associated 2 m resolution topography (Figure 5.17) provide further evidence for the poor performance of the porosity techniques compared to the coarse resolution DSM results. Although there is significant variation in the porosity values with water depth, the volume-depth relationship is basically linear. Below 0.2 m water depth, the storage volume is close to zero and above 0.2 m water depth, the volume-water depth relationship is linear. Therefore, as the variation is limited to the first 0.2 m, there is little impact of this variation on the flow. Overall, this further highlights the point that small-scale topography does not substantially affect the dyanmics of floodwave propagation and therefore, if a DTM-based model is a good predictor of flood extents, a reprojection strategy is suitable to retrieve detailed depth information (Horritt and Bates, 2001a).

As the ηVAR approach over-predicts flood extents and depths at coarse resolutions, the use of the boundary based porosity (ηBVAR) may provide an alternative. Figure 5.18 shows the spatial distribution of predicted flood depths after 600 s for the 32 m resolution water height dependent areal and boundary porosity methods. The ηBVAR technique appears to underestimate flood depths throughout the domain, as observed when using the ηBOUND

approach. Indeed, this approach also seems to alter the dominant flow paths, over-predicting flooding in the north and under-predicting flooding in the south of the domain. The evolution of RMSE and bias of flood depths during the simulation at resolutions of 16 and 32 m is shown in Figure 5.19. Although there is a significant degree of variability during the simulation, in the main the coarse resolution DTM approach appears to outpeform the porosity approaches at both 16 and 32 m resolution. In addition, the ηVAR techniques generally provides better predictions than ηBVAR techniques at both model resolutions.

These results suggest that although small-scale topography irregularities may control the initial rate of wetting of a cell, coarse resolution descriptions of topography retain enough detail (up to ratios of at least 1:16), to simulate the broad scale features of the floodwave. Furthermore, as long as the predictions of flood extent are satisfactory (i.e. wave celerity is accurately represented), reprojection onto a high resolution DEM provides good estimates of local flood depths. In addition, the simplistic scaling of fluxes and depths based on water height dependent porosity values, do not appear to provide an improvement to results compared to the coarse DSM results. However, explicit inclusion of small-scale topography and slope relationships (as in Yu and Lane, 2006b) may provide a viable alternative. Nevertheless, it would seem that if the effect of structures can be incorporated into coarse resolution models (i.e. through ηFIX values), flood predictions at these resolutions may provide the trade-off between detail and computation time required for practical applications. In order to test this hypothesis, the analysis that follows will apply the four porosity approaches to simulation of a wave over actual urban topography.

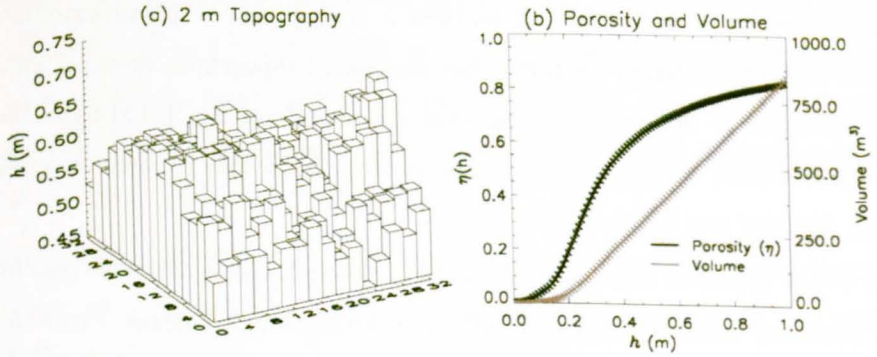

Figure 5.17: Water height dependent areal porosity for a singel coarse resolution cell of complex topography where (a) shows the variation of sub-grid scale 2 m topography for the 32 m cell and (b) shows the associated porosity and volume functions with increasing water depth.

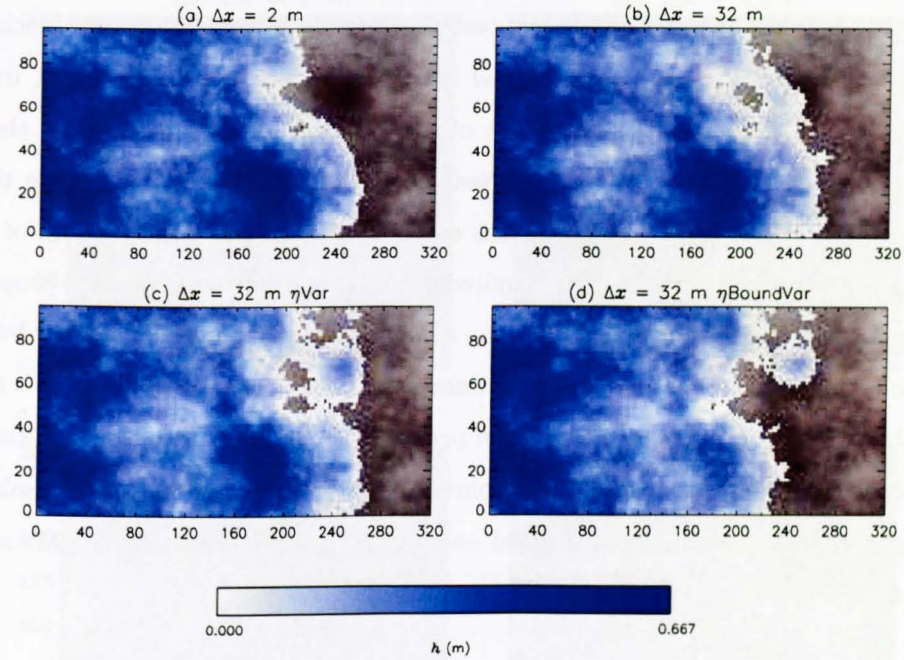

Figure 5.18: Distribution of simulated water depths (h) after 600 s using the ηVAR and ηBVAR porosity techniques reprojected onto the high resolution DEM (z) where (a) is the benchmark 2 m simulation, (b) is the coarse resolution DSM, (c) is the ηVAR and (d) is the ηBVAR at 32 m resolution.

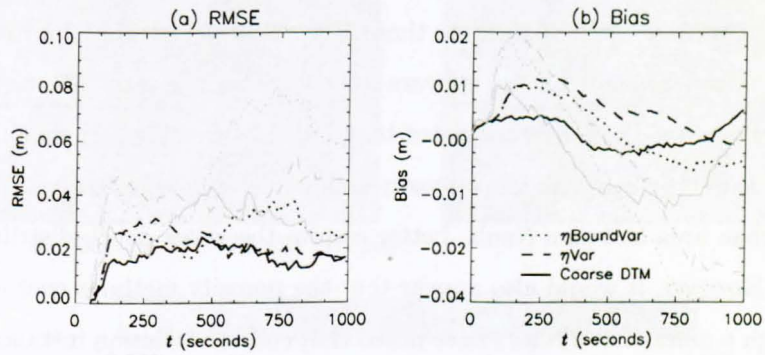

Figure 5.19: Evolution of RMSE and bias of water depth predictions at 16 and 32 m resolution using the DTM, ηVAR and ηBVAR methods where the dark line corresponds to the 16 m resolution and the grey line corresponds to the 32 m resolution.

5.5.4 Flow through complex urban environments

The use of idealised urban configurations does not replicate the true variability of urban topography and therefore is not a stringent test of utility of the different porosity techniques. In this test case, a floodwave is propagated over a subset of processed LiDAR from the Carlisle region. This 200 by 200 m subset of Carlisle is from the area around the River Petteril classified as the West Petteril in Neal *et al.* (2009a). The authors note that the area is characterised by building separations of ~2 m and longest building axes of ~15 m suggesting a grid resolution of 2 m is required to fully capture the floodwave propagation in this region. Furthermore, coupled with the combination of aligned and rotated buildings, relative to regional flow direction, and long terraces of houses, this site will act as a rigorous test for the porosity techniques. Firstly, the performance of the four porosity methods will be assessed with respect to a benchmark solution. Secondly, the effect of the resolution of the sub-grid topography will be examined and finally, the sensitivity to the Manning's n friction parameter will be analysed.

Sensitivity to grid resolution

Figure 5.20 shows the spatial distribution of predicted water depths after 400 s of the simulation for the porosity techniques compared to the high resolution benchmark and the coarse resolution DSM approach at 20 m grid solution. The effect of using a coarse DSM appears two-fold in this case. Firstly, there is a significant loss of detail in predicted water depths around individual buildings once the water depths are reprojected. This could be resolved by intelligent reprojection of water surfaces in those areas, however such an approach would not be mass conservative. Secondly, there appears to be significant retardation of the floodwave as the coarse resolution DSM overestimates building sizes causing significant blockages to flow paths. On the other hand, all four porosity techniques appear to resolve the propagation through the urban area and as a result, better resolve the water depth distribution around the buildings. However, it would also appear that the porosity methods over-estimate flood extent, although a number of authors have noted that coarse resolution instances of diffusion wave models often portray this characteristic (Hunter *et al.*, 2005b; Yu and Lane, 2006a). However, these results only provide a qualitative assessment of floodwave predictions.

Accordingly, the evolution of global model performance measures for the four porosity and coarse DSM approaches thoughout the simulation will be analysed (Figure 5.21). In general,

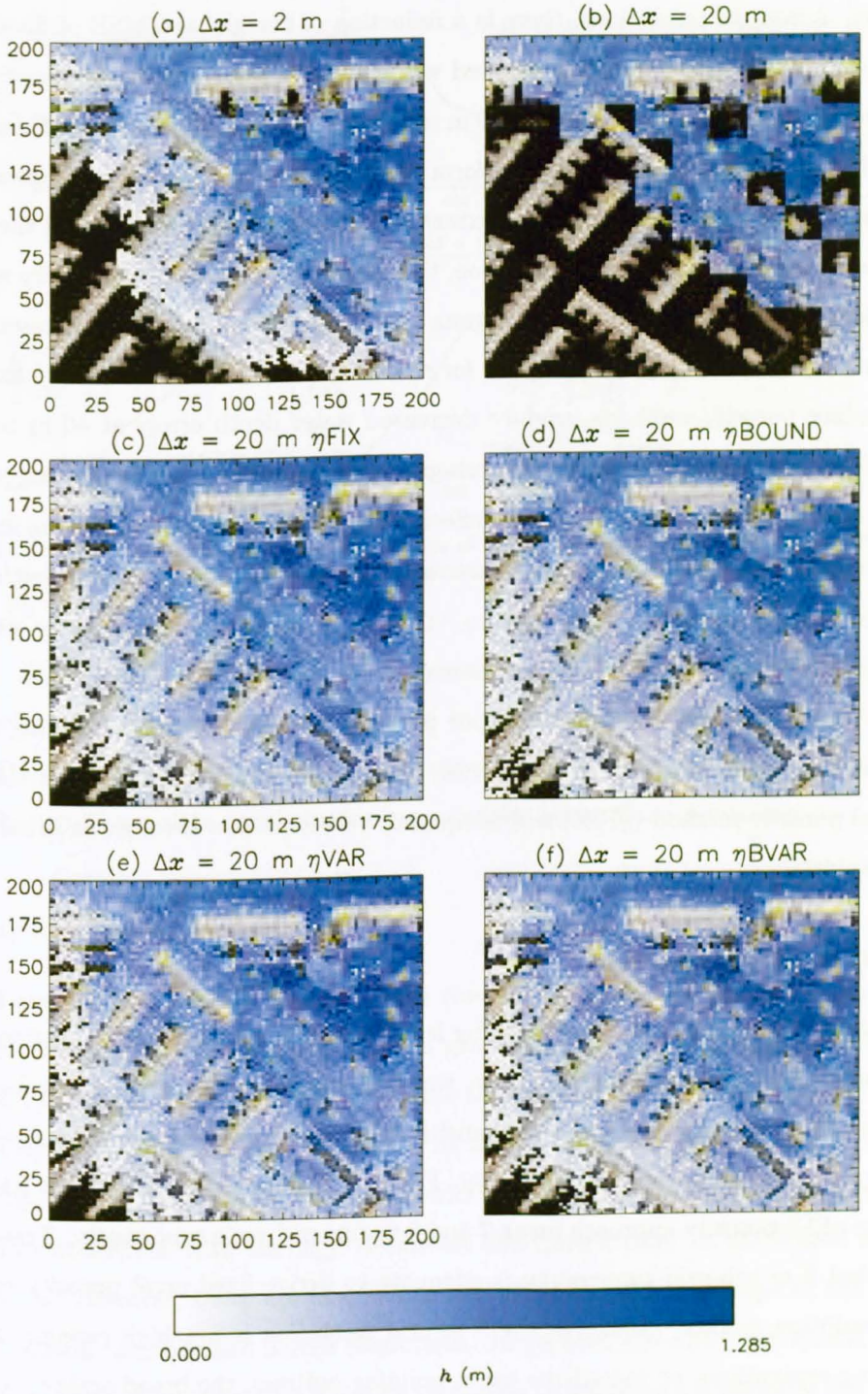

Figure 5.20: Spatial distribution of water depths after 400 s for (a) the 2 m resolution benchmark, (b) the coarse resolution DSM and (c)-(f) the four porosity approaches at 20 m resolution.

these results suggest that, using the porosity methods, there is considerable improvement of model results over the coarse DSM models across all grid resolutions throughout the simulation. Across all resolutions, there is a reduction of the global RMSE of flood depths from ~0.4 m to ~0.1 m, which is associated with correctly resolving the wetting front and depths around buildings. Specifically, at 10 m resolution, the boundary porosity formulations (ηBOUND and ηBVAR) appear to out-perform the areal porosity approaches in terms of both the prediction of water depths and flood extent throughout the simulation until the domain is completely wet. At 20 and 40 m resolution, the difference between the boundary and areal formulations is less pronounced which suggests that as resolution decreases, representing the bulk effects on the flow becomes adequate for resolving flood flows. Notably, the fixed areal and boundary porosity methods produce decreased water depth errors at 40 m resolution compared to the water height dependent sub-grid scale methods. This further suggests that at coarse resolutions representing the bulk effect of large-scale obstructions is more important than the small-scale local topography. Moreover, although there is an increase water depth errors from ~0.07 m on the 10 m grid to ~0.12 m at 40 m resolution, these values are within the RMSE of typical elevations measurements from LiDAR instruments. Overall, there is little to distinguish between the four porosity methods and thus, invoking Occam's Razor and the 'point of diminishing returns' (Bergstrom, 1991), suggests that the simple fixed areal porosity method (ηFIX) will adequately represent flow through an urban area at coarse resolutions.

Sensitivity to sub-grid resolution

Neal *et al.* (2009a) noted that the controlling length scale in the West Petteril region was the separation between neighbouring buildings, which was of the order of ~2 m. Consequently, the section that follows will examine the sensitivity of model predictions to the resolution of the sub-grid scale topography in this region. Figure 5.22 shows the evolution of RMSE and F^2 for the ηFIX porosity approach using 2 and 5 m sub-grid scale topography. These results suggest that 5 m sub-grid topography is adequate to derive fixed areal porosity values for coarse resolution models. Although the 5 m grid resolution is not high enough to resolve all building separations, or indeed the exact building outlines, the broad scale effect on the flow is still captured implicitly in the porosity values. Notably there is a slight reduction in the ability of the model to predict water levels at 10 m resolution using the 5 m sub-grid topography. However, in this case, the value of porosity can only vary by 5 discrete values

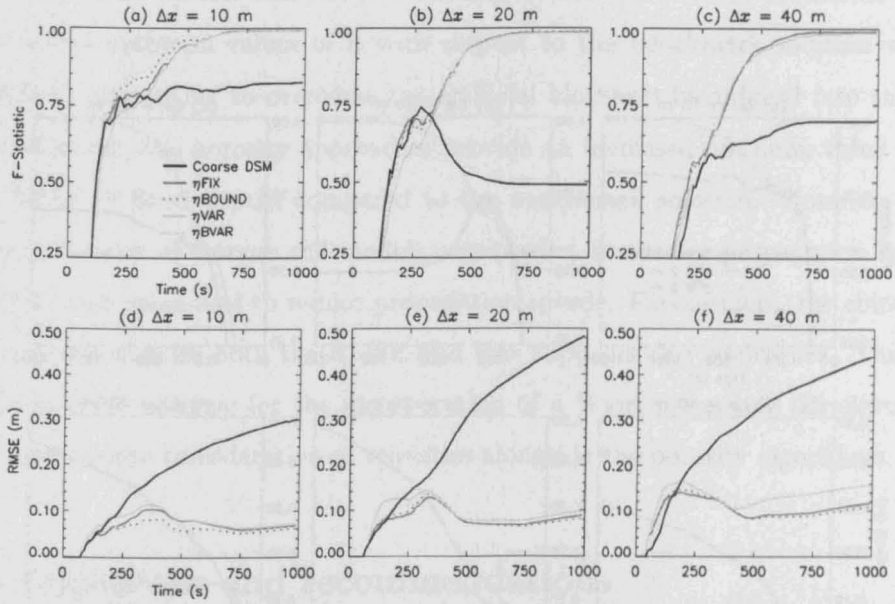

Figure 5.21: Evolution of global performance measures of model performance throughout the simulation at 10, 20 and 40 m resolution for the coarse resolution DSM and four porosity techniques where (a) corresponds to F^2 and (b) corresponds to RMSE.

and therefore will be more greatly influenced by the misrepresentation of the buildings in the 5 m DSM. As the porosity results do not appear affected at coarse scales, this somewhat relaxes the significant data requirements proposed for urban flood modelling.

Sensitivity to floodplain friction

Yu and Lane (2006b) suggest that at coarse resolutions, floodplain friction is an effective parameter that can be re-introduced when a greater degree of topographic information is present in the model (i.e. using a sub-grid scale treatment). Figure 5.23 shows the response surface of RMSE and bias of water depths for 10, 20 and 40 m resolution models to variations in Manning's n. As expected, for any given friction value, the porosity techniques provide results more consistent with the high resolution benchmark than do the coarse resolution DSM models. However, there are also substantial differences in the shape of the response surfaces between methods and across resolutions. In general, the ηFIX and ηVAR methods provide physically and numerically intuitive responses to Manning's n whereby the optimum value is well defined and identifiable for both the RMSE and bias. In the coarse DSM models, the optimum friction value varies significantly with resolution and the response is not predictable *a priori* (i.e. 10 and 40 m models have a lower optimum value than

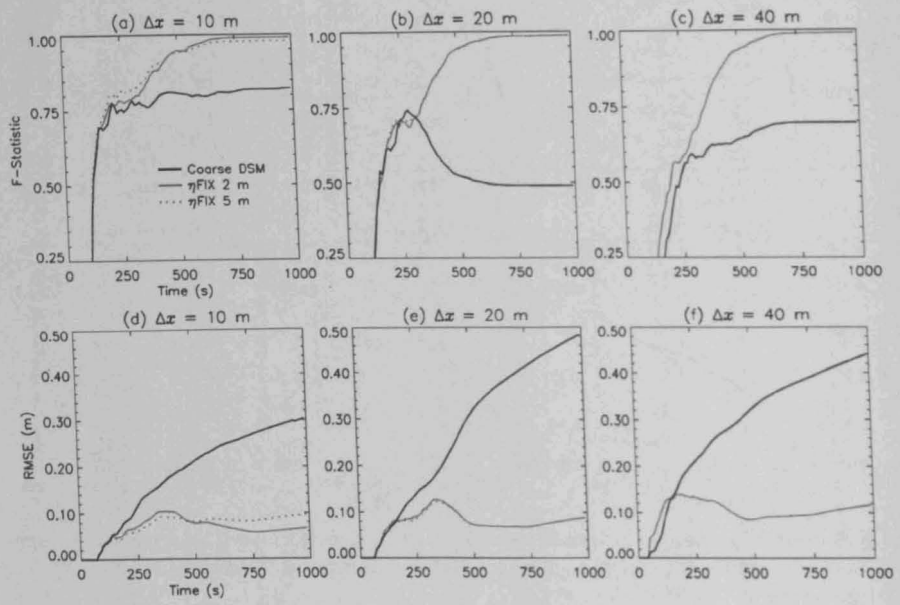

Figure 5.22: Evolution of global performance measures of model performance throughout the simulation at 10, 20 and 40 m resolution for the coarse resolution DSM and ηFIX technique for sub-grid resolutions of 2 and 5 m where (a) corresponds to F^2 and (b) corresponds to RMSE.

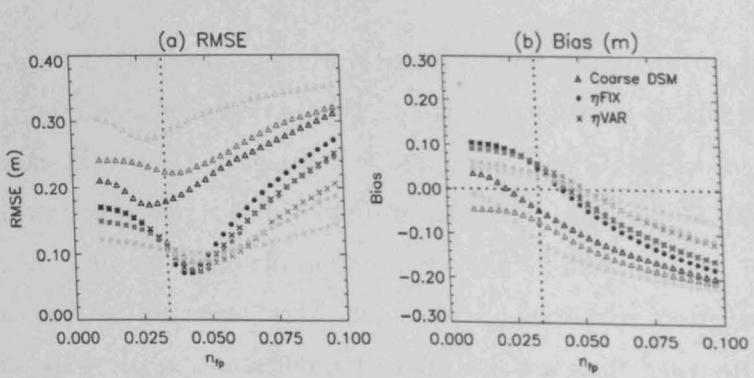

Figure 5.23: Model response of RMSE and bias for the ensemble of varying friction coefficient simulations at $t = 400$ s for each resolution using the coarse DSM and ηFIX and ηVAR porosity approaches. The dotted line represents the Manning's n friction value used in the benchmark 2 m solution. Note that the black represents the 10 m models, the dark grey represents the 20 m model and the light grey represents the 40 m model.

the 20 m model for RMSE and bias). Nonetheless, the coarse DSM models do appear to have decreased optimum values of n with respect to the benchmark solution which may be a result of attempting to overcome the artificial blockages introduced into these model grids. In contrast, the porosity approaches provide an increased optimum value of friction for the RMSE of flood depths compared to the benchmark solution. However, as coarse scale configurations of storage cell models over-predict floodwave propagation speeds, the increased friction value acts to reduce propagation speeds. Furthermore, the coincidence of optimum values of n for both the RMSE and bias supports this conjecture. These results suggest that there is scope for the incorporation of a %wet parameter (Bradbrook *et al.*, 2004) or appropriate consideration of velocities alongside the porosity algorithms.

5.6 Conclusions and recommendations

The review of current sub-grid scale porosity approaches (in Chapter 2) has highlighted the significant number of techniques of varying complexity, that have been developed over the last 20 years for inundation models of varying complexity. These techniques have generally been shown to improve predictions of flooding variables in coarse resolution models with a view to providing satisfactory assessments of flood risk over wide areas. The dichotomy in flood risk that requires fine scale, detailed predictions over wide areas provides an continuing need for the development of such techniques. However, given the variability in approach to specifying porosity and the models in which the techniques were applied, there was a clear need to rigorously test a number of different algorithms within a consistent modelling framework.

In response to this need, four porosity techniques of increasing numerical and data requirement complexity have been developed and applied to a simple finite difference storage cell inundation model, LISFLOOD-FP. The four techniques consist of: (i) a simple areal scaling based on the ratio of unblocked to total area of grid cell (ηFIX), (ii) a water height dependent version of the areal porosity (ηVAR), (iii) the incorporation of boundary cells governing inter-cellular fluxes (ηBOUND) and (iv) a water height dependent version of the boundary based porosity (ηBVAR). A procedure of testing on verifiable cases whereby porosity results were compared to high resolution benchmark solutions provided a framework for checking the conceptual model, the numerical implementation and the utility of the different approaches.

Testing of the simple fixed areal and boundary porosity methods suggested improve-

ments in predictions of the water height distribution around single buildings and collections of buildings compared to standard grid resampling method. However, these porosity approaches appeared to over-estimate the impact the buildings by reducing water levels although this is likely to be an effect of the increased wave propagation speeds in coarse resolution configurations of storage cell codes. In the case of flow over complex topography, the water height dependent porosity methods did not appear to provide an improvement over standard gridding techniques. However, Horritt and Bates (2001a) suggest that where a coarse resolution DTM adequately represents the underlying topography, a reprojection strategy will adequately resolve the spatial flood depth distribution. This result suggests that representing the bulk effect of buildings on the flow direction and flow paths is sufficient to improve predictions of floodwave propagation. Applying the four methods to flow through a complex urban area, showed significant improvement over the coarse resolution DSM approaches widely used in the literature. However, the porosity methods are largely indistinguishable which further suggests that representing the bulk effect is the most important factor, and therefore, the simple areal scaling porosity provides the best compromise between data requirements and numerical complexity.

The preceding chapter has shown the utility of various porosity approaches for improving predictions of floodwave propagation through idealised urban areas. However, to rigorously evaluate these methods, it is necessary to apply the suite of approaches to floods of varying type (e.g. fluvial, pluvial) and magnitude, and to different urban areas (e.g. Glasgow, Greenwich). This evaluation will form the basis of Chapter 6.

CHAPTER 6

Application of sub-grid scale porosity techniques

The preceding chapter has documented the development and subsequent testing of four sub-grid scale porosity techniques to enhance predictions of flood variables in coarse resolution models. These tests have illustrated the utility of such techniques at resolving water level predictions in the near-field of structures on the floodplain. In addition, representing the bulk effect of the building configuration appears to be sufficient to improve model performance at coarse resolutions. Furthermore, the water height dependency of porosity values did not appear to provide significant advantages over simple fixed areal-based porosity methods. The implementation of these porosity methods within the same modelling framework allows for consistent testing across a wide range of applications, both idealised and real-world. Furthermore, the sub-grid scale methods developed here are broadly representative of those currently available in the literature and the results of this study thus allow robust evaluation of their utility, independent of model structure.

The porosity techniques developed in the literature have thus far generally only been applied to single observed flooding scenarios (McMillan and Brasington, 2007) or to laboratory scale experiments (Sanders *et al.*, 2008; Soares-Frazão *et al.*, 2008). Application of these methods to flooding scenarios of varying magnitude and in different urban settings and configurations will allow rigorous evaluation of appropriate techniques. In addition, few studies have considered the detailed dependence of porosity methods to grid and sub-grid scale resolutions. This chapter will, therefore, document the application of these four techniques to benchmark scenarios in Greenfield and Greenwich (as in Chapter 4) and to observed data from the Carlisle event of January 2005.

6.1 Greenfield, Glasgow, UK

Chapter 4 documented the significant effect of model resolution on predictions of flooding at the Greenfield test site. In addition, the non-stationary response of optimum friction parameter values in coarse resolution models was highlighted. The following sections discuss

the use of increasing complexity porosity formulations for prediction of flooding in coarse grid models at this site.

6.1.1 Fixed porosity approaches

Figure 6.1 shows the spatial distribution of areal porosity (ηFIX) values for 8, 16 and 32 m grid resolutions based on the 2 m LiDAR survey of the Greenfield site. These were derived by assuming buildings remain as blockages throughout the full range of flow depths for this flood event; a reasonable assumption as water depths do not generally exceed ~1 m at all resolutions (Δx = 2, 4, 8, 16 & 32m). At 8 m resolution, the pattern of porosity broadly mirrors the building locations (overlain as black lines from MasterMap® data) which is consistent with the analysis of building separations from Chapter 4. However, it does highlight the offset to building locations caused by the use of a regular grid model, even at resolutions below the critical length scale. In fact, Schubert *et al.* (2008) have shown the utility of unstructured grid models for representing buildings at this site. The porosity values at 16 and 32 m resolution show progressively more uniform values representing the composite effect of the dense building configuration rather than individual buildings.

The evolution of global performance measures of the fixed areal porosity method (dotted line) compared to the original DSM gridding method (solid line) benchmarked against the high resolution 2 m solution is shown in Figure 6.2. In this case, it would appear that the porosity technique provides considerable improvement to predicted flood depths and flood extents across all model resolutions. In fact, the ηFIX model performance at any given resolution is now roughly equal to the performance of the DSM model at a subsequent higher resolution. This is likely to be a result of the porosity technique better resolving water depths around buildings, where coarse DSM models do not predict flooding due to the overestimation of buildings size. At 32 m resolution, the improved prediction of flood depths becomes apparent during the ponding phase when the porosity method enhances floodwave propagation to the souther-most streets which is prevented in the DSM model at this resolution by the mis-representation of building size. The ratio between fine and coarse grid models is 1:8 and 1:16, for the 16 m and 32 m models, respectively which confirms the conjectures from Chapter 5 regarding the significant ratios between model grid and sub-grid topographic resolutions required to justify the use of porosity methods. However, in order to assess this with any certainty, it is necessary to analyse the water depths at the same four control points as used in Chapter 4.

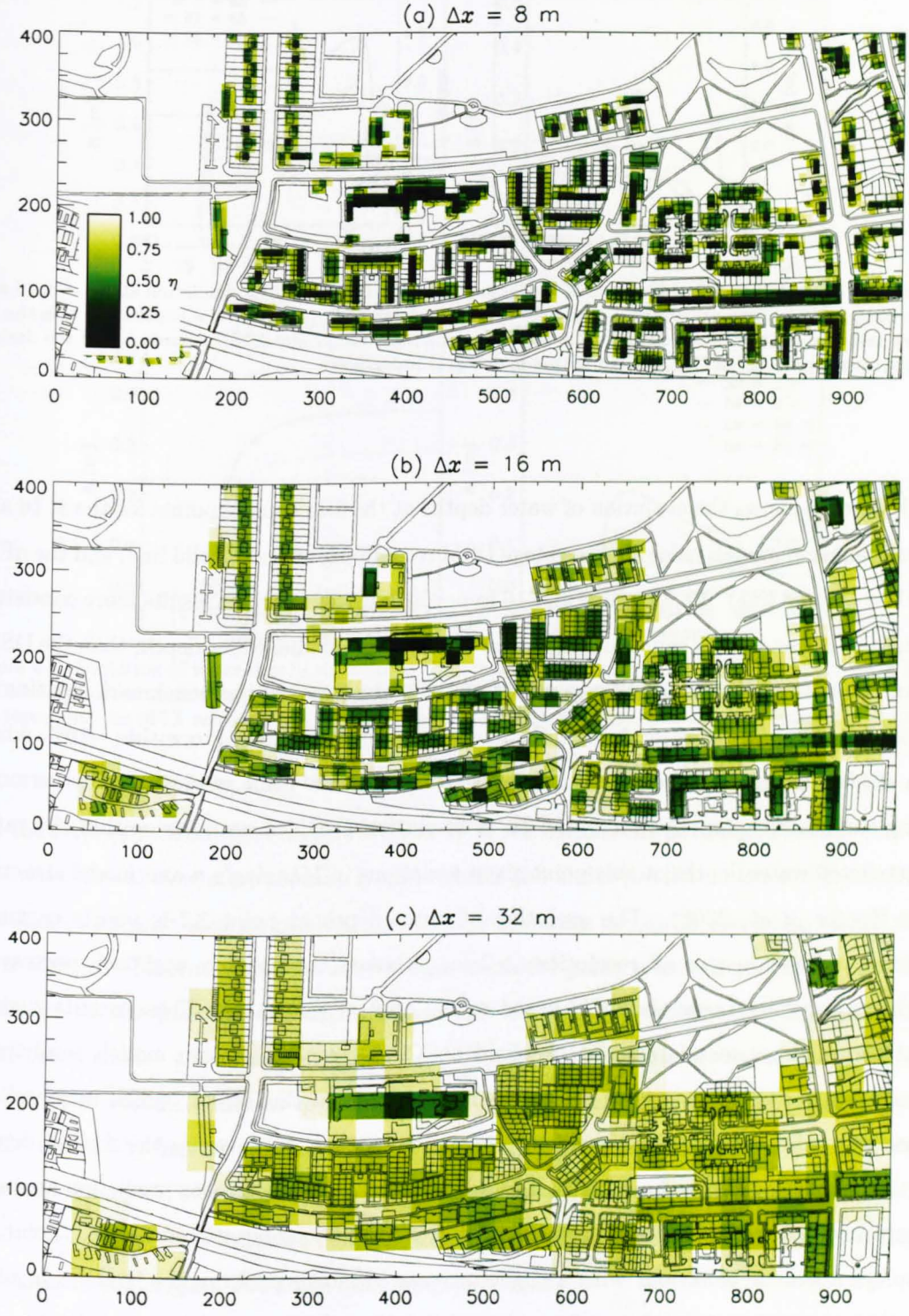

Figure 6.1: Spatial distribution of η using the fixed areal porosity approach for the 8, 16 and 32 m resolution DTMs using the 2 m benchmark DSM and MasterMap® data.

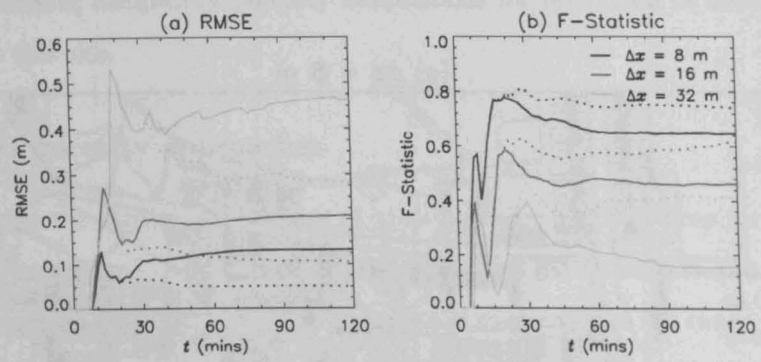

Figure 6.2: Evolution of global measures of model performance throughout the simulation at $\Delta x = 8$, 16 and 32 m compared to the benchmark solution where *a*) is the RMSE of predicted flood depths and *b*) is the F^2 binary measure of fit of flood extents. The solid line represents the original DSM approach and the dashed line represents porosity ηFIX approach with 2 m sub-grid topography.

Figure 6.3 shows the evolution of water depths at the four control points for the 8, 16 and 32 m resolution models using the two-stage DSM resampling method (solid line) and the ηFIX method (dotted line). At X1, the 8 and 16 m porosity models provide results more consistent with the 2 m benchmark solution, in terms of flood peak and final water depth, than the DSM-based models. Although the 32 m porosity model under-predicts the benchmark solution by ~25% in terms of peak water depths, the final water depth is resolved to within ~10%, which is a marked improvement over the DSM-based model of the same resolution. Furthermore, using the porosity approach at 8 and 16 m resolution provides estimates within the range of predicted water depths at this point given variations in Manning's n and model structure (see Hunter *et al.*, 2008). The evolution of water depth at point X2 is poorly captured in both methods across all resolutions >2 m, although the porosity approach portrays a slight improvement over the DSM-based model at 8 m resolution. These results suggest that the road network is not well resolved at X2 in coarse resolution models implying a small-scale topographic control on the propagation down this street, which may well be resolved by the water height dependent porosity techniques. However, as the shallow depths at this point are likely to have little effect on estimates of damage, poor prediction at coarse resolution may be an acceptable trade-off for increased computational speed. Point X4 displays a similar behaviour with a slight increase in model performance in the 8 m ηFIX model but no change to the performance of the 16 and 32 m models using the porosity approach over the DSM-based approach. At X3, the fixed areal porosity technique at 8 m resolution appears to overestimate water depths compared to both the benchmark solution

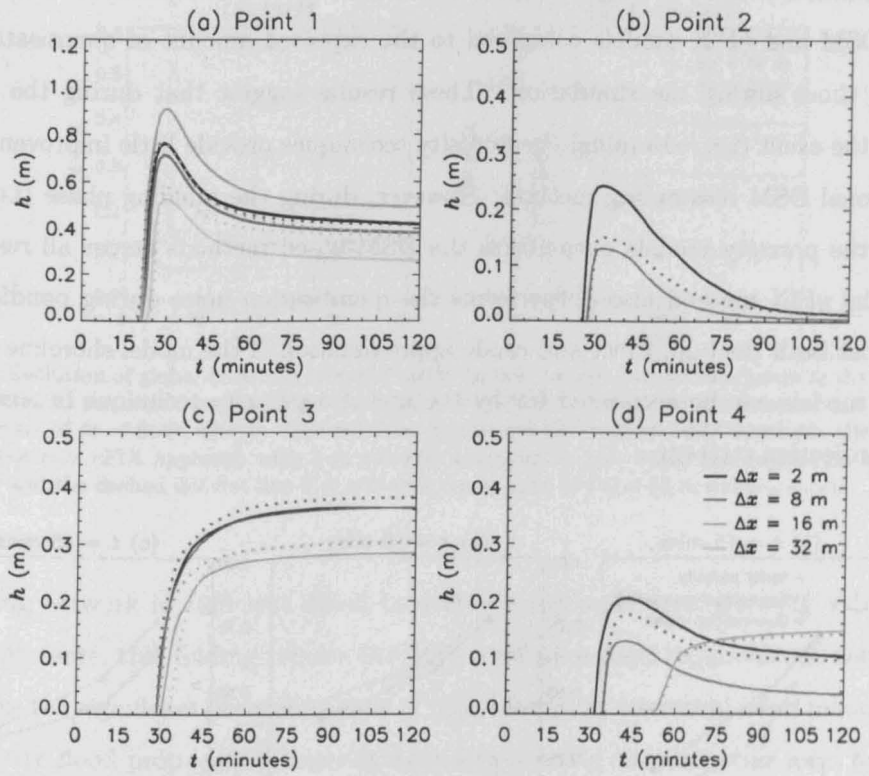

Figure 6.3: Evolution of water depths throughout the simulation at four control points, X1-4, at $\Delta x = 8$, 16 and 32 m grid resolution using ηFIX approach. The solid line represents the DSM approach and the dotted line represents the ηFIX results. Note the black line in each diagram represents the benchmark 2 m solution.

and the respective DSM model. However, at 16 m resolution, the porosity approach resolves floodwave arrival time more accurately and reduces the under-prediction evident in the DSM model, a factor that may be resolved further if considering the water elevations rather than water depths. The most substantial increase in model performance is visible in the 32 m model where the porosity approach resolves the water depth evolution at X3, unlike the DSM-based model which doesn't predict any water reaching this location. However, the 16 and 32 m models (DSM or ηFIX) do not provide predictions within the range of water depths created by friction parameterisation and model choice outlined in Hunter *et al.* (2008). Internal verification of water depths therefore suggests an increase in model performance at resolutions below the minimum distance between buildings (~8 m) in the ηFIX method compared to the original two-stage resmpling technique.

Horritt and Bates (2001a) postulate that coarse resolution models will be subject to i) quantisation noise resulting from a crude approximation of the model shoreline and ii) a bulk effect caused by the change in model scale, which in the urban case results from

misrepresentation of the building configuration. Figure 6.4 shows the modelled fit statistic from the DSM and ηFIX models compared to the expected amount of quantisation noise at varying times during the simulation. These results suggest that during the dynamic portion of the event (i.e. ~15 mins) the porosity techniques provide little improvement over the traditional DSM resampling method. However, during the ponding phase (i.e. ~30 & 45 mins), the porosity models outperform the DSM-based methods across all resolutions. Notably, the ηFIX method also outperforms the quantisation noise during ponding. This suggests that both the bulk effect and crude approximation of the model shoreline in coarse resolution models can be accounted for by the use of a porosity technique in combination with a reprojection strategy.

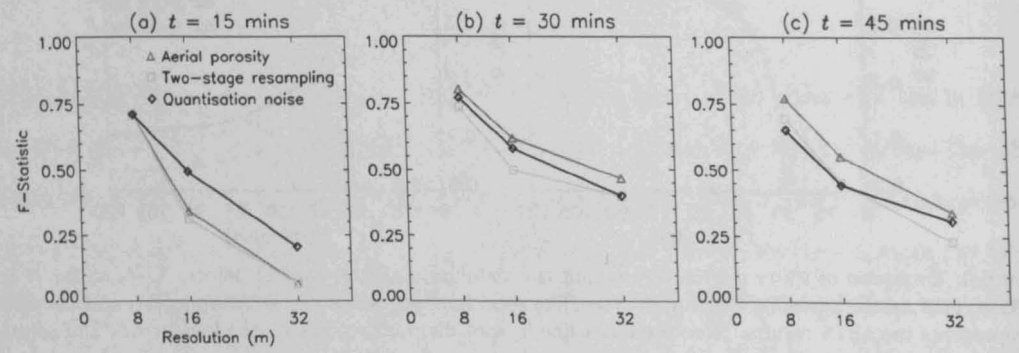

Figure 6.4: Fit between predicted and benchmark inundated area at *a*) $t = 15$, *b*) $t = 30$ and *c*) $t = 45$ mins for the two-stage resampling technique and the ηFIX approach and the maximum expected taking quantisation noise into account.

Sensitivity to sub-grid resolution

In testing a sub-grid scale porosity method, Yu and Lane (2006b) use the sub-grid scale topography in a ratio of 2:1 between fine and coarse resolution topographic datasets, however the sensitivity to such a formulation has not been assessed. The sensitivity of the ηFIX method to the specification of sub-grid scale topography is shown in Figure 6.5 where results for 16 and 32 m porosity models contain sub-grid information from the $\Delta x = 2$, 4 and 8 m DSMs and the 8 m porosity model contain sub-grid information from the $\Delta x = 2$ and 4 m DSMs. The most notable feature of this comparison is the similarity of performance in the ηFIX models regardless of resolution of the sub-grid topography. However, considering the critical length scale in this urban area is ~8 m and that the corresponding model performs adequately, this result is not altogether surprising. The $\Delta x = 8$ m DSM clearly represents

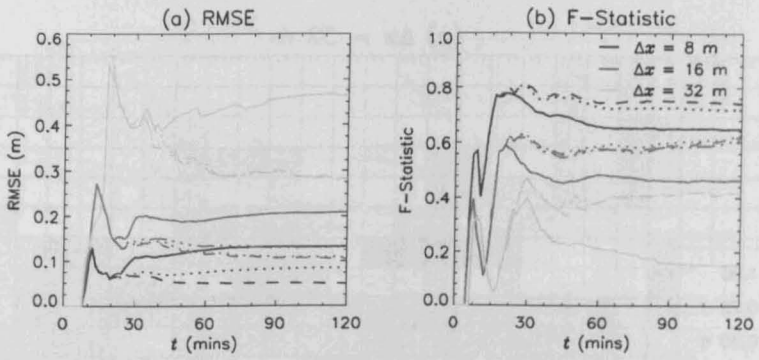

Figure 6.5: Evolution of global measures of model performance throughout the simulation at $\Delta x = 8$, 16 and 32 m compared to the benchmark solution where *a*) is the RMSE of predicted flood depths and *b*) is the F^2 binary measure of fit of flood extents. The solid line represents the original DSM approach, the dashed line represents porosity ηFIX approach with 2 m sub-grid topography, the dotted line represents 4 m sub-grid topography and the dashed dot dot line 8 m sub-grid topography (16 and 32 m models only).

the building network in sufficient detail to derive broad scale areal porosity values at this site. Furthermore, this finding relaxes the high resolution data requirements noted in §3.2 and reduces the significant processing time of high resolution numerical flood models. Nevertheless, where flood propagation depends more significantly on small-scale local topography (i.e. on gentle slopes), the need for the inclusion of a conveyance or boundary porosity as well as a water height dependence may be significant.

Influence of boundary porosities on flood propagation

Sanders *et al.* (2008) note the importance of accurately representing the conveyance (*conveyance porosity* or ηBOUND developed here) between cells as well as the storage (*storage porosity* or ηFIX developed here) in a given grid cell. In contrast, the results from Chapter 5 suggest that just representing the bulk effect of buildings on the flow is sufficient to resolve flood propagation. Figure 6.6 shows the spatial distribution of boundary porosity values compared to the fixed areal porosities. The pattern appears broadly similar although the boundary porosity formulation displays some substantial directional blockages that are underestimated in the areal porosity, especially in the regions around X2 and X3. Figure 6.7 shows the comparison of global performance measures for the fixed areal (ηFIX) and boundary (ηBOUND) porosity formulation throughout the simulation. There appears to be no added value in incorporating a boundary based porosity in coarse resolution models at this site. However, in this particular case, the overall slope, rather than the building configuration, controls broad scale flow direction and the reprojection step accounts for over-

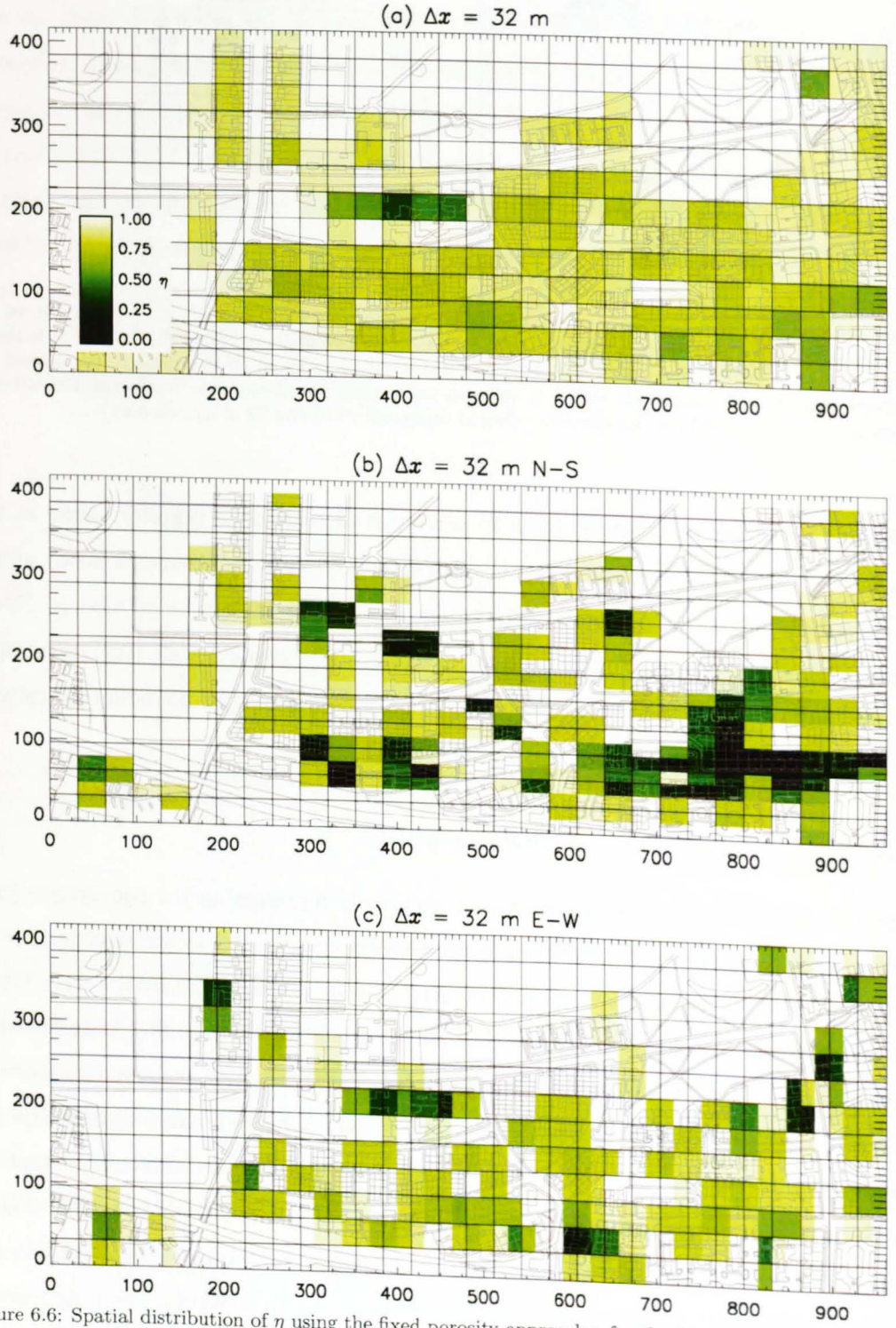

Figure 6.6: Spatial distribution of η using the fixed porosity approaches for the 32 m resolution DTMs using the 2 m benchmark DSM and MasterMap® data where a) represents the ηFIX values (as in Fig 6.2), b) represents the ηBOUND values for the North-South direction and c) represents the ηBOUND values for the East-West direction. Note that two values of boundary porosities are shown in one grid cell for each direction.

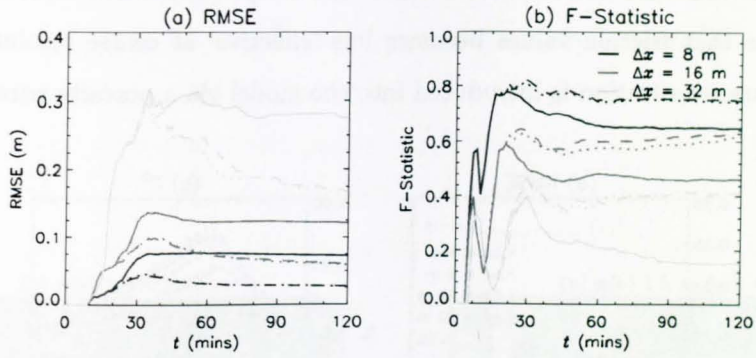

Figure 6.7: Evolution of global measures of model performance throughout the simulation at $\Delta x = 8$, 16 and 32 m compared to the benchmark solution where *a)* is the RMSE of predicted flood depths and *b)* is the F^2 binary measure of fit of flood extents. The solid line represents the original DSM approach, the dashed line represents porosity ηFIX approach and the dotted line represents porosity ηBOUND approach

estimation of flood extents in a particular cell from the ηFIX formulation. Furthermore, as LISFLOOD-FP calculates a volumetric flow rate rather than a velocity between cells, as long as the porosity adequately represents the overall volumetric change, global performance measures are unlikely to be largely affected. In a more complex numerical model that explicitly resolves velocity calculations, the impact of a boundary porosity formulation (e.g. Sanders *et al.*, 2008) may be more substantial.

Sensitivity to friction parameterisation

Results from a porosity technique in a similar class of model (Yu and Lane, 2006b) suggest that as more sub-grid scale topographic information is incorporated into coarse grid models using porosity techniques, the value of Manning's n friction parameter becomes more identifiable with respect to the optimum model parameterisation. Figure 6.8 shows the results of a sensitivity analysis in n for the DSM and ηFIX porosity models across a range of resolutions. These results suggest little change in model response to Manning's n at 4 m resolution using the ηFIX porosity formulation in preference to the DSM approach but substantial effects at coarser resolutions. Notably, there is an increase in the identifiability of the optimum friction value in the 8 and 16 m models using the porosity approach when considering the errors in water depth estimation, a result also found by Yu and Lane (2006b). Furthermore, the porosity models at 8 and 16 m grid resolution show an inherent stationarity of Manning's n with respect to the 2 m benchmark solution value. At 32 m resolution, the model response to friction parameterisation proves to be both non-stationary compared to

the benchmark value and non-identifiable in terms of optimum value. Nevertheless, these results suggests that friction values becomes less 'effective' at coarse resolutions as more topographic parameterisation is introduced into the model via a porosity parameter.

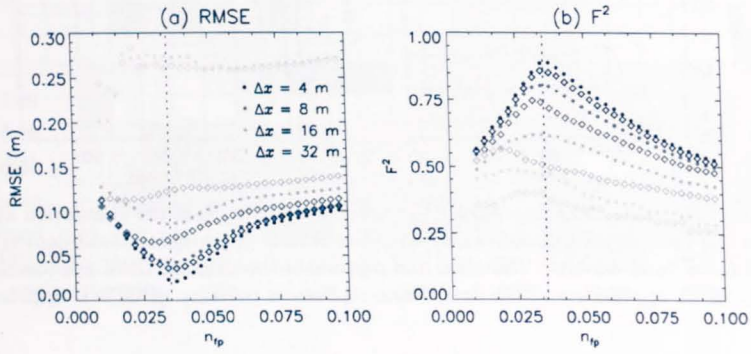

Figure 6.8: Model response of RMSE and F^2 for the ensemble of varying friction coefficient simulations at $t = 30$ mins for each resolution using the DSM (diamonds) and ηFIX porosity (dots) model configurations. The dotted line represents the Manning's n friction value used in the benchmark 2 m solution.

Regardless of the success of the simple areal porosity method, coarse grid models of this site struggle to resolve the high velocity, shallow flows down the northern-most street. The analysis above, coupled with results from Chapter 4 suggest that small-scale topographic variability may control the flow in this region. However, although such shallow flows do not impact on damage estimates, these flows affect the degree of ponding at the western edge of the domain. Therefore, it is important to analyse the effectiveness of water height dependent porosity values at resolving these shallow flows.

6.1.2 Water height dependent porosity approaches

Figure 6.9 shows the spatial distribution of height dependent areal porosity values at various water depth increments on the 16 m grid for the Glasgow test site. There is substantial variability in porosity values with increasing water depth up to depths of 0.5 m, thereafter the porosity values appear to mirror the building configuration as much as is possible at 16 m resolution. The porosity variability at small water depths would imply a strong dependence of floodwave propagation on the local topography. However, as the domain slopes downwards considerably ($S_0 = 0.01$) from east to west, the variation in porosity is actually describing the sloping terrain in the coarse grid cells.

The evolution of global model performance measures for the ηFIX and ηVAR methods compared to the DSM approach are shown in Figure 6.10. The height variable porosity

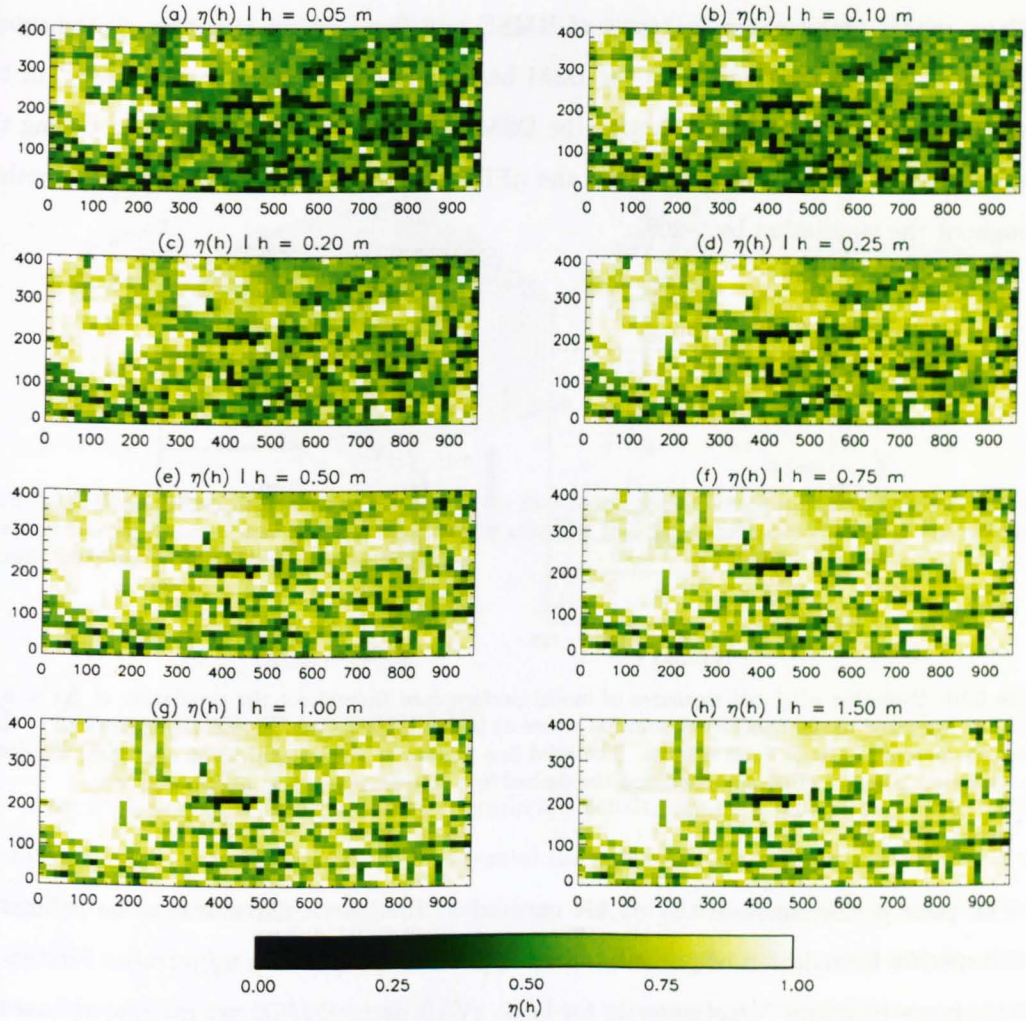

Figure 6.9: Spatial distribution of ηVAR for the 16 m resolution DTMs using the 2 m benchmark DSM and MasterMap$^{®}$ data at various water depth increments.

the benchmark value and non-identifiable in terms of optimum value. Nevertheless, these results suggests that friction values becomes less 'effective' at coarse resolutions as more topographic parameterisation is introduced into the model via a porosity parameter.

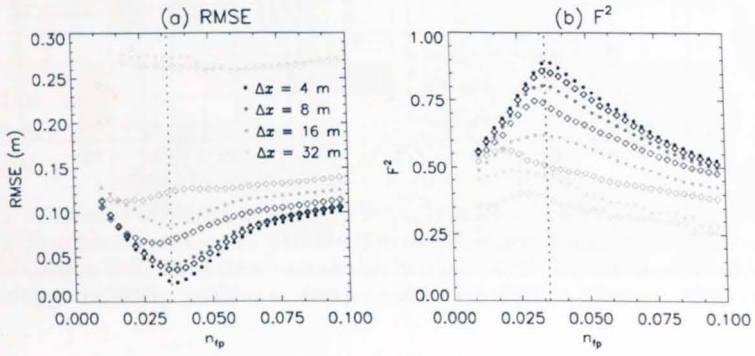

Figure 6.8: Model response of RMSE and F^2 for the ensemble of varying friction coefficient simulations at $t = 30$ mins for each resolution using the DSM (diamonds) and ηFIX porosity (dots) model configurations. The dotted line represents the Manning's n friction value used in the benchmark 2 m solution.

Regardless of the success of the simple areal porosity method, coarse grid models of this site struggle to resolve the high velocity, shallow flows down the northern-most street. The analysis above, coupled with results from Chapter 4 suggest that small-scale topographic variability may control the flow in this region. However, although such shallow flows do not impact on damage estimates, these flows affect the degree of ponding at the western edge of the domain. Therefore, it is important to analyse the effectiveness of water height dependent porosity values at resolving these shallow flows.

6.1.2 Water height dependent porosity approaches

Figure 6.9 shows the spatial distribution of height dependent areal porosity values at various water depth increments on the 16 m grid for the Glasgow test site. There is substantial variability in porosity values with increasing water depth up to depths of 0.5 m, thereafter the porosity values appear to mirror the building configuration as much as is possible at 16 m resolution. The porosity variability at small water depths would imply a strong dependence of floodwave propagation on the local topography. However, as the domain slopes downwards considerably ($S_0 = 0.01$) from east to west, the variation in porosity is actually describing the sloping terrain in the coarse grid cells.

The evolution of global model performance measures for the ηFIX and ηVAR methods compared to the DSM approach are shown in Figure 6.10. The height variable porosity

approach significantly reduces model performance at 8 and 16 m resolution compared to both the ηFIX and DSM based models throughout the simulation. Most notably, model performance decreases dramatically in the ηVAR method at 8 m grid resolution as the model approaches steady state when water is ponded in the low-lying regions (around X3). The 16 m model also portrays a reduction in model performance in terms of F^2 compared to the DSM based model and significantly under-performs the ηFIX model. In contrast, at 32 m, model performance in terms of RMSE and flood extent increases as the model approaches steady state relative to the DSM based approach. However, the RMSE of the 32 m ηVAR rises more steeply than for the DSM and ηFIX model formulations during the dynamic portion of the event. Notably, the ηFIX method outperforms the ηVAR method throughout the simulation by >20%.

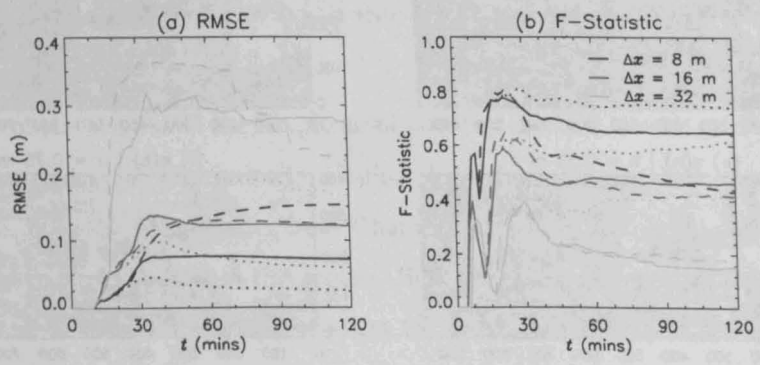

Figure 6.10: Evolution of global measures of model performance throughout the simulation at $\Delta x = 8$, 16 and 32 m compared to the benchmark solution where *a*) is the RMSE of predicted flood depths and *b*) is the F^2 binary measure of fit of flood extents. The solid line represents the original DSM approach, the dotted line represents porosity ηFIX approach and the dashed line represents porosity ηVAR approach

The poor performance of the ηVAR method at this particular site may be a function of the specific formulation of porosity when applied to steeply sloping terrain. Firstly, the storage porosity values (*areal porosity* for both ηVAR and ηBVAR) are calculated based on horizontal water surface profiles. In addition, in LISFLOOD-FP (as in any finite difference approach), elevations are defined at cell centres as a horizontal plane. It can postulated that the combination of these two features may lead to spurious volume-depth conversions in the two-stage look-up table approach of the water height dependent porosity algorithms. Figure 6.11 shows the variation in 2 m sub-grid topography for four 16 m cells of the Glasgow digital terrain model and the variation in porosity for those four 16 m resolution cells. The most notable feature of these porosity functions is the rapid increase in porosity in the range 0 - 0.25

m water depth which may suggest that the linear interpolation between discrete water depth increments does not adequately represent the actual function. It may be that topographic terrain variation within a coarse grid cells must be approximately normally distributed to allow height variable porosity functions to improve model results. These results suggests that as long as the digital terrain model provides a good description of the underlying topography, simple areal based fixed porosity techniques (ηFIX or Soares-Frazão *et al.* (2008)) provide the best trade-off between processing time, data requirements and model performance.

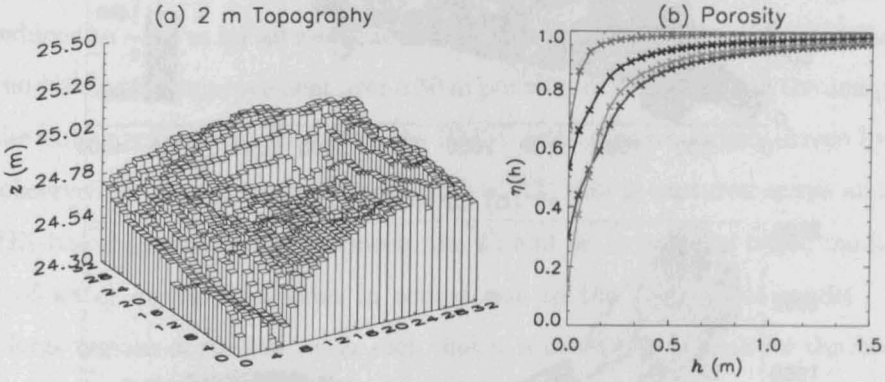

Figure 6.11: Water height dependent areal porosity for four coarse resolution cells of the Glasgow DSM where (a) shows the variation of sub-grid scale 2 m topography for four 16 m cells and (b) shows the associated porosity functions with increasing water depth.

6.2 Greenwich, London, UK

The Greenwich test case highlighted the significant sensitivity of urban areas to the narrow separations between buildings and the potential for substantial alteration of flowpaths and storage in coarse resolution models. In addition, the DTM-based models of this site suggested that some regions were solely controlled by the building configuration and floodwave propagation in other areas was controlled by small-scale topographic irregularities. As a consequence, the fixed and height dependent porosity techniques can be applied in this region to establish the influence of these different controlling mechanisms for flooding at this site.

6.2.1 Fixed porosity approaches

Figure 6.12 shows the spatial distribution of fixed areal porosity values throughout the Greenwich embayment at 10, 25 and 50 m resolution based on the 5 m benchmark DEM. At 10 m resolution, the porosity value echoes the building configuration and highlights the areas of

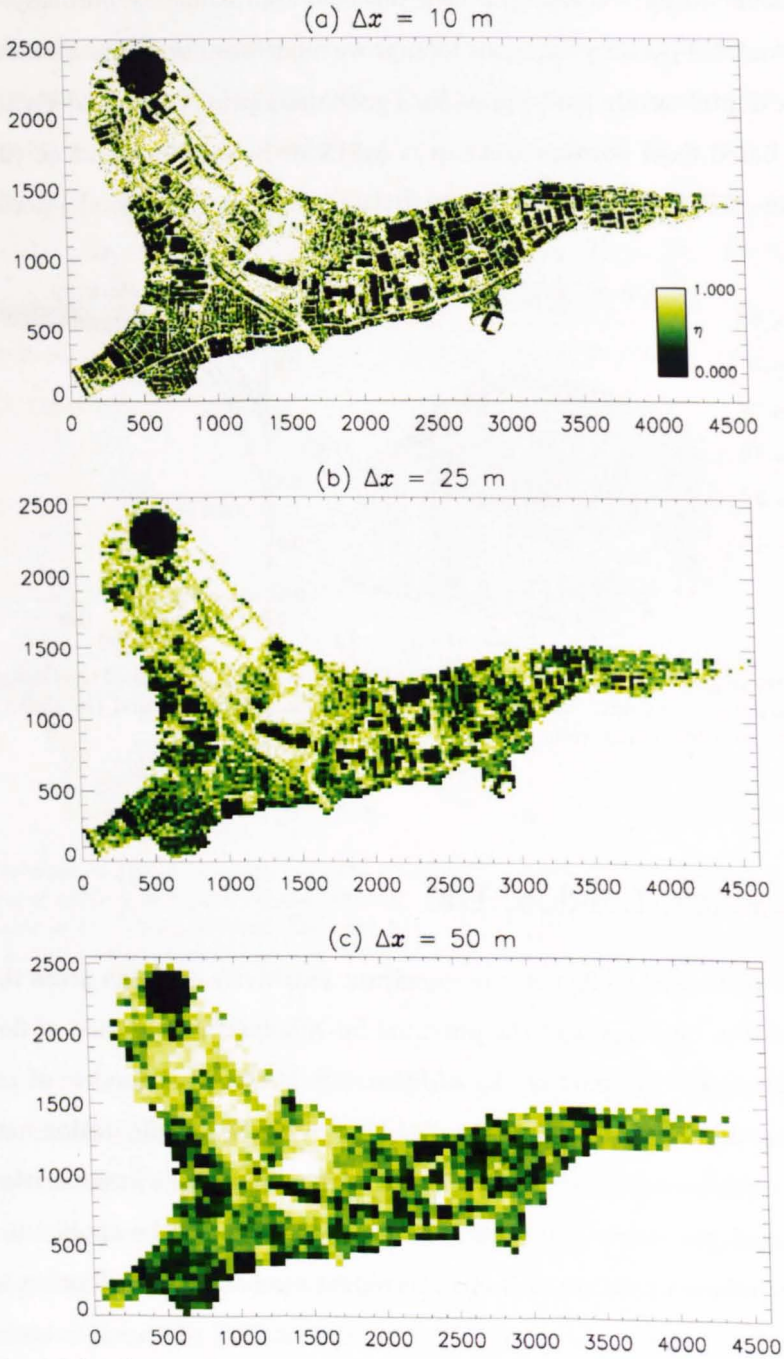

Figure 6.12: Spatial distribution of η using the fixed areal porosity approach for the 10, 25 and 50 m resolution DTMs using the 5 m benchmark DSM and MasterMap® data.

large buildings around X4 and the detailed street network at X1. In contrast, at 25 and 50 m resolution, the porosity values provide aggregate approximations of the building network, in particular around X1. The large variability in porosity values around X2 across all resolutions highlights the complex nature of structures, buildings and open land in industrial areas.

The evolution of global RMSE and F^2 for the DSM and ηFIX models of Greenwich at 10, 25 and 50 m resolution (Figure 6.13) shows considerable improvement of flood depth and extent predictions when employing the porosity based approach. Notably, the RMSE error is reduced to $\sim$0.1 m for all resolutions such that a high resolution 10 m porosity model provides no substantial improvement over a 50 m porosity model, reducing the computational cost for the same performance. However, the RMSE estimates are largely driven by the deep ponding observed in the Blackwall Tunnel (south of X2) that is captured across all resolution in the ηFIX-based approach. Furthermore, the 25 and 50 m porosity based models reduce the error of water depth predictions in comparison to the 10 m DSM model. However, there are large regions of shallow water such that it is necessary to consider the flood extent predictions to adequately evaluate the porosity based models. Figure 6.13b shows that the porosity approaches increase the fit between the benchmark and modelled flood extent. In fact, the 25 and 50 m ηFIX models provide global flood extent fits similar to the 10 m DSM-based model which further justifies the trade-off between resolution and computational cost. In addition, the 10 m ηFIX models yields a 50% improvement over the DSM-based 10 m model at steady state in terms of F^2. An examination of the maximum predicted flood

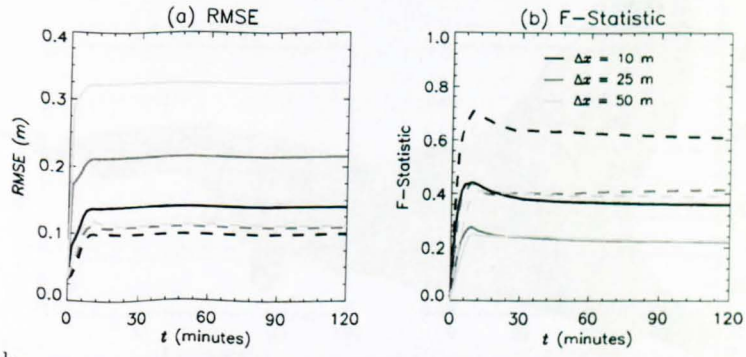

Figure 6.13: Evolution of global measures of model performance throughout the simulation at Δx = 10, 25 and 50 m compared to the benchmark solution where *a)* is the RMSE of predicted flood depths and *b)* is the F^2 binary measure of fit of flood extents. The solid line represents the original DSM approach and the dashed line represents porosity ηFIX approach with 5 m sub-grid topography.

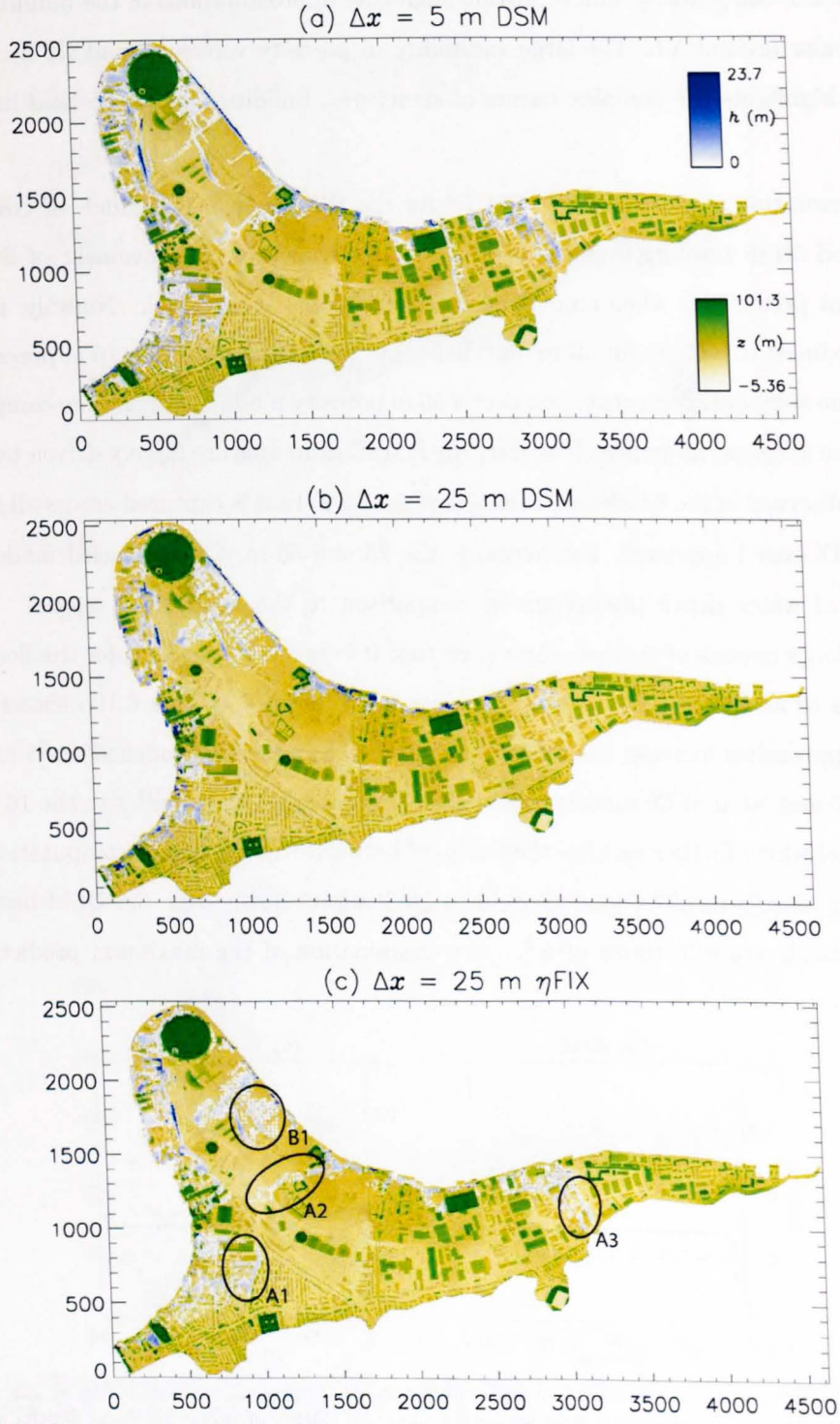

Figure 6.14: Maximum simulated flood extent at 25 m resolution with the surface height (z) from the DEM shown as a grey scale overlain by water depths (h) using (b) the coarse DSM and (c) the ηFIX method.

depths throughout the simulation (Figure 6.14) highlights the localised improvements that produce the global increase in model performance. The flood extent map highlights three areas of significant local improvement to floodwave propagation using the porosity approach (labelled A1-3) and also highlights regions where both the porosity and DSM models over-predict flood extents (labelled B1). The improvement in flood extent prediction in the urban areas around X1 and X4 (A1 and A3, respectively) is a direct result of using the DTM and incorporating the building information to drive flow direction. However, at B1, there is clear over-prediction of flood extents in both the DSM and fixed areal porosity based models which suggests that local topographic irregularities control floodwave direction. Therefore, water height dependent porosity methods may provide the added level of detail required to force floodwave propagation in this region.

Influence of boundary porosities on flood propagation

Figure 6.15 shows the evolution of global performance measures for the ηFIX and ηBOUND porosity approaches at 10, 25 and 50 m resolution using the 5 m resolution sub-grid topography. As observed at the Glasgow site, the incorporation of boundary dependent porosity values does not increase model performance compared to the areal porosity method at resolutions coarser than the building dimensions (i.e. 25 and 50 m). In fact, in this case, model results are almost identical. However, at resolutions similar to the building dimensions, the boundary porosity methods provide contrasting results depending on the performance measure. Considering water depth predictions, the boundary porosity lowers the RMSE

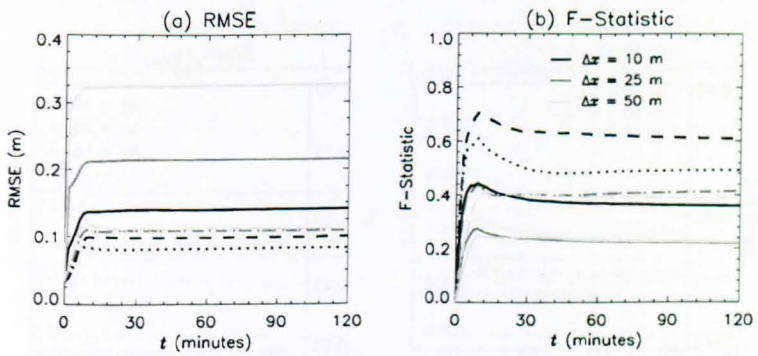

Figure 6.15: Evolution of global measures of model performance throughout the simulation at Δx = 10, 25 and 50 m compared to the benchmark solution where *a*) is the RMSE of predicted flood depths and *b*) is the F^2 binary measure of fit of flood extents. The solid line represents the original DSM approach, the dashed line represents the ηFIX approach and the dotted line represents the ηBOUND approach using 5 m sub-grid topography.

by ~10% but also decreases the F^2 measure from 0.6 to 0.5 when compared to the ηFIX method. This suggests the boundary porosity formulation over-estimates the importance of the single-cell stencil at the boundary and thus under-estimates flood depth predictions - a finding that echoes results from Chapter 5.

Sensitivity to friction parameterisation

Floodwave propagation in Greenwich appears to be controlled either by the building configuration or small-scale topographic irregularities, depending on the region under investigation. As the simple fixed porosity methods have been shown to replicate propagation through a dense urban network (above and in Chapter 5), it may be possible to parameterise the flow over open land using Manning's n. Figure 6.16 shows the variation in RMSE and F^2 for the ensemble of floodplain friction variations documented in Chapter 4 at 10 mins through the simulation for the DSM and ηFIX methods. Although the porosity approach increases model performance across resolutions for any given value of floodplain friction compared to the DSM-based approach, model performance appears insensitive to actual values of floodplain n. There are two possible and contrasting reasons for such a model response. Firstly, the Greenwich test case is characterised by deep water at the inflow locations which may cause the relative insensitivity to friction values. Secondly, the embayment has a number of different land use types such that the global performance measures are compensating for localised differences throughout the domain and providing an aggregate model response. Considering the latter, it may be beneficial to incorporate a spatially varied approach to Manning's n friction parameterisation. In addition, once topography is better represented

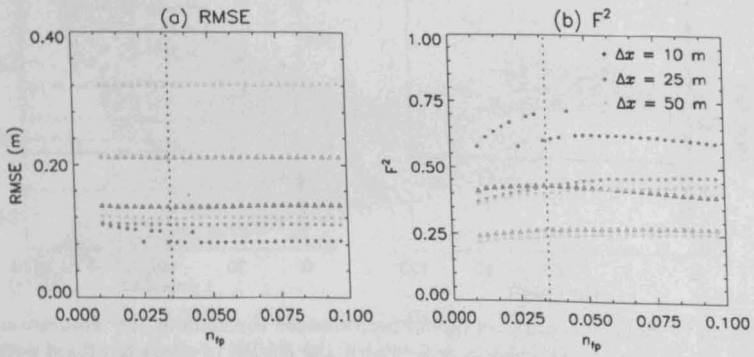

Figure 6.16: Model response of RMSE and F^2 for the ensemble of varying friction coefficient simulations at $t = 10$ mins for each resolution using the DSM (triangles) and ηFIX porosity (dots) model configurations. The dotted line represents the Manning's n friction value used in the benchmark 5 m solution.

in coarse resolution models (i.e. using a porosity-type approach), friction specification may be more physically-based (as suggested in Yu and Lane (2006b)).

6.2.2 Water height dependent porosity approaches

The Greenwich embayment is characterised by extensive areas of open land and terraced housing. The ηFIX method has been shown to improve coarse resolution predictions of flood depths and extents in dense urban areas with respect to coarse DSM models. Floodwave propagation in the areas of open land. however, was poorly represented due to the averaging procedure in transforming high resolution terrain models to coarse resolution terrain models. As a result, the ηVAR method is implemented to determine if small-scale topographic irregularities can be better resolved in coarse resolution models where sub-grid scale flow paths exist. Figure 6.17 shows the evolution of RMSE and F^2 for the height variable areal porosity compared to the original DSM model formulation at 10, 25 and 50 m resolution. In terms of flood depth predictions, the porosity models show an improvement compared to the DSM-based models. However, analysis of the flood extent predictions shows a reduction in model performance in the ηVAR approach which is magnified significantly at 10 m resolution. Visual analysis of flood extents shows that the water height dependent areal porosity approach under-predicts floodwave propagation throughout the domain. In order to diagnose the cause of the under-prediction, the evolution of water volume in the domain is analysed (Figure 6.18). This shows that the ηVAR approach is non-mass conservative which appears to manifest during propagation from the inflow points (i.e. when the inflow point is drying) which may in part be caused by the use of a look-up table for water heights in this

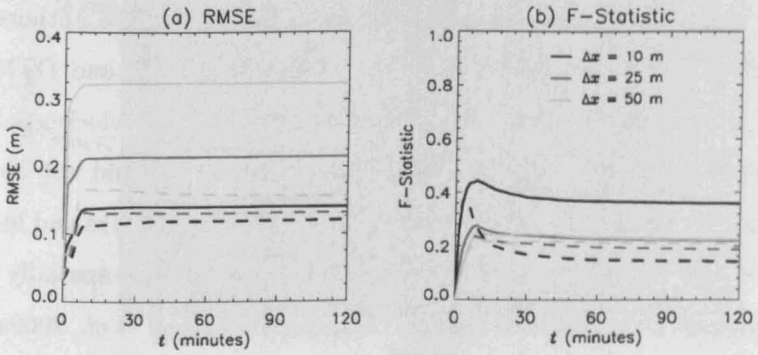

Figure 6.17: Evolution of global measures of model performance throughout the simulation at $\Delta x = 10$, 25 and 50 m compared to the benchmark solution where *a*) is the RMSE of predicted flood depths and *b*) is the F^2 binary measure of fit of flood extents. The solid line represents the original DSM approach and the dashed line represents the ηVAR approach using 5 m sub-grid topography.

method. The look-up table is required as the use of height dependent porosities in a storage cell approach becomes an implicit problem. As a result, this method becomes significantly more complex to implement numerically, artificially adding to model complexity. Therefore, this method fails to meet the aims of the thesis to develop simplistic methods for wide area flood risk assessment. In addition, the ηFIX approach has been shown to significantly improve flood risk estimates at this site such that the additional numerical complexity is not warranted.

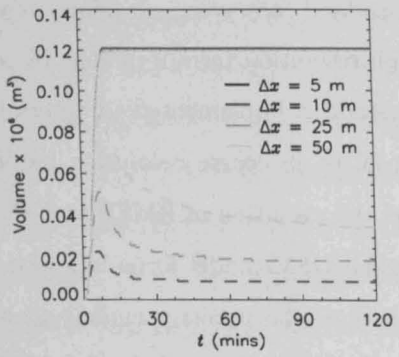

Figure 6.18: Evolution of water volume throughout the simulation at $\Delta x = 10$, 25 and 50 m compared to the benchmark solution. The solid line represents the original DSM approach, the dotted line represents the ηFIX method and the dashed line represents the ηVAR approach using 5 m sub-grid topography. Note the solid and dotted line overplot regardless of resolution.

6.3 Carlisle, Cumbria, UK

Neal *et al.* (2009a) detail the collection and processing of one of the largest water and wrack mark data sets from an urban flood event with complementary LiDAR, digital map and multiple gauge data from the Carlisle 2005 event. In addition, the authors develop and calibrate a LISFLOOD-FP model at 25 m resolution using DSM and DTM descriptions of topography. It was noted in this study that where significant blockages influence flow direction and storage, the 25 m DSM and DTM-based models could not be calibrated to give optimum performance with respect to both floodplain water marks and in-channel stage with a simple two-parameter space. However, there may be scope for spatially varied friction values in the channels given localised channel characteristics (Neal *et al.*, 2009a). In response to localised poor model performance in the DSM-based models and results from the Glasgow and Greenwich test cases, the fixed porosity approach (ηFIX) is implemented on the Carlisle 2005 event. As a result of the significant computation time of the 25 m model, a similar 50

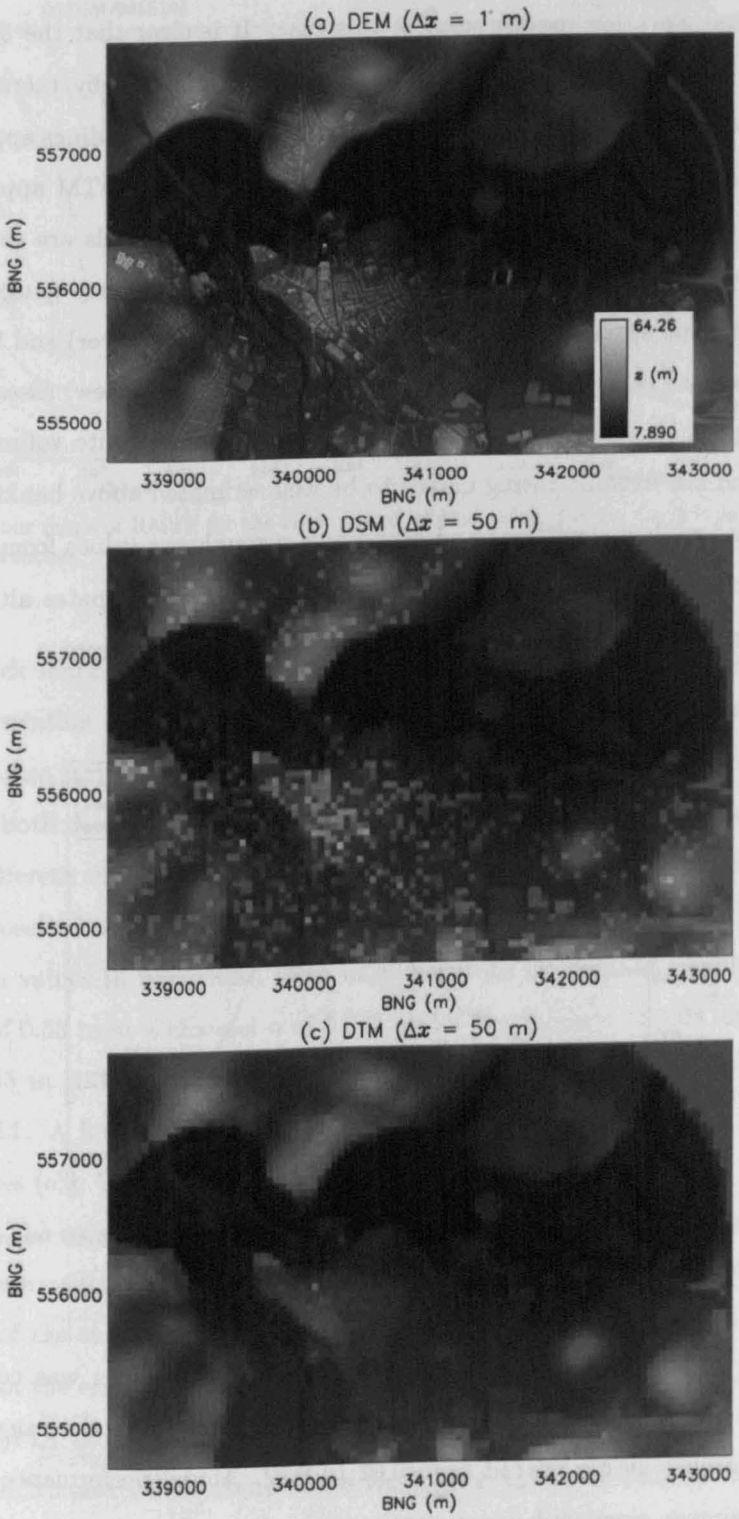

Figure 6.19: Digital elevation models of the Carlisle model domain where (a) is the 1 m DSM, (b) is the 50 m DSM and (c) is the 50 m DTM.

m model using the DSM and ηFIX approaches is tested in this case. Figure 6.19 shows the 1 and 50m digital elevation models used in this case. It is clear that the 50 m resolution DSM does not provide a coherent match to the 1 m DSM whereby there is substantial misrepresentation of the building configuration and in places, the buildings appear as random noise incorporated into the DEM. On the other hand, the 50 m DTM appears to resolve the broad-scale topographic attributes around Carlisle. The models are setup as in Neal *et al.* (2009a) with channel flows derived from Environment Agency gauge data (Figure 6.20), a uniform slope applied to each channel (for the kinematic solver) and LiDAR-derived topography processed as in Mason *et al.* (2007). Horritt *et al.* (in review) assessed the quality of the Environment Agency gauge data using a high resolution finite volume flood model (SFV) and found the existing rating curves to be well estimated above bankfull stage when calibrated using low flow conditions and Manning's n roughness values from the literature. Nevertheless, it is still likely that there are errors in the flow estimates although there is insufficient data to estimate the magnitude or distribution of the errors.

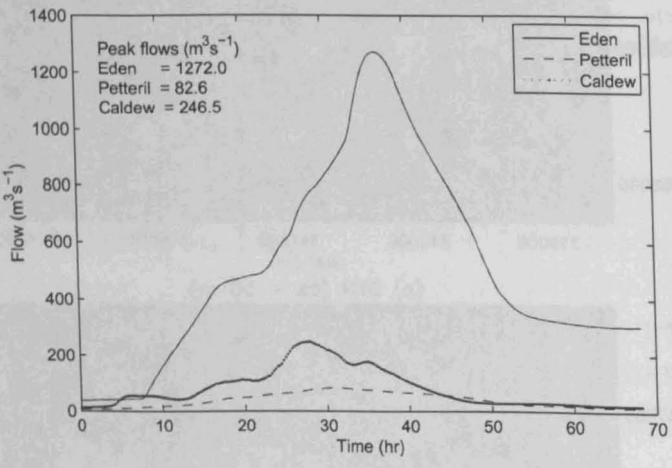

Figure 6.20: Inflows to the Carlisle model from the Rivers Eden, Petteril and Caldew (reproduced from Neal *et al.* (2009a)).

As in Neal *et al.* (2009a), a calibration of Manning's n values was conducted using a matrix of 66 simulations using channel values evenly spaced in the range 0.03 to 0.08 and floodplain values evenly spaced from 0.02 to 0.12. Model performance is assessed by comparing maximum simulated water depths with observed maximum water marks. In order to maintain a consistent model evaluation strategy, the approach employed in Neal *et al.* (2009a) is implemented here such that in the event of a simulated flood extent not

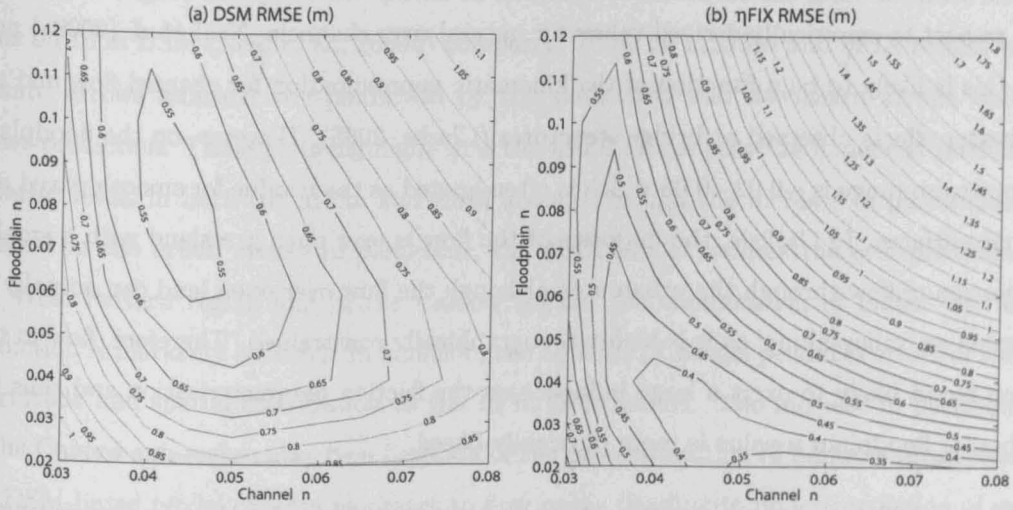

Figure 6.21: Contour maps of RMSE for the ensemble of friction values for the Carlisle area using (a) DSM and (b) ηFIX approaches.

reaching a wrack mark, the water surface of the nearest wet cell is used to calculate the error in the simulation (see Neal *et al.* (2009a) for further justification). Figure 6.21 shows the model response surface to variations in the channel and floodplain Manning's n friction parameters for both the 50 m DSM and ηFIX models. The two model configurations exhibit considerably different shape response surfaces with respect to friction parameterisation, with the ηFIX approach showing a greater sensitivity across the range of both floodplain and channel friction values in particular. The most accurate DSM-based simulation yielded a global RMSE of 0.53 m at a channel n of 0.045 and a floodplain n of 0.08 although optimal solutions (<0.55 m RMSE) exist in the range of channel n of 0.04 to 0.05 and floodplain n of 0.06 to 0.11. A floodplain Manning's n of 0.08 is substantially higher than literature prescribed values (e.g. Chow, 1959) for rural and urban surfaces.

In contrast, the most accurate ηFIX simulation was at a channel friction of 0.06 and a floodplain friction of 0.02 delivering an RMSE of 0.31 m. Neal *et al.* (2009b) showed that a 10 m model of the same event yielded a global RMSE of 0.28 m which is approximately the magnitude of the error in the observational data (J.C. Neal, pers. comm.). The response surface in the ηFIX model portrays the characteristic L-shaped parameter shape whereby lower floodplain friction values compensate for higher values of channel friction (Hunter *et al.*, 2006) as shown by Neal *et al.* (2009a) at 25 m resolution for both the DSM- and DTM-based models. Yu and Lane (2006b) suggested that as more topographic information is incorporated at coarse grid scales, values of Manning's n become less scale dependent. In

this case, the optimum friction values from the ηFIX configuration are high in the channel with respect to empirically derived values for natural river channels. Neal *et al.* (2009a) note that this is likely to be a function of the kinematic approximation for channel flow and the backwater effects observed at bridge structures (Clarke, 2005). However, on the floodplain, the optimum range is ~0.02 - 0.03 which is often quoted as the n value for smooth paved and tarmac surfaces. In Carlisle, the majority of the flow is over open grassland with a smaller proportion of flow through the urban area although the flow over open land can actually be regarded as 'valley-filling' as it is highly topographically constrained. Therefore, flow in this region is not likely to exert a large influence on the friction parameterisation and thus the calibrated floodplain n value is more physically-based.

Figure 6.22 shows the histogram of errors between the simulated and measured water levels for the most accurate simulations in the DSM and ηFIX model configurations. These results show a main peak at -0.25 m and a secondary peak at -1.25 m for the DSM model whereas the ηFIX shows a cluster of errors from -0.5 m to 0.5 m. The DSM model over-predicts water levels by 1.5 m and under-predicts by as much as 2.0 m whereas the ηFIX model over-predicts by 0.75 m and under-predicts by 1.5 m. The small range in the ηFIX-based model explains the increase in global model performance compared to the DSM-based model. The spatial distribution of these errors will provide information on local model performance and will diagnose where the increase in performance from the ηFIX model is

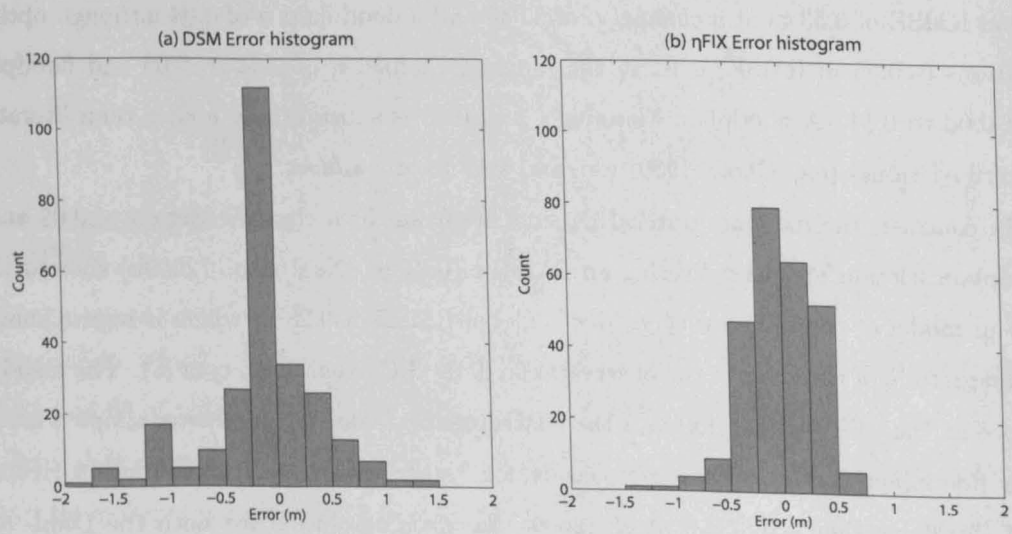

Figure 6.22: Histograms of errors between maximum water level measurements and the most accurate simulations for the Carlisle area (observed - simulated) using (a) DSM and (b) ηFIX approaches.

manifested. Figure 6.23 plots the spatial distribution of errors for the most accurate simulations on 10 m DSM (Neal *et al.*, 2009b) compared to the 50 m DSM and ηFIX results where upward arrows indicate over-prediction by the simulation and downward arrows indicate under-prediction. These plots highlight that the ηFIX model provides enhanced predictions of water levels in both the urban and rural areas, although the increase in performance is greatest in the urban areas. In particular, the ηFIX model reduces the over-prediction in the West Petteril region and in the Caldew region, the combination of under- and over-prediction is markedly reduced. In addition, the 50 m ηFIX model produces errors of similar magnitude and spatial distribution as the 10 m DSM model. The increase in performance in the Caldew sub-region may be a function of the over-estimation of building dimensions in the DSM-based model causing blockages to flow paths (leading to under-prediction of water depths) and backwater effects behind large building artefacts (leading to over-prediction). An investigation of the Manning's n parameter response surface in this region (Figure 6.24) shows that the DSM model is insensitive to floodplain friction which suggests that this area has become hydraulically disconnected such that water is ponding as a result of misrepresenting buildings in the DSM. On the other hand, the ηFIX model produces a response surface that is more sensitive to the specification of channel and floodplain friction values and also displays the characteristic L-shape. The RMSE value is also reduced from 0.55 m for the DSM-based model to 0.29 m for the ηFIX model in this region. Furthermore, the optimum channel roughness has remained stationary with respect to the global estimate of channel n but there has been a slight increase in the optimum floodplain n value.

Around the West Petteril, the ηFIX model reduces the large over-prediction of water depths visible in the DSM-based model (Figure 6.23) and in the histograms of depth error (Figure 6.22). Neal *et al.* (2009a) suggest that these errors correspond to flood extent wrack marks, which are better resolved using porosity as the flows in the urban area are better represented. This region is also characterised by large under-prediction errors which are apparent in both the optimum DSM and ηFIX models. However, Neal *et al.* (2009a) note that these points correspond to water level marks on the sides of buildings and structures which tend to be higher than those taken from flood extent wrack marks which may be caused by local flow conditions, bias in the interpretation of these marks and wrack marks deposited on the falling limb of the hydrograph. Figure 6.25 shows response of RMSE to variations in channel and floodplain n in the West Petteril region for the DSM and ηFIX models. These results suggest it is not possible to calibrate channel and floodplain friction

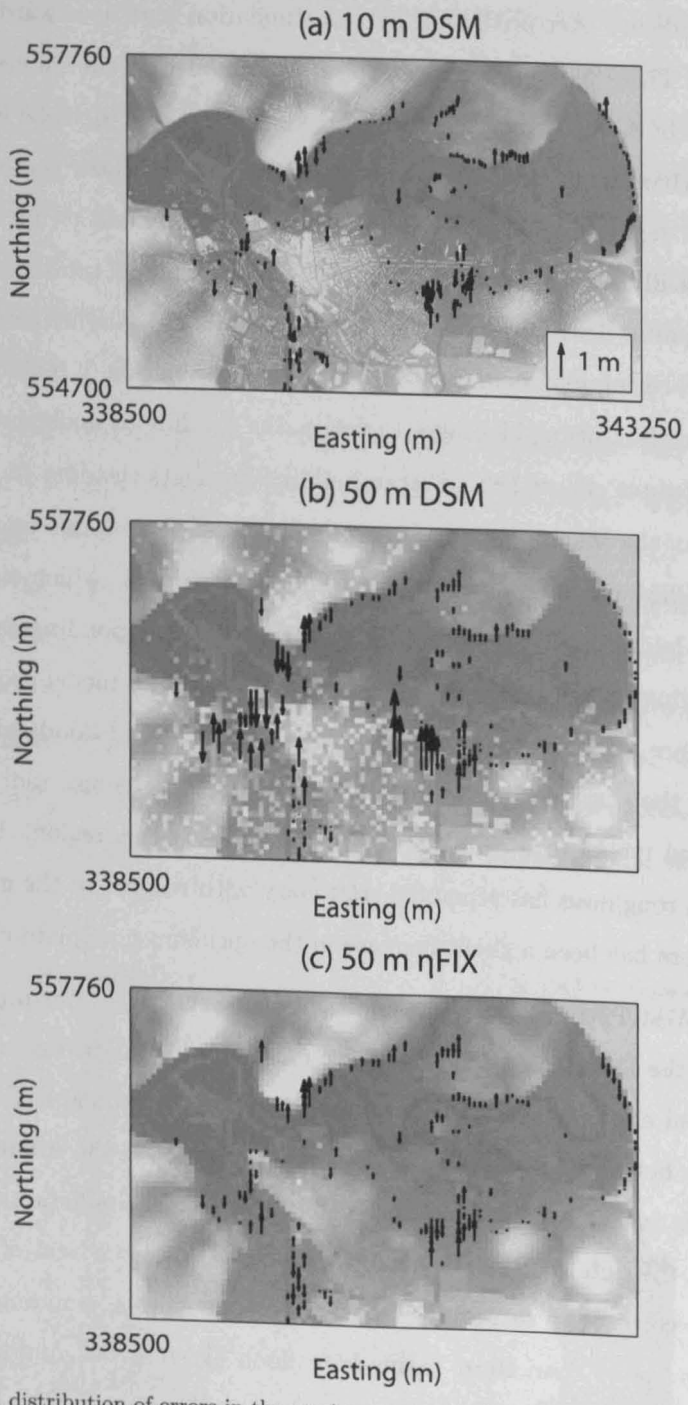

Figure 6.23: Spatial distribution of errors in the most accurate simulations for the Carlisle area from the (a) 10 m DSM (reproduced from Neal *et al.* (2009a)), (b) 50 m DSM, and (c) 50 m ηFIX approaches.

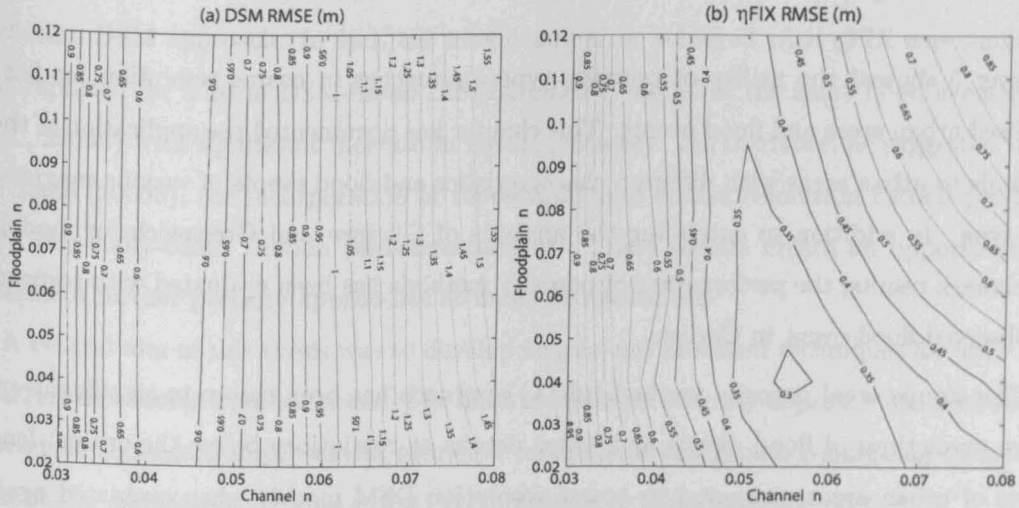

Figure 6.24: Contour maps of RMSE for the ensemble of friction values for the River Caldew sub-region using (a) DSM and (b) ηFIX approaches.

to overcome limitations of topographic representation in coarse resolution DSM models as the error is >0.85 m regardless of friction values. The ηFIX model yields a response surface with a slightly increased optimum floodplain n and slightly decreased channel n with respect to the global and Caldew sub-region RMSE values. However, the model may be attempting to fit to the water mark data in this region thus obtaining a high floodplain n to generate higher water elevations. Nevertheless, the porosity approach provides a more identifiable friction response surface globally and for individual sub-regions than the DSM-based model.

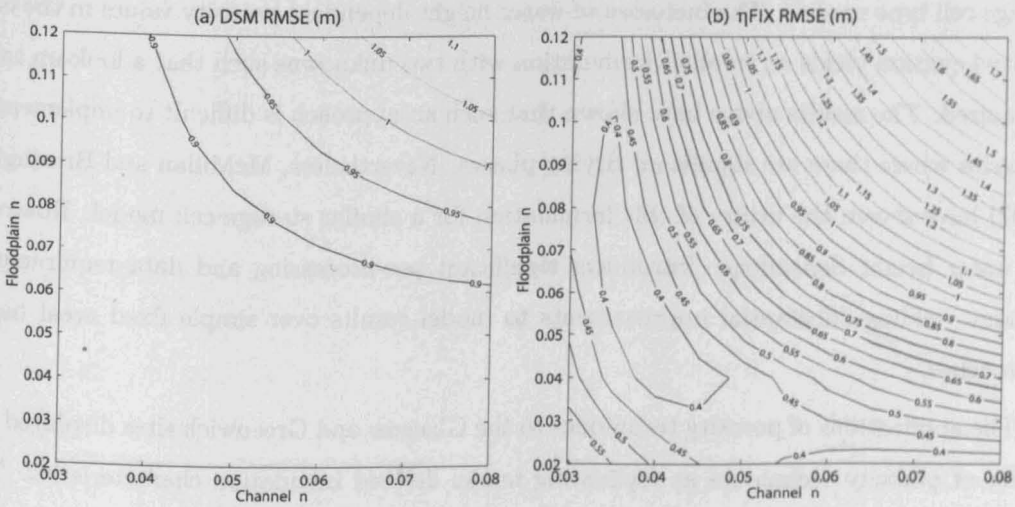

Figure 6.25: Contour maps of RMSE for the ensemble of friction values for the West Petteril sub-region using (a) DSM and (b) ηFIX approaches.

6.4 Conclusions and recommendations

Chapter 5 showed the utility of porosity type approaches in coarse resolution models of idealised urban areas and flood events. This chapter has documented the application of these methods to urban areas with different characteristics and flood events of varying magnitude and type. In addition to extending the analysis of Glasgow and Greenwich for modelled benchmark results, the performance of porosity methods has been evaluated with respect to an observed flood event in Carlisle.

The simple areal porosity method (ηFIX) approach has been shown to significantly improve predictions of flood extent and water depths at resolutions below the critical length scales of urban areas compared to coarse resolution DSM models when evaluated against high-resolution benchmark simulations. The requirements for sub-grid scale topography to define the porosity values in this method appear to be relaxed such that sub-grid scale descriptions that resolve the critical length scales of the urban area are sufficient. Furthermore, the incorporation of a boundary porosity to resolve inter-cellular fluxes at coarse resolution does not improve predictions when compared to benchmark modelled data sets. This suggests that it is sufficient to represent the bulk effect of buildings with simple hydraulic models although this may prove important in more complex numerical schemes.

In Chapter 5, water height dependent porosity approaches did not significantly improve predictions of water propagation. Application of these methods to the Greenwich and Glasgow test cases actually highlighted the practical difficulties of using such an approach within storage cell type models. The inclusion of water height dependent porosity values in the continuity equation yields an implicit formulation with two unknowns such that a look-up table is required. The results above have shown that such an approach is difficult to implement in scenarios where there are significant drying phases. Nevertheless, McMillan and Brasington (2007) have shown the utility of this formulation for a similar storage cell model. However, the water height dependence introduces significant pre-processing and data requirements without yielding substantial improvements to model results over simple fixed areal based approaches.

The applications of porosity techniques to the Glasgow and Greenwich sites displayed the utility of porosity techniques at replicating model derived inundation characteristics. The Carlisle flood event provided the first opportunity to evaluate simple porosity approaches with respect to observed flood data. At a single resolution, the ηFIX porosity method has

been shown to reduce the global error in water depth predicts by ~40% compared to a coarse resolution DSM approach. In fact, the magnitude error achieved with ηFIX was similar to that reported for a 10 m DSM-based LISFLOOD-FP model of the same flood event (Neal *et al.*, 2009b) with significant increase in model efficiency. Furthermore, as suggested in Yu and Lane (2006b), the incorporation of topography into coarse resolution models produces more physcially-based friction parameterisations. These results create an opportunity to implement further porosity approaches at multiple resolutions.

A central aim of this thesis was to develop simple and practical techniques for wide area flood risk assessment in urban areas. The fixed areal based porosity approach has been shown to produce significant improvement to model results over traditional resampling techniques without the addition of significant data requirements or computational cost.

CHAPTER 7

Conclusions, limitations and future work

In the past 20 years, flood inundation models of rural flooding episodes have been extensively built and tested against bulk catchment flow measurements and synoptic scale remotely sensed imagery. However, until recently, urban areas have largely been disregarded in flood modelling studies despite the concentration of risk in urban environments. In addition, recent studies concerning flood risk assessment under climate change scenarios (e.g. Wilby *et al.*, 2008) suggest considerable increase in flood risk throughout the UK. The realisation of this increasing flood risk has recently prompted a proliferation of urban flood inundation modelling studies throughout the hydraulic and hydrological community. Further consideration of flood risk assessment highlights a clear dichotomy between the scales on which information is analysed and the areas over which said information is needed. Specifically, *fine scale* detail is required over *wide areas* for the planning and insurance industries creating a significant computational burden. Computationally efficient techniques are therefore necessary to deliver the required detail within manageable and practical timescales.

Methods and approaches are needed to deliver a compromise between the level of detail, accuracy and the computational burden to adequately assess flood risk. As a result, modelling frameworks, data sources and numerical techniques originally developed for rural flood events have been transferred to the urban setting with varying degrees of success. In response to the limited success, bespoke tools for data processing (e.g. Mason *et al.*, 2007) and numerical modelling (e.g. Yu and Lane, 2006b) specifically targeted to the characteristics of urban areas and urban floods have been defined and implemented. However, the effects of the compromise between detail and computational efficiency on predictive ability and model accuracy have, to date, not been explored in detail.

As flood models are being increasingly applied to urban areas, it is important to elucidate the features of urban areas that modulate flood flows and as such, understand the effects of model resolution and structure. To date, most studies have arbitrarily chosen a model resolution based on modeller knowledge of the test site and a compromise between

project length and computation time. A few studies have considered the effect of model grid resolution on model performance when compared to benchmark high resolution modelled simulations (Neelz and Pender, 2007a; Yu and Lane, 2006a). However, the quality of representation of the urban structures and their detailed effect on flood flows has not been explored in detail. As such the features that control flow through urban environments have not been fully explored.

Despite advances in technology, the computational requirements of high resolution models are restrictive in terms of facilitating fine scale detail over whole cities. A variety of methods exist to address this problem such as using variable resolution grids (VRGs), multi-block grid methods and sub-grid scale topography parameterisation. The research presented here was specifically targeted towards the development of simple methods for practical application and as such, sub-grid scale porosity type approaches present the most appropriate area of research for this application. A variety of sub-grid scale methods, harnessing the availability of high resolution data sets (e.g. LiDAR, MasterMap®) and reducing the computational burden, have been developed. However, the development of the wide variety of sub-grid scale porosity techniques has occurred in a array of model classes and structures (e.g. Molinaro *et al.*, 1994; Sanders *et al.*, 2008; Yu and Lane, 2006b). As a result, the required level of algorithm complexity for a given increase in model performance and the choice of appropriate technique for a given model structure are not well understood. In addition, most techniques have not been tested on floods of varying magnitude in urban areas with substantially different flow and building characteristics. Indeed, a number of methods have only been evaluated against laboratory scale experiments (Sanders *et al.*, 2008; Soares-Frazão *et al.*, 2008). Therefore, it is necessary to standardise the model structure to evaluate required algorithm complexity and subsequently, test the algorithms on a range of flood events and urban areas.

The ultimate goal of this whole area of research is to develop computationally efficient methods for fine scale, wide area predictions using simple to implement, practical approaches for engineers. The research presented in Chapters 4 to 6 has sought to address this aim within a structured framework to provide substantial progress towards a coherent methodology towards flood risk assessment over whole cities.

7.1 Specific conclusions and recommendations

The main conclusions that can be drawn from this thesis are detailed below.

7.1.1 Evaluation of the scale dependence of urban areas

Urban flood modelling practitioners have until recently arbitrarily chosen a model resolution with little physical basis based on modeller skill, and computational and project constraints (e.g. HR Wallingford, 2004; Tarrant *et al.*, 2005). This creates a need for understanding the effects of this choice in terms of model predictive ability and subsequently in terms of management decisions. Therefore, the LISFLOOD-FP model, originally developed by Bates and De Roo (2000) and further improved by Hunter *et al.* (2005b), was applied at a range of model resolutions to flooding scenarios in regions of Glasgow and London in the UK. Due to a lack of observed data from historical floods, a model verification procedure was undertaken whereby coarse grid resolution model results were compared to high resolution benchmark simulations (Lane and Richards, 2001; Yu and Lane, 2006a). Results suggest that coarse representations of urban topography and topology have significant effects on storage and conveyance characteristics of urban areas. Indeed, there appears to be a critical threshold for grid resolution in urban flood modelling studies based on the distribution of gap distances between buildings. Use of digital map data allows the characterisation of urban areas *a priori* such that practitioners can provide a physical basis for model grid resolution that can be study site and flood event dependent and as a result maximise computational efficiency.

Chapter 4 also investigated the utility of different digital elevation data sets and friction parameterisations for enhancing predictions from coarse grid model configurations in an attempt to further optimise computational efficiency. Despite an intelligent use of building data and digital terrain models, there appears to be a limit on model performance similar in magnitude to the quantisation noise introduced at coarse resolutions. In addition, spatially lumped variations in Manning's n do not provide an alternative to topographic representation and cannot be used to enhance the performance of coarse resolution models. Overall, these findings point to a need to characterise the length scales of urban areas prior to any hydraulic modelling study.

7.1.2 Development of porosity algorithms for finite difference models

In response to poor model performance at coarse resolution, and the proliferation of sub-grid scale porosity techniques in the literature, a consistent modelling and testing framework was necessary to evaluate the utility of porosity-type approaches. Engineers and catastrophe modellers require simple and practical methods in order to improve model predictions but as

yet no guidance exists in terms of algorithm complexity. The porosity approaches developed in Chapter 5 were specifically designed to be simple to implement and yet make optimal use of the available data sets.

The fixed areal (ηFIX) and boundary (ηBOUND) based porosity methods assume that the building configuration is the modulating feature of flow in urban areas and thus assume blockage throughout the full range of flow depths. As such, these approaches rely on the coarse resolution terrain models being a good description of the underlying high resolution terrain. Results from the analyses in Chapter 5 suggest that for hypothetical and real urban configurations this assumption holds. The height dependent porosity approaches (ηVAR and ηBVAR) do not appear to enhance predictions of flow over complex topography over and above the results obtained from the fixed porosity techniques. Furthermore, these methods incur significant pre-processing and computational cost as a result of their implicit nature. Therefore the fixed areal based method (ηFIX) appears to be the best compromise between data requirements, pre-processing costs and model performance

7.1.3 Application of porosity approaches to urban floods

Chapter 6 documented the application of the porosity algorithms to the Greenfield and Greenwich test cases (initially analysed in Chapter 4). These results showed the utility of the simple fixed areal porosity method with respect to improving model performance on coarse resolution grids. Notably, the results also suggest that sub-grid scale resolutions for the derivation of porosity values may be of the order of the gap distance between buildings. As a result, this relaxes the data requirements for urban flood studies. In addition, the fixed boundary porosity provided no additional significant increase in model results to warrant the increased algorithm complexity and pre-processing requirements. Furthermore, the height dependent porosity methods proved significantly more complex to implement within the test cases reported here and as such were not deemed 'fit for purpose' as simple and practical methods.

Comparison of the fixed areal porosity results with observed maximum flood depth and extent data for a ~1-in-150 year return period flood event in Carlisle in January 2005 suggests a significant improvement in model performance compared to the standard coarse resolution model approach. Indeed, the ηFIX method at 50 m resolution produced results comparable to a standard 10 m resolution model of the same flood event. In addition, a Manning's n friction parameterisation for this reach suggests a stationarity of optimum floodplain friction

values with respect to empirically-derived values from literature; a result also found at the Glasgow and Greenwich test sites and by other studies (e.g. Yu and Lane, 2006b). Across all the study sites, the inclusion of spatially-distributed fixed areal porosity values delivered model performance similar to that achieved by standard model configurations at double the model resolution. In practical terms, the porosity approach, therefore, provides similar results for significantly less computational cost considering the reduction in number of cells and the increase in model time step.

7.2 Critical assessment of methodology

Through this thesis, a number of limitations have been identified, both within the research presented here and the research upon which some of this work is based.

7.2.1 Limitations of the LISFLOOD-FP model formulation

Hunter (2005) noted that although the adaptive time step formulation improved results obtained from LISFLOOD-FP, the computational constraints imposed by this time stepping procedure mean the model would be most efficiently applied at large grid resolutions (i.e. > 50 m). Nevertheless, Hunter *et al.* (2008) use the LISFLOOD-FP model for a high resolution (2 m) study of urban flood inundation and most model results presented here are at resolution higher than 50 m. In fact, work in parallel with this thesis has shown full 2D hydrodynamic models to be more efficient on grids up to 25 m resolution. In addition, estimates of damage from flooding may be highly dependent on water velocities as well as water depth and the LISFLOOD-FP conceptualisation is not designed to provide realistic estimates of velocity. Hunter *et al.* (2008) also highlight the small-scale local oscillations and reflections that occur during urban floods which LISFLOOD-FP is not capable of resolving. Therefore, in any scenario where these reflections and oscillations in water level have a significant impact on damage estimates (i.e. during a levee breach), a diffusion wave type model is not appropriate. However, diffusion wave type models do represent the broad scale evolution of floodwave dynamics and indeed, the further inclusion of inertial terms may provide a compromise between model complexity and process representation.

7.2.2 Limitations of sub-grid scale porosity techniques

The sub-grid scale porosity techniques evaluated in this thesis have been specifically developed for the finite difference model used here but are indicative of those currently documented in the literature. Although are limited by the simplistic approach to scaling of fluxes and storage area. In contrast, Yu and Lane (2006b) explicitly calculate flow and storage water depths based on the sub-grid topography but only consider ratios of 2:1 between grid and sub-grid resolutions. Similarly, the methods developed here assume that coarse resolution terrain models adequately represent the sub-grid scale variation in the underlying terrain; an important assumption when considering the slope between neighbouring grid cells.

In the work presented here, the boundary based porosity approaches have only been evaluated with respect to a single sub-grid resolution. In fact, as boundary porosities are explicitly calculated using the topography of a single-cell stencil at the edge of a coarse resolution cell, boundary porosities may well be very sensitive to the sub-grid scale topography from which they are derived. However, the results above suggest that the boundary porosity formulation does not significantly influence model results so as to warrant this added algorithm complexity and pre-processing step.

The incorporation of water height dependency into both the areal and boundary-based porosity approaches proved significantly more difficult to i) calculate and ii) implement in the LISFLOOD-FP numerical code. In addition, the utility of such an approach appears to be test case dependent such that incorporating this method into a country-wide flood model (e.g. the RMS UK Flood Model (Lohmann *et al.*, 2009), JFLOW (Bradbrook *et al.*, 2004)) may be unfeasible. However, McMillan and Brasington (2007) used an approach similar to ηBVAR and demonstrated a significant increase in model performance. As a result, more research is required to understand the poor predictions from these methods observed in this research.

7.2.3 Limitations with respect to evaluation strategy

In the majority of this thesis, model evaluation has taken the form of a verification study (Lane and Richards, 2001) comparing coarse resolution results to a high resolution benchmark simulation. This makes the assumption that the high resolution model is a more accurate representation of the actual flooding process than the coarse resolution model; an assumption that may be more applicable in urban areas given the large, high frequency vari-

ations in elevation. Furthermore, the assessment of coarse resolution results will be largely dependent on the method used for comparison to the high resolution benchmark. For instance, Yu and Lane (2006a) evaluate models at the coarse resolution using a wetting front concept whereas in this research, model results are resampled to the high resolution for evaluation.

In the case where observed flood depth and extent data are available, the methods for representing topography in coarse grid models may be evaluated more realistically. The Carlisle test site represents one of the most comprehensive data sets available to date concerning an urban flood event that combines spatially distributed post-event maximum water level and extent measurements with gauged hydragrophs and digital topography and topology data. Nonetheless, problems with the observed data still remain. Most notably, the observational data used here provides a single point measurement in space and time and thus does not provide a method for evaluating the dynamic performance of numerical flood models. In addition, Neal *et al.* (2009a) note the problems of post-event surveys of water depths and extents. Water marks form as a result of the waves and reflections that occur when the floodwave interacts with the building network and wrack marks may be deposited on the falling limb of the hydrograph leading to mis-interpretation of maximum flood elevations.

7.3 Perspectives for future work

The main focus of this research was to develop computationally efficient hydraulic flood models for wide area application while at the same time delivering fine scale detail for the planning and insurance industries. Although a number of approaches have been presented to meet this goal, there remains significant scope for improving wide area predictions of flood risk from hydraulic models. Recent advances in computing technology (e.g. Accelerator boards (ClearSpeed^{TM}, GPUs, etc.) and High Performance Computing clusters (BlueCrystal @ UoB)) has created a significant opportunity to enhance hydraulic models and thus relax the current computational constraints. The responsibility now lies with environmental modellers to adapt current models to take full advantage of the available resources. In fact, recent work using the OpenMP API (Neal *et al.*, in press) for shared-memory processor architectures and the Microsoft DirectX 9 programming language on GPUs (Lamb *et al.*, in press) have demonstrated significant model speed ups for explicit diffusion wave type flood models. Given the raster data structure and simple numerics of LISFLOOD-FP, adaptive or hierarchical

data structures (e.g. quadtree) may provide a framework for variations in grid cell size providing local detail where required and increasing computational speed on the larger grid cells.

The increases in computational efficiency brought by the porosity techniques developed in this thesis also provides an opportunity to move from deterministic to ensembles of simulations. As a consequence, ensembles of simulations may be used, in operational terms, for prediction purposes in flood inundation forecasting or indeed in research terms, for investigating the relative uncertainties in any given flood modelling exercise. The latter is the focus of a NERC Flood Risk for Extreme Events (FREE) programme work package investigating the uncertainty cascade from general circulation models (GCMs) of climatic conditions through to flood inundation estimation.

The fact that the simple porosity technique performs well at a variety of test sites suggests that it may be possible to apply this technique to data sparse areas where high resolution DEM and land use data is not available. Aerial photography and optical satellite sensors may be able to inform areal porosity values through image classification in order to resolve flows through large urban areas. Furthermore, these large scale data sets may be used to characterise different types of urban configurations within a larger urban agglomeration and thus it may be possible to classify large portions of these urban areas by porosity values.

The work presented in this thesis has also recognised the lack of validation data available for model assessment and reliable gauged flow data to accurately parameterise flood events. Recent large flood events in the UK (e.g. summer 2007) that coincide with a number of satellite acquisitions and aerial photography missions provide an increasingly amount of information to study the dynamics of urban floods. In addition, the use of wireless technologies for hydrometric data retrieval (e.g. GridStix project under the NERC FREE programme) will further increase the data available for model evaluation. Nevertheless, the impact of 'off-river' or 'disconnected' flooding in urban areas caused by overwhelming of local drainage systems still presents significant research problems.

The combination of these research directions will provide the tools necessary to assess flood risk over wide areas while still providing local, fine scale detail. In addition, this will allow environmental modellers to more efficiency and exhaustively assess the uncertainty in data sources and model structures, and their effect on model results as the computational burden has been resolved.

References

ABI, 2007. Summer floods 2007: Learning the lessons. Tech. rep., Association of British Insurers.

Aronica, G., Bates, P. D., Horritt, M. S., 2002. Assessing the uncertainty in distributed model predictions using observed binary pattern information within GLUE. Hydrological Processes 16 (10), 2001–2016.

Bates, P., Anderson, M., 2001. Validation of hydraulic models. In: Anderson, M., Bates, P. D. (Eds.), Model Validation: Perspectives in Hydrological Science. John Wiley & Sons Ltd.

Bates, P., Horritt, M., 2005. Modelling wetting and drying processes in hydraulic models. In: Bates, P., Lane, S., Ferguson, R. (Eds.), Computational Fluid Dynamics: Applications in Environmental Hydraulics. John Wiley & Sons Ltd, pp. 121–146.

Bates, P., Stewart, M., Siggers, G., Smith, C., Hervouet, J., Sellin, R., 1998a. Internal and external validation of a two-dimensional finite element code for river flood simulations. Proceedings of the Institution of Civil Engineers - Water and Maritime Engineering 130 (3), 127–141.

Bates, P. D., 2004. Remote sensing and flood inundation modelling. Hydrological Processes 18 (13), 2593–2597.

Bates, P. D., Anderson, M. G., 1993. A 2-dimensional finite-element model for river flow inundation. Proceedings of the Royal Society of London Series A - Mathematical Physical and Engineering Sciences 440 (1909), 481–491.

Bates, P. D., Anderson, M. G., 1996. A preliminary investigation into the impact of initial conditions on flood inundation predictions using a time/space distributed sensitivity analysis. Catena 26 (1-2), 115–134.

Bates, P. D., De Roo, A. P. J., 2000. A simple raster-based model for flood inundation simulation. Journal of Hydrology 236 (1-2), 54–77.

Bates, P. D., Hervouet, J. M., 1999. A new method for moving-boundary hydrodynamic problems in shallow water. Proceedings of the Royal Society of London Series A - Mathematical Physical and Engineering Sciences 455 (1988), 3107–3128.

Bates, P. D., Horritt, M., Hervouet, J. M., 1998b. Investigating two-dimensional, finite element predictions of floodplain inundation using fractal generated topography. Hydrological Processes 12 (8), 1257–1277.

Bates, P. D., Marks, K. J., Horritt, M. S., 2003. Optimal use of high-resolution topographic data in flood inundation models. Hydrological Processes 17 (3), 537–557.

Bergstrom, S., 1991. Principles and confidence in hydrological modelling. Nordic Hydrology 22, 123–136.

Beven, K., 1989. Changing ideas in hydrology - the case of physically-based models. Journal of Hydrology 105 (1), 157–172.

Beven, K., 1995. Linking parameters across scales - subgrid parameterizations and scale-dependent hydrological models. Hydrological Processes 9 (5-6), 507–525.

Beven, K., 2000a. On model uncertainty, risk and decision making. Hydrological Processes 14 (14), 2605–2606.

Beven, K., 2000b. Uniqueness of place and process representations in hydrological modelling. Hydrology and Earth System Sciences 4 (2), 203–213.

Beven, K., 2002. Towards a coherent philosophy for modelling the environment. Proceedings of the Royal Society of London Series a-Mathematical Physical and Engineering Sciences 458 (2026), 2465–2484.

Beven, K., 2006. A manifesto for the equifinality thesis. Journal of Hydrology 320 (1-2), 18–36, Special Issue.

Beven, K., Binley, A., 1992. The future of distributed models: model calibration and uncertainty prediction. Hydrological Processes 6, 279–298.

Box, G. P. E., Jenkins, G. M., 1970. Time series analysis: forecasting and control. Holden-Day, San Francisco.

Bradbrook, K., Lane, S. N., Waller, S., Bates, P. D., 2004. Two dimensional diffusion wave modelling of flood inundation using a simplified channel representation. International Journal of River Basin Management 2 (3), 1–13.

Bradford, S. F., Sanders, B. F., 2002. Finite-volume model for shallow-water flooding of arbitrary topography. Journal of Hydraulic Engineering-Asce 128 (3), 289–298, times Cited: 49.

Braschi, G., Gallati, M., Natale, L., 1989. Simulation of a road network flooding. In: 20th Annual Pittsburgh Conference on Modeling and Simulation. Vol. 4. Pittsburgh, USA, pp. 1625–1632.

Braschi, G., Gallati, M., Natale, L., 1991. Modelling floods in urban areas. In: 15th Annual Conference, Association of State Floodplain Managers. Vol. 1. Denver, USA, pp. 117–122.

Brater, E., Sherril, J., 1975. Rainfall-runoff relations on urban and rural areas. Tech. Rep. EPA-670/2-75-046, United States Environmental Protection Agency.

Butler, J., Martin, D., Stephes, E., Smith, L., 2009. An intergrated approach to modelling surface water flood risk in urban areas. In: Samuels, P., Huntington, S., Allsop, W., Harrop, J. (Eds.), Flood Risk Management: Research and Practice. Taylor & Francis Group, pp. 57–67.

Carling, P., Cao, Z., Holland, M., Ervine, D., Babaeyan-Koopaei, K., 2002. Turbulent flow across a natural compound channel. Water Resources Research 38 (12), 1270.

Carter, R., 1961. Magnitude and frequency of floods in suburban areas. Tech. Rep. 424-B, United States Geological Survey.

Chow, V. T., 1959. Open-channel hydraulics. McGraw-Hill Civil Engineering. McGraw-Hill, London.

Clarke, D., 1st July 2005 2005. Managing flood risk: Dealing with flooding. Tech. Rep. GEHO0605BJDB-E-E, Environment Agency.

Cobby, D. M., Mason, D. C., Horritt, M. S., Bates, P. D., 2003. Two-dimensional hydraulic flood modelling using a finite-element mesh decomposed according to vegetation and topographic features derived from airborne scanning laser altimetry. Hydrological Processes 17 (10), 1979–2000.

Cunge, J., Holly, F., Verwey, A., 1980. Practical aspects of computational river hydraulics. Pitman Publishing, London.

Dawson, R. J., Hall, J. W., Bates, P. D., Nicholls, R. J., 2005. Quantified analysis of the probability of flooding in the thames estuary under imaginable worst-case sea level rise scenarios. International Journal of Water Resources Development 21 (4), 577–591.

Day, A., July 2005. Carlisle storms and associated flooding: Multi-agency debrief report. Tech. rep., UK Resilience.

Defina, A., 2000. Two-dimensional shallow flow equations for partially dry areas. Water Resources Research 36 (11), 3251–3264.

Defina, A., D'Alpaos, L., Matticchio, B., 1994. Modelling of flood propagation over initially dry areas. In: Molinaro, P., Natale, L. (Eds.), Proceedings of the Specialty Conference on Modelling of Flood Propagation Over Initially Dry Areas. Milan, Italy, pp. 72–81.

Di Baldassarre, G., Laio, F., Montanari, A., in press. Design flood estimation using model selection criteria. Physics and Chemistry of the Earth, Parts A/B/C.

Eilertsen, R. S., Hansen, L., 2008. Morphology of river bed scours on a delta plain revealed by interferometric sonar. Geomorphology 94 (1-2), 58–68.

Epsey, W., Winslow, D., Morgan, C., 1969. Urban effects of the unit hydrograph. In: Moore, W., Morgan, C. (Eds.), Effects of watershed changes on streamflow. University of Texas Press, Austin, USA.

Ervine, D., Willetts, B., Sellin, R., Lorena, M., 1993. Factors affecting conveyance in meandering compound flows. Journal of Hydraulic Engineering 119 (12), 1383–1399.

Evans, E., Ashley, R., Hall, J., Penning-Rowsell, E., Sayers, P., Thorne, C., Watkinson, A., 2004. Foresight. Future Flooding. Scientific Summary: Volume II Managing future risks. Office of Science and Technology, London.

Falconer, R., Owens, P., 1987. Numerical-simulation of flooding and drying in a depth-averaged tidal flow model. Proceedings of the Institution of Civil Engineers Part 2 - Research and Theory 83, 161–180.

Fathi-Maghadam, M., Kouwen, N., 1997. Nonrigid, nonsubmerged, vegetative roughness on floodplains. Journal of Hydraulic Engineering-Asce 123 (1), 51–57.

Fawcett, K., Anderson, M., Bates, P., Jordan, J.-P., Bathhurst, J., 1995. The importance of internal validation in the assessment of physically based distributed models. Transactions of the Institute of British Geographers 20, 248–265.

Fisher, K., Dawson, H., 2003. Reducing uncertainty in river flood conveyance: Roughness review. Tech. Rep. W5A-057, UK DEFRA and Environment Agency.

Forlani, G., Nardinocchi, C., Scaioni, M., Zingaretti, P., 2006. Complete classification of raw LiDAR data 3D reconstruction of buildings. Pattern Analysis and Applications 8, 357–374.

Freer, J., Beven, K., 2005. Model structural error and the curse of the errors in variables problem. In: EGU General Assembly. Vienna, Austria.

Freer, J. E., McMillan, H., McDonnell, J. J., Beven, K. J., 2004. Constraining dynamic TOPMODEL responses for imprecise water table information using fuzzy rule based performance measures. Journal of Hydrology 291, 254–277.

Freeze, R., Harlan, R., Nov. 1969. Blueprint for a physically-based, digitally-simulated hydrologic response model. Journal of Hydrology 9, 237–258.

Gouldby, B., Samuels, P., 2005. Integrated flood risk analysis and management methodologies: FLOODsite, language of risk, project definitions. Tech. Rep. T32-04-01, HR Wallingford.

Gouldby, B., Sayers, P., Mulet-Marti, J., Hassan, M., Benwell, D., 2008. A methodology for regional-scale flood risk assessment. Proceedings of the Institution of Civil Engineers - Water Management 161 (WM3), 169–182.

Gouldby, B., Sayers, P., Tarrant, O., Kavanagh, D., April 2007. Thames Estuary 2100: Performance based asset management. Tech. Rep. IA8/10, HR Wallingford.

Guinot, V., Soares-Frazão, S., 2006. Flux and source term discretization in two-dimensional shallow water models with porosity on unstructured grids. International Journal for Numerical Methods in Fluids 50, 309–345.

Haider, S., Paquier, A., Morel, R., Champagne, J. Y., 2003. Urban flood modelling using computational fluid dynamics. Proceedings of the Institution of Civil Engineers-Water and Maritime Engineering 156 (2), 129–135.

Hall, J. W., Dawson, R. J., Sayers, P. B., Rosu, C., Chatterton, J. B., Deakin, R., 2003. A methodology for national-scale flood risk assessment. Proceedings of the Institution of Civil Engineers-Water and Maritime Engineering 156 (3), 235–247.

Han, K. Y., Lee, J. T., Park, J. H., 1998. Flood inundation analysis resulting from levee-break. Journal of Hydraulic Research 36 (5), 747–759.

Hardy, R. J., Bates, P., Anderson, M., 1999. The importance of spatial resolution in hydraulic models for floodplain environments. Journal of Hydrology 216, 124–136.

Herschy, R. (Ed.), 1999. Hydrometry: Principles and practices, Second Edition. John Wiley & Sons Ltd, Chicester.

Hervouet, J. M., Samie, R., Moreau, B., 2000. Modelling urban areas in dam-break flood-wave numerical simulations. In: International Seminar and Workshop on Rescue Actions based on Dam-break Flood Analysis. Vol. 1. Seinajoki, Finland.

Hervouet, J.-M., Van Haren, L., 1996. Recent advances in numerical methods for fluid flow. In: Anderson, M. G., Walling, D. E., Bates, P. D. (Eds.), Floodplain Processes. John Wiley & Sons Ltd, Chichester, pp. 183–214.

Hingray, B., Cappelaere, B., Bouvier, B., Desorbes, M., 2000. Hydraulic vulnerability of elementary urban cell. Journal of Hydrologic Engineering 5 (4), 402–410.

Hollis, G., 1975. The effect of urbanization on floods of different recurrence interval. Water Resources Research 11, 431–435.

Horritt, M., 2004. Development and testing of a simple 2d finite volume model of sub-critical shallow water flow. International Journal for Numerical Methods in Fluids 44 (11), 1231–1255.

Horritt, M., Bates, P., Fewtrell, T., Mason, D., Wilson, M., in review. Modelling the hydraulics of the Carlisle 2005 flood event. Proceedings of the Institution of Civil Engineers - Water Management.

Horritt, M. S., 2000a. Calibration of a two-dimensional finite element flood flow model using satellite radar imagery. Water Resources Research 36 (11), 3279–3291.

Horritt, M. S., 2000b. Development of physically based meshes for two-dimensional models of meandering channel flow. International Journal for Numerical Methods in Engineering 47 (12), 2019–2037.

Horritt, M. S., 2002. Evaluating wetting and drying algorithms for finite element models of shallow water flow. International Journal for Numerical Methods in Engineering 55 (7), 835–851.

Horritt, M. S., Bates, P. D., 2001a. Effects of spatial resolution on a raster based model of flood flow. Journal of Hydrology 253 (1-4), 239–249.

Horritt, M. S., Bates, P. D., 2001b. Predicting floodplain inundation: raster-based modelling versus the finite-element approach. Hydrological Processes 15 (5), 825–842.

Horritt, M. S., Bates, P. D., 2002. Evaluation of 1D and 2D numerical models for predicting river flood inundation. Journal of Hydrology 268 (1-4), 87–99.

Horritt, M. S., Bates, P. D., Mattinson, M. J., September 2006. Effects of mesh resolution and topographic representation in 2d finite volume models of shallow water fluvial flow. Journal of Hydrology 329 (1-2), 306–314.

Horritt, M. S., Di Baldassarre, G., Bates, P. D., Brath, A., 2007. Comparing the performance of a 2-D finite element and a 2-D finite volume model of floodplain inundation using airborne sar imagery. Hydrological Processes 21 (20), 2745–2759.

HR Wallingford, H. ., 2004. Thames embayments inundation modelling. Stage 2a: Model testing. Tech. rep., Halcrow Group Ltd.

Hromadka, T. V., Yen, C. C., 1986. A diffusion hydrodynamic model (DHM). Advances in Water Resources 9 (3), 118–170.

Huber, M., 2004. Reforming the UK flood insurance regime: The breakdown of a Gentleman's Agreement.

Hunter, N., Bates, P., Horritt, M., De Roo, P., Werner, M., 2005a. Utility of different data types for calibrating flood inundation models within a GLUE framework. Hydrology and Earth System Sciences 9 (4), 412–430.

Hunter, N. M., 2005. Development and assessment of dynamic storage cell codes for flood inundation modelling. Ph.D. thesis, University of Bristol.

Hunter, N. M., Bates, P. D., Horritt, M. S., Wilson, M. D., 2006. Improved simulation of flood flows using storage cell models. Proceedings of the Institution of Civil Engineers - Water Management 159 (WM1), 9–18.

Hunter, N. M., Bates, P. D., Horritt, M. S., Wilson, M. D., 2007. Simple spatially-distributed models for predicting flood inundation: A review. Geomorphology 90 (3-4), 208–225.

Hunter, N. M., Bates, P. D., Néelz, S., Pender, G., Villanueva, I., Wright, N. G., Liang, D., Falconer, R. A., Lin, B., Waller, S., Crossley, A. J., Mason, D. C., 2008. Benchmarking 2D hydraulic models for urban flooding. Proceedings of the Institution of Civil Engineers - Water Management 161 (WM1), 13–30.

Hunter, N. M., Horritt, M. S., Bates, P. D., Wilson, M. D., Werner, M. G. F., 2005b. An adaptive time step solution for raster-based storage cell modelling of floodplain inundation. Advances in Water Resources 28 (9), 975–991.

IPCC, 2007. Climate Change 2007: Synthesis Report. Contribution of Working Groups I, II and III to the Fourth Assessment Report of the Intergovernmental Panel on Climate Change. IPCC, Geneva, Switzerland.

Jolley, T., November 2002. Flooding in the east end of Glasgow - 30 July 2002. Tech. rep., Scottish Environmental Protection Agency.

Kirchner, J. W., 2006. Getting the right answers for the right reasons: Linking measurements, analyses, and models to advance the science of hydrology. Water Resources Research 42 (3), w03S04.

Knight, D., Shiono, K., 1996. River channel and floodplain hydraulics. In: Anderson, M. G., Walling, D., Bates, P. (Eds.), Floodplain Processes. John Wiley & Sons Ltd, Chichester, pp. 139–181.

Konikow, L., Bredehoeft, J., 1992. Ground-water models cannot be validated. Advances in Water Resources 15 (1), 75–83.

Lamb, R., Crossley, A., Waller, S., in press. A fast 2D floodplain inundation model. Proceedings of the Institution of Civil Engineers - Water Management.

Lane, S., James, T., Pritchard, H., Saunders, M., 2003. Photogrammetric and laser altimetric reconstruction of water levels for extreme flood event analysis. Photogrammetric Record 18 (104), 293–307.

Lane, S. N., 2005. Roughness - time for a re-evaluation? Earth Surface Processes and Landforms 30 (2), 251–253.

Lane, S. N., 2008. Climate change and the summer 2007 floods in the UK. Geography 93 (2), 91–97.

Lane, S. N., Bradbrook, K. F., Richards, K. S., Biron, P. A., Roy, A. G., 1999. The application of computational fluid dynamics to natural river channels: three-dimensional versus two-dimensional approaches. Geomorphology 29 (1-2), 1–20.

Lane, S. N., Hardy, R. J., Elliott, L., Ingham, D. B., 2002. High-resolution numerical modelling of three-dimensional flows over complex river bed topography. Hydrological Processes 16 (11), 2261–2272.

Lane, S. N., Richards, K., 2001. The validation of hydrodynamic models: some critical perspectives. In: Anderson, M. (Ed.), Model validation: perspectives in hydrological science. John Wiley & Sons Ltd, Chichester, pp. 413–438.

Leopold, L. B., 1973. River channel change with time: An example. Geological Society of America Bulletin 84 (6), 1845–1860.

Lohmann, D., Eppert, S., Hilberts, A., Honegger, C., Steward-Menteth, A., 2009. Correlation in time and space: Economic assessment of flood risk with the Risk Management Solutions (RMS) UK River Flood Model. In: Samuels, P., Huntington, S., Allsop, W., Harrop, J. (Eds.), Flood Risk Management: Research and Practice. Taylor & Francis Group, pp. 1631–1634.

Mark, O., Weesakul, S., Apirumanekul, C., Aroonnet, S. B., Djordjevic, S., 2004. Potential and limitations of 1D modelling of urban flooding. Journal of Hydrology 299 (3-4), 284–299.

Marks, K., Bates, P., 2000. Integration of high-resolution topographic data with floodplain flow models. Hydrological Processes 14 (11-12), 2109–2122.

Martens, L., 1968. Flood inundation and effects of urbanization in metropolitan Charlotte, North Carolina. Tech. Rep. 1591-C, United States Geological Survey.

Mason, D. C., Cobby, D. M., Horritt, M. S., Bates, P. D., 2003. Floodplain friction parameterization in two-dimensional river flood models using vegetation heights derived from airborne scanning laser altimetry. Hydrological Processes 17 (9), 1711–1732.

Mason, D. C., Horritt, M. S., Bates, P. D., Hunter, N., 2007. Use of fused airborne scanning laser altimetry and digital map data for urban flood modelling. Hydrological Processes 21 (11), 1436–1447.

McMillan, H. K., Brasington, J., 2007. Reduced complexity strategies for modelling urban floodplain inundation. Geomorphology 90, 226–243.

Mignot, E., Paquier, A., Haider, S., 2006. Modeling floods in a dense urban area using 2D shallow water equations. Journal of Hydrology 327 (1-2), 186–199.

Molinaro, P., Di Fillippo, A., Ferrari, F., 1994. Modelling of flood wave propagation over flat dry areas of complex topography in presence of different infrastructures. In: Modelling of Flood Propagation Over Initially Dry Areas. Vol. 1. ASCE, New York, pp. 209–228.

Moramarco, T., Melone, F., Singh, V. P., 2005. Assessment of flooding in urbanized ungauged basins: a case study in the upper tiber area, italy. Hydrological Processes 19 (10), 1909–1924.

Morris, M., 2000. CADAM concerted action on dambreak modelling - final report. Tech. Rep. SR 571, HR Wallingford Ltd.

Morton, A., 1993. Mathematical models: Questions of trustworthiness. British Journal for the Philosophy of Science 44 (4), 659–674.

Munson, B., Young, D., Okiishi, T. (Eds.), 2005. Fundamentals of fluid mechanics. John Wiley & Sons Ltd.

Neal, J., Bates, P., Fewtrell, T., Hunter, N., Wilson, M., Horritt, M., 2009a. Hydrodynamic modelling of the Carlisle 2005 urban flood event and comparison with validation data. Journal of Hydrology.

Neal, J., Bates, P., Fewtrell, T., Wright, N. G., Villanueva, I., Hunter, N. M., Horritt, M., 2009b. Modelling the 2005 carlisle flood event using lisflood-fp and trent. In: Samuels, P., Huntington, S., Allsop, W., Harrop, J. (Eds.), Flood Risk Management: Research and Practice. Taylor & Francis Group, pp. 263–272.

Neal, J., Fewtrell, T., Trigg, M., in press. Parallelisation of storage cell flood models using openmp. Environmental Modelling and Software.

Néelz, S., Pender, G., 2006. The influence of errors in Digital Terrain Models on flood flow routes. In: River Flow 2006. IAHR, Lisbon, Portugal, pp. 1955–1962.

Neelz, S., Pender, G., 2007a. Parameterisation of square-grid hydrodynamic models of inundation in the urban area. In: Proceedings of the 32nd IAHR congress.

Neelz, S., Pender, G., 2007b. Sub-grid scale parameterisation of 2d hydrodynamic models of inundation in the urban area. Acta Geophysica 55, 65–72.

Nelson, P. A., Smith, J. A., Miller, A. J., 2009. Evolution of channel morphology and hydrologic response in an urbanizing drainage basin. Earth Surface Processes and Landforms.

NERC, 1975. Flood Studies Report. Vol. 3. Whitefriars Press.

Oreskes, N., Shraderfrechette, K., Belitz, K., 1994. Verification, validation, and confirmation of numerical-models in the earth-sciences. Science 263 (5147), 641–646.

Pappenberger, F., Beven, K., Horritt, M., Blazkova, S., 2005. Uncertainty in the calibration of effective roughness parameters in hec-ras using inundation and downstream level observations. Journal of Hydrology 302 (1-4), 46–69.

Pappenberger, F., Matgen, P., Beven, K. J., Henry, J. B., Pfister, L., Fraipont de, P., 2006. Influence of uncertain boundary conditions and model structure on flood inundation predictions. Advances in Water Resources 29 (10), 1430–1449.

Pender, G., 2006. Briefing: Introducting the flood risk management research consortium. Proceedings of the Institution of Civil Engineers - Water Management 159 (WM1), 3–8.

Prescott, J., 2005. Delivering growth in Thames Gateway and the Growth Areas. Tech. rep., Office of The Deputy Prime Minister.

Prestininzi, P., 2008. Suitability of the diffusive model for dam break simulation: Application to a CADAM experiment. Journal of Hydrology 361 (1-2), 172–185.

Raber, G. T., Jensen, J. R., Hodgson, M. E., Tullis, J. A., Davis, B. A., Berglund, J., 2007. Impact of LiDAR nominal post-spacing on DEM accuracy and flood zone delineation. Photogrammetric Engineering and Remote Sensing 73, 793–804.

Refsgaard, J., 2000. Towards a formal approach to calibration and validation of models using spatial data. In: Grayson, R., Blöschl, G. (Eds.), Spatial Patterns in Catchment Hydrology: Observations and Modelling. University Press, Cambridge, pp. 329–354.

Richards, K., 1982. Rivers: Form and Process in Alluvial Channels. Methuen.

Richards, K., 1996. Samples and cases: generalisation and explanation in geomorphology. In: Rhoads, B., Thorn, C. (Eds.), The scientific nature of geomorphology. John Wiley & Sons Ltd, Chichester, pp. 171–190.

Samuels, P., 1990. Cross-section location in 1-D models. In: White, W., Watts, J. (Eds.), 2nd International Conference on River Flood Hydraulics. John Wiley & Sons Ltd, Chichester, pp. 339–350.

Sanders, B., Schubert, J., Gallegos, H., 2008. Intergal formulation of shallow-water equations with anisotropic porosity for urban flood modelling. Journal of Hydrology 362, 19–38.

Sanders, B. F., 2008. Integration of a shallow water model with a local time step. Journal of Hydraulic Research 48 (4), 466–475.

Sayers, P., Gouldby, B., Simm, J. D., Meadowcraft, I., Hall, J., 2002. Risk, performance and uncertainty in flood and coastal defence - a review. Tech. Rep. FD2302/TR1, HR Wallingford Ltd.

Schmitt, T. G., Thomas, M., Ettrich, N., 2004. Analysis and modeling of flooding in urban drainage systems. Journal of Hydrology 299, 300–311.

Schubert, J. E., Sanders, B. F., Smith, M. J., Wright, N. G., 2008. Unstructured mesh generation and landcover-based resistance for hydrodynamic modeling of urban flooding. Advances in Water Resources 31 (12), 1603 – 1621.

Schumann, G., Hostache, R., Puech, C., Hoffmann, L., Matgen, P., Pappenberger, F., Pfister, L., 2007a. High-resolution 3-D flood information from radar imagery for flood hazard management. Ieee Transactions on Geoscience and Remote Sensing 45 (6), 1715–1725.

Schumann, G., Matgen, P., Hoffmann, L., Hostache, R., Pappenberger, F., Pfister, L., 2007b. Deriving distributed roughness values from satellite radar data for flood inundation modelling. Journal of Hydrology 344 (1-2), 96–111.

Sellin, R., Ervine, D., Willetts, B., 1993. Behaviour of meandering 2-stage channels. Proceedings of the Institution of Civil Engineers - Water Maritime and Energy 101 (2), 99–111.

Shiono, K., Knight, D., 1991. Turbulent open channel flows with variable depth across the channel. Journal of Fluid Mechanics 222, 617–646.

Smith, J. A., Baeck, M. L., Morrison, J. E., Sturdevant-Rees, P., Turner-Gillespie, D. F., Bates, P. D., 2002. The regional hydrology of extreme floods in an urbanizing drainage basin. Journal of Hydrometeorology 3 (3), 267–282.

Soares-Frazão, S., LHomme, J., Guinot, V., Zech, Y., 2008. Two-dimensional shallow-water model with porosity for urban flood modelling. Journal of Hydraulic Research 1, 45–64.

Soares-Frazão, S., Zech, Y., 2008. Dam-break flow through an idealised city. Journal of Hydraulic Research 46 (5), 648–658.

Spear, R. C., Hornberger, G. M., 1980. Eutrophication in Peel inlet - II. Identification of critical uncertainties via generalized sensitivity analysis. Water Research 14 (XX), 43–49.

Syme, W. J., 1991. Dynamically linked two-dimensional/onedimensional hydrodynamic modelling program for rivers, estuaries and coast waters. Mengsc thesis, University of Queensland, Australia.

Tarrant, O., Todd, M., Ramsbottom, D., Wicks, J., 2005. 2D floodplain modelling in the tidal thames - addressing the residual risk. Water and Environment Journal 19 (2), 125–134.

Tayefi, V., Lane, S., Hardy, R., Yu, D., 2007. A comparison of one- and two-dimensional approaches to modelling flood inundation over complex upland floodplains. Hydrological Processes 21 (23), 3190–3202.

Villanueva, I., Wright, N. G., 2006. Linking riemann and storage cell models for flood prediction. Proceedings of the Institution of Civil Engineers, Journal of Water Management 159 (1), 27–33.

Wagener, T., McIntyre, N., Lees, M. J., Wheater, H. S., Gupta, H. V., 2003. Towards reduced uncertainty in conceptual rainfall-runoff modelling: dynamic identifiability analysis. Hydrological Processes 17, 455–476.

Werner, M., Blazkova, S., Petr, J., 2005a. Spatially distributed observations in constraining inundation modelling uncertainties. Hydrological Processes In Press (0), 0.

Werner, M. G. F., 2004. A comparison of flood extent modelling approaches through constraining uncertainties on gauge data. Hydrology and Earth System Sciences 8 (6), 1141–1152.

Werner, M. G. F., Hunter, N. M., Bates, P. D., 2005b. Identifiability of distributed floodplain roughness values in flood extent estimation. Journal of Hydrology 314 (1-4), 139–157.

Wheater, H. S., 2002. Progress in and prospects for fluvial flood modelling. Philosophical Transactions: Mathematical, Physical and Engineering Sciences 360 (1796), 1409–1431.

Wilby, R., Beven, K., N.S., R., 2008. Climate change and fluvial flood risk in the UK: more of the same? Hydrological Processes 22, 2511–2523.

Wilson, M., Bates, P., Alsforf, D., Forsberg, B., Horritt, M., Melack, J., Frappart, F., Famigliette, J., 2007. Modeling large-scale inundation of Amazonian seasonally flooded wetlands. Geophysical Research Letters 34 (15).

Xanthopoulos, T., Koutitas, C., 1976. Numerical-simulation of a 2 dimensional flood wave-propagation due to dam failure. Journal of Hydraulic Research 14 (4), 321–331.

Xiao, Q., McPherson, E. G., Simpson, J., L., U. S., 2009. Hydrologic processes at the urban residential scale. Hydrological Processes in press.

Yu, D., 2005. Diffusion-based modelling of flood inundation over complex floodplains. Ph.D. thesis, University of Leeds.

Yu, D., Lane, S. N., 2006a. Urban fluvial flood modelling using a two-dimensional diffusion-wave treatment, part 1: mesh resolution effects. Hydrological Processes 20 (7), 1541–1565.

Yu, D., Lane, S. N., 2006b. Urban fluvial flood modelling using a two-dimensional diffusion-wave treatment, part 2: development of a sub-grid-scale treatment. Hydrological Processes 20 (7), 1567–1583.

Zanichelli, G., Caroni, E., Fiorotto, V., 2004. River bifurcation analysis by physical and numerical modeling. Journal of Hydraulic Engineering-Asce 130 (3), 237–242.

Zanobetti, D., Longer, H., Preissmann, A., Cunge, J., 1968. Le modèle mathmatique du delta du Mékong. La Houille Blanche 23 (1, 4 and 5).

Zanobetti, D., Longeré, H., Preissmann, A., Cunge, J., 1970. Mekong Delta mathematical model program construction. Journal of the Waterways and Harbors Division 96 (WW2), 181–199.